United States Nuclear Regulatory Commission

Protecting People and the Environment

NUREG/CR-7136
PNNL-20300

Assessment of NDE Methods on Inspection of HDPE Butt Fusion Piping Joints for Lack of Fusion

Office of Nuclear Regulatory Research

AVAILABILITY OF REFERENCE MATERIALS IN NRC PUBLICATIONS

NRC Reference Material

As of November 1999, you may electronically access NUREG-series publications and other NRC records at NRC's Public Electronic Reading Room at http://www.nrc.gov/reading-rm.html. Publicly released records include, to name a few, NUREG-series publications; *Federal Register* notices; applicant, licensee, and vendor documents and correspondence; NRC correspondence and internal memoranda; bulletins and information notices; inspection and investigative reports; licensee event reports; and Commission papers and their attachments.

NRC publications in the NUREG series, NRC regulations, and *Title 10, Energy*, in the Code of *Federal Regulations* may also be purchased from one of these two sources.

1. The Superintendent of Documents
   U.S. Government Printing Office
   Mail Stop SSOP
   Washington, DC 20402–0001
   Internet: bookstore.gpo.gov
   Telephone: 202-512-1800
   Fax: 202-512-2250
2. The National Technical Information Service
   Springfield, VA 22161–0002
   www.ntis.gov
   1–800–553–6847 or, locally, 703–605–6000

A single copy of each NRC draft report for comment is available free, to the extent of supply, upon written request as follows:

Address: U.S. Nuclear Regulatory Commission
Office of Administration
Publications Branch
Washington, DC 20555-0001
E-mail: DISTRIBUTION.RESOURCE@NRC.GOV
Facsimile: 301–415–2289

Some publications in the NUREG series that are posted at NRC's Web site address http://www.nrc.gov/reading-rm/doc-collections/nuregs are updated periodically and may differ from the last printed version. Although references to material found on a Web site bear the date the material was accessed, the material available on the date cited may subsequently be removed from the site.

Non-NRC Reference Material

Documents available from public and special technical libraries include all open literature items, such as books, journal articles, and transactions, *Federal Register* notices, Federal and State legislation, and congressional reports. Such documents as theses, dissertations, foreign reports and translations, and non-NRC conference proceedings may be purchased from their sponsoring organization.

Copies of industry codes and standards used in a substantive manner in the NRC regulatory process are maintained at—

The NRC Technical Library
Two White Flint North
11545 Rockville Pike
Rockville, MD 20852–2738

These standards are available in the library for reference use by the public. Codes and standards are usually copyrighted and may be purchased from the originating organization or, if they are American National Standards, from—

American National Standards Institute
11 West 42nd Street
New York, NY 10036–8002
www.ansi.org
212–642–4900

Legally binding regulatory requirements are stated only in laws; NRC regulations; licenses, including technical specifications; or orders, not in NUREG-series publications. The views expressed in contractor-prepared publications in this series are not necessarily those of the NRC.

The NUREG series comprises (1) technical and administrative reports and books prepared by the staff (NUREG–XXXX) or agency contractors (NUREG/CR–XXXX), (2) proceedings of conferences (NUREG/CP–XXXX), (3) reports resulting from international agreements (NUREG/IA–XXXX), (4) brochures (NUREG/BR–XXXX), and (5) compilations of legal decisions and orders of the Commission and Atomic and Safety Licensing Boards and of Directors' decisions under Section 2.206 of NRC's regulations (NUREG–0750).

DISCLAIMER: This report was prepared as an account of work sponsored by an agency of the U.S. Government. Neither the U.S. Government nor any agency thereof, nor any employee, makes any warranty, expressed or implied, or assumes any legal liability or responsibility for any third party's use, or the results of such use, of any information, apparatus, product, or process disclosed in this publication, or represents that its use by such third party would not infringe privately owned rights.

United States Nuclear Regulatory Commission

Protecting People and the Environment

NUREG/CR-7136
PNNL-20300

Assessment of NDE Methods on Inspection of HDPE Butt Fusion Piping Joints for Lack of Fusion

Manuscript Completed: October 2011
Date Published: May 2012

Prepared by
S. L. Crawford, S. R. Doctor, A. D. Cinson, M. W. Watts,
S. E. Cumblidge, T. E. Hall, and M. T. Anderson

Pacific Northwest National Laboratory
P.O. Box 999
Richland, WA 99352

W. E. Norris, NRC Project Manager

NRC Job Code N6398

Office of Nuclear Regulatory Research

ABSTRACT

The U.S. Nuclear Regulatory Commission (NRC) has a multi-year program at the Pacific Northwest National Laboratory (PNNL) to provide engineering studies and assessments of issues such as the nondestructive evaluation (NDE) of high-density polyethylene (HDPE) butt fusion joints. This work was begun in response to requests from commercial nuclear licensees to employ HDPE materials in nuclear power plant systems. HDPE has been widely used in low-pressure, low-temperature applications such as natural gas lines, water, sewer, and petrochemical applications. There are a number of issues related to its use at the higher temperatures that would be encountered in nuclear applications.

Materials issues associated with the use of HDPE at higher temperatures are being investigated under a separate contract. The work described in this report is being conducted by the NRC at PNNL to assess whether a volumetric inspection method can be applied to the fusion joint that may reliably detect lack-of-fusion (LOF) conditions. Temperatures at or exceeding the design temperature may result in the failure of piping due to LOF.

Twenty-four HDPE pipe specimens were butt fused in 3408 material to contain LOF conditions that could be used to assess the effectiveness of NDE methods applied. (It should be noted that 4710 became the material of choice after this study was initiated [in large part to address some of the issues associated with the higher temperature application]. The NRC plans to assess 4710 material.) A range of NDE measurements were performed using ultrasonic and electromagnetic methods. Destructive evaluations were conducted using several different methods, but eventually were focused on a side-bend test procedure. All of the NDE results and destructive test results have been analyzed and documented in this report.

PAPERWORK REDUCTION ACT STATEMENT

This NUREG does not contain information collection requirements and, therefore, is not subject to the requirements of the Paperwork Reduction Act of 1995 (44 U.S.C. 3501 et seq.).

PUBLIC PROTECTION NOTIFICATION

The NRC may not conduct or sponsor, and a person is not required to respond to, a request for information or an information collection requirement unless the requesting document displays a currently valid OMB control number.

FOREWORD

The American Society of Mechanical Engineers (ASME) is developing provisions to address the use of high-density polyethylene (HDPE) in nuclear power plant buried piping systems. The initial provisions were published as Code Case N-755 (Revision 0), "Use of Polyethylene (PE) Plastic Pipe Section III, Division I and Section XI." The purpose of the Code Case is to provide ASME-approved requirements to address the construction of ASME Class 3 buried piping systems and the repair or replacement of PE as a Section XI activity. ASME relied on existing American Society for Testing and Materials (ASTM) specifications, Plastic Pipe Institute (PPI) technical reports, and polyethylene industry experience to develop Code Case N-755.

By letter dated October 26, 2006, Duke Power Company submitted a request to use many of the provisions of the Code Case to manage the replacement of portions of Class 3 steel service water system piping with HDPE piping at Catawba Nuclear Station, Units 1 and 2 (U.S. Nuclear Regulatory Commission's (NRC's) Agencywide Documents Access and Management System [ADAMS] Accession No. ML063120215). By letter dated August 30, 2007, Union Electric Company submitted a similar request to use HDPE at Callaway Plant Unit 1 (ADAMS Accession No. ML072550488).

The licensee requests were approved with conditions placed on fabrication processes, nondestructive evaluation (NDE) examinations, and the associated qualifications of procedures, equipment, and personnel. The safety evaluations by NRC's Office of Nuclear Reactor Regulation conditionally approving the requests are available in ADAMS under Accession Nos. ML082240386 (Catawba) and ML082640007 (Callaway).

PE piping has been used extensively in natural gas lines, water, sewer, and petrochemical applications for over 50 years. Nuclear application is different from these applications in that service temperatures and piping thickness and diameter can be much greater. Based on the information that has been made available to support the use of HDPE in nuclear applications, the service temperature could equal or exceed the operating design temperature of HDPE.

The consideration of temperature and pipe size raises questions with regard to butt fusion joint integrity, slow crack growth resistance of thick-section pipe, and long-term service life. In addition, questions exist regarding the ability of current NDE methods to adequately examine HDPE joints. HDPE has been installed in the service water system at Sizewell B in the United Kingdom. However, due to the concerns discussed above, Sizewell B limited the service temperature to well below the operating design temperature.

Currently, the industry is conducting research on these issues and NRC is conducting confirmatory research at PNNL. The research described in this report provides the initial assessment from the confirmatory NDE-related research. The research is ongoing, and additional results will be provided in future reports.

As discussed in this report, it has been shown that a combination of NDE methods may be required in order to detect flaws in butt fusion joints. NRC and PNNL staff have been in contact with national and international researchers who are investigating the NDE of HDPE. While the

goal of these efforts is to improve current methods or develop new methods that are successful, there is no guarantee that the efforts will prove to be fully satisfactory. Accordingly, the best way to eliminate the potential for poor joints being placed in-service may be to gain a better understanding of the essential fabrication variables and their effect on joint integrity, and what constitutes a satisfactory joint (e.g., degree of cross polymer linking). Several national and international researchers have recently initiated programs investigating fabrication equipment and methods. The results of these investigations will be reviewed with respect to the outcomes of the NDE-related research.

CONTENTS

ABSTRACT iii
FOREWORD v
FIGURES ix
TABLES xii
EXECUTIVE SUMMARY xiii
ACKNOWLEDGMENTS xv
ACRONYMS AND ABBREVIATIONS xvii
1 BACKGROUND 1-1
2 HDPE TEST SAMPLES 2-1
2.1 Material Properties of HDPE 2-1
2.1.1 General Properties of HDPE 2-1
2.1.2 Measured Properties of 3408 and 4710 HDPE Specimens at PNNL 2-2
2.1.3 Measured Properties of Low Carbon 4710 HDPE 2-3
2.1.4 Measured Properties of Callaway 4 Inch Thick 4710 HDPE 2-4
2.2 Ultrasonic Transducer Wedge Materials 2-4
2.3 Fused Pipes 2-4
3 NDE METHODS STUDIED IN THIS ASSESSMENT 3-1
3.1 Visual Testing 3-1
3.1.1 Weld Bead Profile 3-1
3.1.2 Inspection of the Fusion Zone 3-4
3.2 Millimeter Wave 3-4
3.2.1 Ku-Band Cylindrical Tests of HDPE Pipe Samples 3-4
3.2.2 U-Band Cylindrical Tests of HDPE Pipe Samples 3-5
3.3 Ultrasonic Time-of-Flight Diffraction 3-6
3.3.1 Fluor/NDT Innovations, Inc. TOFD 3-7
3.3.2 PNNL TOFD 3-8
3.4 Ultrasonic Phased Array 3-13
3.4.1 4 MHz PA Probe 3-13
3.4.2 1.5 MHz PA Probe 3-15
3.5 Microwave 3-19
4 DESTRUCTIVE TEST RESULTS 4-1
4.1 Slicing 4-1
4.1.1 Fusion Joint Evaluation 4-3
4.1.2 Base Material Evaluation 4-7

4.2 Mechanical Testing 4-7
4.2.1 High Speed Tensile Test 4-7
4.2.2 Guided Bend Test 4-15
4.2.3 Side-Bend Test 4-16
5 DISCUSSION OF NDE AND DE RESULTS 5-1
6 SUMMARY AND CONCLUSIONS 6-1
7 REFERENCES 7-1
APPENDIX A – TOFD INSPECTION RESULTS ON 24 FUSION JOINTS IN 3408 HDPE PIPE AS DETERMINED BY FLUOR/NDT INNOVATIONS, INC. A-1
APPENDIX B – TOFD INSPECTION RESULTS ON 24 FUSION JOINTS IN 3408 HDPE PIPE AS ACQUIRED BY FLUOR/NDT INNOVATIONS, INC. B-1
APPENDIX C – PNNL TOFD INSPECTION RESULTS ON 12 FUSION JOINTS IN 3408 HDPE C-1
APPENDIX D – PNNL PA INSPECTION RESULTS ON 12 FUSION JOINTS IN 3408 HDPE D-1
APPENDIX E – SUMMARY PLOTS OF NDE RESULTS IN SPECIMENS NOT SUBJECTED TO DE E-1

FIGURES

2.1 Several of the Butt Welded 3408 Pipes are shown with 12-in. Scales on the Center Pipe, One in the Horizontal Direction and One in the Vertical 2-5

3.1 Butt Fusion Bead Dimensional Guideline (ASTM F2620-06) 3-1

3.2 Weld Bead Profiles Taken Left to Right from a Pipe Fused at Conditions 1–6 3-2

3.3 Bead Width-to-Height Ratio Comparison for the 24 Fused Pipes.....3-2

3.4 Pipes 121–1212: Fusion Pressure During the Heat Cycle 3-3

3.5 Pipes 1213–1224: No Fusion Pressure During the Heat Cycle.....3-3

3.6 Fusion Zone Anomalies.....3-4

3.7 Ku-Band mm-Wave Laboratory System Setup 3-5

3.8 Typical U-Band Image Slice at the ID Surface.....3-6

3.9 Schematic of the TOFD Signals Received from an Embedded Flaw 3-7

3.10 TOFD Image Showing the OD and ID Surface Signals and a Flawed Area 3-8

3.11 Area Identified as Incomplete Fusion.....3-9

3.12 Possible Flaw Indications in One of the “Good” Pipes 3-9

3.13 TOFD Probe Assembly.....3-10

3.14 PNNL TOFD Results from Four ID-Connected Sawcuts.....3-11

3.15 TOFD Data Acquired on Pipe 125, First and Second Quadrants, by PNNL in the Top and by Fluor/NDT Innovations, Inc. in the Bottom.....3-12

3.16 TOFD Data Acquired on Pipe 125, Third and Fourth Quadrants, by PNNL in the Top and by Fluor/NDT Innovations, Inc. in the Bottom.....3-12

3.17 Phase Array Beam Modeling Results at 40 Degrees on the Left and 60 Degrees on the Right.....3-13

3.18 Manual Phased Array Probe Assembly in Position to Inspect a Fusion Joint.....3-14

3.19 Phased Array Results on HDPE Pipe 125, Quadrant 4 Showing a Possible Lack of Fusion in the Noted Flaw Area 3-15

3.20 Gel Wedge in an Aluminum Frame for the 1.5-MHz PA Probe 3-16

3.21 Beam Simulations for the 1.5-MHz PA Probe at 35, 45, 55, and 65 Degrees.....3-17

3.22 Pipe Joint 127 Quadrant 1 from the Stamped Side Showing Flaw Indications 3-18

3.23 Pipe Joint 1220 Quadrant 4 from the Unstamped Side Showing a Flaw Indication with Diffraction Pattern 3-18

3.24 Pipe Joint 1223 Quadrant 1 from the Unstamped Side Showing No Flaw Indications in the Sample Made Using the Optimal Fabrication Procedure 3-19

3.25 4-in. Pipe Standard.....3-20

3.26 Image of Parent Material on Pipe 123 3-20

3.27 Microwave Results for Pipe Joint 123 Showing Possible LOF in Areas 1 and 2 with an Inclusion at 15 in. 3-20

3.28 Microwave Results for Pipe Joint 127 Showing LOF in Area 1, Pinholes at 15, 21, 22.5, and 24.2 in., and a Possible Inclusion at 12 in. and Area 4 3-21
3.29 Microwave Results for Pipe Joint 1212 Showing Large Areas with LOF 3-21
3.30 Microwave Results for Pipe Joint 1214 Showing Cold Fusion in Area 1 and LOF in Area 2 3-21
3.31 Microwave Results for Pipe Joint 1218 Showing LOF or Cold Fusion in Area 1 and 2 with General LOF in Area 3 3-21
3.32 Microwave Results for Pipe Joint 1223 Showing Cold Fusion.....3-22
3.33 Evisive Microwave Results on Two Pipe Joints After ID Beam Removal 3-22
4.1 Cold Fusion and Good Joint in PE Material 4-1
4.2 Rotary Manual Microtome Used to Slice HDPE Pipe Sections. 4-2
4.3 Setup for Photographing the Bulk Specimen 4-2
4.4 A Slice from HDPE Pipe 125, Quadrant 4 at Approximately 8.6 Inches 4-3
4.5 Surface of HDPE Pipe 125, Quadrant 4 at Approximately 8.6 Inches 4-4
4.6 PNNL TOFD, Fluor/NDT Innovations, Inc. TOFD, and PNNL PA Data from the Fourth Quadrant of Pipe 125 4-5
4.7 Slice from HDPE Pipe 1224, Quadrant 4 at Approximately 3.4 Inches 4-5
4.8 Surface of HDPE Pipe 1224, Quadrant 4 at Approximately 3.4 Inches 4-6
4.9 Ultrasonic Responses from Quadrant 4 of Pipe 1224 Show No Flaw Indications 4-6
4.10 Base Material Slices from 3408 on the Left and 4710 on the Right Show Swirls from Non-uniform Mixing 4-7
4.11 Areas Marked for Tensile Testing as Shown by the Lower Arrows in the NDE Images for Pipe 126, Quadrant 4.....4-8
4.12 Areas Marked for Tensile Testing as Shown by the Lower Arrows in the NDE Images for Pipe 1215, Quadrant 4.....4-9
4.13 Area Marked for Tensile Testing as Shown by the Lower Arrows in the NDE Images for Pipe 1224, Quadrant 2. 4-10
4.14 Coupon 1 from Pipe 1215 Quadrant 4 with a Long Open/Close Time of 20 sec Showing a Ductile Failure Outside of the Joint 4-12
4.15 Coupon 2 from Pipe 1215 Quadrant 4 with a Long Open/Close Time of 20 sec Showing a Ductile Failure at or Near the Joint.....4-13
4.16 Coupon 3 from Pipe 126 Quadrant 4, Fused with Fusion Pressure During the Heat Cycle and a 20-sec Open/Close Time.....4-13
4.17 Coupon 4 from Pipe 126 Quadrant 4, Fused with Fusion Pressure During the Heat Cycle and a 20-sec Open/Close Time.....4-14
4.18 Coupon 5 from Pipe 1224 Quadrant 2, Fused with Procedure F2620 and Expected to be Good.....4-14
4.19 Coupon 6 Base Material Shows a Ductile Failure 4-15

4.20 Failure Energy Show a Quantitative Measure of Failure Among the Six Coupons 4-15
4.21 Side-Bend Test Apparatus with an HDPE Test Specimen from Pipe 1224 Undergoing Testing – Example of a Dark Green SBT Result 4-17
4.22 Another HDPE Specimen Undergoing Side-Bend Testing Showing the Dial Indicator Used to Track Travel of the Ram Which, in This Case, is Showing the Maximum Travel of 2.5 Inches as Shown by the Upper Right and Lower Left Dials 4-18
4.23 Specimen from Pipe 126 Part Way Through the Side-Bend Test Showing the Early Stages of Failure 4-19
4.24 The Specimen from Pipe 126 at the End of the SBT – Example of a Red SBT Result 4-19
4.25 Sample from Pipe 1224 Failed the SBT and Was Removed Adjacent to the Specimen Shown in 4.21, Which Did Not Fail – Example of a Red SBT Result 4-20
4.26 Example Where Only One Ligament Remained at Location +12 on Pipe 1224 – Example of a Yellow SBT Result 4-22
4.27 SBT Results for Pipe 1224 4-23
4.28 Largest Base Material Flaw Found in the 22 Base Material Samples Tested for Pipe 1224 4-24
4.29 SBT Results for Pipe 123 4-24
4.30 SBT Results for Pipe 1212 4-25
4.31 SBT Results for Pipe 1214 4-25
4.32 SBT Results for Pipe 1218 4-26
4.33 SBT Results for Pipe 1223 4-26
5.1 DE Results as Determined from the SBT Results Do Not Correlate with Any of the NDE Results 5-2
5.2 Evisive is the Only NDE Technique that Correlates with the SBT Light Green DE Results Although It has Many False Calls 5-3
5.3 SBT Yellow Region was Detected with the NDE PA-SI, PA-PNNL, TOFD-PNNL, and TOFD-Flour. 5-4
5.4 SBT Yellow Region was Detected by NDE Evisive in Part, PA-PNNL, and TOFD-PNNL 5-5
5.5 SBT Red Region was Detected with PA PNNL, TOFD PNNL, and TOFD Fluor 5-6
5.6 SBT Red Region was Detected in Part by Evisive and by PA PNNL, TOFD PNNL, and TOFD Fluor 5-7
5.7 Most of This Specimen Showed Some Type of Failure in the SBT 5-8
5.8 SBT Failure Regions were Only Detected with NDE TOFD-Fluor; However, There were False Call Regions as Well 5-9

5.9 SBT Failure Regions Covered Most of This Quadrant and were Partially Detected with Evisive NDE 5-10
5.10 SBT Failure Regions Covered Most of This Quadrant and were Partially Detected with Evisive and TOFD Fluor NDE....5-11
5.11 SBT Failure Regions Covered Most of This Quadrant and were Well Detected with Evisive NDE 5-12
5.12 Majority of This Quadrant Failed in the SBT to Some Extent 5-13
5.13 Approximately Half of the Quadrant Showed Signs of Failure in the SBT in the Yellow or Light Green Range....5-14
5.14 SBT Red Failure Regions were Partially Detected with Evisive NDE and a Very Small Region with PA SI NDE 5-15
5.15 SBT Failure Regions were Not Detected by Any of the NDE Techniques 5-16
5.16 Quadrant Showed SBT Failures Over Most of the Quadrant 5-17
5.17 Several Flawed Regions were Noted with the SBT DE Results. 5-18

TABLES

2.1 HDPE Pipe Characteristics, 2.25-MHz, 0.375-inch Diameter Transducer, Longitudinal Wave 2-3
2.2 Wedge Material Properties 2-5
2.3 HDPE 3408 Pipe Fusion Conditions to Produce Lack of Fusion 2-5
4.1 High-Speed Tensile Test Results From 5 HDPE Fusion Joints and 3 Base Material Coupons 4-11
4.2 SBT Results on Pipe 127....4-21

EXECUTIVE SUMMARY

The U.S. Nuclear Regulatory Commission (NRC) has a multi-year program at the Pacific Northwest National Laboratory (PNNL) to provide engineering studies and assessments of issues related to the use of nondestructive examination (NDE) methods for the reliable inspection of nuclear power plant components. As part of this program, a task was initiated to assess issues related to the NDE of high-density polyethylene (HDPE) butt fusion joints. This work was begun in response to requests from commercial nuclear licensees to employ HDPE materials in nuclear power plant systems. HDPE has been widely used in low-pressure, low-temperature applications such as natural gas lines, water, sewer, and petrochemical applications. There are a number of issues related to its use at the higher temperatures that would be encountered in nuclear applications.

The industry is pursuing American Society of Mechanical Engineers (ASME) Code Case N-755 entitled, *Use of Polyethylene (PE) Plastic Pipe for Section III, Division 1, Construction and Section XI Repair/Replacement Activities,* and contains the requirements for nuclear power plant applications of HDPE. This Code Case requires that inspections be performed after the fusion joint is made by visually examining the extruded material bead that is formed and conducting a pressure test of the joint. These tests are generally only effective if gross through-wall flaws exist in the fusion joint. The NRC is interested in determining whether a volumetric inspection method can be applied to the fusion joint that may reliably detect lack-of-fusion (LOF) conditions. The NRC requested PNNL to conduct the work described in this report to assist in resolving this issue.

Twenty-four HDPE pipe specimens were butt fused in 3408 material to contain LOF conditions that could be used to assess the effectiveness of NDE methods applied. Basic ultrasonic material properties were measured and used to guide the use of phased array (PA) and time-of-flight diffraction (TOFD) work that was conducted. An electromagnetic millimeter (mm) wave technique was also used to inspect several assemblies. Fluor and NDE Innovations, Inc., two companies that routinely conduct HDPE examinations for industries other than nuclear, used their commercially available TOFD equipment on all 24 specimens. These NDE inspection results were reviewed, which led to several of the specimens being selected for destructive evaluation using a microtome to extract slices of small portions of parent and fusion joint material. Additionally, five joint zones with and without ultrasonic flaw indications were subjected to a high-speed tensile test. The results did not provide a high degree of correlation between the ductile/brittle failure mode and the ultrasonic findings. A second phase of testing was pursued in which 12 joints were evaluated at PNNL with TOFD and PA ultrasonic technologies. Six of these joints were evaluated by the company Evisive with their microwave technology. Structural Integrity, Inc., also inspected several of these joints using their phased array technology. Destructive evaluations were conducted using several different methods, but eventually were focused on a side-bend test (SBT) procedure. All of the NDE results and destructive test results have been analyzed and documented in this report.

Additional investigation is required in order to draw significant conclusions from this study. The SBT results were graded based on the extent of breakage and it has not yet been established as to which of these conditions would constitute failure versus passing the SBT. For some LOF

conditions, there were a number of NDE techniques that produced a response that was interpreted to be from a flaw condition. In other cases, virtually none of the NDE methods were able to obtain a response. Most of the NDE methods tended to produce false calls. The fusion bead width-to-height ratio rejected all of the fusion joints that were made when pressure was applied during the heat cycle and the SBT results for these joints included the full range of breakage conditions. The applied NDE methods detected some material anomalies but only qualitative conclusions can be drawn. In order to detect most of the conditions included in this study, a combination of NDE methods was needed. Clearly, further investigation is needed to refine this study and resolve the issues identified.

ACKNOWLEDGMENTS

The reported work was sponsored by the U.S. Nuclear Regulatory Commission (NRC) under job code N6398. Wallace Norris was the NRC manager of this work and provided valuable guidance and technical direction. The Pacific Northwest National Laboratory (PNNL) acknowledges Mr. Norris for his contributions.

The authors express their gratitude to Bill Adams at WL Plastics Corporation, James Craig at McElroy Manufacturing, Inc., and Gordon Forster at Ameren UE Callaway Plant for supplying materials.

PNNL thanks Raul Leon at NDT Innovations, Inc., Clayton Smith at Fluor Nuclear Power, Robert Stakenborghs at Evisive, Dave Zimmerman at Duke-Energy, and Caleb Frederick formerly at Structural Integrity for conducting nondestructive evaluations.

The authors also thank James Craig for conducting high-speed tensile tests on several specimens. Lastly, the authors are grateful to Robert Coma at Bartels and Stout, Inc. for the loan of a Lecia microtome for slicing through a fusion zone.

The authors would also like to thank the members of the ASME Code Special Working Group on HDPE for many fruitful discussions, insights, and suggestions as this work progressed. Dudley Burwell of ISCO Industries provided the procedure and related experience in applying the side-bend test.

At PNNL the authors thank Kay Hass for preparing the manuscript and her attention to detail. PNNL is operated by Battelle for the U.S. Department of Energy under Contract DE-AC05-76RL01830.

ACRONYMS AND ABBREVIATIONS

A	axial
ASME	American Society of Mechanical Engineers
ASTM	American Society for Testing and Materials
DE	destructive evaluation
DIPS	ductile iron pipe size
DR	dimension ratio (pipe's average outside diameter divided by the minimum wall thickness)
Emc^2	Engineering Mechanics Corporation of Columbus
FMCW	frequency modulated continuous wave
HDPE	high density polyethylene
GBT	guided bend test
ID	inner diameter
IPS	iron pipe size
ISO	International Organization for Standards
LOF	lack of fusion
mm	millimeter
MWD	molecular weight distribution
NDE	nondestructive examination
NRC	Nuclear Regulatory Commission
OD	outer diameter
PA	phased array
PE	polyethylene
PENT	Pennsylvania Notch Test
PNNL	Pacific Northwest National Laboratory
PPI	Plastic Pipe Institute
PT	liquid penetrant testing
R	radial
SBT	side bend test
SCG	slow crack growth
SNR	signal-to-noise ratio
SWG	Special Working Group
TLR	technical letter report
TRL	transmit receive longitudinal
TOFD	time-of-flight diffraction
UT	ultrasonic testing
VT	visual testing

1 BACKGROUND

The U.S. Nuclear Regulatory Commission (NRC) has a multi-year program at the Pacific Northwest National Laboratory (PNNL) to provide engineering studies and assessments of issues related to the use of nondestructive examination (NDE) methods for the reliable inspection of nuclear power plant components. As part of this program, subtask 2D under project JCN-N6398 was set up to assess a range of issues related to the performance of NDE on butt fusion joints in high-density polyethylene (HDPE) piping. This work was initiated in response to requests from commercial nuclear power licensees to employ HDPE materials in certain plant systems. HDPE has been widely used in low-pressure, low-temperature applications such as natural gas lines, water, sewer, and petrochemical applications. There are a number of issues related to its use at the higher temperatures that would be encountered in nuclear applications.

PNNL conducted initial work under a previous project, JCN-Y6604, with two primary activities being pursued. The first of these activities was to enlist Dr. Prabhat Krishnaswamy of Engineering Mechanics Corporation of Columbus (Emc^2) to conduct a thorough literature review relative to background and history of HDPE along with its applications (including its very limited nuclear application). A technical letter report (TLR) entitled *Review of Literature on the Use of Polyethylene (PE) Piping in Nuclear Power Plant Safety-Related Class 3 Service Water Systems*, dated October 27, 2006, was produced, describing the scope of the effort and findings. PNNL also provided limited input to the TLR regarding NDE studies that had been conducted and reported in the open literature for inspecting HDPE fusion joints.

The second primary activity was a literature review of published results on the effectiveness and reliability of NDE methods to detect flaws in PE pipe joints. A letter report was submitted to the NRC on December 1, 2006. The significant aspect about this second TLR was that it clarified the direction of research that was needed in order to try to fill in the gaps identified by the literature reviews. The current report is an update on the work that PNNL has been conducting to initially assess NDE methods and quantification of their effectiveness for the inspection of HDPE butt fusion joints.

The objective of the research at PNNL is to confirm certain analyses performed by the industry in support of the use of HDPE in nuclear applications and assess the capabilities and effectiveness of NDE. American Society of Mechanical Engineers (ASME) Code Case N-755 was developed to provide a basis and requirements for nuclear power plant applications of HDPE. It was reported that Callaway installed nearly 40,000 feet (12,192 m) of HDPE, using provisions of the Code Case. This Code Case requires that inspections be performed after the fusion joint is made by visually examining the bead that is formed and conducting a pressure test of the joint. These tests are only effective, in general, if gross through-wall flaws exist in the fusion joint. The NRC is interested in determining whether a volumetric inspection can be conducted that will reliably detect lack-of-fusion (LOF) conditions that may be produced during joint fusing. The NRC requested PNNL to conduct the work described in this report to assist in resolving this issue.

This report presents the current status of an initial assessment of NDE effectiveness that PNNL has been conducting. Section 2 covers the material properties and discusses the fusion joints that PNNL had manufactured for the studies. Section 3 addresses the NDE methods that were evaluated in the initial assessment of NDE effectiveness to detect lack-of-fusion conditions, and describes areas sectioned for mechanical testing from both flawed regions and non-flawed regions, as reported by the NDE applied. Section 4 then presents destructive examination (DE) results for some of the test samples that were used in these studies, and Section 5 provides an integration of NDE and DE results along with a discussion of these results. Finally, Section 6 contains a summary and conclusions, and Section 7 provides a list of references used when developing this document.

2 HDPE TEST SAMPLES

2.1 Material Properties of HDPE

2.1.1 General Properties of HDPE

Polyethylene is thermoplastic, meaning that it can be re-melted to shape, reform, or recycle, the material. It was invented in 1933 and at that time could only be formed under high pressures. In the 1950s, a low-pressure technique made it safer and more economical to produce. Polyethylene resins are characterized by their density, molecular weight, and molecular weight distribution (PPI 2006). These three characteristics in turn determine the material behavior and are discussed below.

The density of the material is determined by the amount of side branching (from the bonding of short polymer chains to the main long polymer chains). The more branching, the more material density will be reduced. Density or packing is also viewed in terms of the presence of a crystalline structure, which is tightly packed and ordered, or the absence of such a structure, which is an amorphous state. Polyethylene has both crystal and amorphous regions, and thus is called a semi-crystalline material. Resin density influences the physical properties of the material such as tensile yield strength and stiffness; both are directly proportional to density.

The molecular weight of polyethylene is an average value of all atomic weights of the atoms making up the molecule. This property directly influences the durability of the material. Long-term strength, toughness, ductility, and fatigue-endurance improve with increasing molecular weight. The molecular weight also affects the ability of the material to flow in the molten state, characterized by the melt index or melt flow rate. The melt index is inversely related to the molecular weight.

The molecular weight distribution (MWD) is generally Gaussian-, or bell-, shaped. A narrow distribution indicates a material with similar molecular weights. Such a material will crystallize at a faster and more uniform rate and will lead to less distortion during solidification. A broad distribution due to a wider range of chain lengths in the material is desirable for environmental stress crack resistance, impact resistance, and processing. More recently materials with bimodal distributions have been formed by blending two different polymer populations to give both good physical properties and favorable processing characteristics.

The American Society for Testing and Materials (ASTM) specification *Standard Specification for Polyethylene Plastics Pipe and Fittings Materials* (ASTM D3350-06) documents the identification of polyethylene materials according to a cell classification system. Based on this standard, the density, melt index, flexural modulus, tensile strength at yield, slow crack growth (SCG) resistance, and hydrostatic strength are classified. The test method for determining SCG resistance is known as the Pennsylvania Notch Test (PENT); this method is documented in *Standard Test Method for Notch Tensile Test to Measure the Resistance to Slow Crack Growth of Polyethylene Pipes and Resins* (ASTM F1473-07). University of Pennsylvania researchers found that one hour of PENT approximated 13 years of service life (Performance Pipe 2007). In referencing a pipe material, the naming starts with PE for polyethylene, followed by 4 numbers.

The first number designates the density and the second the SCG resistance. The last two digits indicate the hydrostatic design stress divided by 100. Materials involved in the PNNL study thus far have been PE3408 and PE4710. According to the classification system, the PE3408 material has a density in the cell class 3, 0.941–0.947 gm/cm^3, an SCG cell class 4, PENT value greater than 10 hours, and an 800-psi hydrostatic design stress for water at 73 degrees Fahrenheit. PE3408 is unimodal HDPE; that is, resin produced using one catalyst in one reactor. Similarly, the PE4710 material has a density in the cell class 4, 0.948–0.955 gm/cm^3, SCG cell class 7, PENT value greater than 500 hours, and a hydrostatic design stress of 1000 psi. PE4710 is a bimodal resin; that is, the combination of two polymers—a high molecular weight polymer and a low molecular weight. Bimodal resins provide improved performance and longer service life.

PE pipe is additionally classified based on outside diameter (OD) as specified in ASTM specification *Standard Specification for Polyethylene (PE) Plastic Pipe (SDR-PR) Based on Outside Diameter* (ASTM F714-06a). Three standard outside-diameter pipe sizing systems are discussed. These systems are the International Organization for Standards (ISO) metric system, the Iron Pipe System (IPS), and the Ductile Iron Pipe System (DIPS). A relationship between the pipe stress, pressure, pipe size, and wall thickness is given. The dimension ratio (DR) of a pipe is defined as the pipe's average OD divided by the minimum wall thickness. This DR is inversely related to the design internal pipe pressure. Tables of pipes listed by DR values are available and show pressure ratings for DR values and PE material types; that is, for 3408 or 4710.

2.1.2 Measured Properties of 3408 and 4710 HDPE Specimens at PNNL

HDPE pipe material obtained for evaluation at PNNL included a series of 24 assemblies of 3408 butt-fusion joints and two pipe sections of 4710 material, one with a yellow stripe. Pipes are color-coded for use by the American Public Work Association standard and yellow indicates a gas, oil, and steam-type of application. All pipe material was 12-in. (30.5-cm) IPS DR11. The 4710 black pipe material was made on October 8, 2007, and the 3408 material was made on April 7, 2005, as noted from the print line information on the pipe. Some fundamental acoustic material properties of the HDPE were thought to be needed to understand how to inspect these materials with ultrasound. To make these measurements, rectangular sections of material were cut from the base material in each of the three types of pipe. Smooth and parallel sides were machined on the three pairs of faces. From such a test piece, the acoustic velocity and attenuation were measured in the through-wall direction of the pipe (inner diameter, ID), from the radial (R), or circumferential direction, and from the axial (A) direction of the pipe. The results are shown in Table 2.1. Velocities from face-to-face within a material type vary only by 1% and velocities are comparable from material-to-material with, at most, a 2% change. Attenuation is also comparable from material to material. Face-to-face variation in attenuation for the 3408 material is starting to be noticeable at 3 dB. The 2 dB change in the 4710 materials is within experimental error.

Table 2.1 HDPE Pipe Characteristics, 2.25-MHz, 0.375-inch (0.95-cm) Diameter Transducer, Longitudinal Wave

	Velocity (in./µsec) [mm/µsec]			Attenuation (dB/in.) [dB/cm]		
Pipe Material	3408	4710	4710 Yellow Stripe	3408	4710	4710 Yellow Stripe
Face[(a)]						
ID	0.089 [2.26]	0.091 [2.31]	0.091 [2.31]	11 [4.3]	10 [3.9]	10 [3.9]
R	0.090 [2.29]	0.090 [2.29]	0.092 [2.34]	8 [3.2]	8 [3.2]	8 [3.2]
A	0.090 [2.29]	0.091 [2.31]	0.091 [2.31]	8 [3.2]	9 [3.5]	8 [3.2]

(a) ID face – pipe thickness; R face – radial (circumferential) direction; A face – axial direction.

Additionally, in the 3408 cube, the frequency response evaluation showed that approximately 1.3–1.8 MHz was returned through 2 in. (5.08 cm) of material (round trip path) from a 2.25-MHz transducer. At 5-MHz incident, the return was 2.2 MHz, and at 10 MHz, the return was 3.5 MHz showing the loss of the main excitation frequency of the probe. Attenuation was also less at 1 MHz with the ID face value measured at 6 dB/in. (2.4 dB/cm), and at 5 dB/in. (2.0 dB/cm) for the A and R faces. A shear wave velocity in the 3408 material was measured at 0.035 in./µsec (0.889 mm/µsec) in the through-wall direction (from the ID face). Only one echo was detected so the attenuation was not measured, but it is assumed to be significant.

2.1.3 Measured Properties of Low Carbon 4710 HDPE

A concern was raised that ultrasonic evaluations of fusion joints and base materials in HDPE pipes were merely detecting variations in the carbon content of the material rather than defects in the fusion joints. To address this concern, a run of 4710 pipe was made by William Adams at WL Plastics Corp. in which the carbon input was shut off. One hundred feet of this pipe was shipped to PNNL. As the run progressed and carbon was bleeding out of the crevices in the pipe die, the carbon content decreased. The carbon content was measured at the beginning of the run and every 10 feet thereafter. The carbon was first measured at a normal 2.09%, followed by readings of 0.55%, 0.13%, 0.07%, and so on until the last two readings were measured at 0.01%. PNNL measured the acoustic velocity and attenuation from material taken at the beginning of the run and at the end of the run. Two independent sets of measurements were made on these blocks for attenuation and velocity from the OD/ID—the A and R faces. The average velocity measurements from face to block face, same carbon content, varied slightly (less than 1.7%). The average velocity variation from normal carbon block to low carbon block showed an increase in velocity of 2–3%. From this limited data set, one could say that the face-to-face velocities are the same and the low carbon material has at most a 3% higher velocity.

The density of each block was also measured to calculate acoustic impedances. It is primarily a change in acoustic impedance that is detected in the presence of a flaw. These samples showed only a 0.5% variation in density leading to a minimal 1.6–2.6% change in impedance.

Attenuation measurements showed a 1- or 2-dB/in. (0.4- or 0.8-dB/cm) higher attenuation on the ID/OD face as compared to the A or R face at the same carbon content. This is

insignificant. The variation from normal carbon to low carbon for a given face was only 1-dB/in. (0.4-dB/cm) change, with the low carbon sample having the lower attenuation. These results are basically indicating no change in attenuation due to the carbon content. As a result of these fundamental measurements, one can assume that carbon variations in the 2% range will not introduce reflectors in an ultrasonic image that would be confused with a flaw indication.

2.1.4 Measured Properties of Callaway 4 Inch Thick 4710 HDPE

Material from the Callaway Plant in Fulton, Missouri, became available through Gordon Forster, Ameren UE. PNNL received a half pipe section of this 4-in. (10.2-cm) thick material with an approximate 3-ft (91.4-cm) diameter. The material was made by WL Plastics with Dow Chemical DG2490/92 resin and is not commercially available. The pipe section has three joints fused with abnormal conditions. PNNL plans to inspect these joints but to date has only cut out a cube from one of the pipe ends for materials characterization. The ultrasonic velocity and attenuation were measured with a 1-MHz, 0.5-in. (1.27-cm) diameter transducer. Velocities over the three cube faces were nearly identical at 0.093–0.094 in./μsec (2.4 mm/μsec). However, attenuation was measured at 3-dB/in. (1.2 dB/cm), which is less than the 12-in. (30.5-cm) diameter DR11 samples. As previously stated, the joints are yet to be inspected, but having similar velocity, with lower attenuation, as compared to the other HDPE materials evaluated at PNNL, indicates inspection of this thicker material is quite possible.

2.2 Ultrasonic Transducer Wedge Materials

Various wedge materials were investigated for use in ultrasonic contact testing of the pipe. The measured velocity and attenuation values are listed in Table 2.2. Low-density PE was also considered and has a slower velocity than HDPE but its attenuation is large. The challenge is to find a material with a slower velocity to produce an ultrasonic beam over a range of angles as determined with Snell's Law, but also having low attenuation. For both time-of-flight diffraction (TOFD) and phased-array (PA) inspection, one would like to insonify the material at angles up to 60 degrees or greater. Dr. Mark Lozev, formerly at the Edison Welding Institute, uses either Rexolite or Plexiglas. Rexolite with its lower attenuation was chosen for the wedge material in the TOFD examinations at PNNL. Plexiglas was not considered because of its higher velocity. Later in Section 3.4.2, a novel gel wedge design that PNNL developed is discussed.

2.3 Fused Pipes

James Craig at McElroy was contracted to heat fuse a series of butt welds in 3408 pipe containing a variety of kissing bond–LOF conditions. This kissing bond or LOF is characterized by contact in the joint between the two compressed surfaces, but there are either no, or a reduction in the number of, molecular ties across the interface. This bond could also be defined as the perfect contact between two surfaces that transmit no shear stress so it is lacking in strength (Brotherhood et al. 2003). Six fusion conditions were selected with the parameters shown in Table 2.3. Four butt fusion joints of each condition were fabricated. The sixth condition is the ideal or control condition and is fused according to an ASTM F2620 Procedure (ASTM F2620-06). The other five conditions are expected to produce LOF in the pipe welds.

Several of the pipes are shown in Figure 2.1. Each butt fusion welded pipe section is approximately 2 ft (61 cm) long.

Table 2.2 Wedge Material Properties

Wedge Material	Velocity (in./μsec) [mm/μsec]	Attenuation (dB/in.) [dB/cm]
Rexolite	0.092 [2.34]	8 [3.2]
Teflon	0.051 [1.30]	21 [8.3]
Delrin	0.098 [2.49]	23 [9.1]
Wax	0.091 [2.31]	28 [11.0]
Indium	0.102 [2.59]	10 [3.9]
Plexiglas A	0.109 [2.76]	

Table 2.3 HDPE 3408 Pipe Fusion Conditions to Produce Lack of Fusion

Fusion Condition	Description
1	Fusion pressure during heat cycle
2	Fusion pressure during heat cycle plus 20 sec open/close
3	Fusion pressure during heat cycle plus 10 sec open/close
4	Long open/close time only (20 sec)
5	Grease in joint area – print line area after heating
6	Good joint fused with 75 psi interfacial pressure and 425°F heater surface temperature

Figure 2.1 Several of the Butt Welded 3408 Pipes are shown with 12-in. (30.5-cm) Scales on the Center Pipe, One in the Horizontal Direction and One in the Vertical. The pipe assemblies are approximately 2 ft (61 cm) long.

3 NDE METHODS STUDIED IN THIS ASSESSMENT

The NDE methods evaluated for fusion butt weld assessment were visual testing (VT), millimeter wave, ultrasonic testing (UT), and microwave. The fusion zone groove between the weld beads was examined visually and suspect areas were photographed. The bead width and height were also measured. A preliminary evaluation with millimeter wave imaging and microwave imaging was conducted. Most of the effort was directed towards evaluating the welds with ultrasonic TOFD and PA techniques. Preliminary results are presented below.

3.1 Visual Testing

3.1.1 Weld Bead Profile

According to ASTM standard F2620 on heat fusion joining of PE pipe, the weld bead should be rounded and uniform in size and shape on both sides and roll back to the pipe surface. The width of the beads should be approximately 2 to 2½ times the bead height. The v-groove between the beads should not be deeper than half the bead height (see Figure 3.1). PNNL did not measure the v-groove depth.

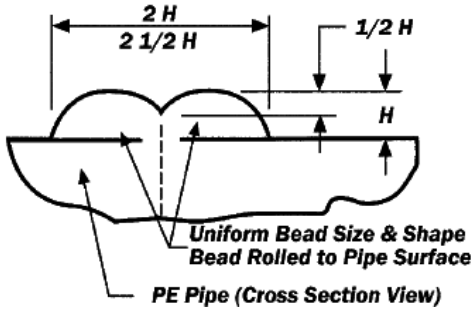

Figure 3.1 Butt Fusion Bead Dimensional Guideline (ASTM F2620-06). Reprinted, with permission, from *ASTM F2620-09 Standard Practice for Heat Fusion Joining of Polyethylene Pipe and Fittings*, copyright ASTM International, 100 Barr Harbor Drive, West Conshohocken, PA 19428.

The left and right weld bead widths, total width, and left and right bead heights were measured for the 24 fused pipes at 8 positions around the pipe or approximately every 45 degrees. Figure 3.2 shows, from left to right, two profiles taken from one pipe in each of the six fusion conditions. The top profile was taken at 0 degree, the print line of the pipe, and the lower profile at 135 degrees. Notice that the beads in conditions 1–3 are smaller than the beads fused with conditions 4–6. The average difference in left and right bead width and height was 0.62 and 0.34 mm (0.025 and 0.013 in.), respectively for fusion conditions 1–5. For the good fusion condition, number 6, the average difference in left and right bead width and height was 0.90 and 0.35 mm (0.035 and 0.014 in.) This shows a slightly larger difference in left and right bead width in the pipes fused under standard conditions. Bead height differences, left and right, are

similar in all pipe joints. The average bead width-to-height ratio, which should be in the 2 to 2½ range, was also calculated. Figure 3.3 shows the results for this calculation for each of the 24 pipes. The single plotted value for each pipe joint represents an average of the eight measurements taken circumstantially around the pipe at approximately 45-degree increments. Joints fused with fusion pressure during the heat cycle, conditions 1-3, were out of bounds in the width-to-height ratio and the beads were smaller in these joints as already mentioned. With fusion pressure during the heat cycle, the weld bead width was approximately 15 percent smaller and the bead height was 32 percent smaller than a bead with a normal heat cycle.

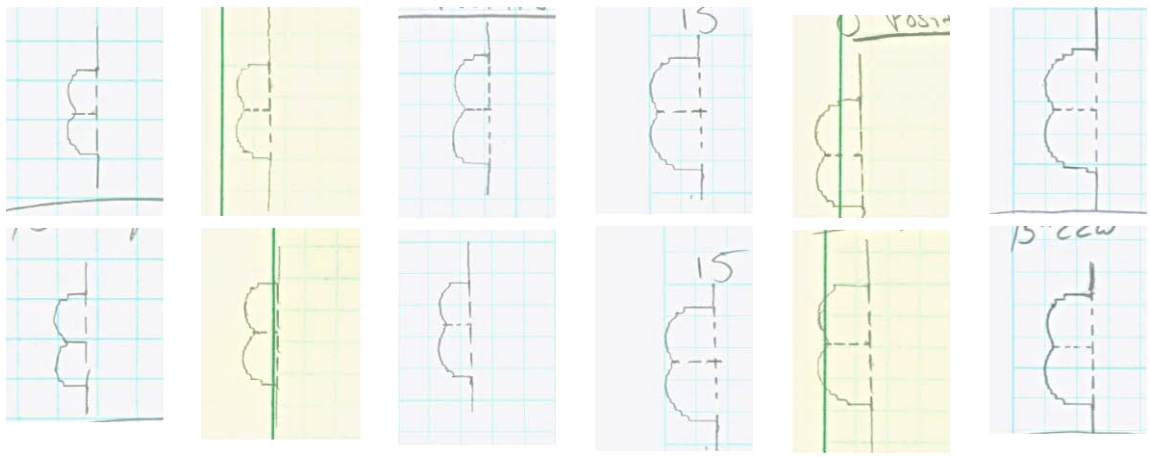

Figure 3.2 Weld Bead Profiles Taken Left to Right from a Pipe Fused at Conditions 1–6. The top profile was acquired at zero degrees and the bottom at 135 degrees. The grid spacing is 0.25 in. (0.64 cm).

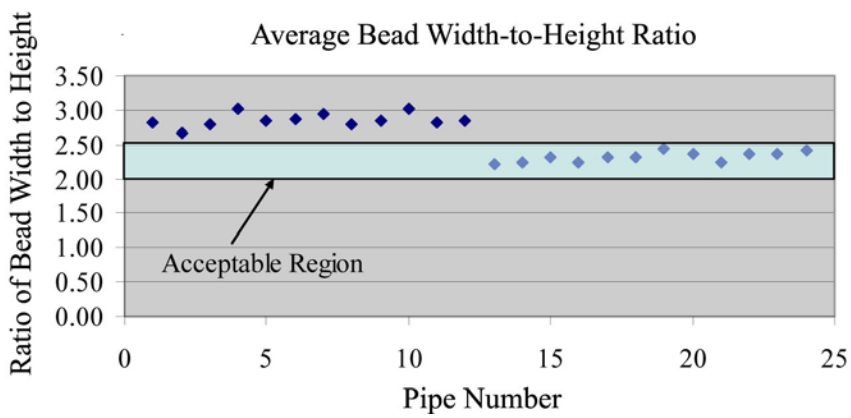

Figure 3.3 Bead Width-to-Height Ratio Comparison for the 24 Fused Pipes

Plots below show the ratio of OD bead width to height for each pipe at each of the eight circumferential locations where the measurements were acquired. Figure 3.4 contains data from pipes 121–1212, which were fused with fusion pressure applied during the heat cycle. All

but three data points lie above the 2.5 bead width-to-height ratio line. This criterion would reject all but these three positions, if the VT method was used as one of the inspection techniques. The points that fall in the acceptable range are from pipe 122, two points, and pipe 123. Figure 3.5 represents pipes 1213–1224, which were not fused with fusion pressure applied during the heat cycle. Furthermore the last four pipe joints, 1221–1224, represent joints fused with the acceptable F2620 procedure. All of the data presented are above the 2.0 ratio line; however, pipes 1219 and 1222 each have a point above the acceptable 2.5 bead width-to-height ratio.

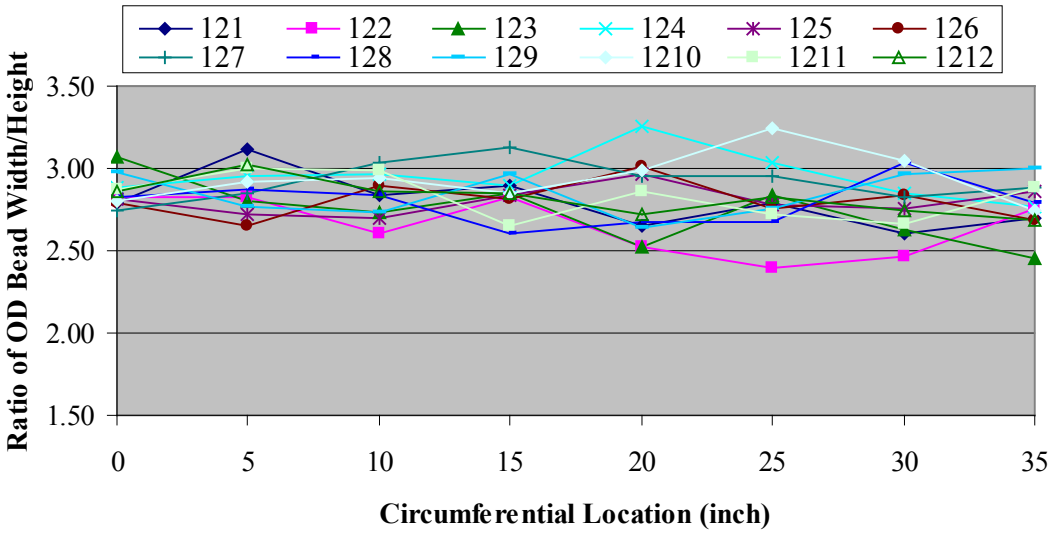

Figure 3.4 Pipes 121–1212: Fusion Pressure During the Heat Cycle

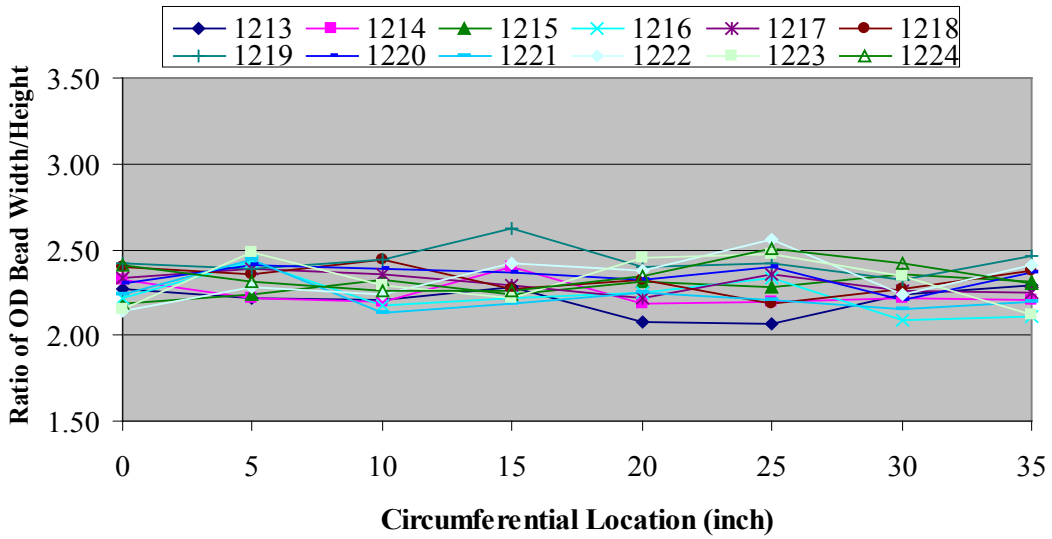

Figure 3.5 Pipes 1213–1224: No Fusion Pressure During the Heat Cycle

3.1.2 Inspection of the Fusion Zone

The weld bead fusion zone from the OD of each pipe was visually inspected and areas with anomalies were photographed. Typical anomalies were voids or dimples in the v-groove between the weld beads as shown in Figure 3.6. In general, there was little or no correlation between the VT results and the ultrasonic TOFD data from the Fluor/NDT Innovations, Inc. workshop, which is discussed later. As an example, one pipe contained many TOFD indications with 70 percent of the pipe fusion zone showing flaw signals. From the VT results, only four small defective areas were noted in the fusion joint from an OD inspection.

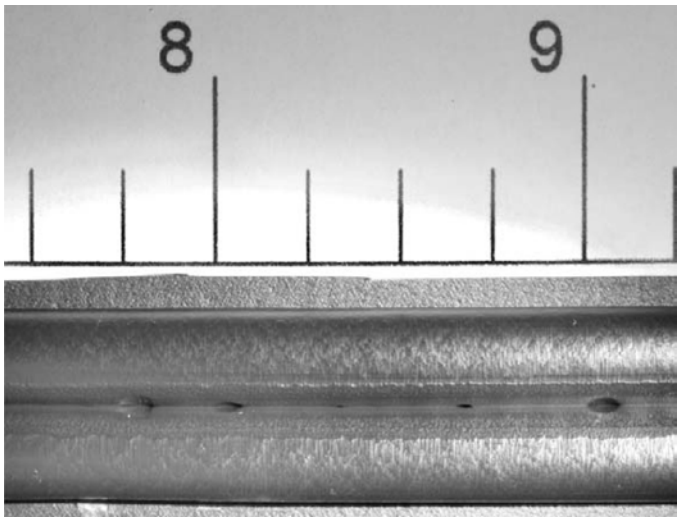

Figure 3.6 Fusion Zone Anomalies. The scale is in inches (1 in. = 2.54 cm).

3.2 Millimeter Wave

In November 2007, experiments were performed at PNNL to explore application of existing mm-Wave imaging technology at PNNL on HDPE pipe fusion joint inspection. The strategy was to implement PNNL's three-dimensional cylindrical imaging method that has been successfully deployed in other rapid inspection applications (Sheen et al. 1999; Sheen et al. 2000, 2006). To efficiently use resources and personnel, this initial effort was limited to using available transceivers and components in the mm-Wave laboratory. A scanner capable of performing cylindrical scans was available in the laboratory with two transceivers. The transceivers described in this test are Ku-band (10-20 GHz) and U-band (40–60 GHz). Both use yttrium-iron-garnet oscillators in a frequency-modulated continuous wave (FMCW) mode.

3.2.1 Ku-Band Cylindrical Tests of HDPE Pipe Samples

The initial part of this test implemented the lower frequency transceiver. The Ku-band illumination has a center frequency wavelength of 0.79 in (2 cm) in free space. The measured wave speed in the HDPE samples was 7.09×10^9 in./sec (1.8×10^8 m/sec) (60% free space).

Therefore, the wavelength in the material is about 0.47 in. (1.2 cm) in the HDPE material. The wavelength and effective aperture (F-number) determine the lateral resolution. In this case, 0.47-in. (1.2-cm) lateral resolution can be expected. The transceiver bandwidth determines the down-range (depth) resolution. The 10-GHz bandwidth calculates to about 0.71-in. (1.8-cm) depth resolution.

A sub-set of the pipe samples was chosen to provide a diverse set of joint conditions. Also it was determined the samples would not be modified in these tests. For example, the outside bead would not be removed.

Figure 3.7 shows a picture of this initial setup. A number of configurations were employed in this lower frequency test. Polarization tests with co-Pol and cross-Pol Circular and co-Pol and cross-Pol linear were tried. A cylindrical reflector was placed in the center to act as a mirror.

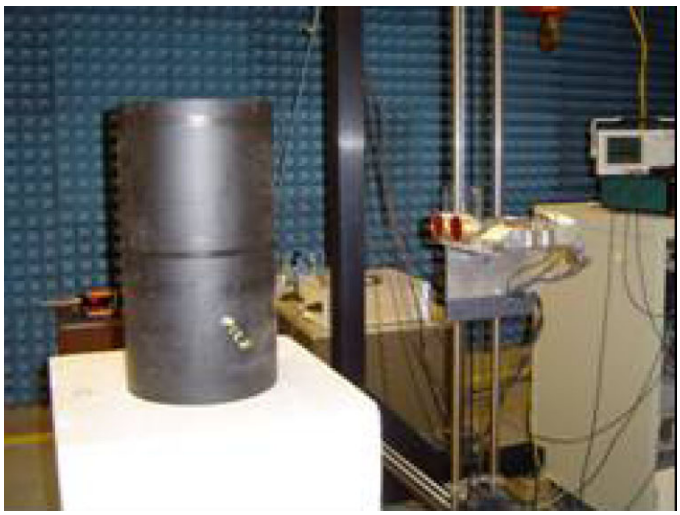

Figure 3.7 Ku-Band mm-Wave Laboratory System Setup

The conclusion of this effort was that linear co-polarization provided the best results, but that higher frequency would be necessary to achieve sufficient lateral resolution to see defects in this material. The HDPE material was quite transparent, but the ID and OD surfaces provided very good reflectivity.

3.2.2 U-Band Cylindrical Tests of HDPE Pipe Samples

A U-band transceiver (40–60 GHz) was implemented because of the need for higher lateral imaging resolution. This system provided for a more promising scenario due to the much higher illumination frequency and higher bandwidth. Figure 3.8 shows a characteristic image slice of one of the pipe samples. The fusion joint is readily seen. However, any defect features are obscured by the outside bead and the geometry of the illumination.

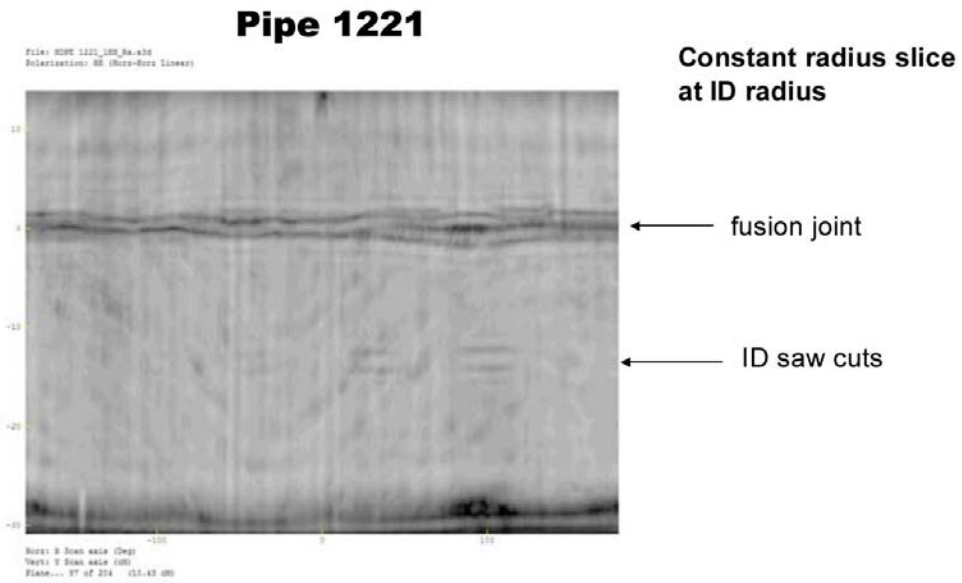

Figure 3.8 Typical U-Band Image Slice at the ID Surface

The method of displaying the image of the ID surface showed promise as it shows the shadow of the material variations.

3.3 Ultrasonic Time-of-Flight Diffraction

The TOFD technique applied to the fusion joint inspection has the advantage over standard pulse-echo or pitch-catch inspection in that it is a volumetric inspection method without raster scanning. Data is acquired as a single-line scan with the transmitter on one side of the fusion weld and the receiver on the other side. The pair of transducers is moved circumferentially around the pipe, collecting information on the material in between. Typically, longitudinal waves are used because the diffraction is stronger than with shear waves (in steel) (Baby et al. 2002). The technique is generally not amplitude-dependent. The schematic in Figure 3.9 shows the response from an embedded flaw. A lateral wave, which is a wave that travels just below the surface, is received first. The upper and lower crack tip signals are received next in time and are from the forward-scattered diffracted signals originating at the crack or flaw tips. Finally, the bounce off the back wall or pipe ID is received. As a flaw tip extends upward or downward close to the OD or ID, it starts to interfere with the lateral wave or back wall echo, respectively. Similarly, an OD- or ID-connected flaw response would also ideally show a disruption of the lateral or back wall signals, respectively. In all of the TOFD data presented in this report, both the lateral wave and back wall echo are evident in the B-scan images. Diffracted signals that indicate the presence of a flaw will fall between these two signals and are typically parabolic in shape.

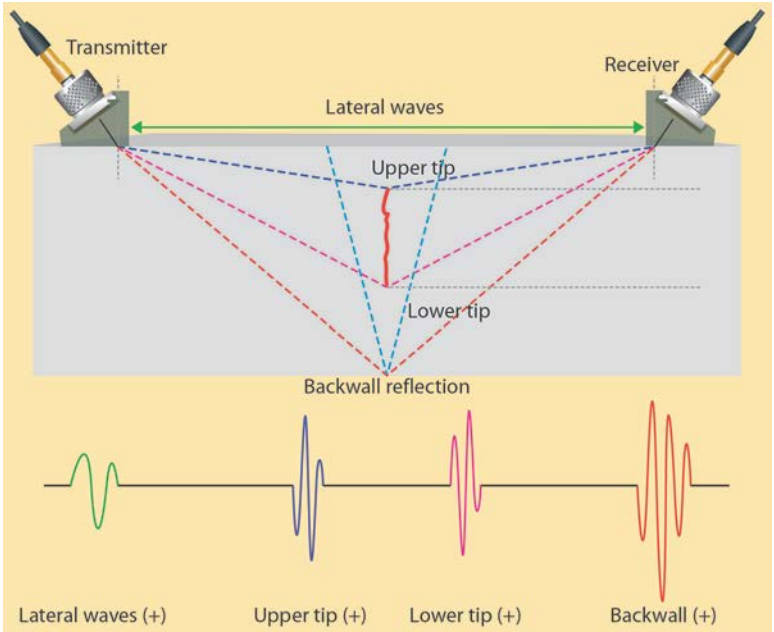

Figure 3.9 Schematic of the TOFD Signals Received from an Embedded Flaw (Olympus Corp. 2011). Reproduced with the permission of Olympus NDT.

3.3.1 Fluor/NDT Innovations, Inc. TOFD

Arrangements were made for Fluor and NDT Innovations, Inc. personnel to visit and inspect the fusion zone of all 24 PNNL test pipes. Fluor in partnership with NDT Innovations has a patented (Messer and Yarmuch 2007) ultrasonic time-of-flight diffraction inspection system based on Olympus (formerly RDTech) Omniscan equipment. This system has been used extensively in the mining and gas pipeline industry for more than four years with reported good success. NDT Innovations personnel inspected all 24 PNNL pipes with the patented system at the Fluor Hanford building and presented the results at a workshop. The pipe inspection was conducted as a blind test with PNNL staff invigilating the process.

The NDT Innovations' findings were summarized in a flaw table and are listed in Appendix A. An indication was classified as planar, longitudinal, incomplete fusion, porosity, or multiple-porosity. The majority of the calls were porosity or multiple-porosity. Because of the proprietary nature of their system, an open discussion of the inspection technique did not occur.

A screen capture for a 10-in. (25.4-cm) section of pipe, one quadrant, is shown in Figure 3.10. The upper portion of the image shows the A-scan, amplitude–time trace. The lower portion shows the B-scan gray-scale image of the inspected 10 in. (25.4 cm) of fusion zone. An OD surface signal (lateral wave) runs across the top of the B-scan image and towards the bottom is the ID surface signal (back wall echo). Embedded flaw signals occur between these two signals. An OD-connected flaw typically disrupts the OD surface signal and an ID surface-connected flaw typically disrupts the ID surface signal. Several flaw signals are noted in the left portion of the image and are representative of the hyperbolic diffracted signals seen in a TOFD

inspection. The technique relies on a disturbance of the base material signals caused by flaw tip diffracted signals.

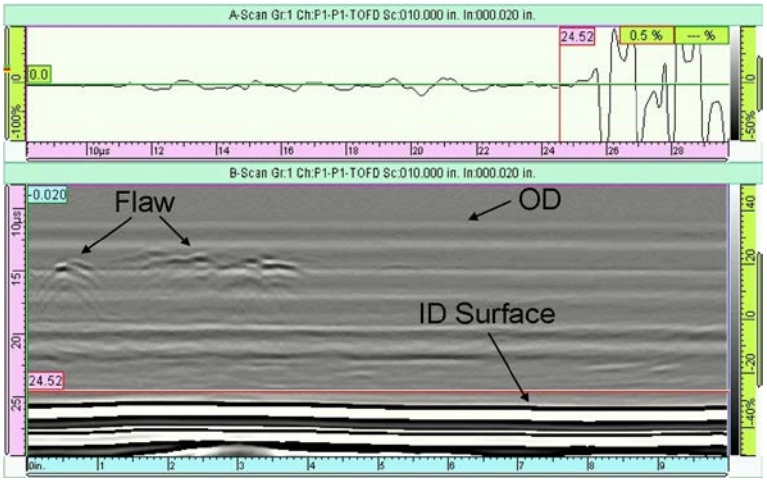

Figure 3.10 TOFD Image Showing the OD and ID Surface Signals and a Flawed Area

In general, the technique appeared to detect acoustical anomalies in many of the pipes. Figure 3.11 shows an area that was identified as having incomplete fusion. Figure 3.12 shows an area called flawed in one of the good pipes, fusion condition 6. Images of all the data are shown in Appendix B. These calls, as noted on the images, were made by NDT Innovations personnel during their two-day inspection of all 24 joints. Some of the calls are obvious, as in Figure 3.10, and others are less obvious, as in Figure 3.11. It should be noted that the original data was of high resolution and contrast, which unfortunately, is somewhat reduced in the figures of this report.

3.3.2 PNNL TOFD

Initially, the TOFD technique was applied in an immersion (in water) mode to avoid wedge material velocity and attenuation issues and the possible need for damping of signal reflections in the wedge. The water velocity of 0.0584 in./μsec (1.48 mm/μsec) is slower than the HDPE pipe material thus allowing insonification at high angles. Sawcuts were placed in the base material of two pipes and most of these were detected in the immersion mode.

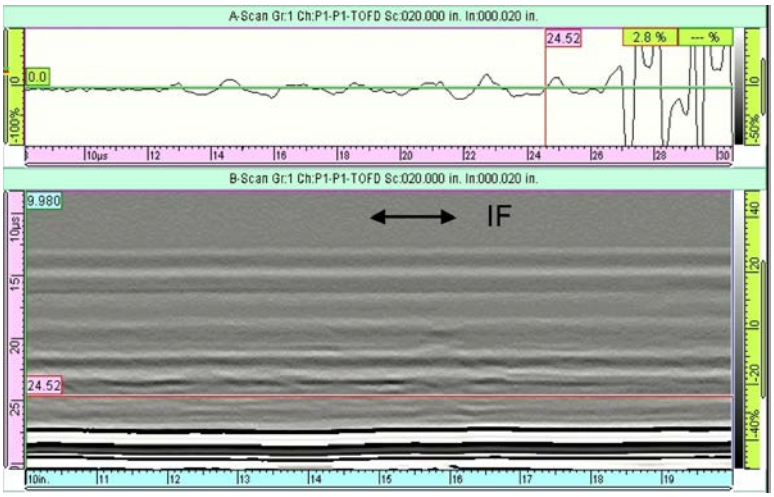

Figure 3.11 Area Identified as Incomplete Fusion

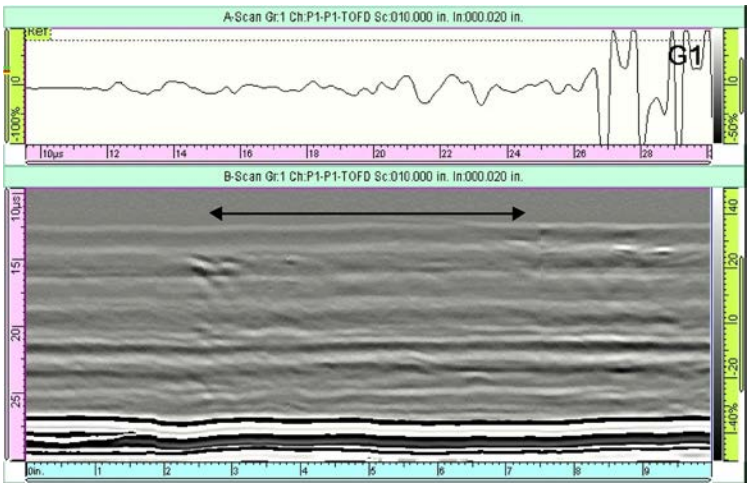

Figure 3.12 Possible Flaw Indications in One of the "Good" Pipes

After these initial and encouraging immersion tests, contact testing was attempted with wedges made of Rexolite and a pair of 1.5-MHz piezo-composite transducers. Sawcuts machined from the OD at through-wall depths of 75, 50, and 25 percent were detected. The 5 and 10 percent deep OD sawcuts were not detected. ID sawcuts were detected at all but the 5 percent depth. The weld fusion zone on one pipe from each of the six fusion conditions was examined with a mechanical scanner controlling the probe motion. Running water was applied at the base of the probes for coupling. With this inspection setup, the data collection was very inconsistent. It was difficult to repeat the results and the flowing water introduced signals that interfered with the signals from the material. At this point, manual scanning was determined to be more effective with a water-wetted surface so the mechanical scanning was abandoned. A small amount of dish soap was added to the water to act as a surfactant. The manual operator needs to apply a firm and consistent pressure on the transducer wedges to ensure uniform contact between the

wedge and the pipe surface as the transducer pair is moved circumferentially around the pipe. This takes some practice and attention to acquire data that is repeatable. The wedges were also machined to fit the pipe curvature.

A pair of 2.25-MHz, 0.5-in. (1.27-cm) diameter, TOFD-style probes was acquired from Olympus/ Panametrics. These piezo-composite probes are highly damped (broadband) and very sensitive. With the increase in sensitivity over the 1.5-MHz pair of probes, defect signals in the fusion zone were detected. A manual probe fixture with an attached encoder wheel was designed and assembled and is shown in Figure 3.13. This allowed circumferential positional information to be recorded with the ultrasonic signal as the probe was moved around the pipe. A ZETEC Tomoscan III system was used in the TOFD mode for data acquisition.

Responses from the ID sawcuts acquired at 52 dB of hard gain and no additional soft gain are shown in Figure 3.14 for the 75, 50, 25, and 10 percent through-wall deep flaws. These sawcuts were placed in the base material. The 5 percent deep notch was not detected. Note that the deeper two flaws are saturated and greater in response than the lateral wave. The 25 percent deep sawcut is 5 dB lower in amplitude and the 10 percent deep notch is 18 dB lower than full scale at the base gain level of 52 dB. The time or depth (vertical direction) window shown in these sawcut images extends beyond the ID or back wall echo. This allows viewing of mode-converted signals (longitudinal to shear) that can add additional information to the material inspection. This is an area for further investigation.

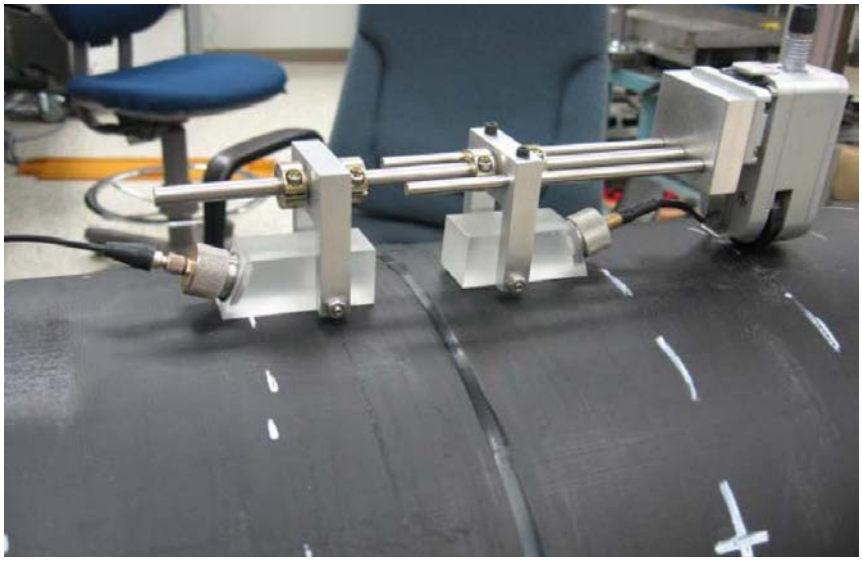

Figure 3.13 TOFD Probe Assembly

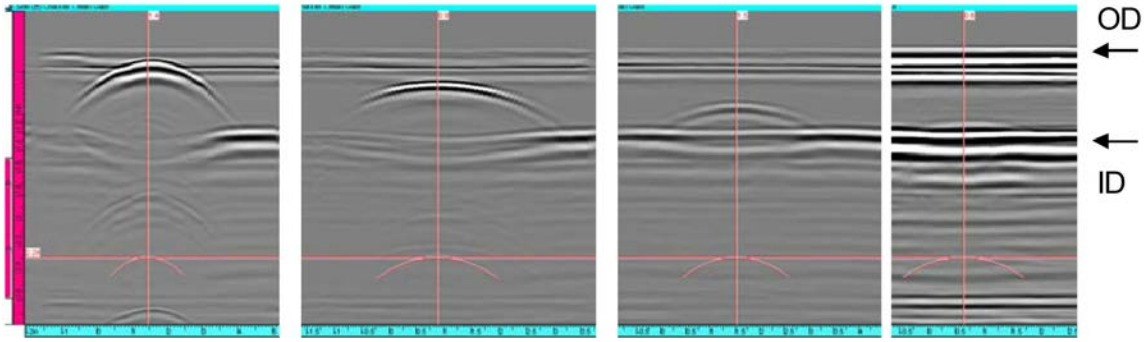

Figure 3.14 PNNL TOFD Results from Four ID-Connected Sawcuts. From left to right the through-wall depths are 75, 50, 25, and 10%.

The worst-case condition for pipe fusion, out of the McElroy batch of 24 test assemblies, and the one most likely to produce LOF, was condition 2, with fusion pressure during the heat cycle and a 20-second open/close time. One of these pipes was examined with TOFD by PNNL showing results comparable to those presented by Fluor/NDT Innovations, Inc. The data are shown in Figure 3.15 and Figure 3.16 for the four pipe quadrants, with the PNNL data shown in the top of each figure and the Fluor/NDT Innovations, Inc. data at the bottom of each figure. Notice that the PNNL data show the mode-converted signals beyond the longitudinal-wave back wall (ID) echo. The time window was extended to include the slower mode-converted signals with the thought that this additional data would enhance the detection of defects. The Fluor/NDT Innovations, Inc. data images are cropped at the ID and additionally do not have the saturated OD lateral wave signal seen in most TOFD images and in the PNNL data. This set-up results in a cleaner looking image and should provide better near-surface sensitivity to flaws. Fluor/NDT Innovations, Inc. data is also much more sensitive, due most likely to their patented processing of the raw data. Regardless, in this data comparison, flaw indications are identified at similar locations by both PNNL and Fluor/NDT Innovations, Inc. Each quadrant represents approximately 10 in. (25.4 cm) of pipe circumference.

Section 4.2.1 discusses tensile testing results on five coupons extracted from the fusion joint in three pipes as compared to TOFD and PA findings. These results showed promise but also raised questions. To further address the relevance of TOFD as a volumetric inspection technique, 12 additional pipe joints were evaluated with the TOFD technique at PNNL. The results of this evaluation are shown in Appendix C. Selected areas from seven of these joints were destructively analyzed to validate the TOFD findings. These results are discussed in Section 4.2.3 and Section 5.

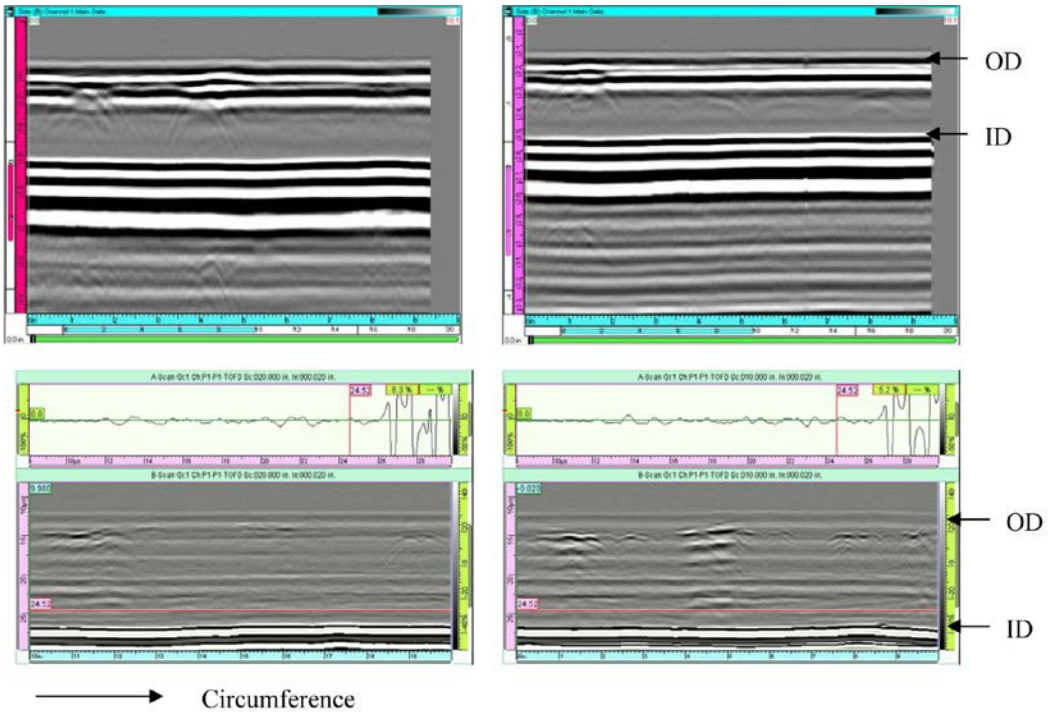

Figure 3.15 TOFD Data Acquired on Pipe 125, First and Second Quadrants (left and right), by PNNL in the Top and by Fluor/NDT Innovations, Inc. in the Bottom

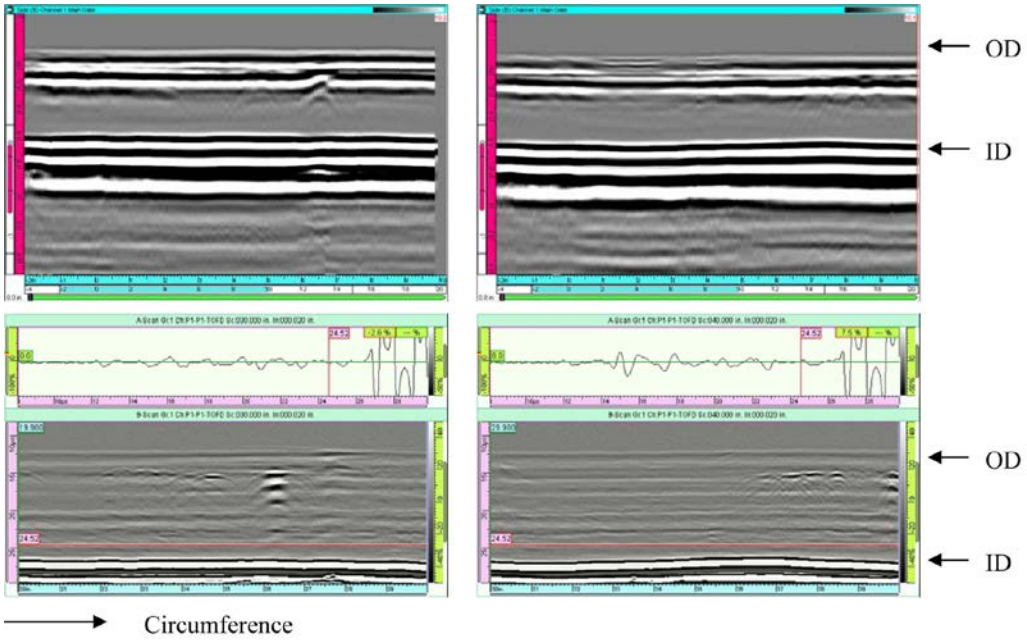

Figure 3.16 TOFD Data Acquired on Pipe 125, Third and Fourth Quadrants (left and right), by PNNL in the Top and by Fluor/NDT Innovations, Inc. in the Bottom

3.4 Ultrasonic Phased Array

PNNL had several PA probes in house that were designed for the inspection of steel components. Two of these probes were applied to the evaluation of HDPE pipe joints. These probes consist of two PA transducers that are mounted side by side on wedges to provide a transmit-receive configuration. The first probe to be applied was a 4-MHz one-dimensional (1-D) design for the transmit transducer and a 1-D design for the receive transducer. Each array contained 32 elements for a total probe aperture of 32 × 2 elements with a footprint of 60 × 27 mm (2.36 × 1.06 in.). The second probe was a 1.5-MHz 1.5-dimensional (1.5-D) design for the transmit transducer and a 1.5-D design for the receive transducer. Each array contained 10 × 3 elements for a total probe aperture of 10 × 6 elements with a footprint of 61.0 × 63.5 mm (2.4 × 2.5 in.).

3.4.1 4 MHz PA Probe

Several HDPE pipe sections were evaluated with the 4-MHz probe that is composed of two 1-D linear arrays operating in a transmit-receive-longitudinal (TRL) mode. The probe was designed to produce shear waves in steel, but longitudinal focal laws were successfully developed for inspecting the HDPE pipe. Beam modeling showed a good longitudinal response in the HDPE material over approximately 30 to 60 degrees of insonification was possible, using the original wedge designed for generating shear waves in steel. The simulated beams produced at 40 and 60 degrees are shown in Figure 3.17. An evaluation on the pipe sawcuts showed that OD notches at depths of 25, 50, and 75 percent through-wall were detected while the shallow 5 and 10 percent notches were not detected. All of the ID notches were detected.

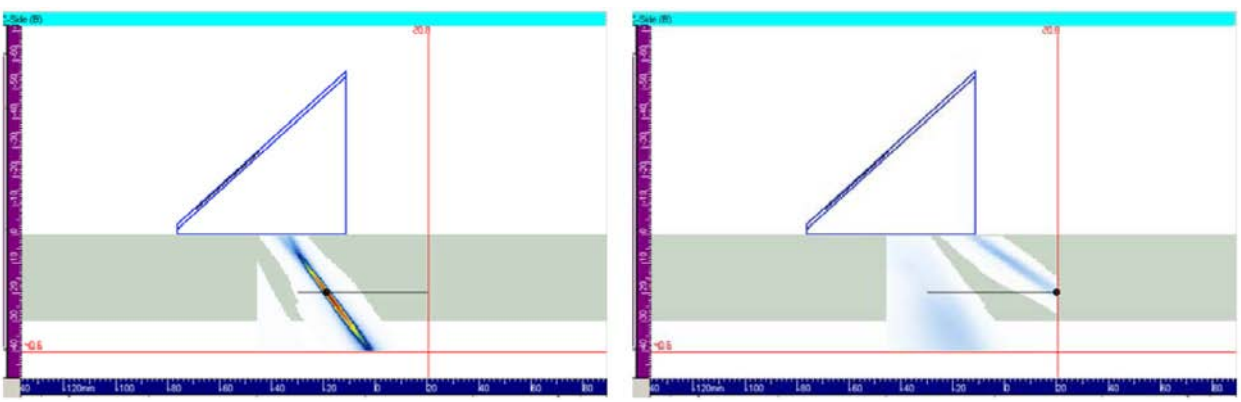

Figure 3.17 Phase Array Beam Modeling Results at 40 Degrees on the Left and 60 Degrees on the Right

As with the TOFD data collection, the PA data were acquired with manual scanning. The same manual scanner assembly used in the PNNL TOFD inspection was used with a new yoke for the PA probe. This assembly is shown in Figure 3.18. Constant and firm pressure on the wedges was also necessary for acquisition of repeatable data. Gel couplant was also used to aid scanning.

PA data was acquired on the fusion joint from pipe 125, a worst-case condition for joint integrity, and is displayed in Figure 3.19. The side view on the left shows the ID signal at the angle sweep start of 30 degrees. Data is acquired from 30 to 60 degrees at 1-degree increments. The highlighted flaw indication was centered at approximately 55 degrees as shown by the black line at the flaw indication in the side view. The associated end view at 55 degrees is shown on the top right with the flaw signal noted. Its circumferential extent is approximately from 7 to 9 in. (17.8–22.9 cm) in quadrant 4. The bottom right shows the A-scan trace from the position marked by the red horizontal line in the end view image.

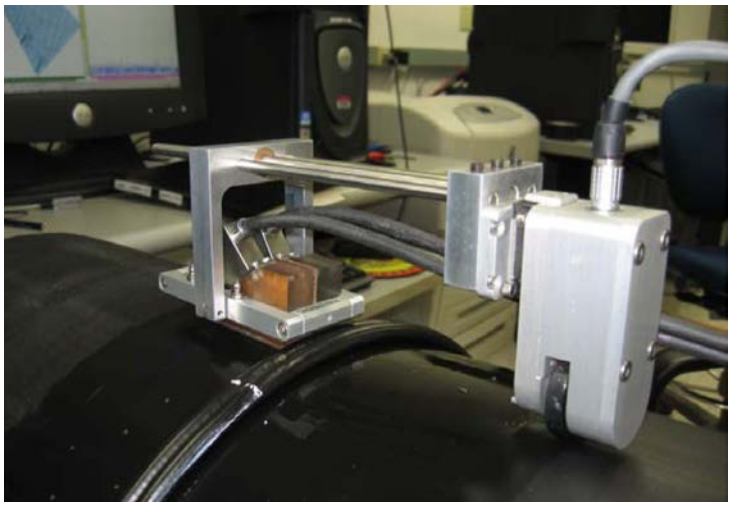

Figure 3.18 Manual Phased Array Probe Assembly in Position to Inspect a Fusion Joint

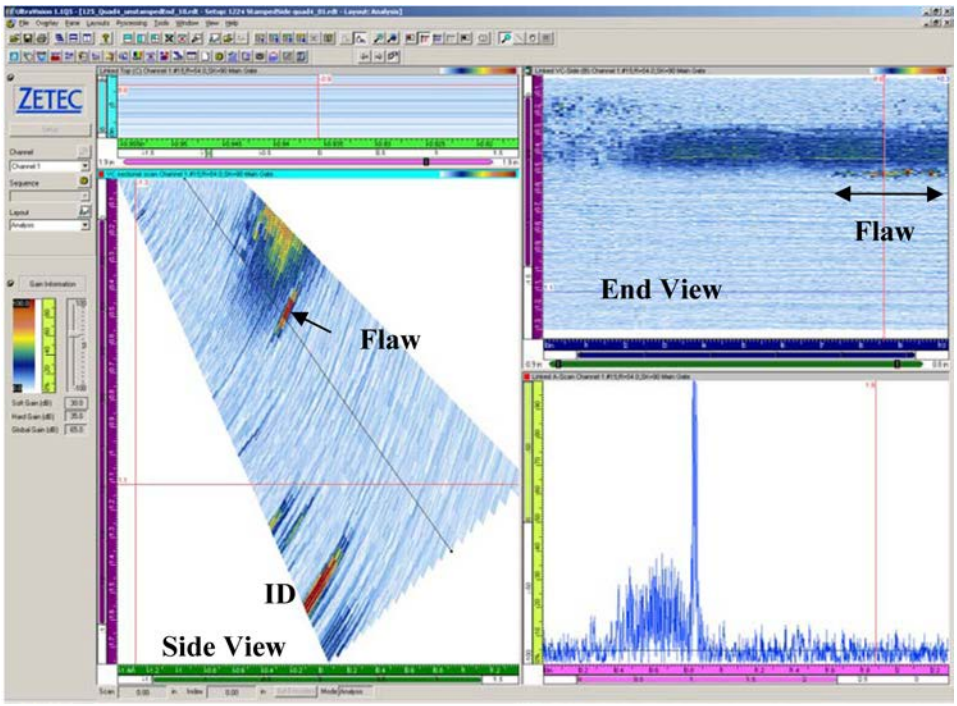

Figure 3.19 Phased Array Results on HDPE Pipe 125, Quadrant 4 Showing a Possible Lack of Fusion in the Noted Flaw Area

3.4.2 1.5 MHz PA Probe

A TRL 1.5-MHz, 10 × 3 elements, phased-array probe also designed for the inspection of steel components was employed for the HDPE pipe joint evaluation. It was desirable to insonify the joint at angles higher than those obtained with the 4-MHz probe to fully evaluate the through-wall extent of the joint and specifically the outer region. This required a new wedge material with a different acoustic velocity. To generate higher angles in the relatively slow HDPE material, it is necessary to use a wedge material with an even slower acoustic velocity as governed by Snell's Law. If the wedge is medium 1 and the HDPE pipe is medium 2, Snell's Law states that:

$$\sin(\theta_1) / \sin(\theta_2) = \text{velocity}_1 / \text{velocity}_2$$

A search for a slower wedge material but still with acceptable acoustic attenuation was conducted. Teflon with a velocity of 0.05 in./μsec was acceptable but it is too attenuative at 20 dB/inch. Water is a good medium with a velocity of 0.058 but requires a water column and is cumbersome. Eventually a gel material was selected and evaluated.

Given the velocity of the gel, a specific wedge assembly was then designed for the evaluation of the HDPE joint with the existing 1.5-MHz PA probe. The final assembly mounted on a pipe for data acquisition can be seen in Figure 3.20.

Figure 3.20 Gel Wedge in an Aluminum Frame for the 1.5-MHz PA Probe

The simulated beams produced at 35, 45, 55, and 65 degrees are shown in Figure 3.21 for this 1.5-MHz probe. The probe responses and detection capability were evaluated on the ID and OD notches. All of the ID notches were detected. All but the 5% OD notches were detected, and this probe was able to detect the 10% OD notch that was undetected with the earlier 4-MHz probe. The 4-MHz probe has a smaller wavelength in the pipe at approximately 0.025 in., compared to the 0.060 in. wavelength at 1.5 MHz, but it does not adequately provide insonification at the higher angles. The 1.5-MHz probe insonifies at the high angles but with a larger wavelength, and as a result, has diminished resolution. Ideally, one would design a PA probe specifically for the inspection of HDPE material with a gel wedge.

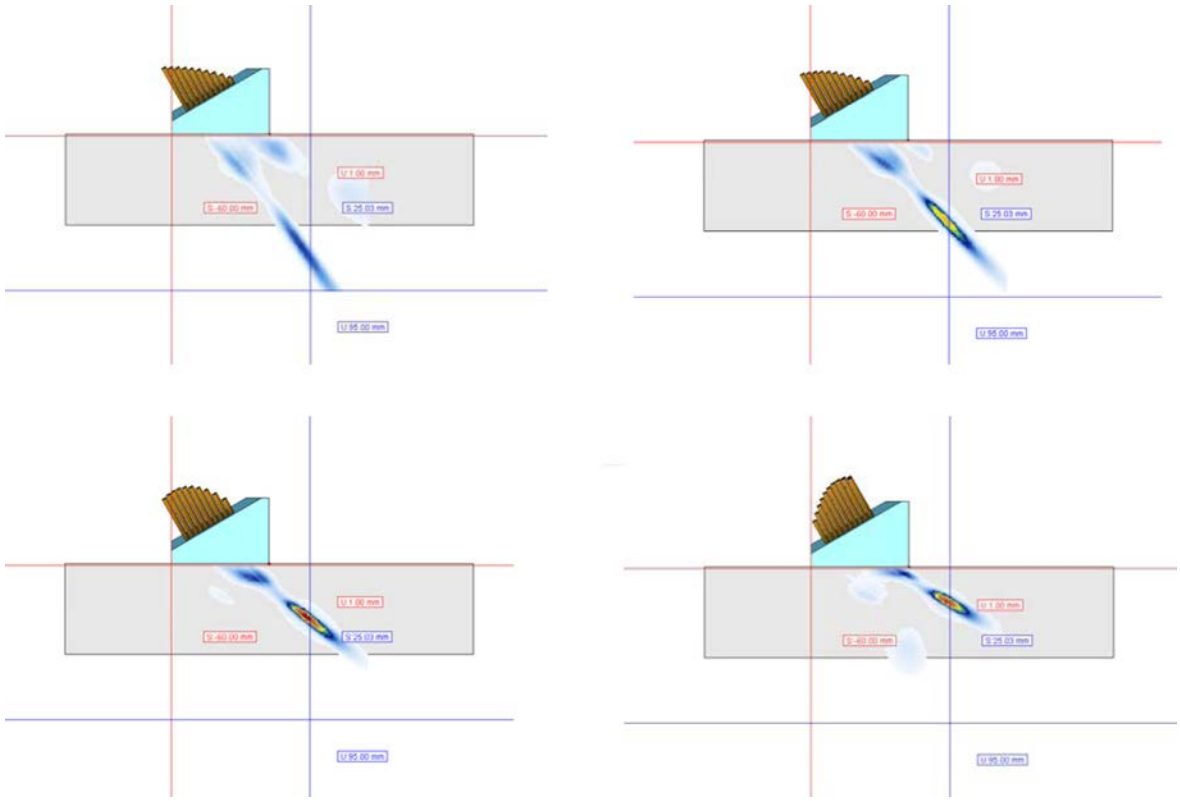

Figure 3.21 Beam Simulations for the 1.5-MHz PA Probe at 35, 45, 55, and 65 Degrees

Data was acquired from 12 pipe joints, two pipes from each of the six joint conditions with this probe. Scan imaging results for all of these joints are shown in Appendix D. The joint was scanned from both sides of the weld bead as it was found that the flaw responses varied from side to side. This is particularly evident in the images from pipe joints 127 and 128 shown in Appendix D.3 and D.4. Circumferential line scans were acquired with the weld bead acting as a guide for the probe. Representative data from some of the joint conditions are shown in Figures 3.22 through 3.24. The worst joint condition is represented in Figure 3.22. Flaw indications are clearly seen with a good signal-to-noise ratio (SNR); the SNR was calculated at 21.7 dB. Another type of flaw indication seen in the joints is shown in Figure 3.23. In the end view, a diffraction pattern is evident. The peak signal SNR is 16.2 dB and the diffraction rings are at approximately 10.2 dB. The stronger signal is likely a specular reflection and is accompanied by weaker diffracted signals. The sweep of angles provided by phased-array inspection as compared to a single-angle inspection give a better detection. Data from a reported good pipe is shown in Figure 3.24. In this image, there is clearly no indication of a flaw. Figures 3.22 and 3.24 show the extreme conditions of bad and good joint from the 12 pipes that were imaged. Much of the data was not as obvious, as can be observed by viewing the images in Appendix D. From the beam simulations, one could expect to see some smaller amplitude signals in the near surface data. This is observed in the three data images below.

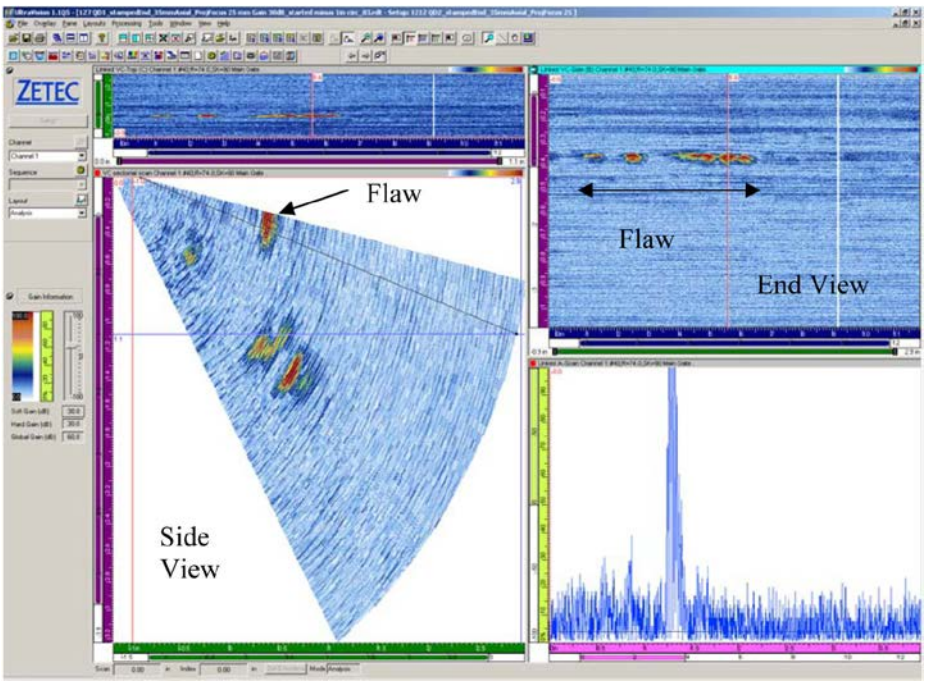

Figure 3.22 Pipe Joint 127 Quadrant 1 from the Stamped Side Showing Flaw Indications. This is the worst joint condition of the six possible.

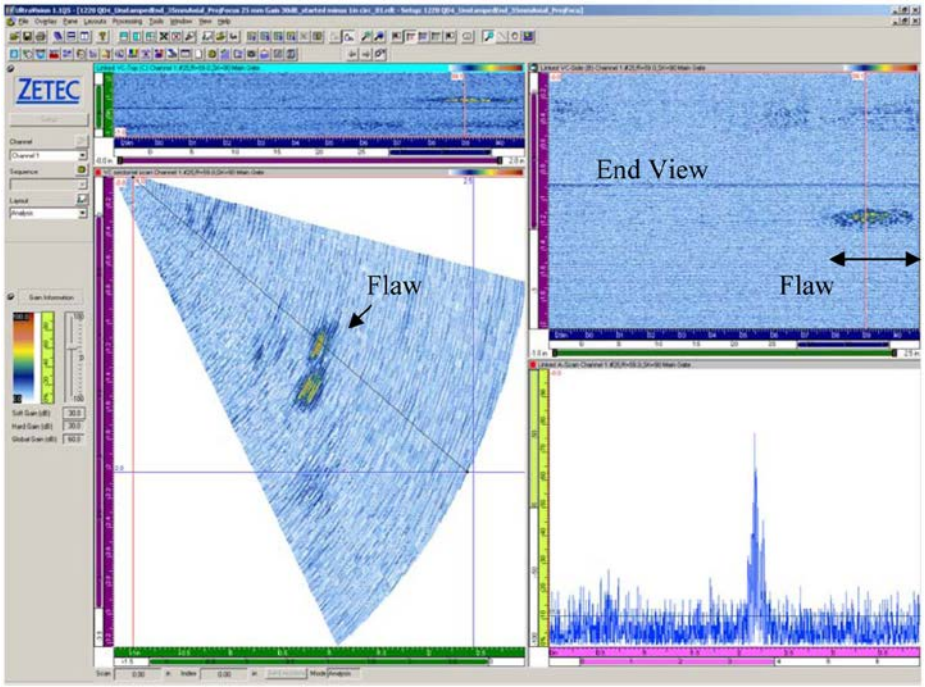

Figure 3.23 Pipe Joint 1220 Quadrant 4 from the Unstamped Side Showing a Flaw Indication with Diffraction Pattern

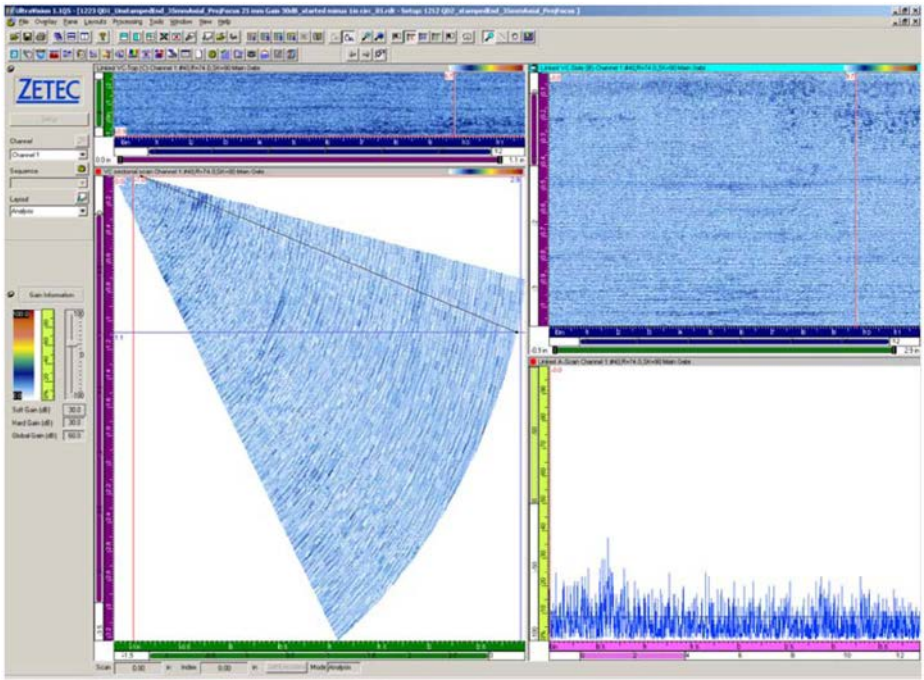

Figure 3.24 Pipe Joint 1223 Quadrant 1 from the Unstamped Side Showing No Flaw Indications in the Sample Made Using the Optimal Fabrication Procedure

3.5 Microwave

The Evisive microwave technology was patented in the early 1990s primarily for the inspection of dielectric materials such as rubber and soft plastics. Delaminations, cracks, impurities, and similar flaws cause a change in the dielectric constant of the material which can be detected and imaged as a specimen is scanned. Arrangements were made for six of the pipes, one from each of the six fusion conditions, to be sent to Robert Stakenborghs at Evisive in Louisiana for evaluation with the microwave technology.

Data images from a 4-in. pipe joint were used as a standard for this evaluation. One of the images from the standard, showing strong and fairly consistent signals from the weld joint, is displayed in Figure 3.25. The horizontal axis represents the pipe circumference and the joint is in the middle of the vertical axis.

A section of parent material from one of the PNNL pipes was imaged with results shown in Figure 3.26. The approximate 40-in. (101.6-cm) circumference is shown horizontally. The magenta band between 5 and 10 in. (12.7 and 25.4 cm) is repeated at nearly 25 to 30 inches (63.5 to 76.2 cm) and represents a pipe thickness variation. This occurrence is approximately 180 degrees apart in the pipe circumference and likely is attributed to the pipe manufacturing and cooling processes.

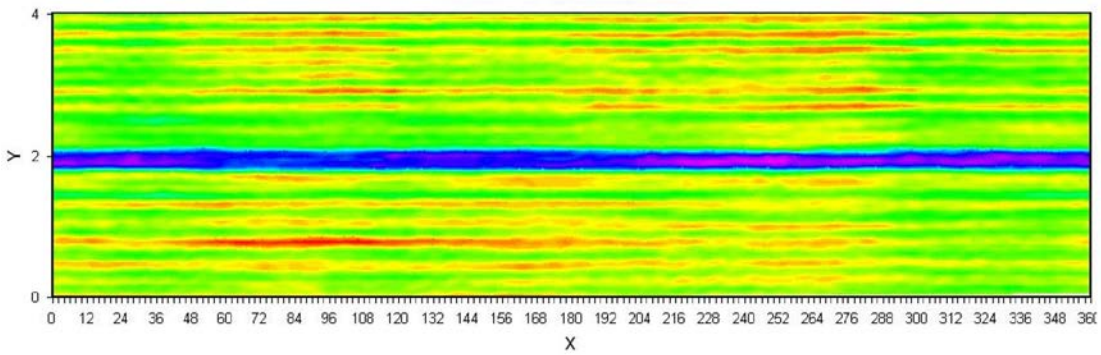

Figure 3.25 4-in. Pipe Standard

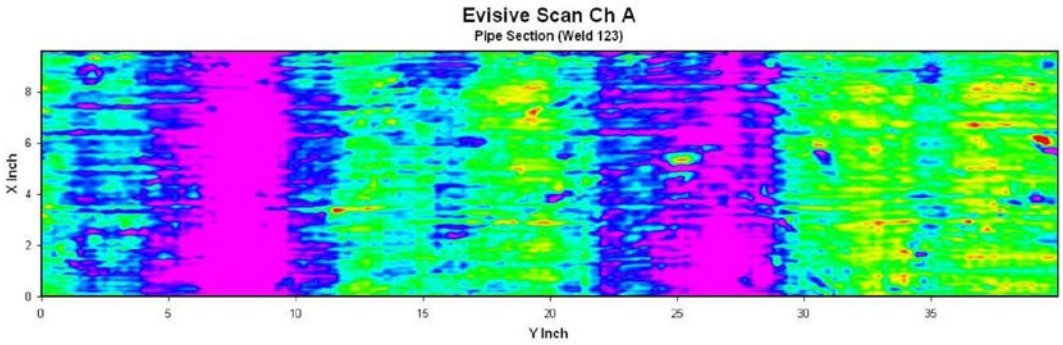

Figure 3.26 Image of Parent Material on Pipe 123

Images from the six pipe joints that were scanned are shown in Figures 3.27–3.32. Potential problem areas are circled with areas containing LOF or cold weld, and point indications noted as inclusions or pinholes. All six of the joints were called unacceptable. The outer weld bead was removed prior to imaging each joint.

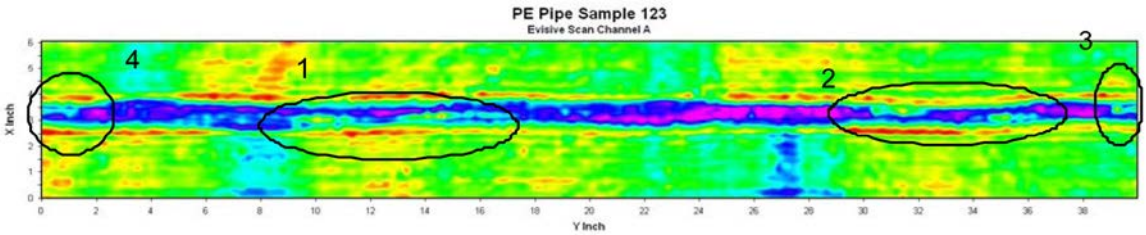

Figure 3.27 Microwave Results for Pipe Joint 123 Showing Possible LOF in Areas 1 and 2 with an Inclusion at 15 in. (38.1 cm). Areas 3 and 4 show a disruption in the center of the weld bead.

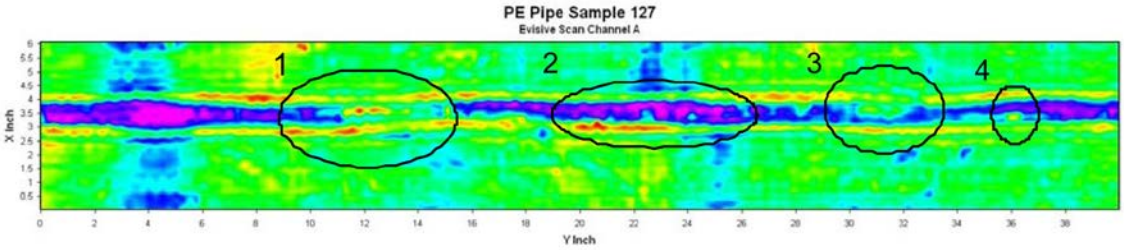

Figure 3.28 Microwave Results for Pipe Joint 127 Showing LOF in Area 1, Pinholes at 15, 21, 22.5, and 24.2 in. (38.1, 53.3, 57.2, and 61.5 cm), and a Possible Inclusion at 12 in. (30.5 cm) and Area 4. Area 3 shows weld zone disruption.

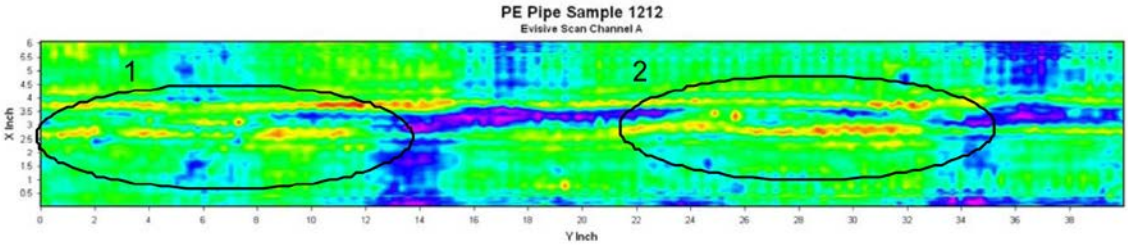

Figure 3.29 Microwave Results for Pipe Joint 1212 Showing Large Areas with LOF

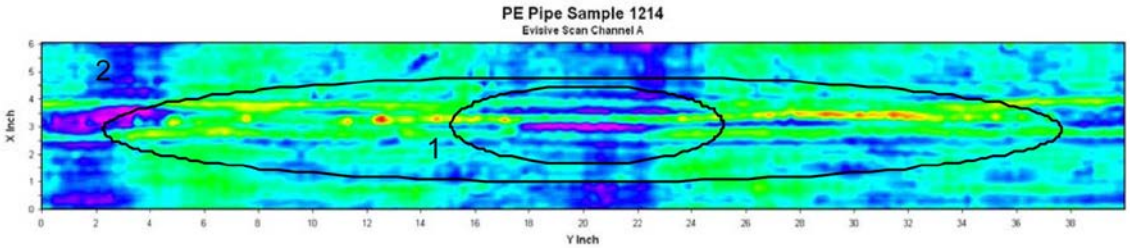

Figure 3.30 Microwave Results for Pipe Joint 1214 Showing Cold Fusion in Area 1 and LOF in Area 2. Possible inclusions at 7.5, 11.5, and 12.5 in. (19.1, 29.2, and 31.8 cm).

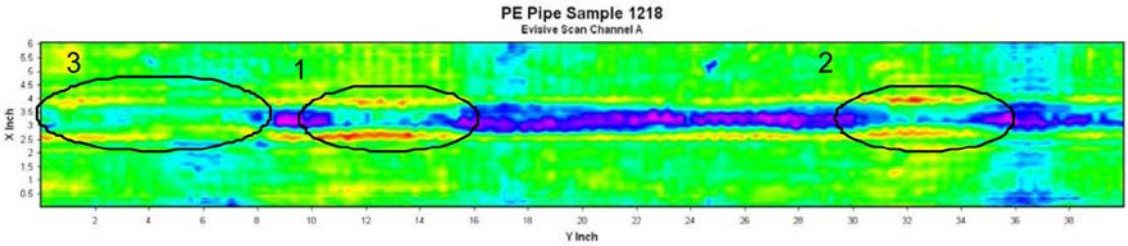

Figure 3.31 Microwave Results for Pipe Joint 1218 Showing LOF or Cold Fusion in Area 1 and 2 with General LOF in Area 3

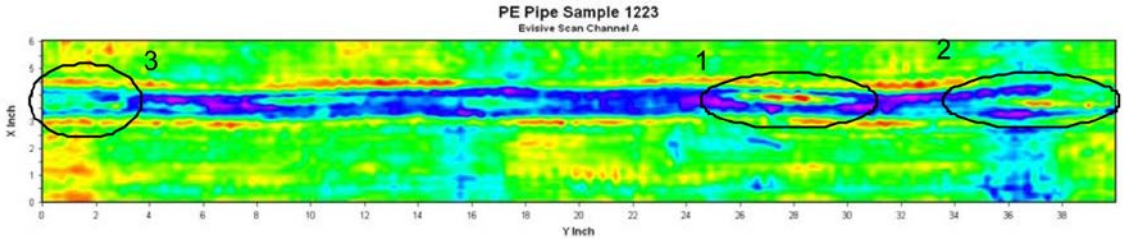

Figure 3.32 Microwave Results for Pipe Joint 1223 Showing Cold Fusion. Other problem areas are at 10 and 17 in. (25.4 and 43.2 cm).

After discussing the initial results with Evisive, it was agreed to remove the inner weld bead from two pipes and rescan the joints. The images with both inner and outer bead removed from pipe 1214 and 1223 are displayed in Figure 3.33. Mr. Stakenborghs stated that the defective areas appear the same in both scans with and without the ID bead.

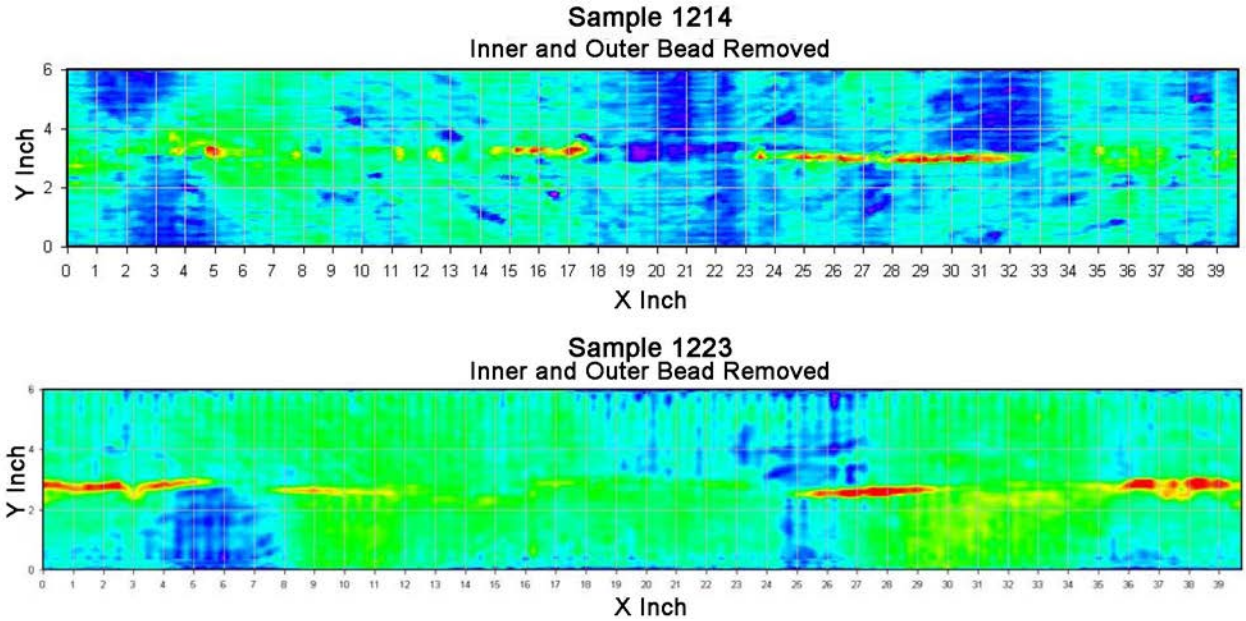

Figure 3.33 Evisive Microwave Results on Two Pipe Joints After ID Beam Removal

4 DESTRUCTIVE TEST RESULTS

Varied destructive evaluation (DE) methods have been applied to HDPE material and the fusion joints. Mechanical tests include the bend back test and a high-speed tensile impact test (ASTM F2634-07 2007). The tensile test is the industry standard and selected PNNL samples were subjected to this test. Another DE technique reported by others, including Fluor personnel and Frank Schaaf, Sterling Refrigeration Corp., is to slice the fusion zone or base material, and look for porosity, lack of fusion, or other anomalies in the thin slices of material. A photo from Mr. Schaaf, showing both a good joint and LOF, is shown as Figure 4.1. A microtome was used to slice perpendicular to the joint, in the axial pipe direction, thus showing a cross section of the fusion area. PNNL conducted an assessment of microtome analysis as part of their efforts to validate the true state of HDPE material being studied. Additionally, because there was an interest in being able to efficiently conduct further testing on many more samples of HDPE, PNNL decided to investigate the side bend test process that had been developed by the plastic industry. Dudley Burwell described this new procedure (McGraff and McElyen 2009) and provided a copy of it for PNNL to evaluate. An extensive number of tests were conducted using this procedure.

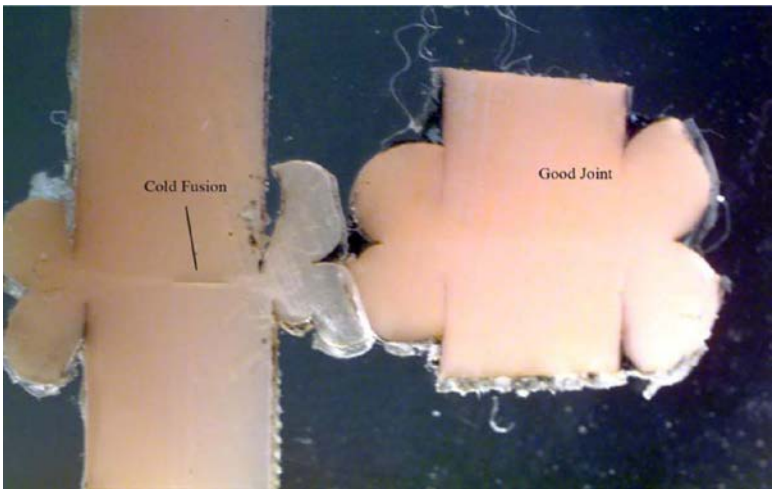

Figure 4.1 Cold Fusion and Good Joint in PE Material. Photo courtesy of Frank Schaaf.

4.1 Slicing

PNNL used a Leica microtome, on loan from from Bartels and Stout, Inc., for slicing HDPE material in order to assess this DE method. Figure 4.2 shows the rotary manual slice (model RM 2245) unit with a weld section cut-out and positioned in the vise. As the wheel (out of the photo) is turned, the specimen moves down and past the razor knife blade that is behind the red knife guard. A thin slice of material is peeled off the specimen and the specimen is advanced in position ready for the next slice. Slices in the 25–35-micron-thick range were ideal for allowing sufficient light through to view details of the material. Thinner slices tended to fall apart.

Figure 4.2 Rotary Manual Microtome Used to Slice HDPE Pipe Sections. The unit was on loan from Bartels and Stout, Inc.

The slices of material were viewed with a light table, or light source, behind the slice. Bulk specimens were also viewed via microscope or magnifying glass, with a light source on top or to the side. A diffuse light box was also helpful on several bulk specimens. Both the slice and the bulk specimen were photographed using a high-resolution camera. A bulk specimen and the camera setup are shown in Figure 4.3 with the light source positioned to the side.

Figure 4.3 Setup for Photographing the Bulk Specimen

4.1.1 Fusion Joint Evaluation

A fusion area from pipe 125 containing a flaw indication at an approximate 7–9 in. (17.8–22.9 cm) circumferential position was cut out of the pipe. Slices were made in the axial direction, perpendicular to the weld. These slices were in the 25–35-micron-thick range, making them thin enough to transmit visible light yet thick enough to maintain their integrity. A tomographic slice at approximately 8.6 in. (21.8 cm) in the pipe circumference is shown in Figure 4.4. Because of uneven mixing of carbon black in the 3408 base material of the pipe, light and dark swirls are observed. When joining two pipe sections, this swirl pattern changes direction due to melting and fusing in the joint, causing a pattern that runs along the fusion line. These light and dark lines in the fusion zone camouflage LOF in this region. Evidence of LOF is, however, seen on the cut (or sectioned) pipe surface as shown in Figure 4.5. The microtome cut was made from the bottom of the piece to the top, leaving cut marks that run perpendicular to the fusion line. Sufficient and diffuse lighting, and/or tilting of the pipe section, highlights these LOF lines in the joint. A liquid penetrant test (PT) of this surface was also performed in attempts to enhance the LOF indication. A red dye was applied to the cut surface and allowed to soak for at least one hour. Normally during this dwell time the liquid penetrant is absorbed into surface discontinuities by capillary action. After the dwell time, the surface was wiped clean of the dye and a white developer applied. The developer typically draws dye out of discontinuities and maps out the flaw shape/opening on the surface of the specimen. No flaw was seen on this specimen face with the PT. It is assumed that these LOF areas are so tight that the dye could not seep into the discontinuity.

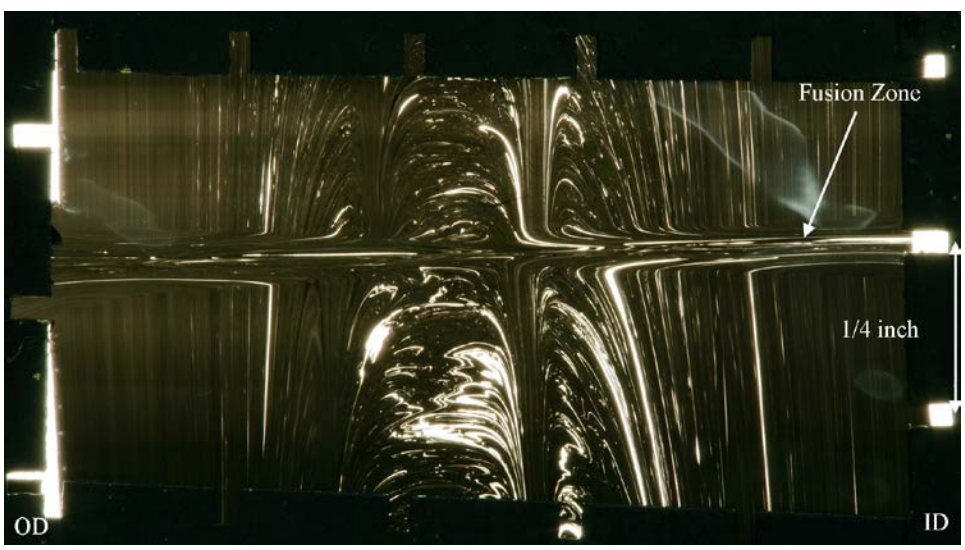

Figure 4.4 A Slice from HDPE Pipe 125, Quadrant 4 at Approximately 8.6 Inches (21.8 cm). Lack of fusion in the fusion zone is not evident due to light colored material streaks and swirls from uneven base material mixing.

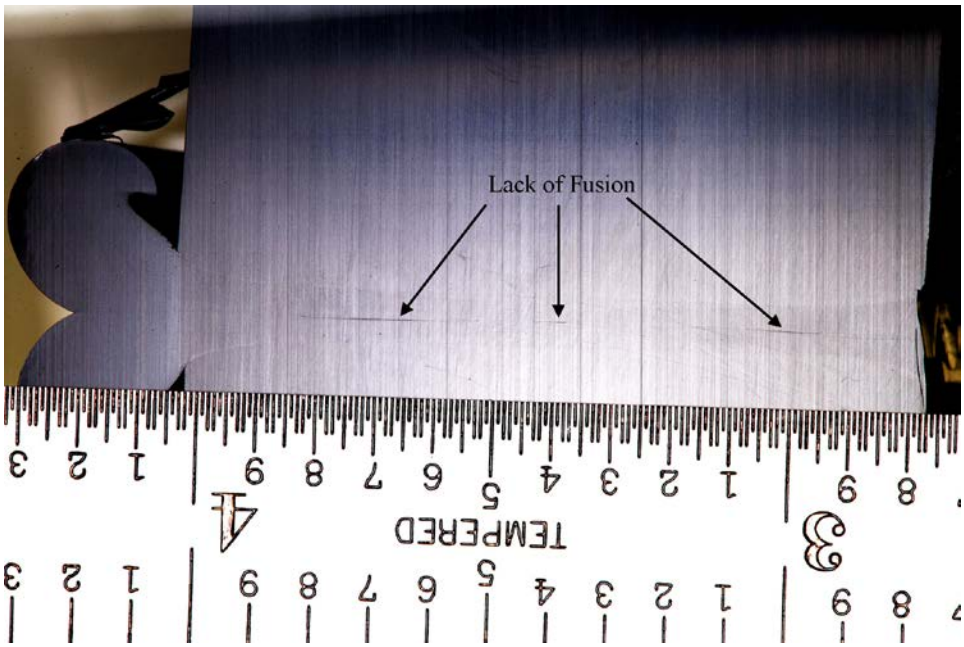

Figure 4.5 Surface of HDPE Pipe 125, Quadrant 4 at Approximately 8.6 Inches (21.8 cm). Areas of lack of fusion are noted. Units displayed in scale are inches.

The TOFD and PA ultrasonic results from the fourth quadrant of pipe 125 are shown in Figure 4.6. The approximate area of the slice and surface shown in Figures 4.4 and 4.5 is identified by a vertical black arrow in each of the ultrasonic images of Figure 4.6. Both the PNNL TOFD (upper left in the figure) and Fluor/NDT Innovations, Inc. TOFD (upper right in the figure) data show a flaw indication in the end of the B-scan image. The PA data shown in the lower part of the figure also contains a flaw indication at the end of the circumferential scan line. This confirms that these ultrasonic techniques were able to detect this LOF.

For comparison, a piece of a reportedly good fusion joint was also evaluated. TOFD and PA ultrasonic examinations showed no indications in quadrant 4 of pipe 1224 at 3 to 4 in. (7.6–10.2 cm). This area was cut out and sectioned. Figure 4.7 shows a slice from this fusion joint at approximately 3.4 in. (8.6 cm). As in pipe 125, streaks of light material due to uneven mixing with the dark carbon black pipe material are evident and make a lack-of-fusion detection from the slice difficult or impossible. The pipe surface after slicing appears to be a better indicator of the fusion joint condition. Figure 4.8 shows the cut surface with no evidence of LOF in the fusion zone. Figure 4.9 shows the ultrasonic results with no flaw indications in the area that was sliced.

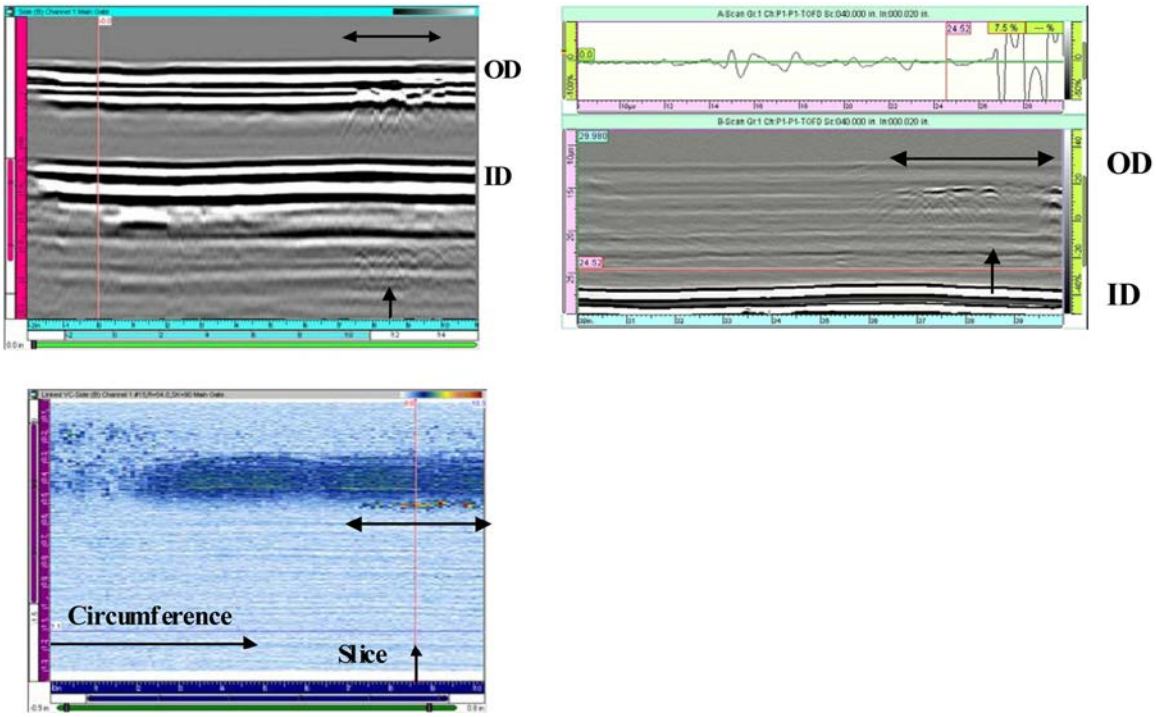

Figure 4.6 PNNL TOFD (upper left), Fluor/NDT Innovations, Inc. TOFD (upper right), and PNNL PA Data from the Fourth Quadrant of Pipe 125. All images show a flaw indication in the approximately 7–9 inch (17.8–22.9 cm) circumferential position.

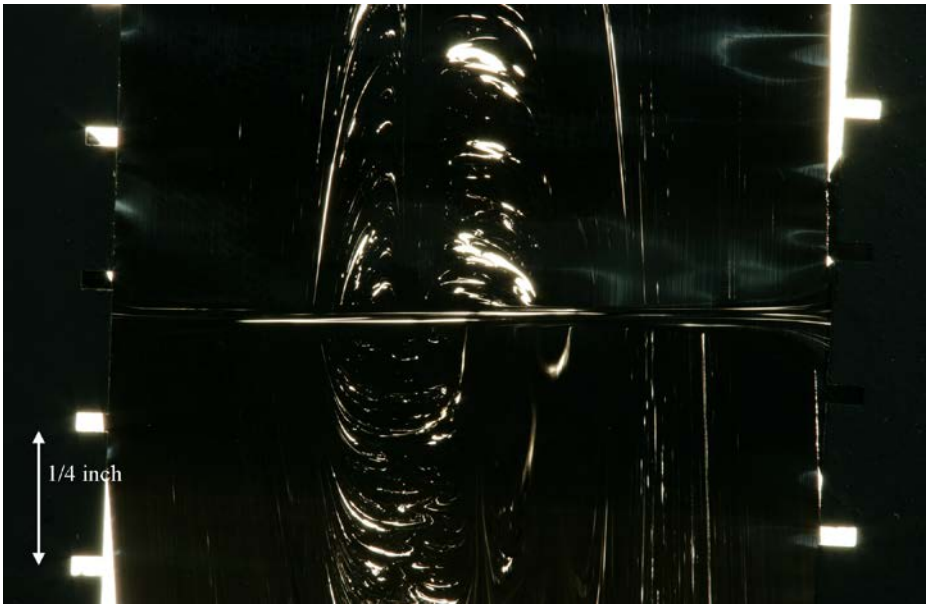

Figure 4.7 Slice from HDPE Pipe 1224, Quadrant 4 at Approximately 3.4 Inches (8.6 cm)

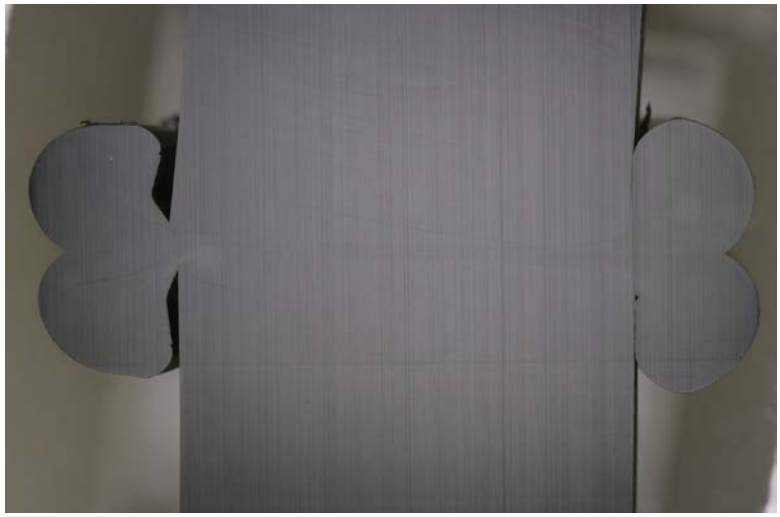

Figure 4.8 Surface of HDPE Pipe 1224, Quadrant 4 at Approximately 3.4 Inches (8.6 cm). No lack of fusion is seen.

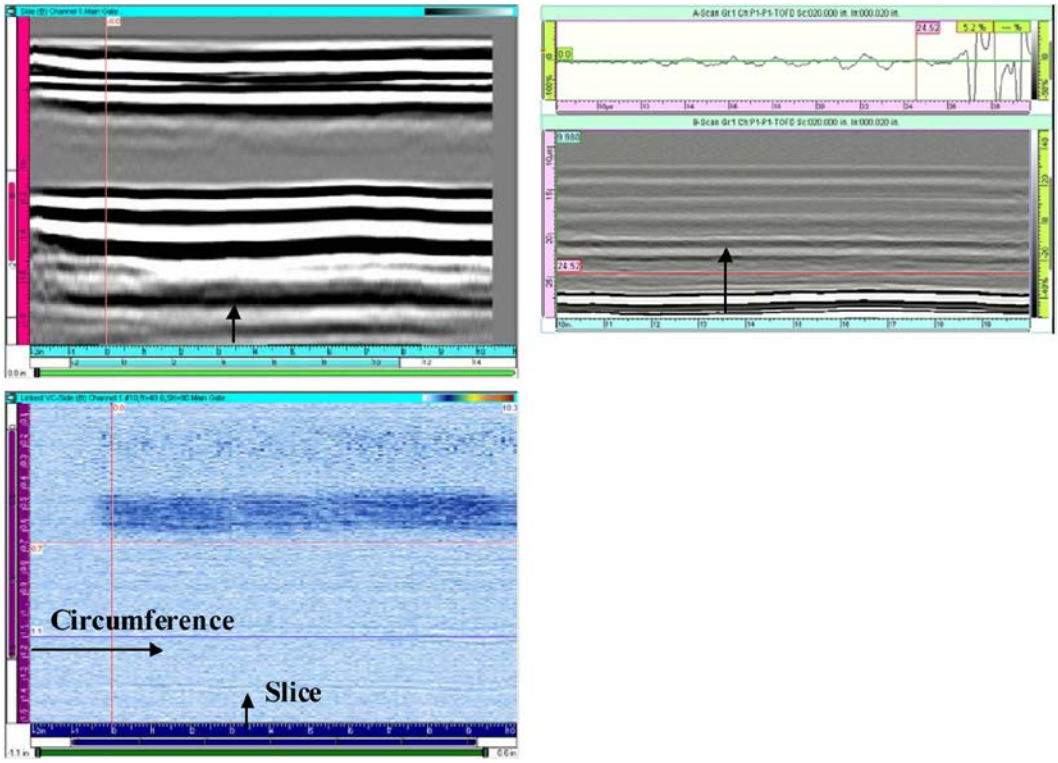

Figure 4.9 Ultrasonic Responses from Quadrant 4 of Pipe 1224 Show No Flaw Indications. The PNNL TOFD data is in the upper left, Fluor TOFD data in the upper right, and PNNL PA data in the lower left. The vertical arrows show the approximate location of the slice of material at 3.4 inch (8.6 cm), see Figure 4.8.

4.1.2 Base Material Evaluation

A preliminary evaluation of base material showed no ultrasonic indications in one 3408 pipe and one 4710 pipe. Slices from the 3408 and 4710 base material are shown in Figure 4.10, left and right, respectively. The spacing between fiducial notch marks on the edge of each image is 0.25 in. (0.64 cm). It is obvious that the 3408 material is less uniformly mixed, with the 4710 material showing some lack of uniformity, but to a lesser extent. However, even with this reduced amount of swirling, it would likely remain difficult to detect LOF when examining a thin slice of material removed through a 4710 fusion joint. No porosity was found in the few slices that were collected through base material. In fact, only one or two areas were found with a single pin hole or porosity in or near a fusion joint in the numerous fusion joint slices evaluated. This would represent an approximate 1 percent or less rate of porosity detected in this material.

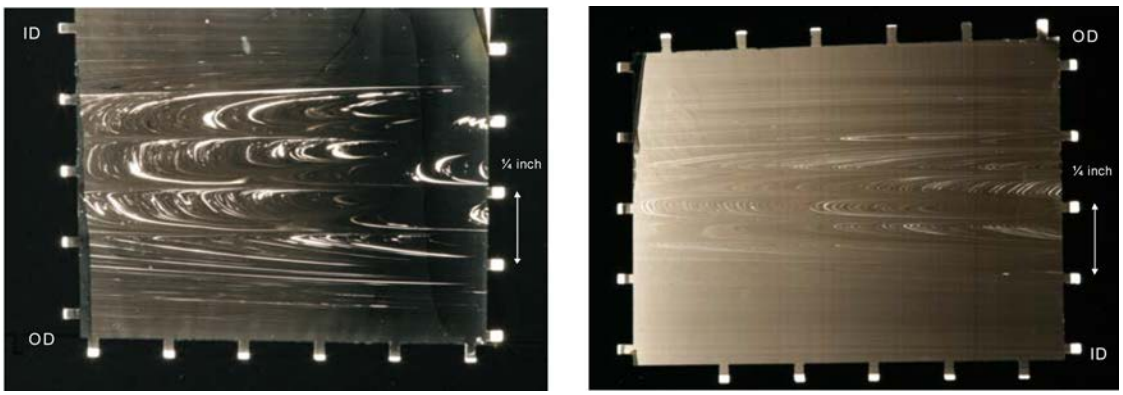

Figure 4.10 Base Material Slices from 3408 on the Left and 4710 on the Right Show Swirls from Non-uniform Mixing. The spacing between edge notches is 0.25 in. (0.64 cm).

4.2 Mechanical Testing

Five fusion joint specimens were mechanically tested with the industry-standard, high-speed tensile test. The results are fully discussed in this section but the failure of an expected “good” joint showed the need for further mechanical testing. After a second round of NDE testing on six pipes, an easily conducted side-bend test was used extensively on the six pipes. These results are also discussed.

4.2.1 High Speed Tensile Test

Several sections of pipe fusion zone were identified for mechanical testing. These specimens were sent to James Craig at McElroy for high-speed tensile testing. Two areas from pipe 126, which was fused under condition 2, most likely to produce LOF, were identified for testing. The TOFD (PNNL and Fluor results) and 4-MHz PA images are shown in Figure 4.11 from quadrant 4 of pipe 126. The solid arrows on the top of each image show areas called potentially defective. The dashed arrows on the bottom of the images show the areas selected for the

tensile testing. Note that an approximately 2-in. (5.1-cm) area was selected for testing and only a 0.4-in. (1.0 cm) area along the pipe circumference was actually tested. Since PNNL was not involved in the machining of these test specimens, it was assumed that the test area was near the center of the marked area. The marked area to the left in the images was identified for testing and was called flawed in all three ultrasonic images in Figure 4.11. The marked area to the right in the images was also identified for testing and was called flawed only in the Fluor TOFD data.

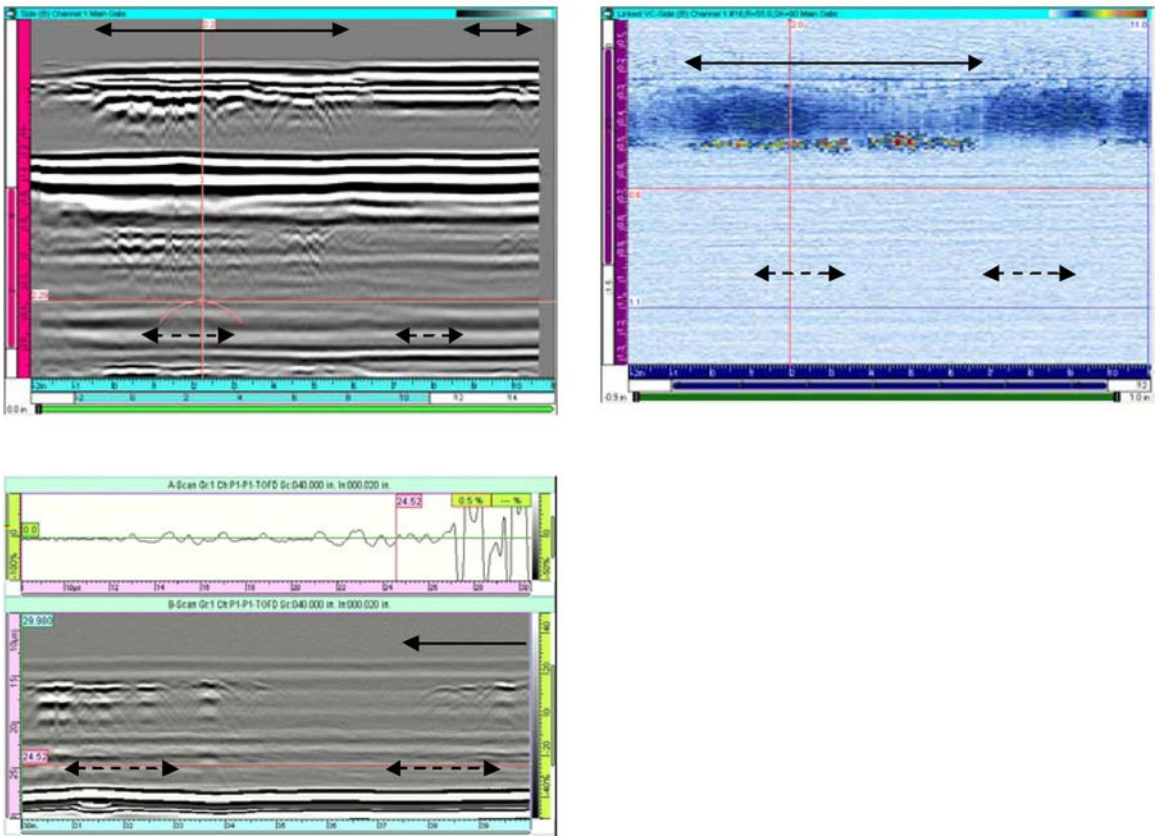

Figure 4.11 Areas Marked for Tensile Testing as Shown by the Lower Arrows in the NDE Images for Pipe 126, Quadrant 4. Upper arrows in the NDE images show regions called defective. Results are for PNNL TOFD, upper left, PNNL PA, upper right, and for Fluor TOFD, lower left.

Two areas from pipe 1215, fused under a less severe condition, were selected for tensile testing, shown in Figure 4.12. The left area produced a TOFD indication noted by Fluor/NDT Innovations, Inc. but not by PNNL TOFD or PA. The other area produced no detected ultrasonic indications.

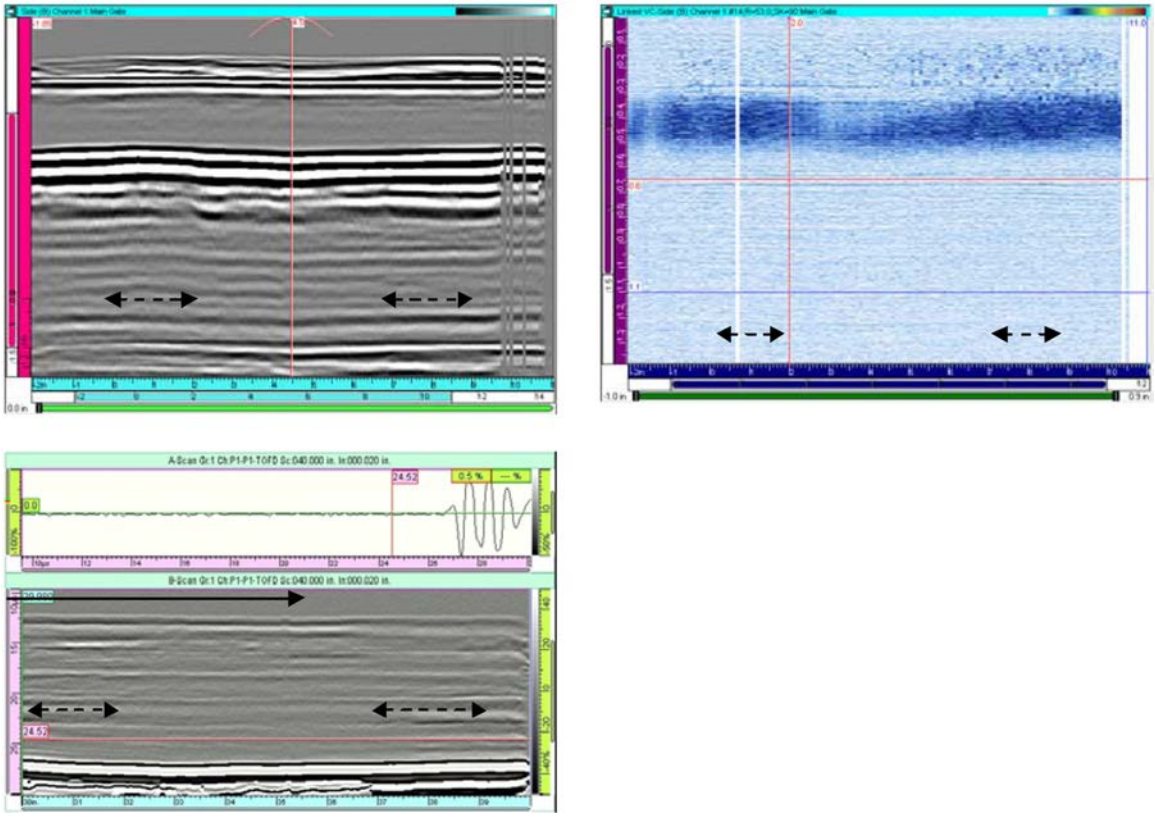

Figure 4.12 Areas Marked for Tensile Testing as Shown by the Lower Arrows in the NDE Images for Pipe 1215, Quadrant 4. Upper arrow in the NDE images show regions called defective. Results are for PNNL TOFD, upper left, PNNL PA, upper right, and for Fluor TOFD, lower left.

One area from pipe 1224, fused as a good pipe, was also selected and is shown in Figure 4.13. In addition to these five joint specimens, the base material was also tested. These tests were performed in April 2008.

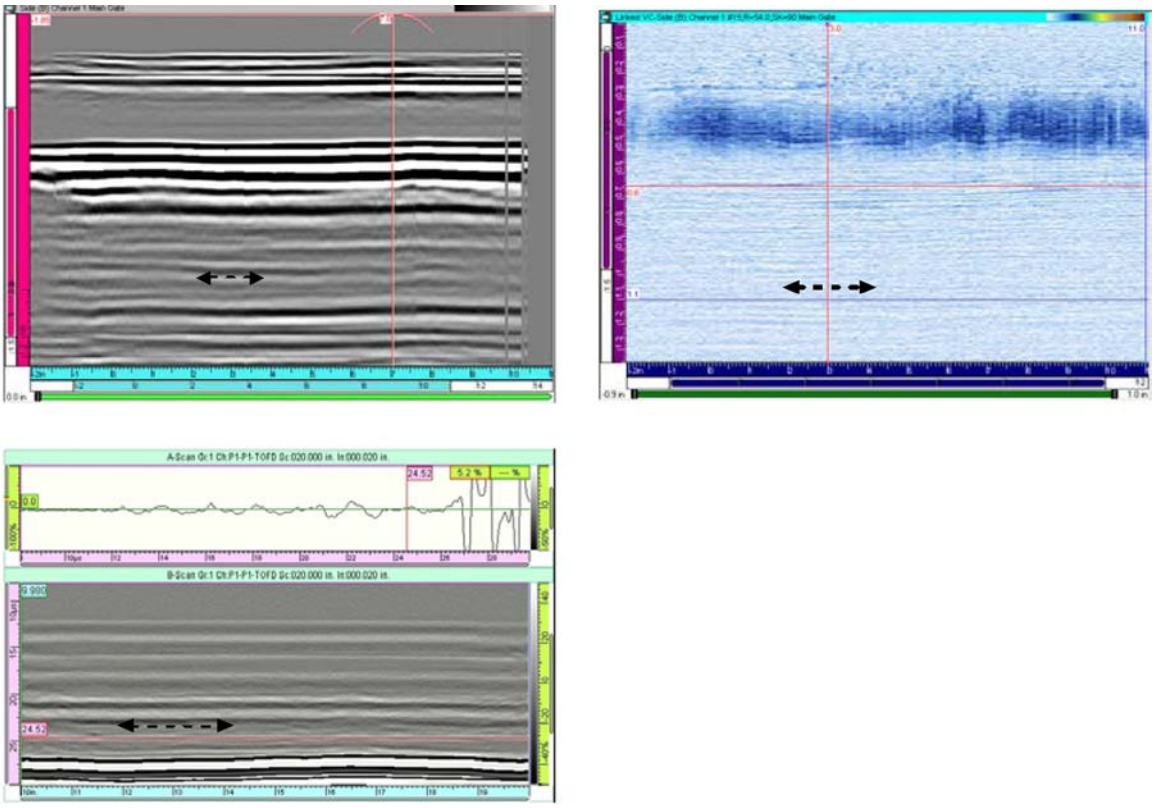

Figure 4.13 Area Marked for Tensile Testing as Shown by the Lower Arrows in the NDE Images for Pipe 1224, Quadrant 2. This was fused as a "good" joint. Results are for PNNL TOFD, upper left, PNNL PA, upper right, and for Fluor TOFD, lower left.

The five marked areas were subjected to the high-speed tensile impact test. The test was performed according to the ASTM F2634 Procedure (ASTM F2634-07), which specifies a testing speed of 6 in./sec (152 mm/sec) for wall thickness of up to 1.25 in. (32 mm). Note that at greater wall thickness, the testing speed is 4 in./sec (102 mm/sec). Table 4.1 shows the test results from the five marked areas and three base material specimens. From these results, it appears that pipe 1215 samples are both good (ductile failure) and that pipe 126 samples are both bad (brittle failure). A surprise is that the 1224 "good" pipe sample also failed in the brittle mode, which indicates an unacceptable fusion area.

Figures 4.14 through 4.19 show six coupons from side and end views, and further illustrate the location and properties of the high-speed tensile test failures. Coupon 1 in Figure 4.14 clearly shows a ductile failure outside the joint area, with necking of the material. Coupon 2 (Figure 4.15) shows a ductile failure at or near the joint so there are differences in the failures between these two coupons (1 and 2) from pipe 1215. The failure in coupon 3, Figure 4.16, is clearly brittle with no ductility shown by the smooth face over the entire joint. Coupon 4 in Figure 4.17 shows a brittle failure with some tearing or cross linking in the material at the ID (top surface in Figure 4.17); thus, we see differences in these two coupons (3 and 4) from the same pipe 126.

Table 4.1 High-Speed Tensile Test Results From 5 HDPE Fusion Joints and 3 Base Material Coupons

Coupon	Wall, in.	Width, in.	Area, in^2	Max Force, lb	Yield Stress, PSI	Yield Energy, in.-lb	Failure Energy, in.-lb	Yield Energy Density, in.-lb/$in.^2$	Failure Energy Density, in.-lb/$in.^2$	Failure Mode	Failure Location	Pipe[(a)]	Circ. Loc. of Coupon, in.	Fluor Call	PNNL Call
1	1.22	0.41	0.49	1879	3803	463	1884	937	3814	Ductile	O/S	1215	7-9	good	good
2	1.22	0.41	0.49	1869	3798	422	1441	858	2929	Ductile	O/S	1215	0-2	bad	good
3	1.23	0.41	0.50	955	1909	43	47	86	94	Brittle	HAZ	126	1-3	bad	bad
4	1.21	0.41	0.49	1839	3752	371	399	757	814	Brittle	HAZ	126	7-9	good/bad	good
5	1.22	0.41	0.50	1899	3813	476	609	956	1223	Brittle	HAZ	1224	2-4	good	good
6	1.19	0.40	0.48	1788	3734	409	1685	854	3518	Ductile	GAGE	Base			
7	1.23	0.41	0.50	1909	3826	497	1773	996	3553	Ductile	GAGE	Base			
8	1.23	0.40	0.49	1879	3803	428	1771	866	3585	Ductile	GAGE	Base			

(a) Note: 1215 q4: long open/close time only 20 sec
126 q4: fusion pressure during the heat cycle plus a 20 sec open/close time
1224 q2: fused as a good joint

Conversions

1 inch = 2.54 cm | 1 $inch^2$ = 6.45 cm^2 | 1 lb (force) = 4.448 N or (kg)(m)/s^2

1 PSI = 1 lb/in^2 = 6894.76 N/m^2 | 1 in-lb = 0.11299 joule (J) | 1 in-lb/in^2 = 175.135 J/m^2

Coupon 5 in Figure 4.18 failed at the joint in the brittle mode but showed some signs of tearing. This coupon 5 sample was removed from pipe 1224, which was fused to be a “good” joint. Lastly, Figure 4.19 shows one of the base material coupons with necking and failure in the ductile (good) mode.

In summary, DE results from coupons 1 and 2 show a good joint in both locations, based on the ductile failure mode call, but there are obvious differences in viewing the test coupons. Coupon 1 failed away from the joint whereas coupon 2 failed at or near the joint and showed less ductility. The PNNL UT results agree on both joints (good call) while Fluor UT calls coupon 1 good and coupon 2 bad. DE results from coupons 3 and 4 show a bad joint in both locations but coupon 4 showed some signs of tearing on the ID surface. PNNL called coupon 3 bad and coupon 4 good, while Fluor called coupon 3 bad with coupon 4 on the edge of good to bad. Finally, the brittle failure on coupon 5 was unexpected as PNNL and Fluor both called it good and it was made to be a good joint. The coupon failed at the joint but some signs of tearing were evident. Figure 4.20 plots the failure energy as a function of coupon and gives some quantitative differences in the failure modes of the eight total coupons.

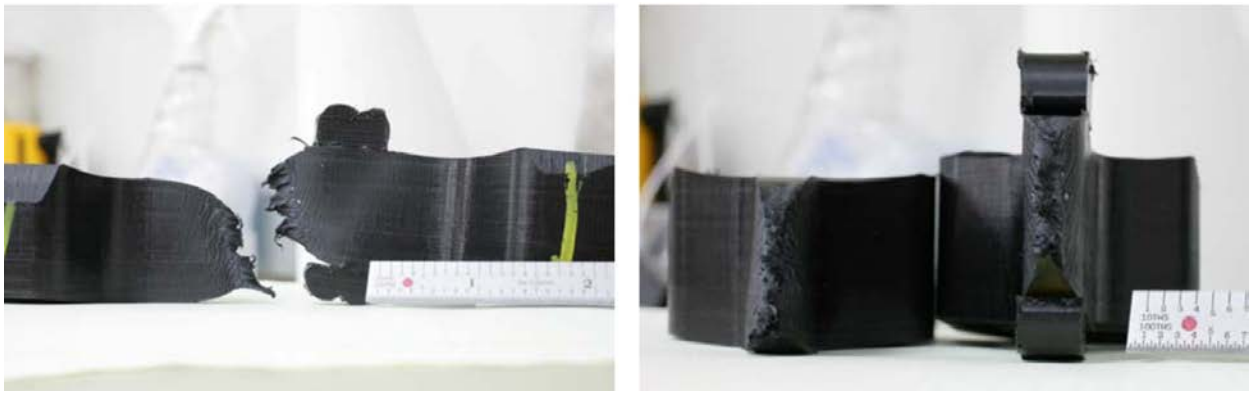

Figure 4.14 Coupon 1 from Pipe 1215 Quadrant 4 with a Long Open/Close Time of 20 sec Showing a Ductile Failure Outside of the Joint. Both PNNL and Fluor called this area good.

Figure 4.15 Coupon 2 from Pipe 1215 Quadrant 4 with a Long Open/Close Time of 20 sec Showing a Ductile Failure at or Near the Joint. PNNL called this area good and Fluor called it bad.

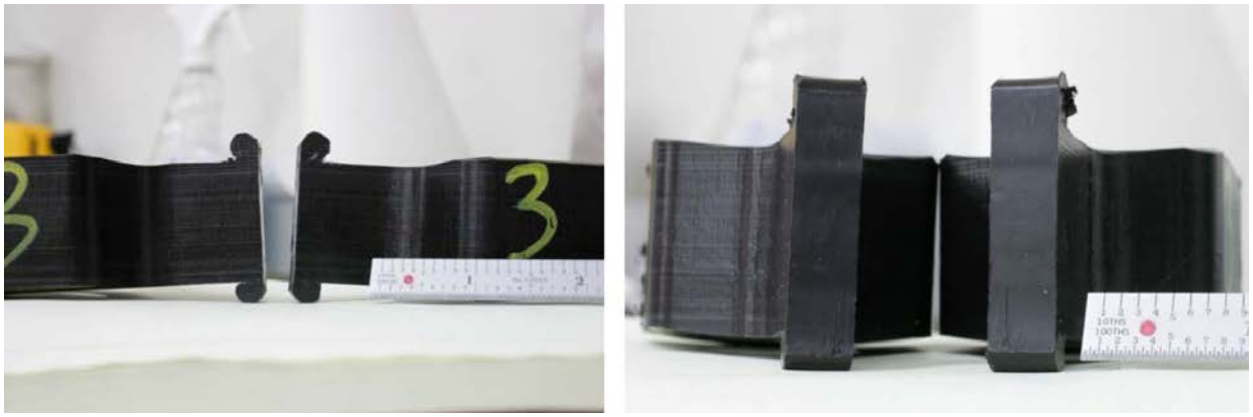

Figure 4.16 Coupon 3 from Pipe 126 Quadrant 4, Fused with Fusion Pressure During the Heat Cycle and a 20-sec Open/Close Time. The failure mode is brittle. Both PNNL and Fluor called this area bad.

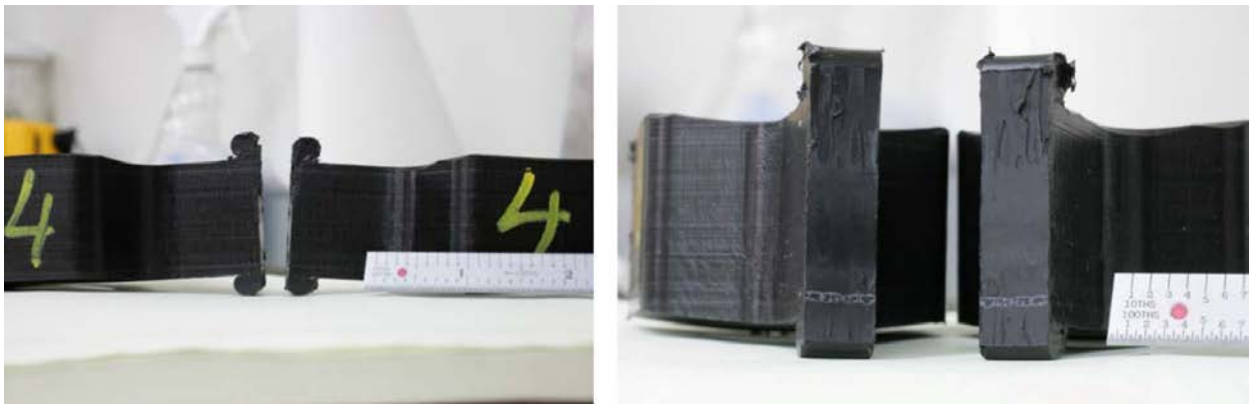

Figure 4.17 Coupon 4 from Pipe 126 Quadrant 4, Fused with Fusion Pressure During the Heat Cycle and a 20-sec Open/Close Time. The failure mode is brittle but shows some tearing at the top (ID) in the right figure. PNNL called this area good and the Fluor call was on the edge of a good-to-bad region.

Figure 4.18 Coupon 5 from Pipe 1224 Quadrant 2, Fused with Procedure F2620 and Expected to be Good. The failure mode was brittle at the joint but shows some ductility. Both PNNL and Fluor called this area good.

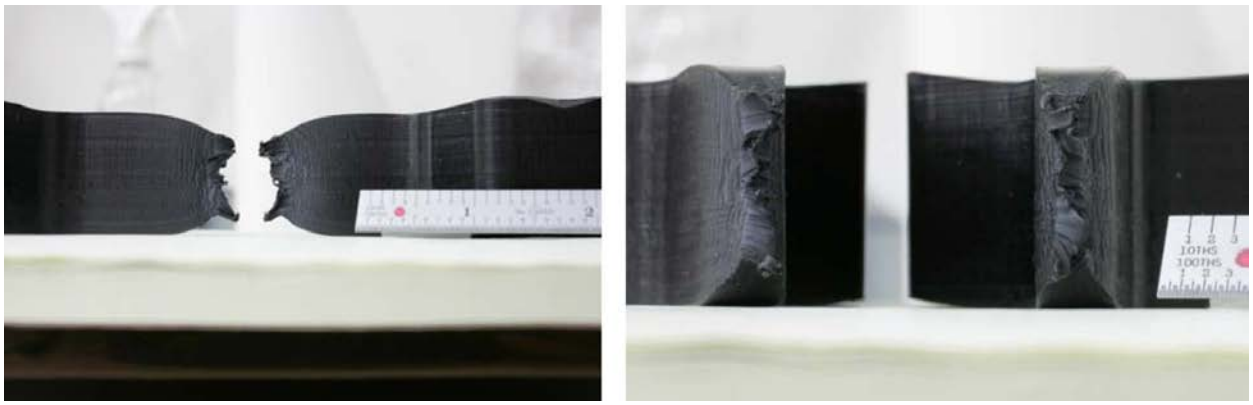

Figure 4.19 Coupon 6 Base Material Shows a Ductile Failure

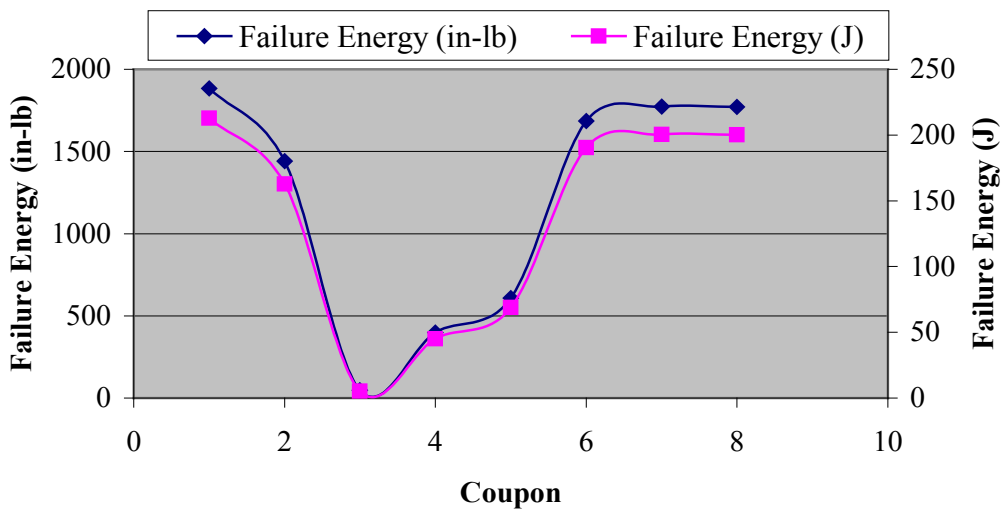

Figure 4.20 Failure Energy Show a Quantitative Measure of Failure Among the Six Coupons. Coupon 3–5 failed in the brittle mode but with differences. Coupons 1, 2, 6–8 failed in the brittle mode but with differences.

4.2.2 Guided Bend Test

The guided bend test (GBT) was recommended by Harvey Svetlik of Independent Pipe Products, Inc. The basic guided bend test places either the pipe ID (root bend), pipe OD (face bend), or entire joint (side bend) in tension with a die and plunger arrangement. This test uses a coupon that is bent in three-point bending to a specified number of degrees of arc, typically, 60 to 90 degrees, and no more than 120 degrees. A strip is cut out of the pipe for testing or the whole pipe can be cut into strips, allowing testing of practically the entire pipe joint. In the test, the specimen is bent around a radiused, or cylindrically shaped, plunger so that all portions of the weld zone are subjected to the same tensile yield strain level. This test is derived from the ASTM Standard Test Method for Guided Bend Test for Ductility of Welds (ASTM E190-92). The GBT for polyethylene pipe recommends a ratio of the plunger radius of curvature to pipe wall

thickness at 2:1. This produces a strain in the joint that is nominally 2.3 times the lower limit yield strain. The test, therefore, strains the joint beyond yield and permanent deformation occurs across the fusion joint. This test has the potential for fairly easily evaluating most of a pipe joint because there is minimal material wasted, unlike the machining of “dog-bones” in a tensile test.

4.2.3 Side-Bend Test

Through discussions with ASME Code participants involved with the Special Working Group (SWG) on HDPE, PNNL learned further about the side-bend test (SBT). This test is easily implemented in the laboratory in order to support the assessment of NDE with respect to fusion joint quality. A procedure for this test was developed, but there have not been any studies conducted to compare SBT results with those provided by the high-speed tensile test, which is the accepted industry standard for assessing HDPE fusion joint quality. The procedure (McGraff and McElyen 2009) developed by ISCO Industries that was provided for the SBT systematically leads one through the steps necessary to design a simple test apparatus and subsequently conduct the bend tests. PNNL chose to pursue the SBT and was able to perform these tests in the same building where the NDE inspections were conducted.

PNNL acquired an inexpensive pipe-bending apparatus from a local discount tool store. The setup allowed the hydraulic cylinder to be driven by a manual pump, or by a switch-activated air supply that was advantageous for a laboratory system where hundreds of samples could potentially be tested. Figure 4.21 shows the pipe-bending apparatus that was purchased along with the mandrels and ram machined according to the guidance in the ISCO Industries procedure. The air-operated switch was used in all testing; this switch had a screw-adjustable limit that was used to set the rate of ram travel to what was directed in the ISCO Industries procedure. The ram speed was specified at approximately 1 inch (25 mm) in 20 seconds and the PNNL system was set to 1 inch (25 mm) in 18 seconds. During actual testing, the ram was moved a fixed distance and stopped so that if a flaw appeared it was documented with a picture and measurements of its size. In this way, the flaw growth was tracked for potential later evaluation if there was a need. A dial indicator as shown in Figures 4.21 and 4.22 was set to zero when the ram was just in contact with the HDPE specimen, and when a crack occurred, the ram travel distance was recorded.

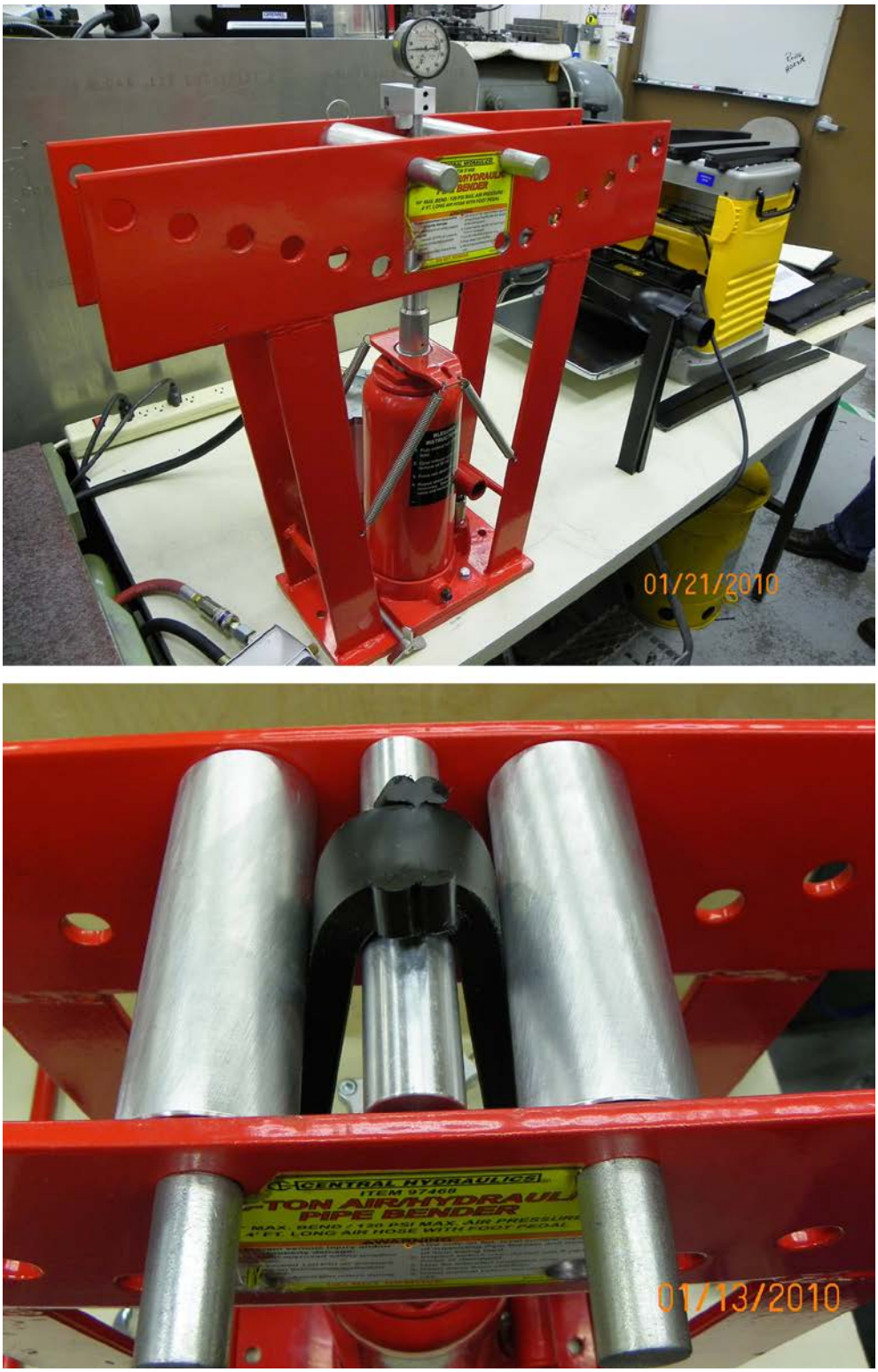

Figure 4.21 Side-Bend Test Apparatus (top) with an HDPE Test Specimen from Pipe 1224 Undergoing Testing (bottom) – Example of a Dark Green SBT Result

Figure 4.22 Another HDPE Specimen Undergoing Side-Bend Testing Showing the Dial Indicator Used to Track Travel of the Ram Which, in This Case, is Showing the Maximum Travel of 2.5 Inches (63.5 mm) as Shown by the Upper Right and Lower Left Dials. This is an example of a light green SBT result.

While awaiting arrival of a planar for preparing SBT specimens, it was decided to simply cut off (using a saber saw) HDPE samples from several of the pipes and use a milling machine to produce flat samples with a ½-inch (12.7-mm) thickness in the circumferential direction. The first specimen chosen was 1224 because it was manufactured under the best conditions and would provide a sample that should successfully pass the SBT. Figure 4.21 shows the end result, a pass, for this specimen. The next specimen selected was from pipe 126 in a zone where there were many NDE indications. The test was performed and the specimen failed the SBT as shown in Figures 4.23 and 4.24 after a total ram movement of 2.5 inches (63.5 mm). This is the maximum displacement used in the side-bend testing and at this position of 2.5 inches (63.5 mm) the included angle between the sides of the test specimen was 17 degrees. When the planar arrived, it was decided to try it out on another sample from pipe 1224. The specimen was cut out of the pipe with a saber saw and then run through the planar to achieve test dimensions. Figure 4.25 shows that this specimen from pipe 1224 failed the SBT. It should be noted that this second sample was removed adjacent to the first sample that was tested and did not fail as shown in Figure 4.21.

Figure 4.23 Specimen from Pipe 126 Part Way Through the Side-Bend Test Showing the Early Stages of Failure

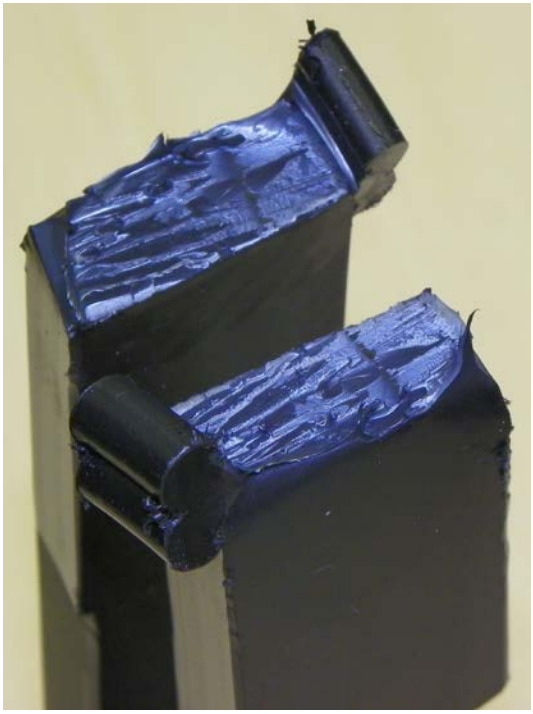

Figure 4.24 The Specimen from Pipe 126 at the End of the SBT – Example of a Red SBT Result

Figure 4.25 Sample from Pipe 1224 Failed the SBT and Was Removed Adjacent to the Specimen Shown in Figure 4.21, Which Did Not Fail – Example of a Red SBT Result

Considering these confusing results, it was decided to move cautiously forward and cut out some key areas from specimen 127, because of the multiple NDE indications on this specimen. The areas selected were referenced to their location from the zero reference mark that was employed by the NDE teams. The test locations described herein are the distance from the zero reference location to the center of the SBT specimen. Test results are listed in Table 4.2. The locations of 3.5, 15.5, 21, 34.5, and 36 inch (88.9, 393.7, 533.4, 876.3, and 914.4 mm) were selected because most all of the NDE methods reported indications in these zones. The location at 8-inch (203.2 mm) was selected because none of the NDE methods made any defect calls at this location, and 9.25 inch (235.0 mm) was selected because only the microwave technique reported an indication at this location.

Table 4.2 SBT Results on Pipe 127

Location, inch (mm)	Result	Comment
3.5 (88.9)	Partial failure	Flaw in middle of fusion area popped in at 1 inch (25.4 mm) of ram travel; flaw grew to ¾ inch (19 mm) in through-wall size at 2.5 inches (63.5 mm) of ram travel.
8.0 (203.2)	Burst apart	Broke at 0.47 inch (11.9 mm) of ram travel.
9.25 (235.0)	Burst apart	Broke at 0.41 inch (10.4 mm) of ram travel.
15.5 (393.7)	Broke	Broke at 0.22 inch (5.5 mm) of ram travel but only bead was holding the two pieces together; did not run ram to maximum travel to see if beads would break.
21 (533.4)	Broke apart	Broke at 0.2 inch (5.1 mm) of ram travel.
34.5 (876.3)	Broke apart	Went to 0.25 inch (6.4 mm) of ram travel and were observing the specimen when it suddenly popped into two pieces.
36 (914.4)	Broke apart	Broke at 0.35 inch (8.9 mm) of ram travel.

Based on the results in Table 4.2 for pipe 127, failure at all test locations, it was decided that conducting other tests such as a high-speed tensile test would not provide any new information on the quality of the fusion joint in this pipe. These results were studied, discussions were made with members of ASME Code SWG on HDPE, and the NDE results for other pipes were also studied to try to determine what would be the most effective way to assess the true structural condition of the fusion joints for which there were extensive NDE results. It was decided to take an entire section of a pipe and cut it into ¾-inch (19-mm) thick slabs that could be planed to ½ inch (12.7 mm) for conducting SBTs. Specimen 1224 was selected for further study because it was joined under ideal conditions but had shown failure in the high-speed tensile test. Additional data from slicing part of the joint was also available and several SBTs had been performed. To complete the study on this specimen, it was decided to section the remaining joint material into as many pieces as possible for the SBT. As this work began, the effort on how best to capture the results for the SBT so that they could be presented and easily interpreted was expanded. One issue was to determine what it means to fail a side-bend test. This issue became more complex as the actual SBT results were being generated. After much discussion and several efforts to plot the results, it was finally decided that a color scheme would be used to capture the final condition of each SBT specimen.

It was decided that if a SBT sample survived a full bend with no flaw result, as is shown in Figure 4.21, this sample would be color-coded as **dark green**. If any flaws that happened to be in the base material were observed, then these would be recorded but because the test was on the fusion joint, base material flaws would not alter the decision on what color to use for the test result. It was decided that if there was a flaw that occurred but that there were remaining ligaments at both the ID and the OD of the specimen, then this condition would be recorded as a **light green**. Such a flaw is shown in Figure 4.22. It was also decided that if the test specimen completely separated into two pieces without any ID or OD ligaments, then it would be color-coded **red**, as is illustrated in Figures 4.24 and 4.25. The only other unique condition

was a flaw in which there was still a remaining ligament on either the ID or the OD. This condition was color-coded **yellow** and an example is shown in Figure 4.26.

Figure 4.26 Example Where Only One Ligament Remained at Location +12 on Pipe 1224 – Example of a Yellow SBT Result

This color scheme was then applied to the results of each of the SBT specimens. Figure 4.27 shows the SBT results for pipe 1224. The blank zone located at the 2 o'clock (2:00) position was an area that had been removed in order to conduct some slicing of the fusion joint to assess its integrity; this process was described in Section 4.1. For this region, the slicing did not reveal any flaws and could be colored green. The area from about 6:30 to 9:00 was a piece cut out and subjected to the high-speed tensile testing that was described in Section 4.2. In this region, the high-speed tensile test produced a brittle failure and this region could be colored red.

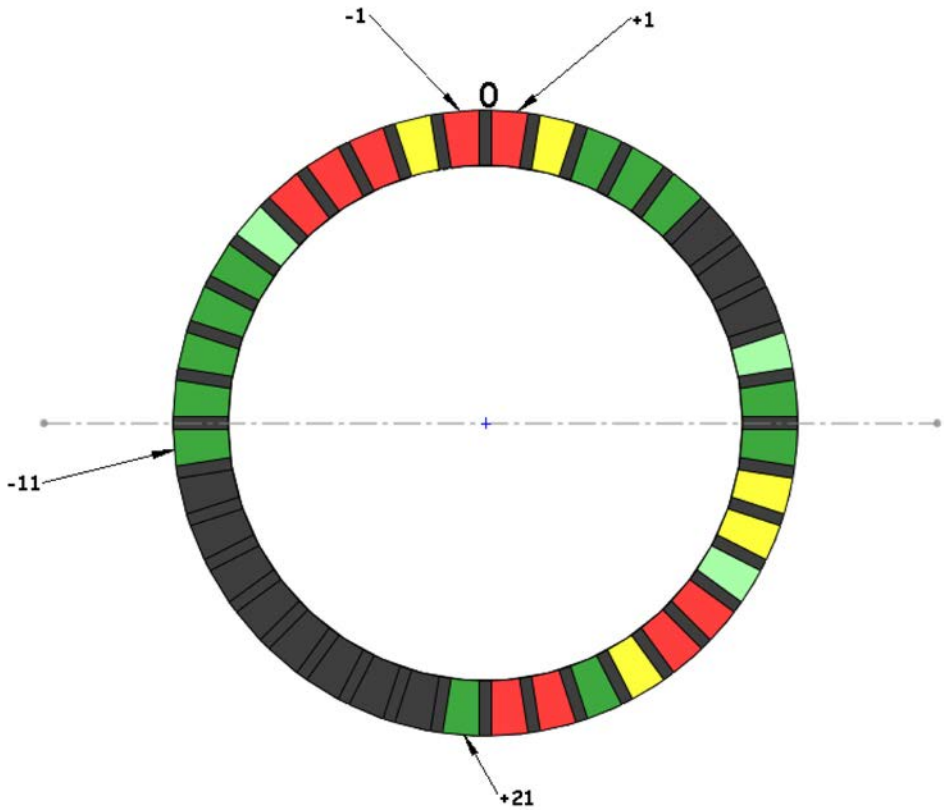

Figure 4.27 SBT Results for Pipe 1224

Based on the results from pipe 1224, additional discussions with plastic pipe experts, and further examination of NDE results, there was certain disagreement in the result and this had implications on how to proceed with the destructive testing. One proposal surfaced and suggested that inherent flaws contained in the base material were leading to the surprising destructive test results. To investigate this theory, PNNL took the base material that was in the already failed segments of pipe 1224 SBT test specimens and subjected the base material on both sides of the fusion joint to a SBT. There were 11 failed SBT specimens thus providing 22 segments for testing. None of these base material segments failed. There were, however, eight very small flaws that were found; the largest of these flaws is shown in Figure 4.28.

Next, patterns were noticed in the NDE results. It appeared that two quadrants in each pipe had a higher numbers of defect calls and two quadrants had a smaller number of defect calls. It was decided to select one quadrant that had the higher incidence of calls and one that had a smaller number of calls for further SBT testing. These two quadrants from each pipe would be cut into approximately ¾-inch (19-mm) slabs that would be planed to ½ inch (12.7 mm) and subjected to SBT. The remaining two quadrants would be reserved for future study if it was determined that further study would provide closure to any research questions. The SBT of two quadrants was performed and the resulting SBT results are shown in Figures 4.29 through 4.33 for pipes 123, 1212, 1214, 1218, and 1223.

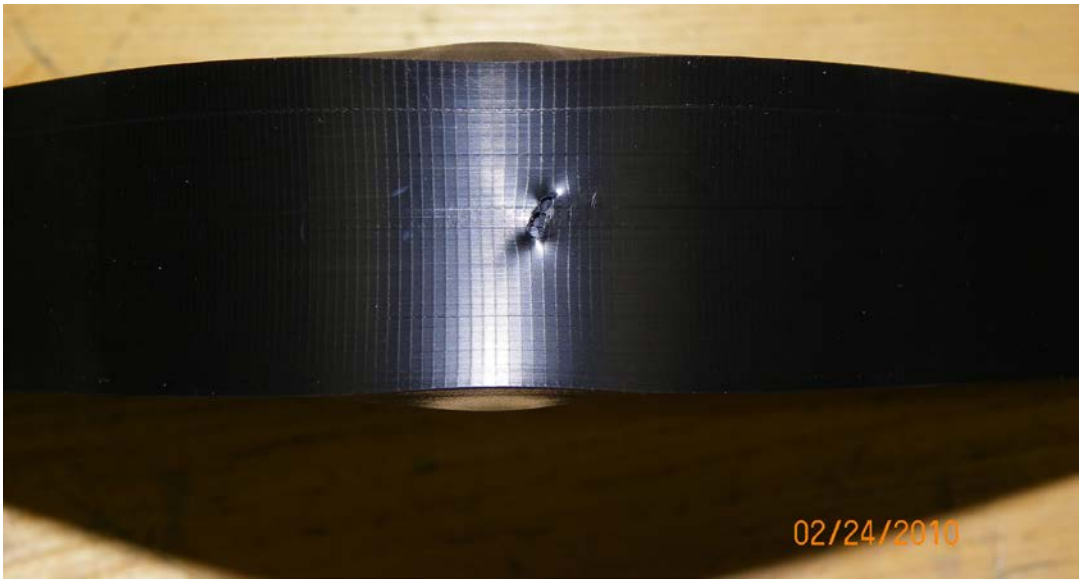

Figure 4.28 Largest Base Material Flaw Found in the 22 Base Material Samples Tested for Pipe 1224

The next step in this process is to combine these destructive testing results with the NDE inspection results to try to develop correlations on what each NDE technique can detect and what it does not detect. These results are discussed in the next section.

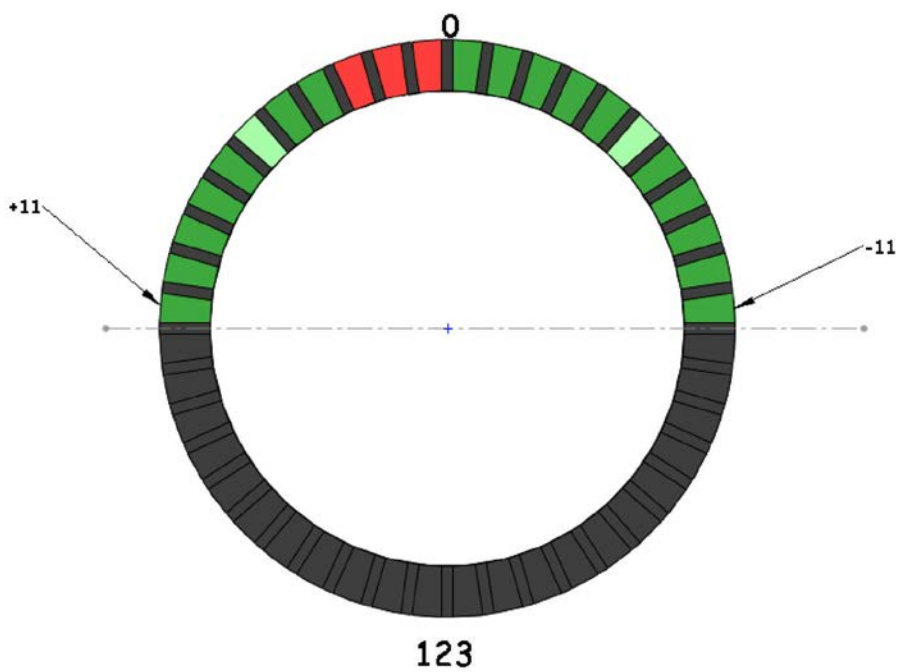

Figure 4.29 SBT Results for Pipe 123

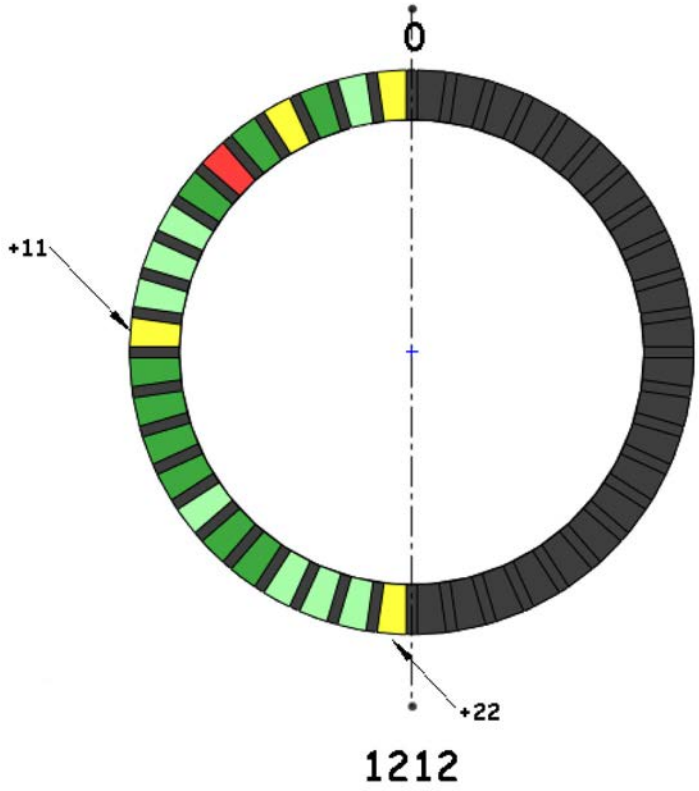

Figure 4.30 SBT Results for Pipe 1212

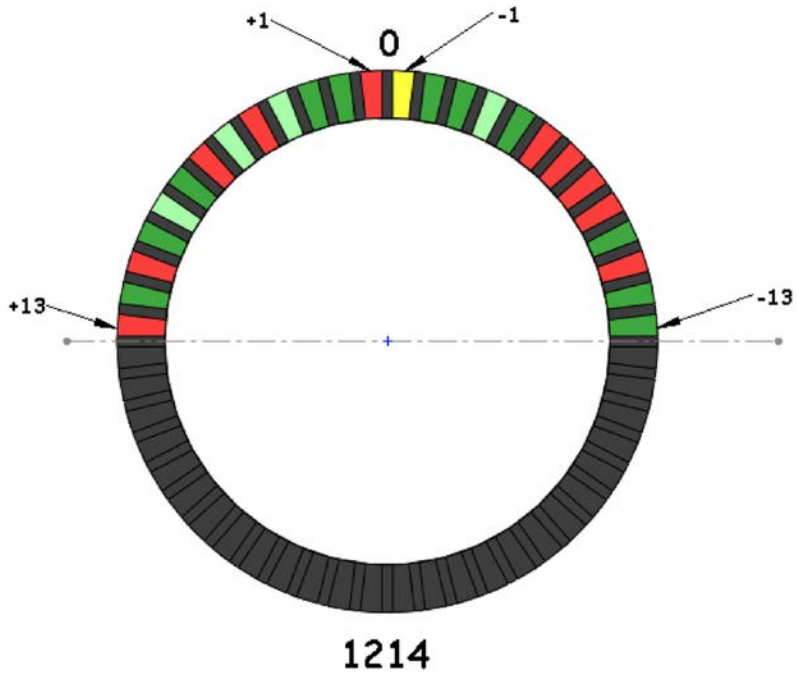

Figure 4.31 SBT Results for Pipe 1214

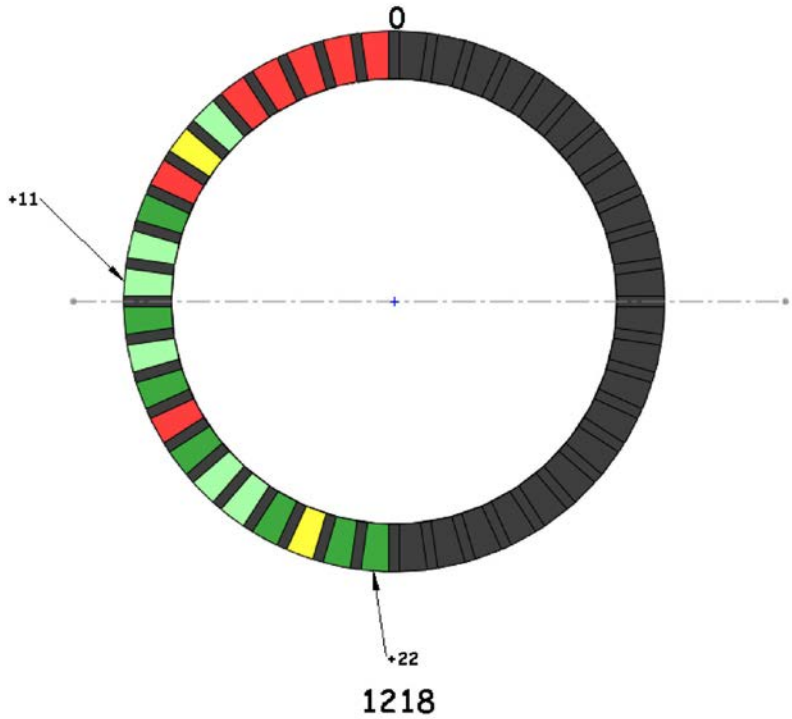

Figure 4.32 SBT Results for Pipe 1218

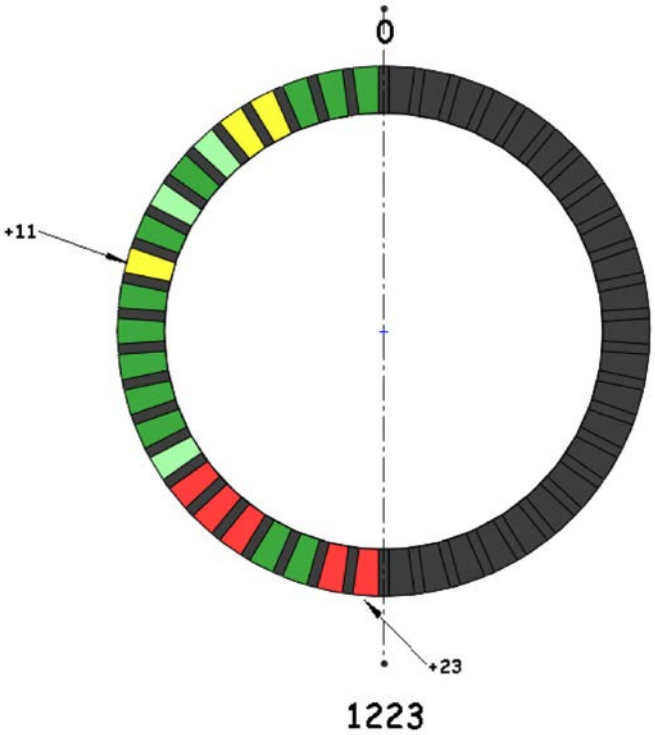

Figure 4.33 SBT Results for Pipe 1223

5 DISCUSSION OF NDE AND DE RESULTS

This section includes discussion intended to integrate the NDE results from Section 3 with the DE results from Section 4. The goal is to try to understand what fusion conditions each NDE technique can detect, or not detect, and correlate these indications with actual joint integrity findings, as determined from mechanical tests. If all flaws are detected and false calls are not made, then the work could be considered fairly complete, thus only limited additional studies would be needed to examine other inspection variables, or to validate the initial results. If some conditions are detectable and others are not, then a direction for further work can be derived. The first challenge is to come up with a means to integrate the NDE and DE data onto a single visual display, such as a chart, graph, or figure, where all data can meaningfully be depicted to assist in this correlation. The strategy that will be followed involves providing the results for each butt fusion pipe joint, but only where there is mechanical test data created through destructive testing. The quadrants that were not destructively characterized have been summarized into a similar format as those containing DE data; however, these are only presented in Appendix E, so that the reader is not confused between quadrants containing DE data and those that do not.

The testing that was performed included a variety of different NDE and DE methods; for clarity, if a particular method was employed on a specimen, that method will be listed in a legend box under each figure. The locations where an NDE method detected a flawed condition in the fusion joint are plotted with a solid line. In locations where NDE methods produced responses that were different from background noise, but possibly similar to flaw-type responses, the plotting protocol employs a dashed line. This should be considered as a marginal call. Finally, to keep the plots from becoming too cluttered, it was decided not to plot areas where destructive testing found no flaws, which are the dark green test results. Thus, the legend will only show SBT Red, SBT Yellow, and SBT Light Green. However, there are two exceptions to this rule: (1) DE on specimen 127 was performed on a limited basis to preserve areas that had interesting NDE responses. All seven areas cut out for the SBT failed as either Red or Yellow. It was decided that based on these results, there would be little value in conducting further DE testing, so the remaining material was saved for potential additional NDE. (2) The other exception was specimen 1224, where only limited DE was performed on quadrants 2 and 4 using the SBT because a portion of quadrant 2 was subjected to the high-speed tensile test and an area of quadrant 4 was sliced using a microtome.

The following figures summarize the NDE and DE results with the captions commenting on the findings. The visual and bead profile results will not be included in the discussion as the visual results are considered a surface evaluation, not volumetric, and the bead profile results were an indication of fusion pressure applied during the heat cycle, which is an abnormal condition. Marginal calls, as represented by the dotted lines, will not be discussed either since they are not definite flaw calls.

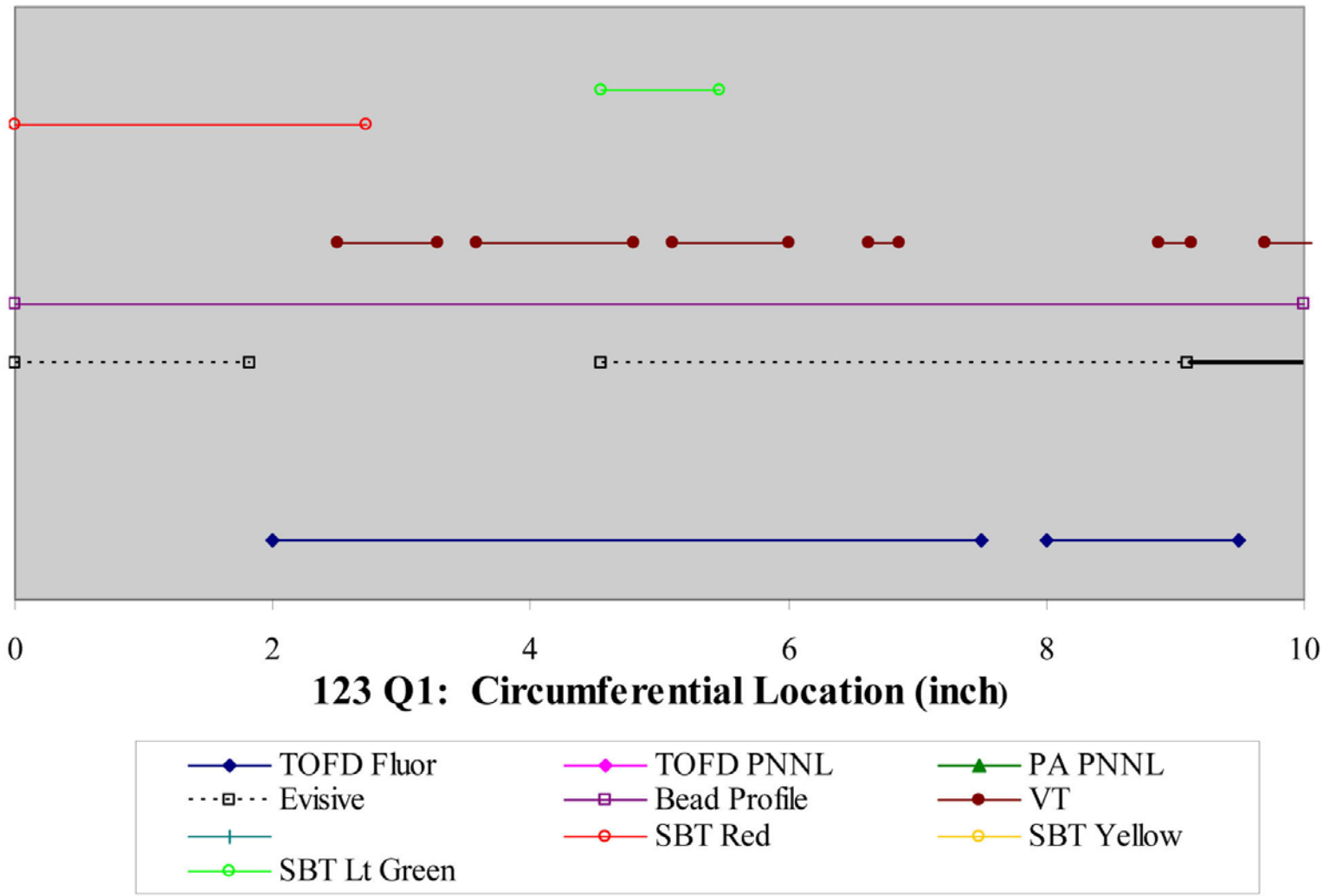

Figure 5.1 **DE Results as Determined from the SBT Results Do Not Correlate with Any of the NDE Results. TOFD Fluor captures the SBT Light Green but misses most of the SBT Red region and has a large false call rate. Evisive has a false call region on the right.**

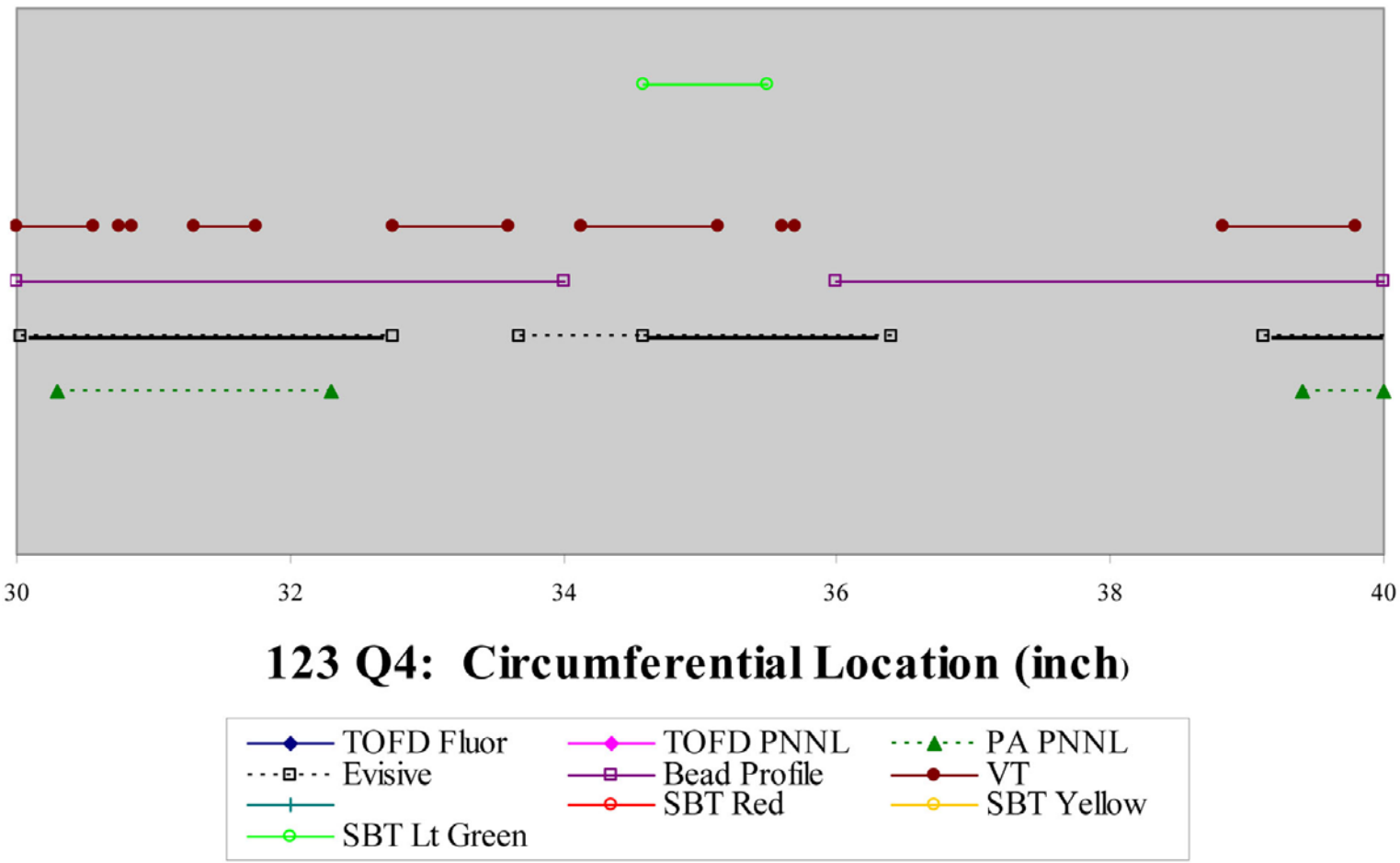

Figure 5.2 Evisive is the Only NDE Technique that Correlates with the SBT Light Green DE Results Although It has Many False Calls

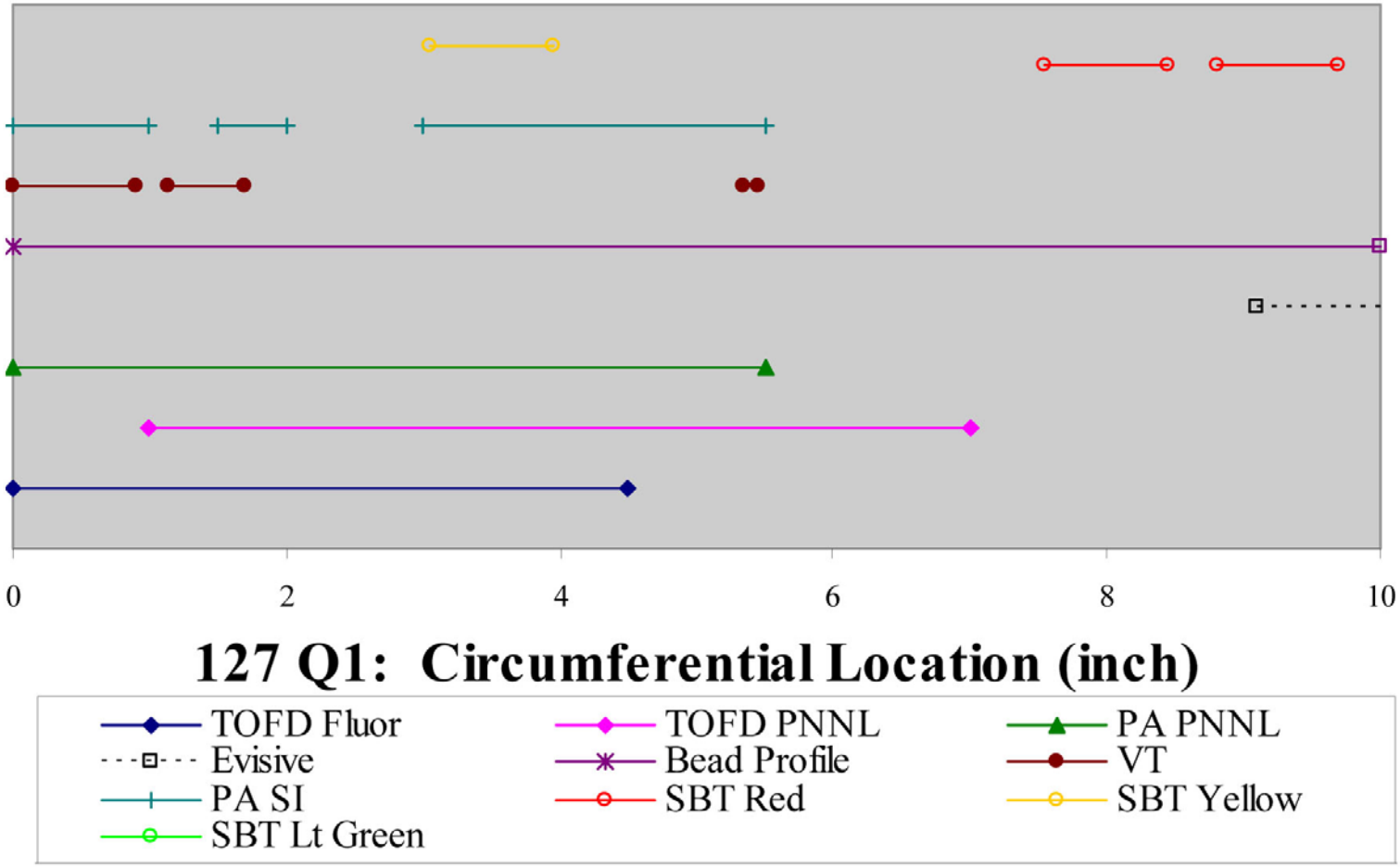

Figure 5.3 SBT Yellow Region was Detected with the NDE PA-SI, PA-PNNL, TOFD-PNNL, and TOFD-Flour. The SBT Red region was not detected by any of the NDE techniques. Note that only a select few regions from pipe 127 were subjected to the SBT and they all failed in the Yellow or Red mode. It was assumed that the entire pipe joint was bad so these plotted summary results should be used only for a correlation of the plotted SBT results and the NDE results and not as an indicator of false calls.

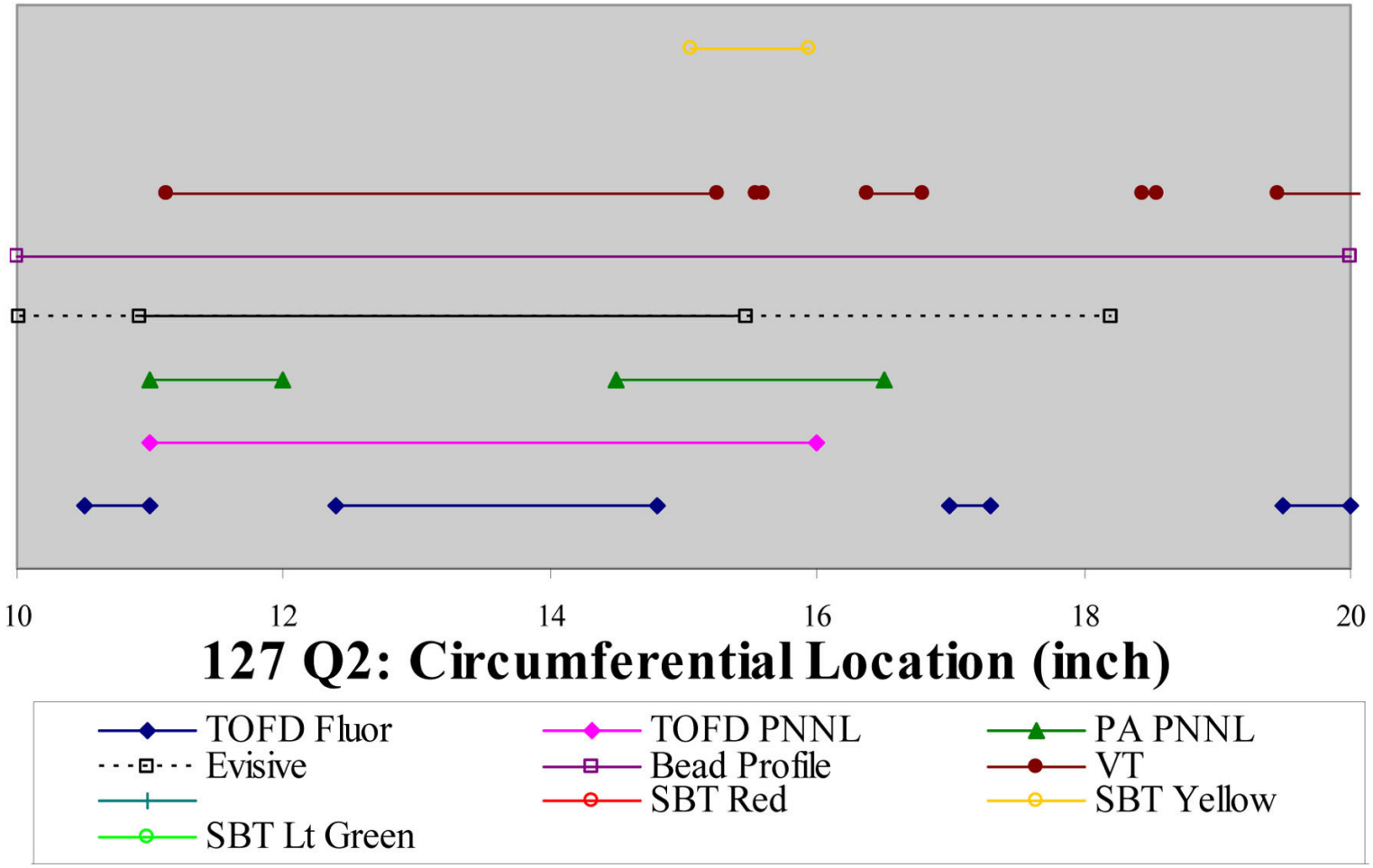

Figure 5.4 SBT Yellow Region was Detected by NDE Evisive in Part, PA-PNNL, and TOFD-PNNL. Note that only a select few regions from pipe 127 were subjected to the SBT and they all failed in the Yellow or Red mode. It was assumed that the entire pipe joint was bad so these plotted summary results should be used only for a correlation of the plotted SBT results and the NDE results and not as an indicator of false calls.

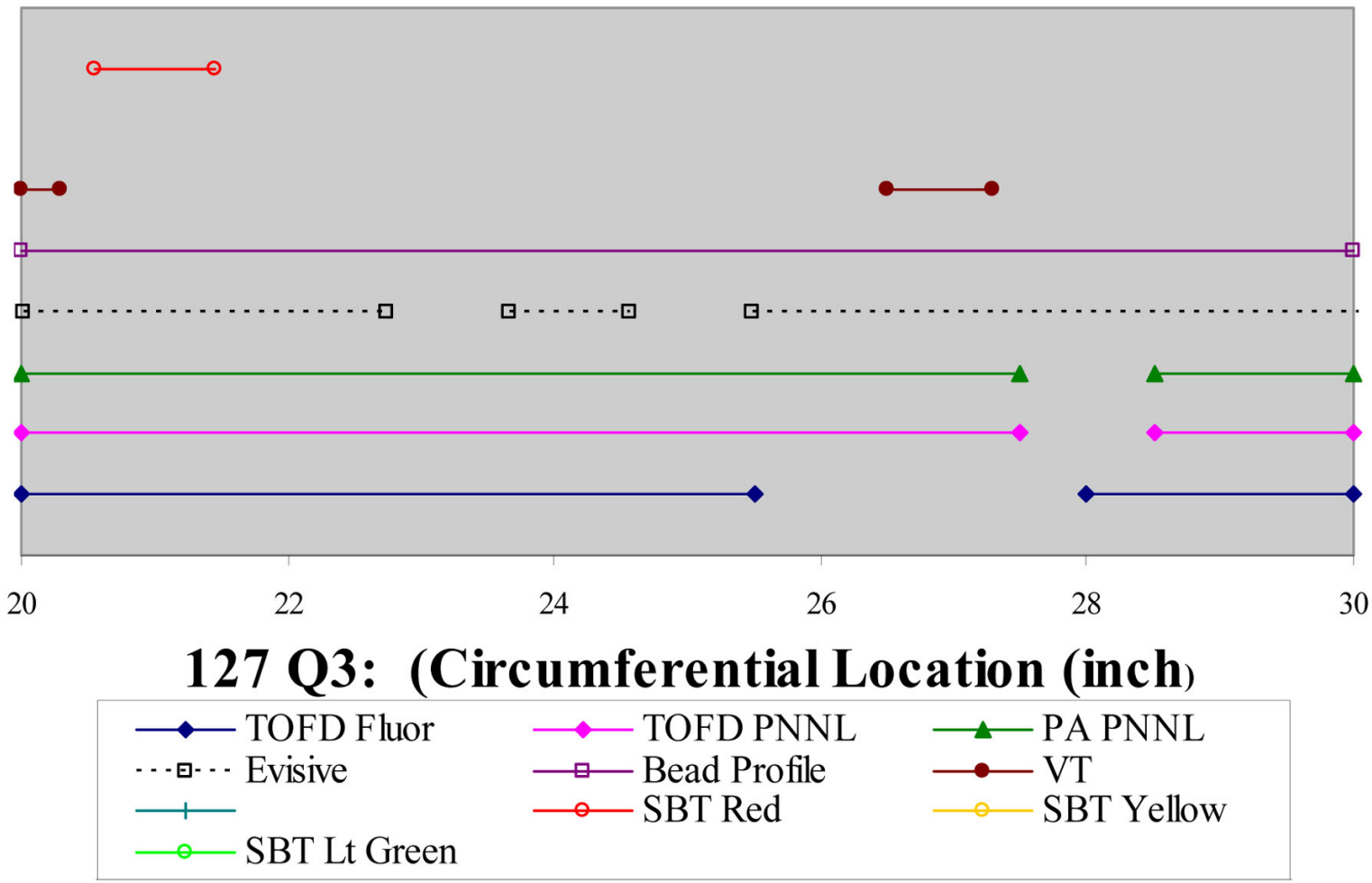

Figure 5.5 SBT Red Region was Detected with PA PNNL, TOFD PNNL, and TOFD Fluor. Note that only a select few regions from pipe 127 were subjected to the SBT and they all failed in the Yellow or Red mode. It was assumed that the entire pipe joint was bad so these plotted summary results should be used only for a correlation of the plotted SBT results and the NDE results and not as an indicator of false calls.

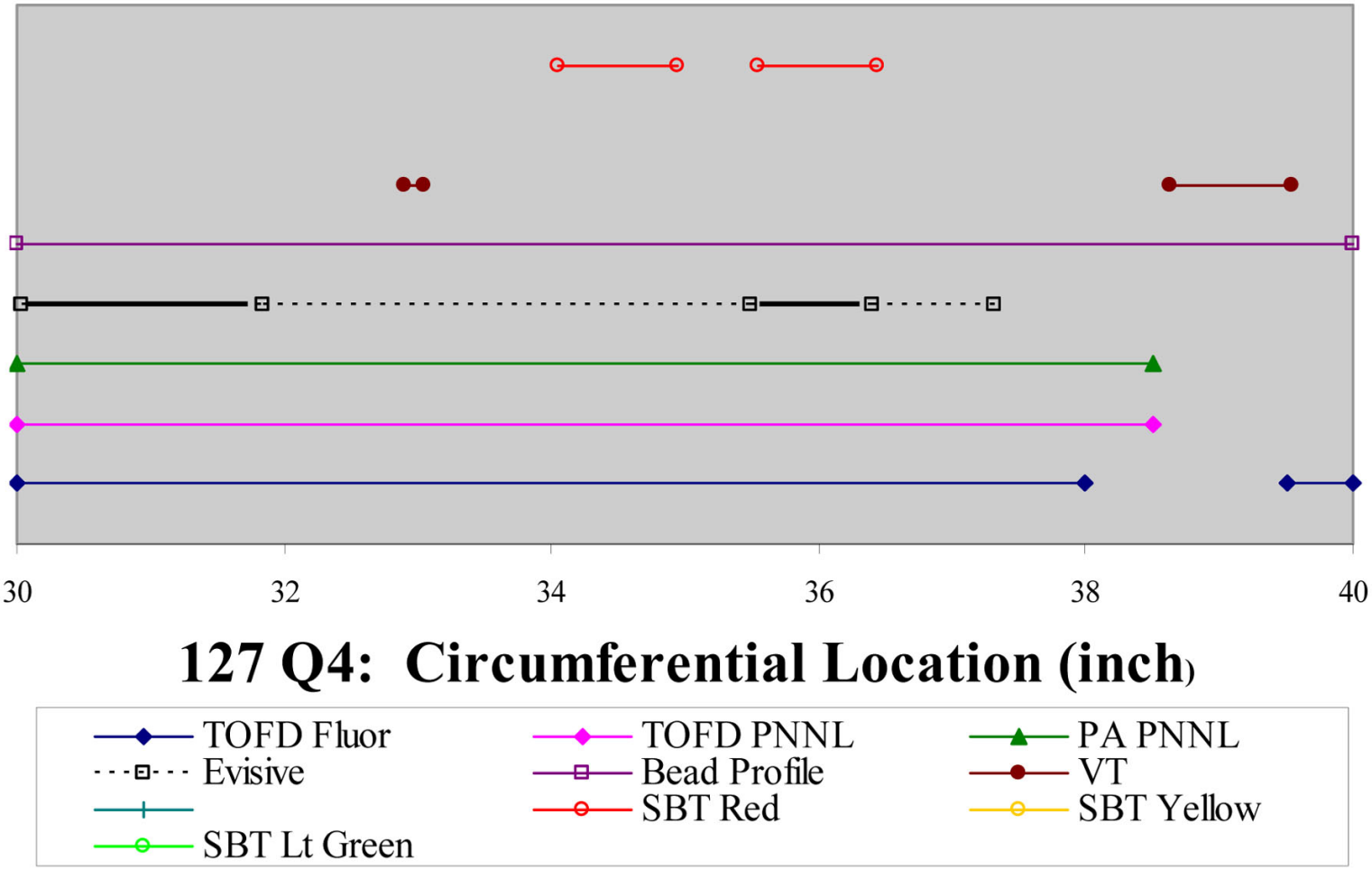

Figure 5.6 SBT Red Region was Detected in Part by Evisive and by PA PNNL, TOFD PNNL, and TOFD Fluor. Note that only a select few regions from pipe 127 were subjected to the SBT and they all failed in the Yellow or Red mode. It was assumed that the entire pipe joint was bad so these plotted summary results should be used only for a correlation of the plotted SBT results and the NDE results and not as an indicator of false calls.

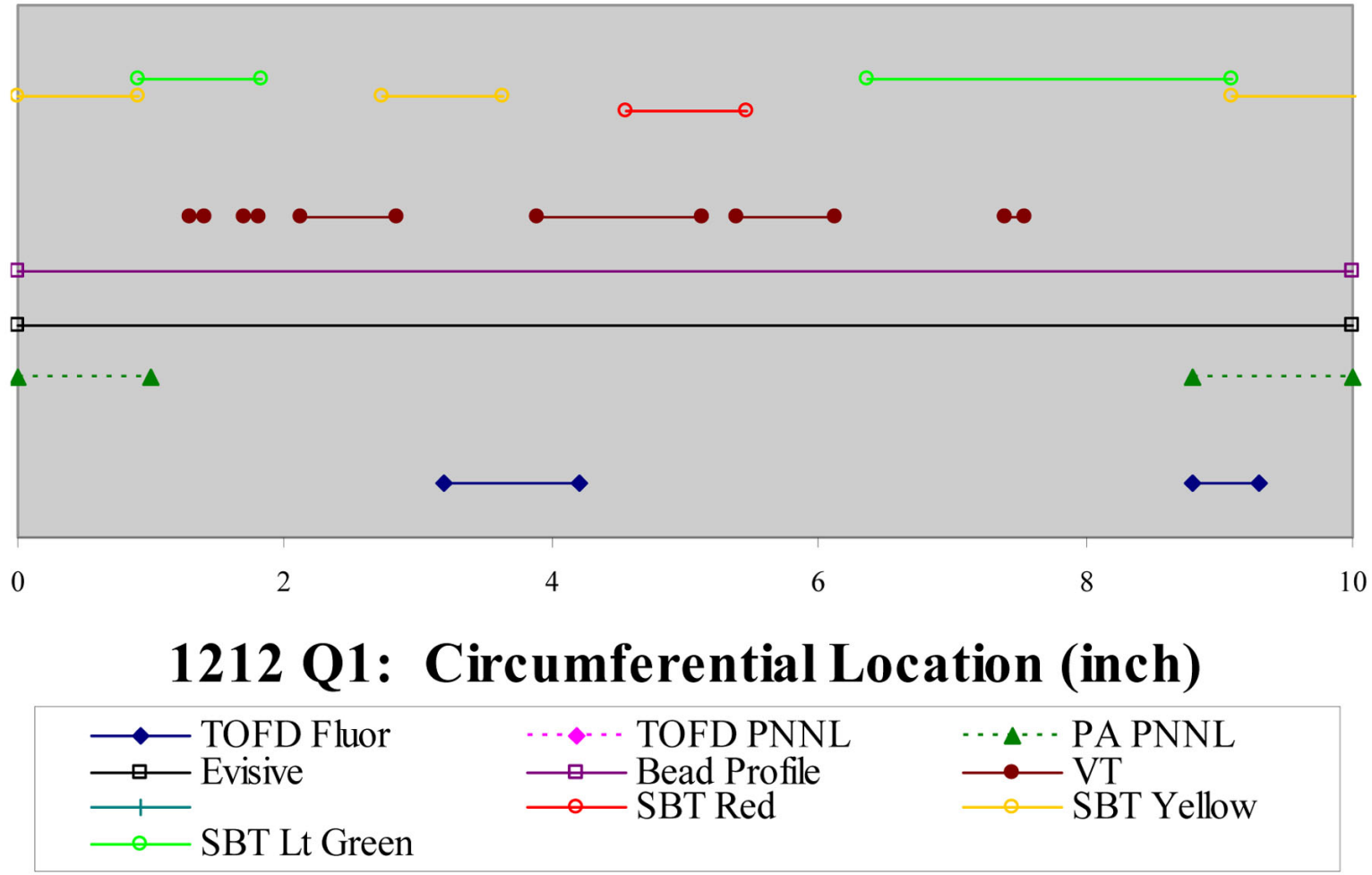

Figure 5.7 **Most of This Specimen Showed Some Type of Failure in the SBT. Evisive NDE detected flaws over the entire quadrant and TOFD Fluor detected two flawed regions.**

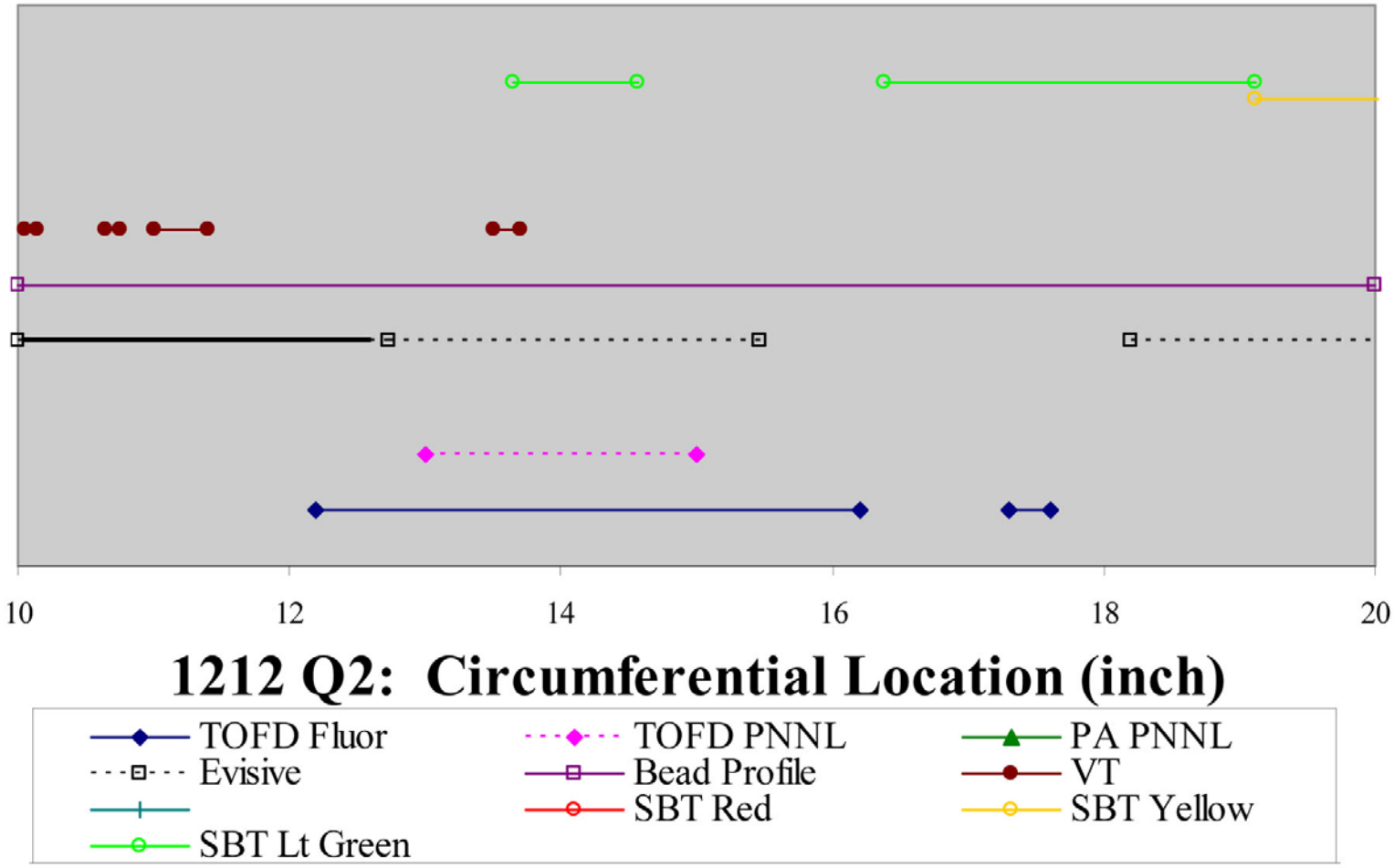

Figure 5.8 SBT Failure Regions were Only Detected with NDE TOFD-Fluor; However, There were False Call Regions as Well

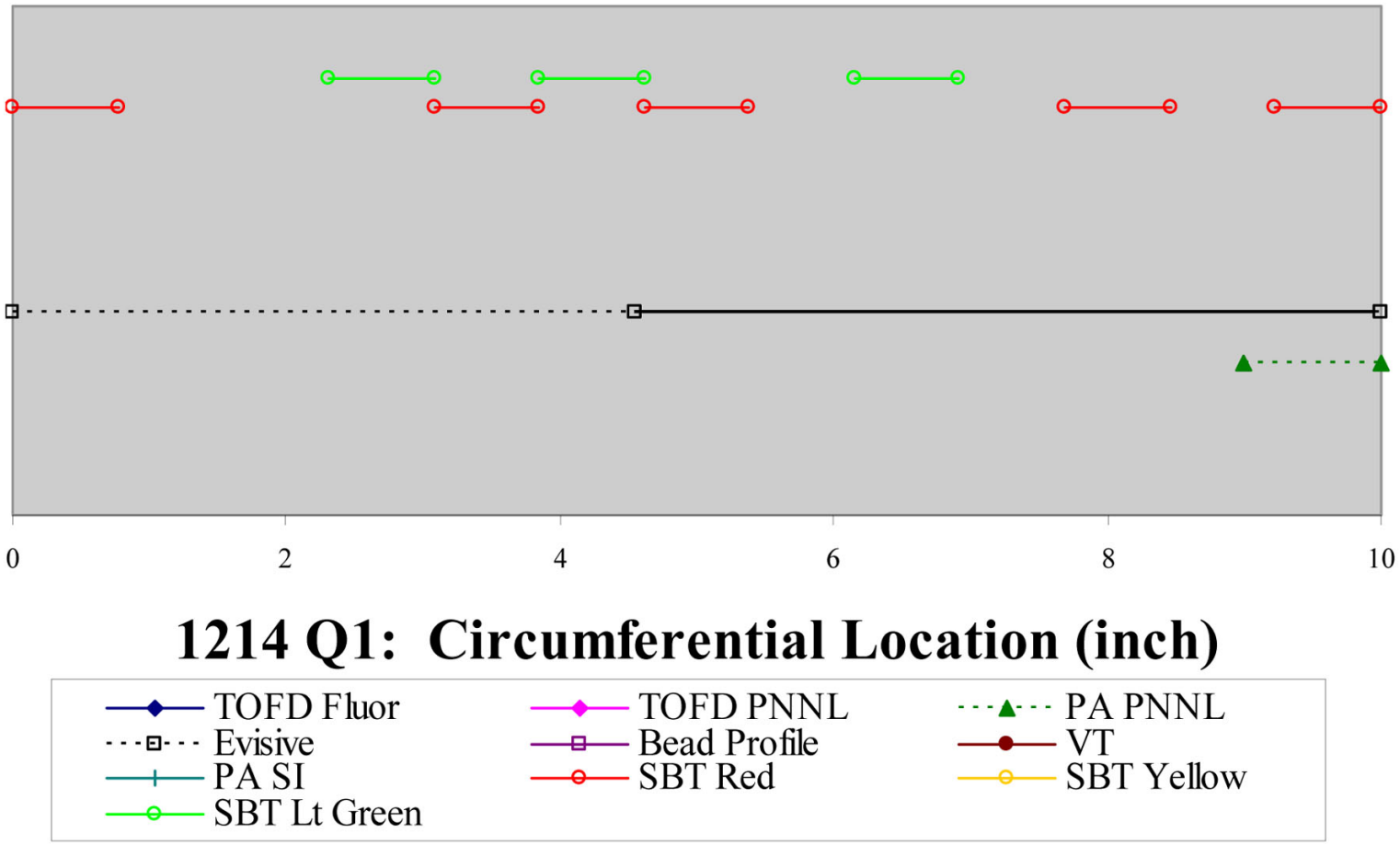

Figure 5.9 SBT Failure Regions Covered Most of This Quadrant and were Partially Detected with Evisive NDE

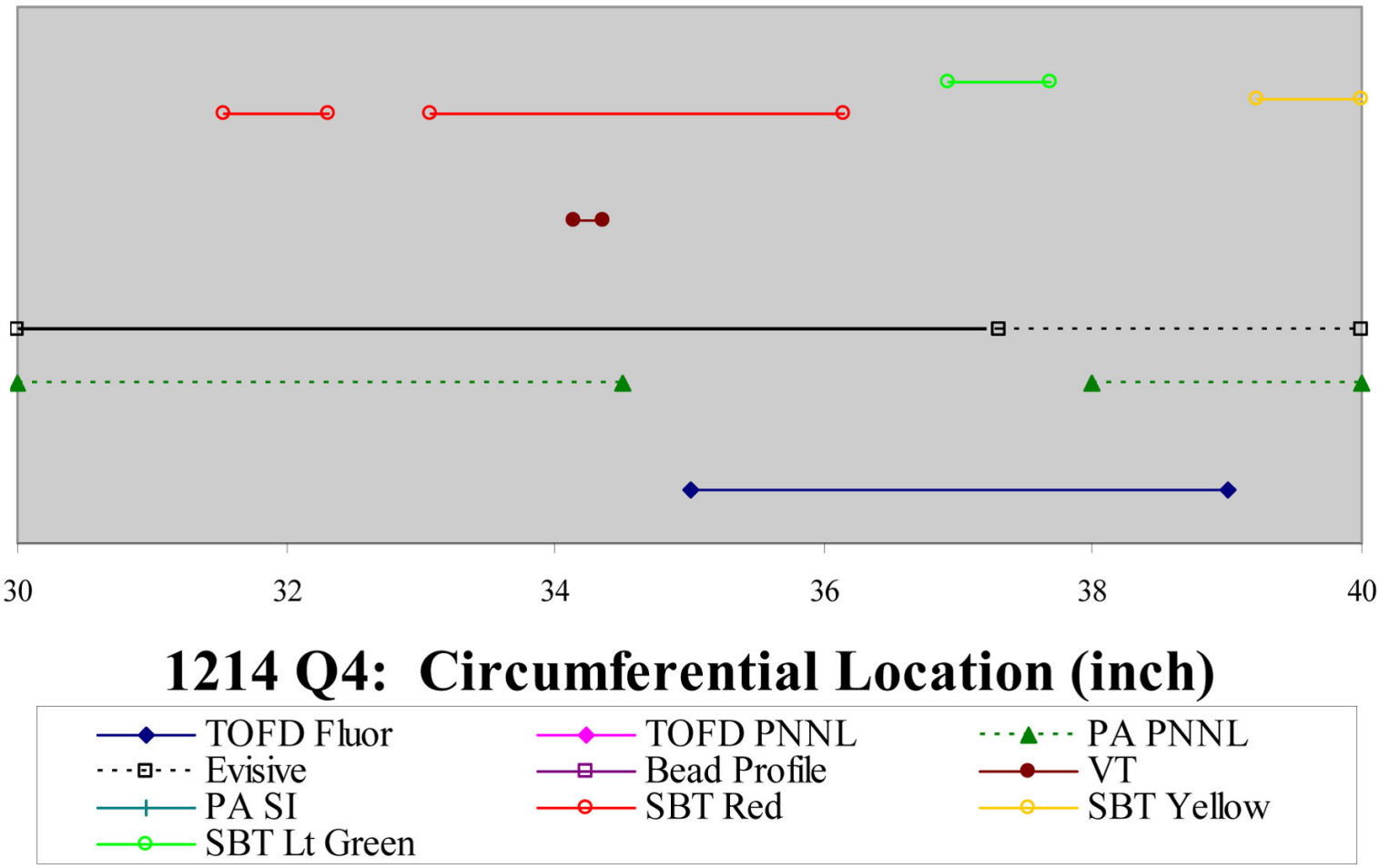

Figure 5.10 SBT Failure Regions Covered Most of This Quadrant and were Partially Detected with Evisive and TOFD Fluor NDE

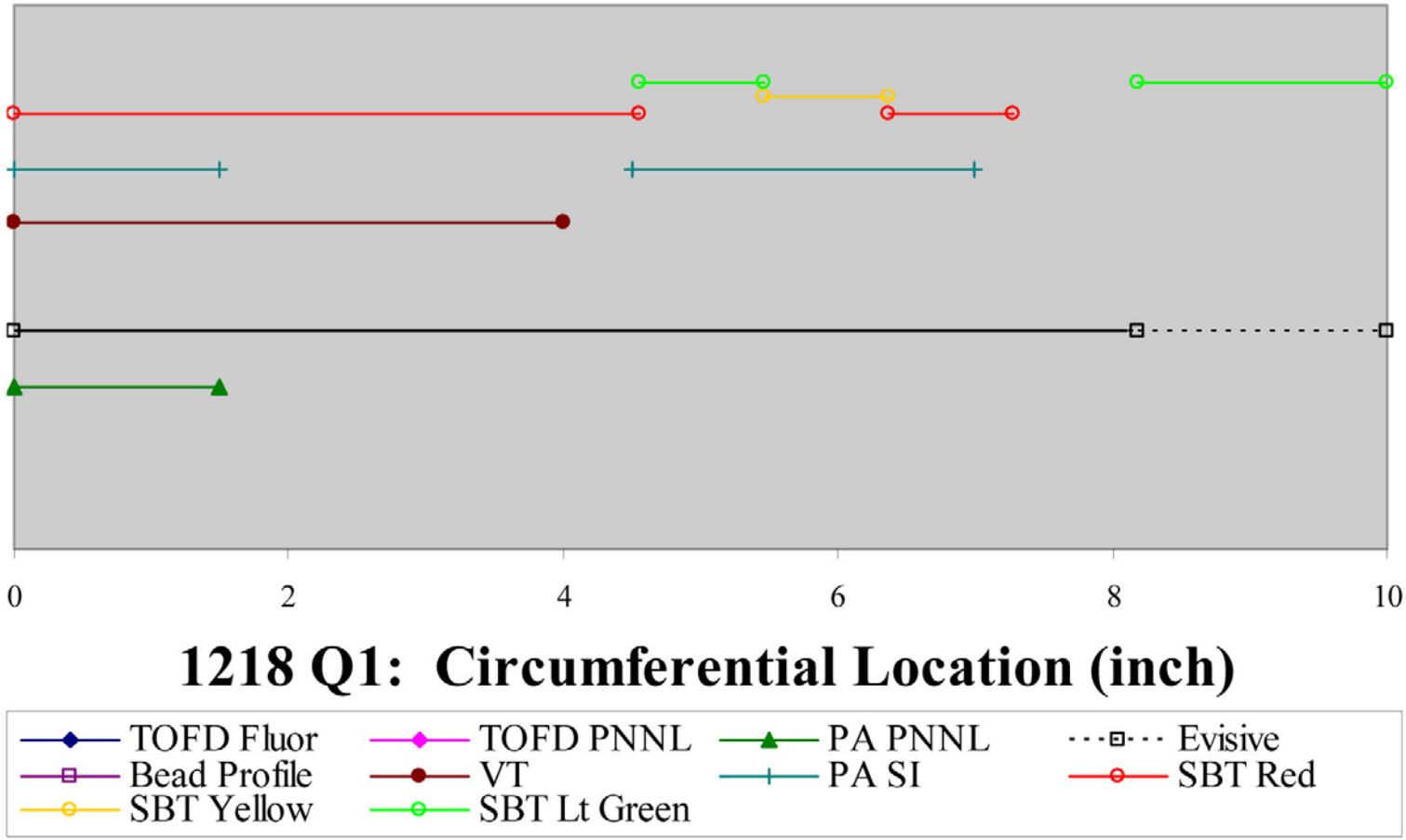

Figure 5.11 SBT Failure Regions Covered Most of This Quadrant and were Well Detected with Evisive NDE. PA SI and PA PNNL detected some of the failure regions.

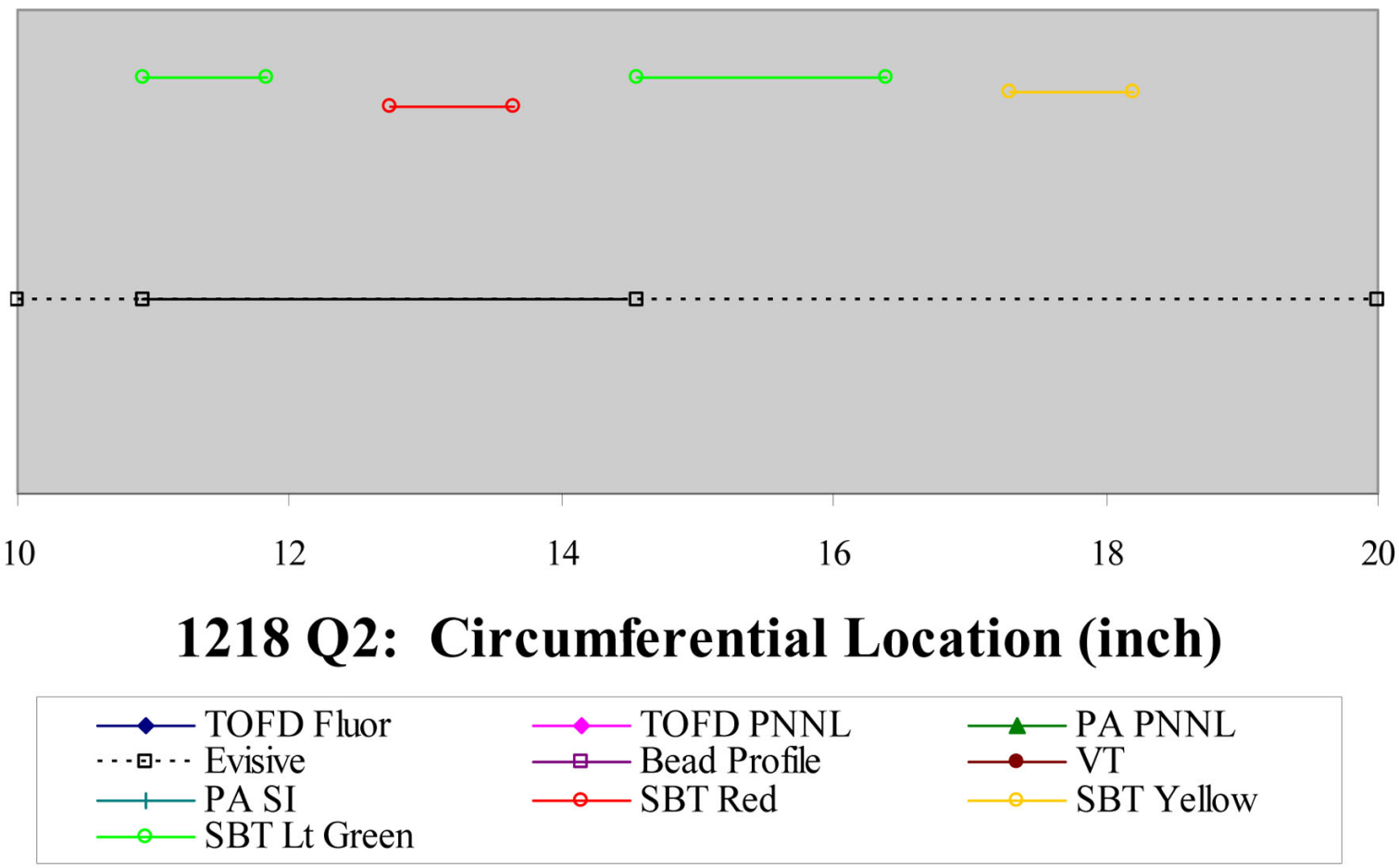

Figure 5.12 Majority of This Quadrant Failed in the SBT to Some Extent. Only the Evisive NDE technique called any flaws. There were false call areas as well.

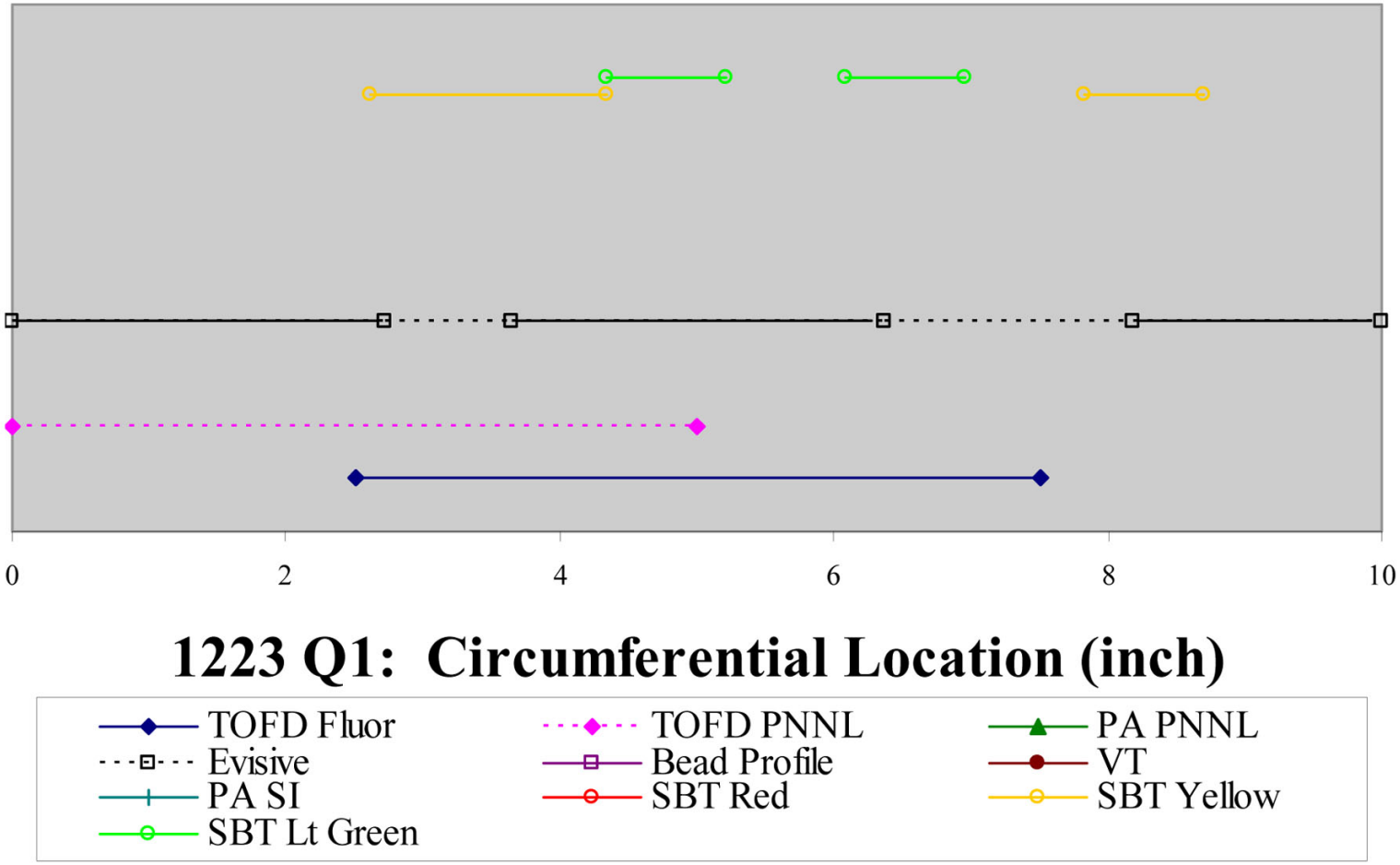

Figure 5.13 Approximately Half of the Quadrant Showed Signs of Failure in the SBT in the Yellow or Light Green Range. Evisive and TOFD Fluor NDE detected these regions; however, Evisive had false calls.

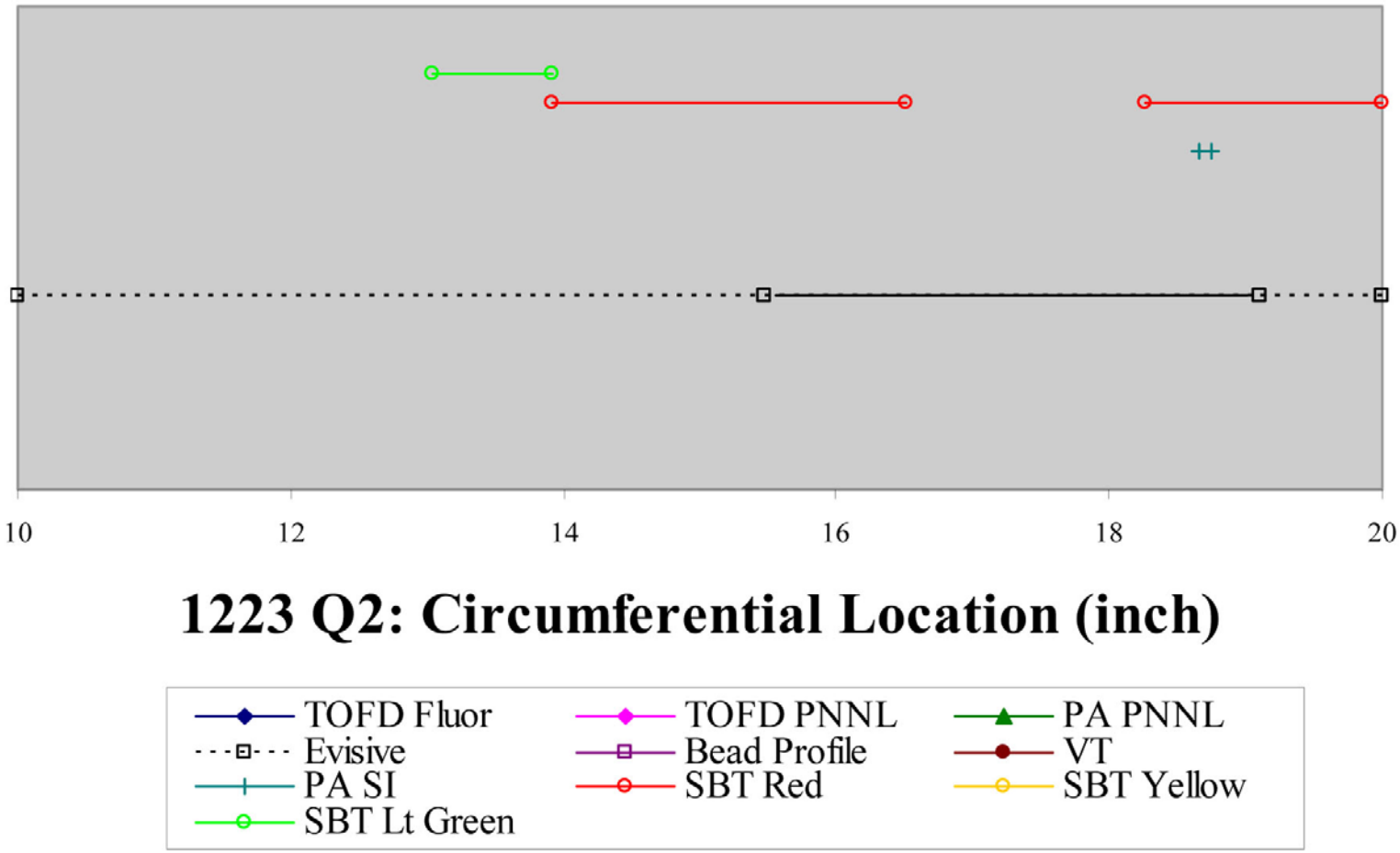

Figure 5.14 SBT Red Failure Regions were Partially Detected with Evisive NDE and a Very Small Region with PA SI NDE. Evisive NDE had a false call region.

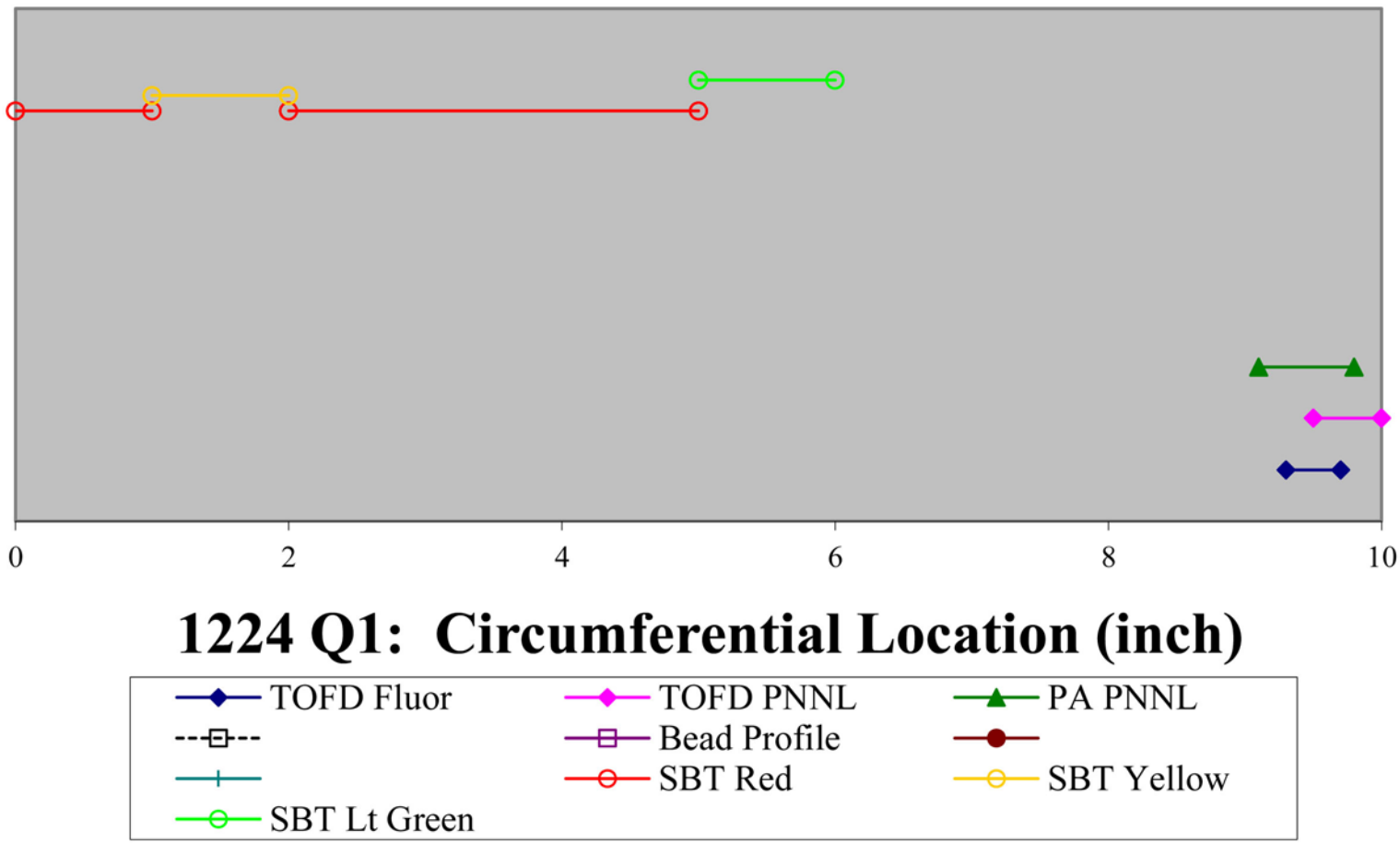

Figure 5.15 SBT Failure Regions were Not Detected by Any of the NDE Techniques. PA PNNL, TOFD PNNL, and TOFD Flour had small false call regions.

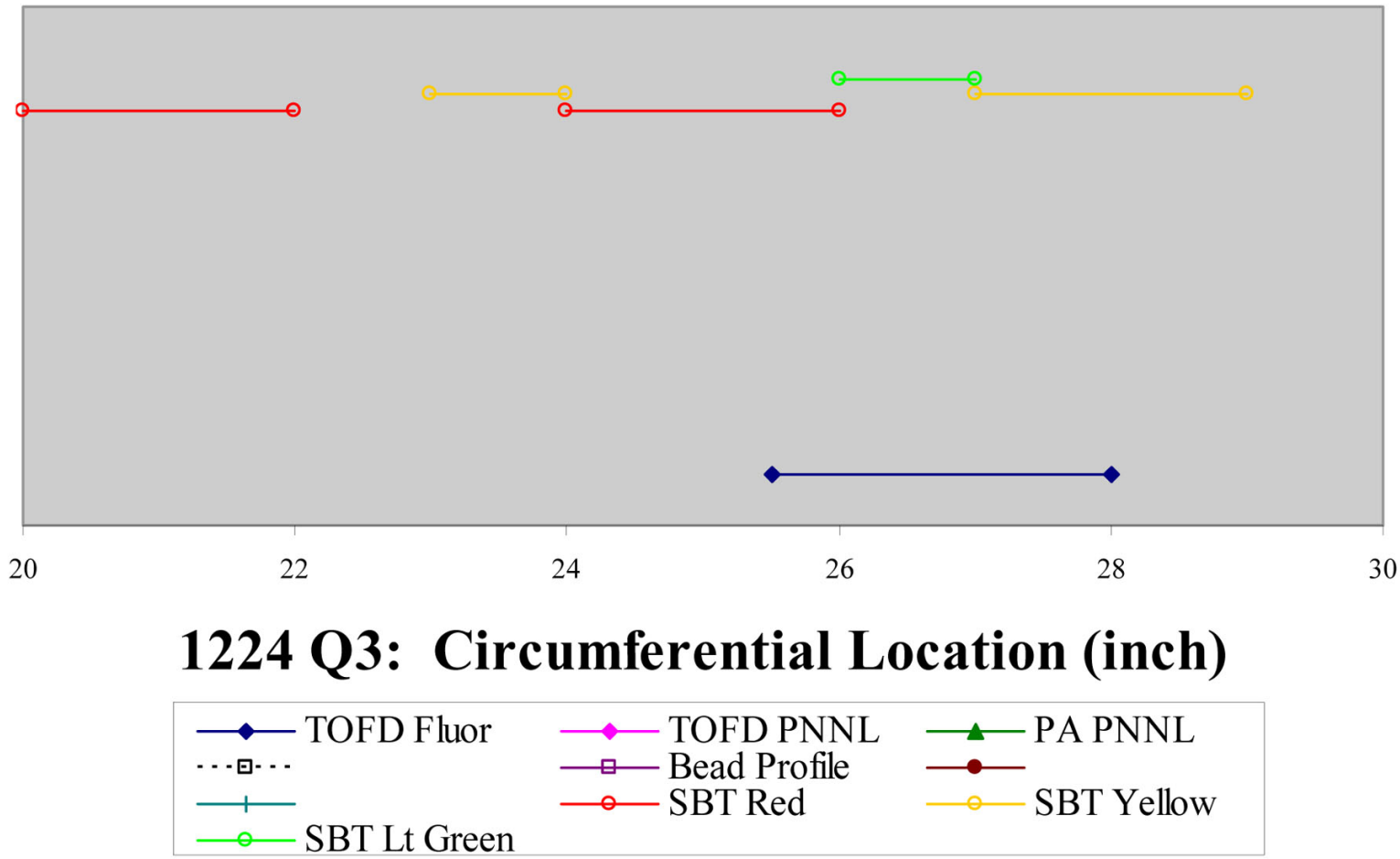

Figure 5.16 Quadrant Showed SBT Failures Over Most of the Quadrant. TOFD Fluor NDE detected part of the SBT Red region, the SBT Light Green region, and part of a SBT Yellow region. No other NDE techniques detected flaws.

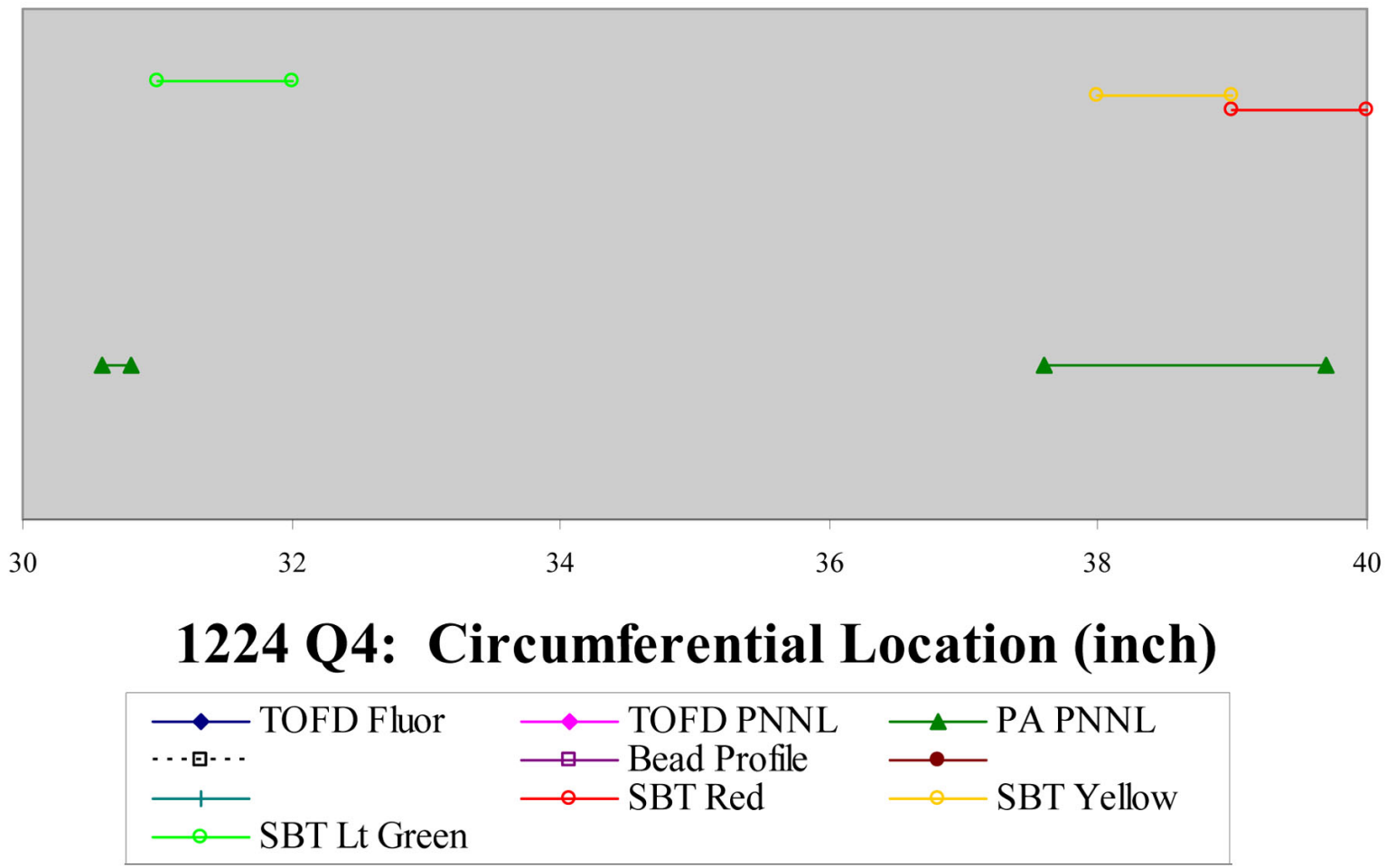

Figure 5.17 Several Flawed Regions were Noted with the SBT DE Results. PA PNNL detected two of the regions and possibly part of the third region with a positional error.

A considerable amount of effort went into carefully reviewing these plots to try to establish any correlations between the NDE methods and the DE results. This was very challenging because it is not clear as to what constitutes a failed SBT and what fusion conditions NDE should be detecting. Clearly, the Red areas are unacceptable, and most likely the Yellow areas should be considered unacceptable as well. Further work is needed by fracture mechanics/flaw evaluation experts to provide insights and a technical foundation for the NDE scoring basis. It was decided that a qualitative approach would be used for an initial assessment.

In examining the fusion joint data shown in Figures 5.1 through 5.17, it is a challenge to find an NDE technique which produced indications correlating with the DE results. Most commonly, a particular NDE method would find certain flaw type conditions, but would miss others. In fact, most of the NDE methods also produced responses in locations where the material passed the SBT. Additionally, some of the NDE techniques were only applied to a subset of the specimen conditions because of time limitations when the inspection team could perform the inspections.

A failure to meet an acceptable bead width-to-height ratio is identified as “bead profile” in the plots. If the ratio was between 2.0 and 2.5, it was acceptable (see Figure 3.3) and nothing is plotted on the Figures 5.1 through 5.17. However, if the results were outside this range, this is then plotted in Figures 5.1 through 5.17, comparing NDE and DE results. All specimens that failed this bead condition requirement had pressure applied during the heat cycle, including specimens 123, 127, and 1212.

Specimens 1223 and 1224 seemed to be the most challenging for NDE, as exhibited by the lack of responses. These were fabricated under the ASTM 2620 procedure and should have been good joints. These passed the bead test and have very few NDE responses. The Evisive microwave technique seemed to get more responses than the UT techniques, but there was not a strong correlation between SBT failed areas and areas which passed the SBT. This clearly shows that more work is needed to refine these NDE methods to detect the conditions in this set of specimens.

The lack of firm conclusions from this study raise questions and highlights many issues that remain to be addressed. There is a need for standardizing methods and interpreting the meaning of results that should be used to assess the quality of a joint undergoing destructive testing. There are a number of DE tests that can be employed, but it is unclear as to which may be the best, or proper one, for use on HDPE fusion joints. During discussions with several research colleagues, it has been suggested that while there are differences between various DE test results, within a given test method, there may be a high level of consistency. It is unknown whether this is true, but if so, either the industry or the regulator will ultimately need to select what DE test method would be acceptable, thus establishing it as the preferred method. In the past, the high-speed tensile test has been considered the standard to be employed. This works well in a laboratory environment, but is not convenient for field testing where something like the SBT offers a very simple method that could be applied.

Other issues to be addressed include the number of test samples that are needed to determine the quality of a butt fusion joint. Based on the results of this study, it is unclear whether one specimen every 90 degrees around the pipe circumference (the current protocol for the smaller

diameter pipes), is adequate to determine overall quality of the joint. However, the number of circumferential test specimens required to provide the basis for acceptance is also not clear. Cutting a pipe fusion joint into multiple ¾-inch (18-mm) slices and subjecting all of them to a SBT would be a significant effort. Definitive studies have yet to be conducted to establish a technical basis for what type and scope of mechanical field tests are needed. These studies need to be challenged and validated by the HDPE community. In addition, a clarification of what constitutes the failure of a SBT, or whatever DE is being conducted, is needed. Four conditions (red, yellow, light green, and dark green) were reported in this work; however, a technical basis for which of these conditions may be unacceptable needs to be established. Furthermore, if multiple test samples are removed from a butt fusion joint, it remains to be determined how many of these need to fail before the fusion joint should be considered as unacceptable.

Based on the NDE results, volumetric testing was clearly able to detect some of the fusion-type flaws that were introduced into these specimens. However, there were a number of conditions that were deemed to be not acceptable, for which there were very little, or no, NDE responses. This clearly identifies areas where improvements are needed and where NDE researchers need to concentrate future efforts.

Overall, this initial study encountered many issues that diminished the ability to draw conclusive results related to volumetric NDE capabilities for fusion joints in HDPE. However, the study provided insights for identifying important issues that will need to be resolved in order to reach the stated objective, and was very beneficial from a standpoint of establishing guidance for future research.

6 SUMMARY AND CONCLUSIONS

PNNL has been assessing the capabilities of NDE techniques to detect lack of fusion in HDPE butt fusion joints. The initial studies are complete, but only limited conclusions, as discussed in Section 5, can be drawn at this point.

The ultrasonic TOFD and PA methods, and the electromagnetic millimeter (mm)-wave technologies, show promise in the inspection of HDPE fusion welds. Higher frequencies are likely needed in order to reliably detect the tight LOF conditions. The parent HDPE material is homogeneous and other material variables such as dielectric and acoustic properties are quite conducive to electromagnetic techniques, and likewise for ultrasonic testing.

Visual testing of the joint bead does not appear to be a viable method to reveal subtle conditions such as LOF in the butt fusion joint. This is a surface evaluation technique and, alone, does not provide sufficient insight as to the volumetric quality of the joint. Research conducted to date shows that VT only detects gross butt fusion joint defects, and is not expected to detect more innocuous conditions that may be unacceptable for long-term service. However, VT was very effective in detecting conditions where pressure was applied during the heat cycle and should be included as one of the first tests recommended for assessing butt fusion joint quality.

It has been shown that a combination of NDE methods may be needed to detect most of the conditions in the test samples that were studied, and subsequently failed the SBT. However, these NDE methods exhibited a number of false calls and would need improvement before they would be considered reliable. While this study was in progress, researchers worldwide have been addressing this issue and there are new and improved NDE methods evolving that may overcome some of the shortcomings found in this study. Only qualitative conclusions can be drawn from this study because of issues that were discussed in Section 5 concerning a lack of definition for unacceptable flaw conditions, and how these may be validated by DE, such as the SBT results. All of the NDE techniques showed promise in detecting some areas that later failed the SBT. None of the NDE techniques provided a true correlation between areas that failed the SBT and those that passed the SBT. Most of the NDE techniques had responses in areas that successfully passed the SBT. For the specimens that failed the fusion bead width-to-height ratio, some of the areas failed the SBT and some passed the SBT. Thus, this work has provided an insight into the challenges associated with inspecting HDPE butt fusion joints for lack-of-fusion conditions and supports the need for more extended studies.

7 REFERENCES

ASTM D3350-06. 2006. *Standard Specification for Polyethylene Plastics Pipe and Fittings Materials*. ASTM International, West Conshohocken, Pennsylvania.

ASTM E190-92. 2008. *Standard Test Method for Guided Bend Test for Ductility of Welds*. ASTM International, West Conshohocken, Pennsylvania. Reapproved 2008.

ASTM F714-06a. 2006. *Standard Specification for Polyethylene (PW) Plastic Pipe (SDR-PR) Based on Outside Diameter*. ASTM International, West Conshohocken, Pennsylvania.

ASTM F1473-07. 2007. *Standard Test Method for Notch Tensile Test to Measure the Resistance to Slow Crack Growth of Polyethylene Pipes and Resins*. ASTM International, West Conshohocken, Pennsylvania.

ASTM F2620-06. 2006. *Standard Practice for Heat Fusion Joining of Polyethylene Pipe Fittings*. ASTM International, West Conshohocken, Pennsylvania.

ASTM F2634-07. 2007. *Standard Test Method for Laboratory Testing of Polyethylene (PE) Butt Fusion Joints using Tensile-Impact Method*. ASTM International, West Conshohocken, Pennsylvania.

Baby S, T Balasubramanian, RJ Pardikar, M Palaniappan and R Subbaratnam. 2002. "Time of Flight Diffraction (TOFD) Technique for Accurate Sizing of Surface Breaking Cracks. NDE2002 Predict, Assure, Improve." In *National Seminar of ISNT*, Chennai, India.

Brotherhood CJ, BW Drinkwater and S Dixon. 2003. "The detectability of kissing bonds in adhesive joints using ultrasonic techniques." *Ultrasonics* 41(7):521-529.

McGraff S and A McElyen. 2009. *Side Bend Testing on Pipe Weld Samples Using Testing Fixture w/ Hand Hydraulic Pump*. ISCO-Shop 134, Rev. 0, ISCO Industries, Louisville, Kentucky.

Messer B and MAR Yarmuch. 2007. "Configurations and Methods for Ultrasound Time of Flight Diffraction Analysis." U.S. Patent 7,255,007.

Olympus Corp. 2011. *Flaw Detectors TOFD*. Waltham, Massachusetts. Accessed October 31, 2011. Available at http://www.olympus-ims.com/en/ultrasonic-transducers/tofd/.

Performance Pipe. 2007. *PE3608 & PE4710 Materials Designation Codes and Pipe Pressure Ratings*. Technical Note PP 816-TN, Chevron Phillips Chemical Company LP, Plano, Texas. Available at http://www.cpchem.com/hb/getdocanon.asp?doc=857&lib=CPC-Portal.

PPI. 2006. *Handbook of Polyethylene Pipe, First Edition*. Plastics Pipe Institute (PPI), Irving, Texas. http://plasticpipe.org/publications/pe_handbook.html.

Sheen DM, DL McMakin and TE Hall. 2000. "Combined Illumination Cylindrical Millimeter-Wave Imaging Technique for Concealed Weapon Detection." In *Proceedings of SPIE, Volume 4032 - Passive Millimeter-Wave Imaging Technology IV*, pp. 52-60. April 26, 2000, Orlando (Kissameee), Florida. Society of Photo-Optical Instrumentation Engineers (SPIE), Bellingham, Washington.

Sheen DM, DL McMakin and TE Hall. 2006. "Cylindrical Millimeter-Wave Imaging Technique and Applications." In *Proceedings of SPIE, Volume 6211 - Passive Millimeter-Wave Imaging Technology IX*, pp. 62110A-10. May 5, 2006, Orlando (Kissimmee), Florida. The International Society for Optical Engineering (SPIE), Bellingham, Washington.

Sheen DM, DL McMakin, TE Hall and RH Severtsen. 1999. "Real-Time Wideband Cylindrical Holographic Surveillance System." U.S. Patent 5,859,609.

APPENDIX A

TOFD INSPECTION RESULTS ON 24 FUSION JOINTS IN 3408 HDPE PIPE AS DETERMINED BY FLUOR/NDT INNOVATIONS, INC.

APPENDIX A

TOFD INSPECTION RESULTS ON 24 FUSION JOINTS IN 3408 HDPE PIPE AS DETERMINED BY FLUOR/NDT INNOVATIONS, INC.

Inspection Matrix - Blind Samples					
Sample No	Diameter	Dimension Ratio	Actual Thickness	Defect Location	Defect Type
121	IPS 12	DR11	1.16”	13.25	PL
				14.5	IF
				20	IF
				25	IF
				32.5	L
				35	P
				39	IF
122	IPS 12	DR11	1.16”	3	MP
				8.7	PL
				13.5	PL
				14.5	PL
				23.5	IF
				28	MP
123	IPS 12	DR11	1.16”	2	MP
				8	MP
				11	MP
				13	L
				16	L
124	IPS 12	DR11	1.16”	3.5	L
				11.4	L
				26.5	L
				32.2	P
				38	L
125	IPS 12	DR11	1.16”	0.5	MP
				7.5	MP
				18	MP
				20.5	MP
				25.5	L
				35.5	P
				36	MP
126	IPS 12	DR11	1.16”	5.5	MP
				8.5	MP
				12.5	L
				15	PL
				20	MP
				37.5	MP

Inspection Matrix - Blind Samples					
Sample No	Diameter	Dimension Ratio	Actual Thickness	Defect Location	Defect Type
127	IPS 12	DR11	1.16”	0.5	P
				1.5	MP
				10.5	P
				10.8	P
				12.4	P
				12.8	MP
				17	MP
				19.5	MP
				28	MP
				39.5	P
128	IPS 12	DR11	1.16”	0	MP
				21.5	MP
				26.4	P
				32.5	MP
129	IPS 12	DR11	1.16”	2.4	P
				34	PL
				38.7	P
1210	IPS 12	DR11	1.16”	3	IF
				10	IF
				16.5	P
				21	IF
				28.5	PL
				32	MP
				39	L
1211	IPS 12	DR11	1.16”	4	L
				6.2	L
				9.1	PL
				16	MP
				26.5	PL
1212	IPS 12	DR11	1.16”	3.2	MP
				9.1	P
				12.2	PL
				17.3	PL
				22	P
				22.5	P
				24.5	L
				31.5	MP
1213	IPS 12	DR11	1.16”	15	IF
				23.5	P
				27	L
				30	PL
				36	PL
1214	IPS 12	DR11	1.16”	12	L
				14.5	MP
				19	IF
				35	MP

Inspection Matrix - Blind Samples					
Sample No	**Diameter**	**Dimension Ratio**	**Actual Thickness**	**Defect Location**	**Defect Type**
1215	IPS 12	DR11	1.16”	4	MP
				11.5	MP
				23.5	MP
1216	IPS 12	DR11	1.16”	3	L
				5.2	L
				34	MP
1217	IPS 12	DR11	1.16”	1	PL
				9.5	MP
				27.5	P
1218	IPS 12	DR11	1.16”	20.5	MP
				25.5	L
				27.3	PL
				37.3	P
1219	IPS 12	DR11	1.16”		
1220	IPS 12	DR11	1.16”	2.5	L
				22	MP
1221	IPS 12	DR11	1.16”	17.7	PL
1222	IPS 12	DR11	1.16”	1.5	P
				5	P
				7	P
				15	P
				20	PL
				25.5	P
				27	P
				32	P
				37	P
1223	IPS 12	DR11	1.16”	2.5	MP
				23.5	MP
1224	IPS 12	DR11	1.16”	9.5	P
				25.5	PL

C – Crack	ED – Embedded
PL – Planar	PR – Point Reflector
IF – Incomplete Fusion	BSB – Bottom Surface Breaking
L – Longitudinal	TW – Through Wall
P – Porosity	TSB – Top Surface Breaking
O – Other	

APPENDIX B

TOFD INSPECTION RESULTS ON 24 FUSION JOINTS IN 3408 HDPE PIPE AS ACQUIRED BY FLUOR/NDT INNOVATIONS, INC.

APPENDIX B

TOFD INSPECTION RESULTS ON 24 FUSION JOINTS IN 3408 HDPE PIPE AS ACQUIRED BY FLUOR/NDT INNOVATIONS, INC.

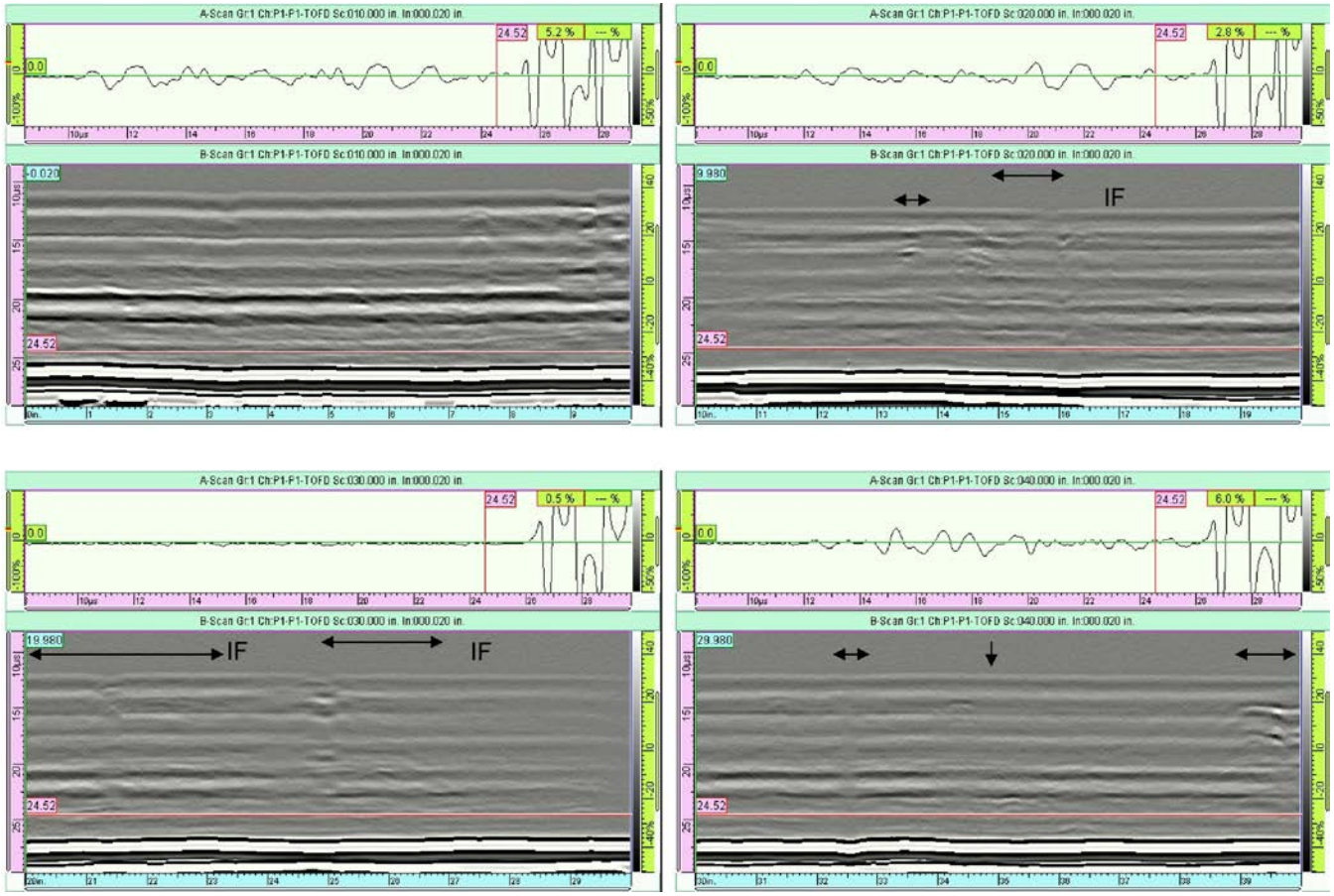

Figure B.1 HDPE Pipe 121, Condition 1

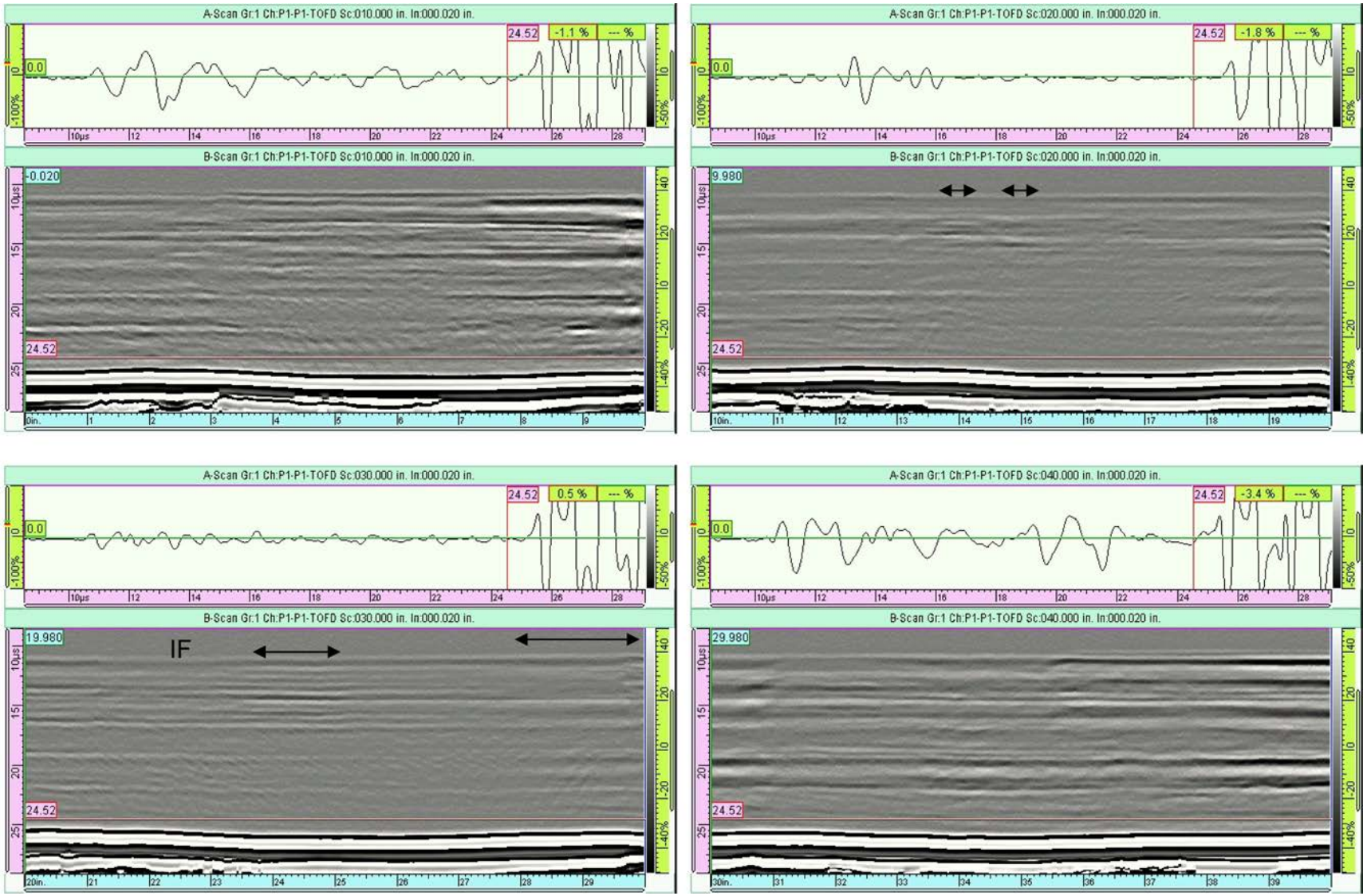

Figure B.2 HDPE Pipe 122, Condition 1

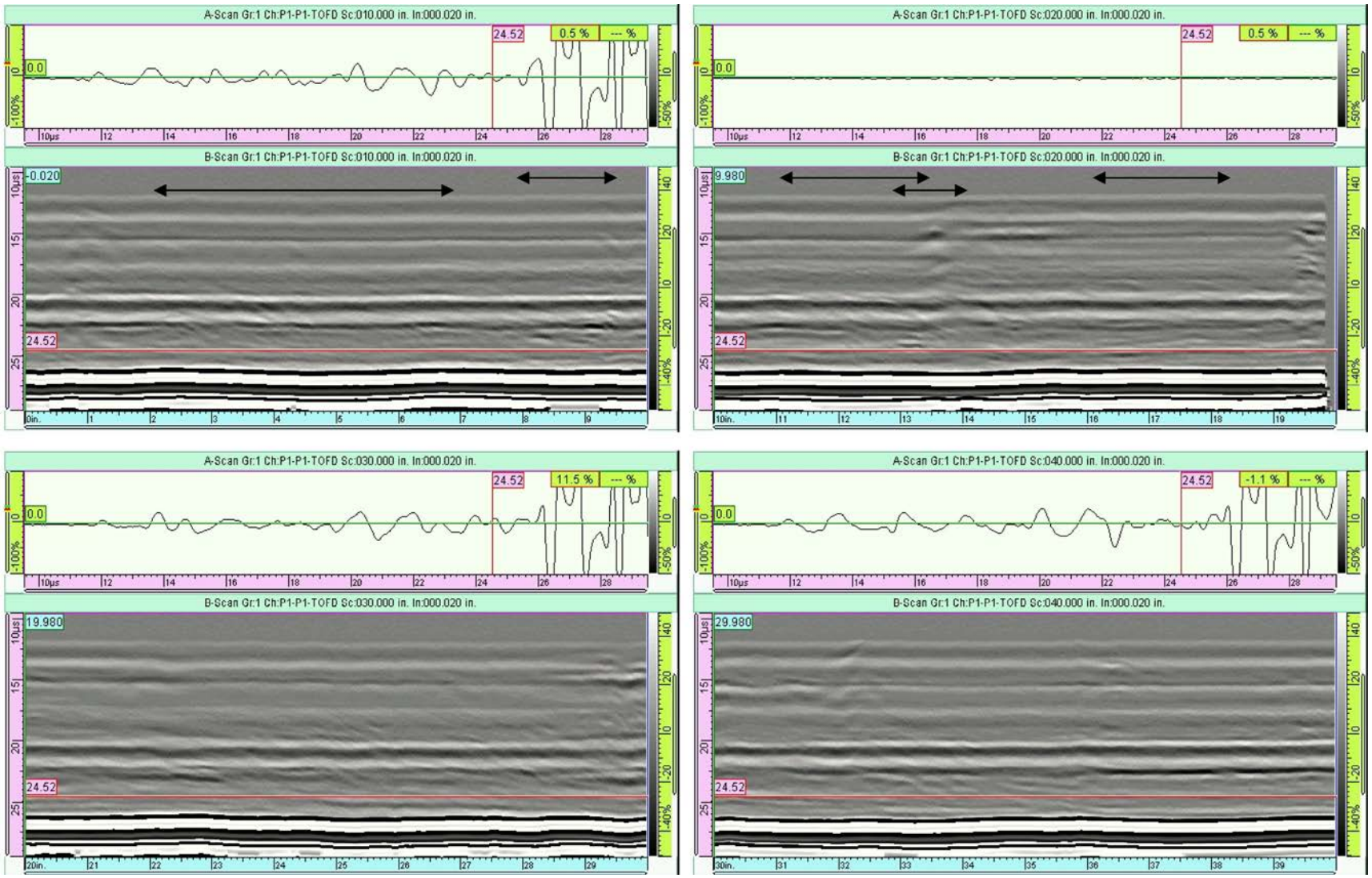

Figure B.3 HDPE Pipe 123, Condition 1

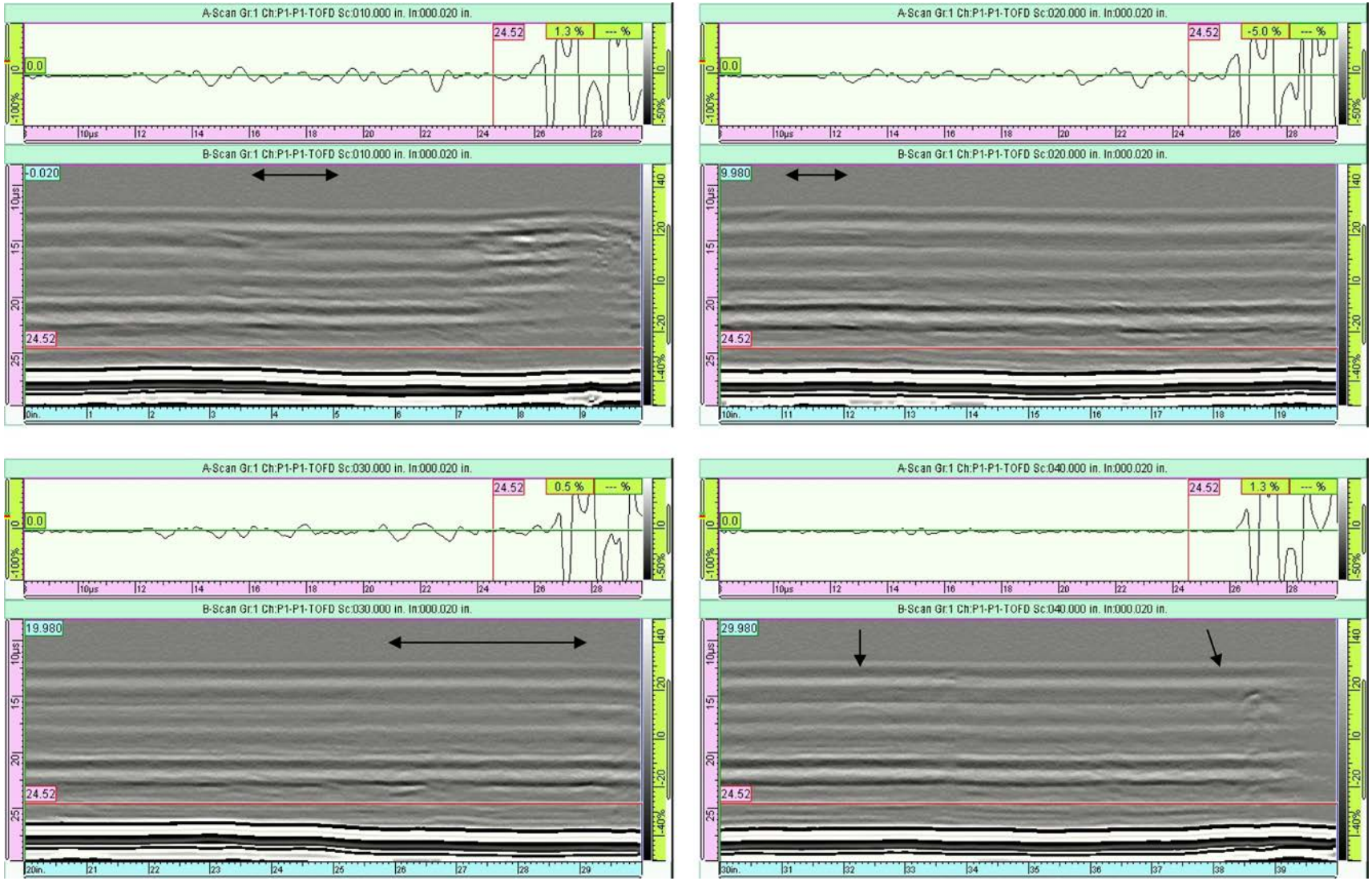

Figure B.4 HDPE Pipe 124, Condition 1

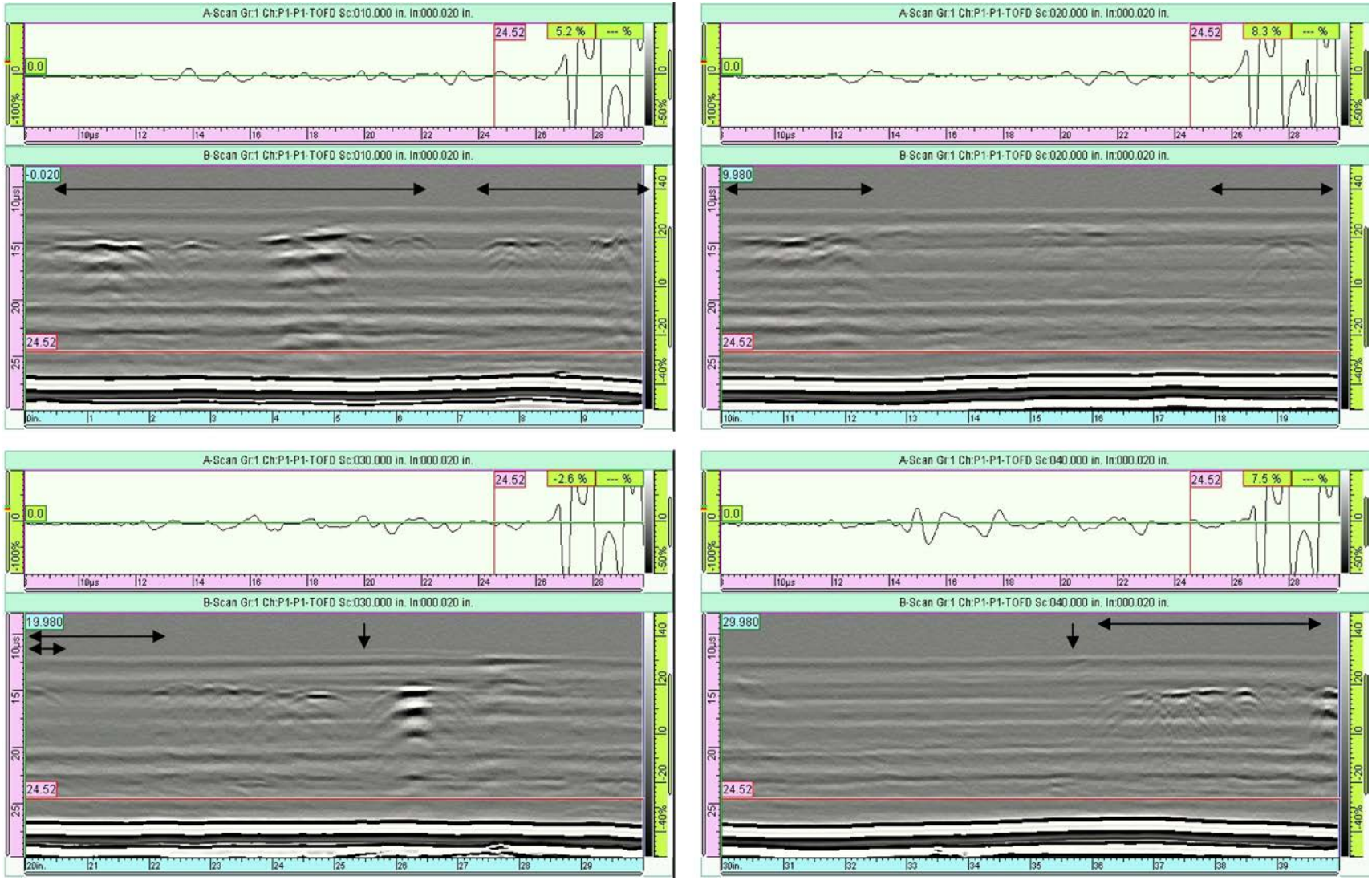

Figure B.5 HDPE Pipe 125, Condition 2

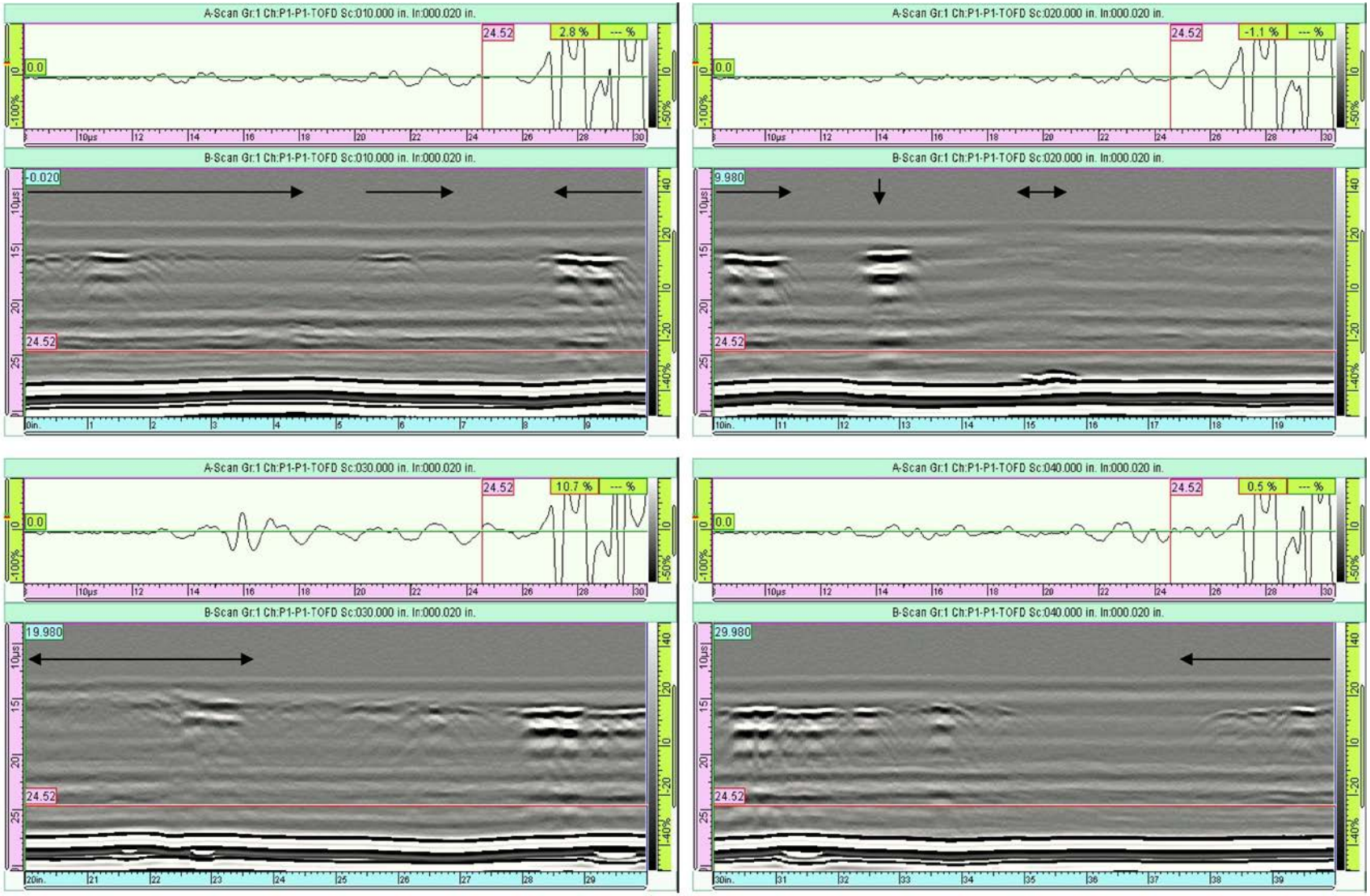

Figure B.6 HDPE Pipe 126, Condition 2

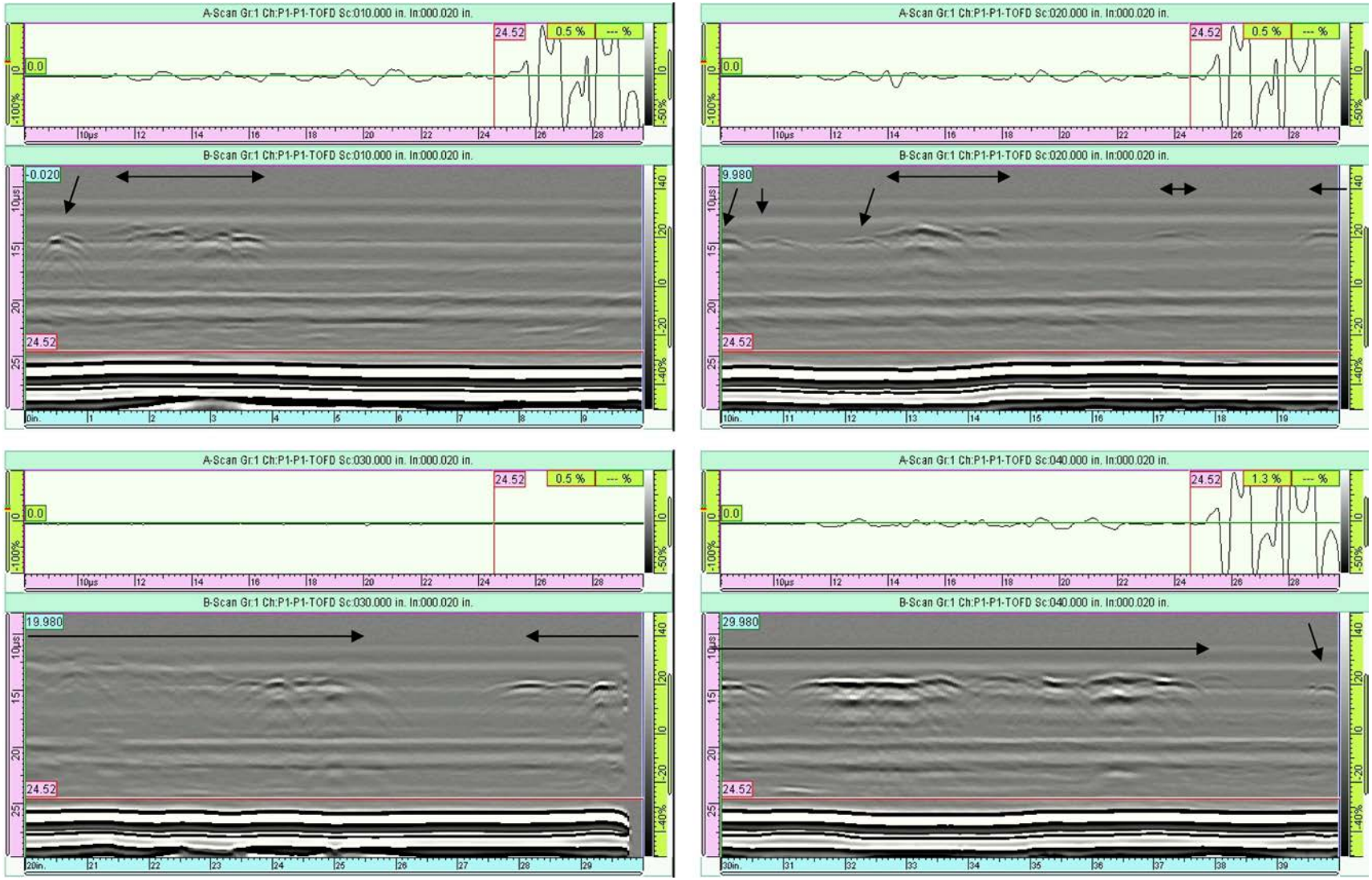

Figure B.7 HDPE Pipe 127, Condition 2

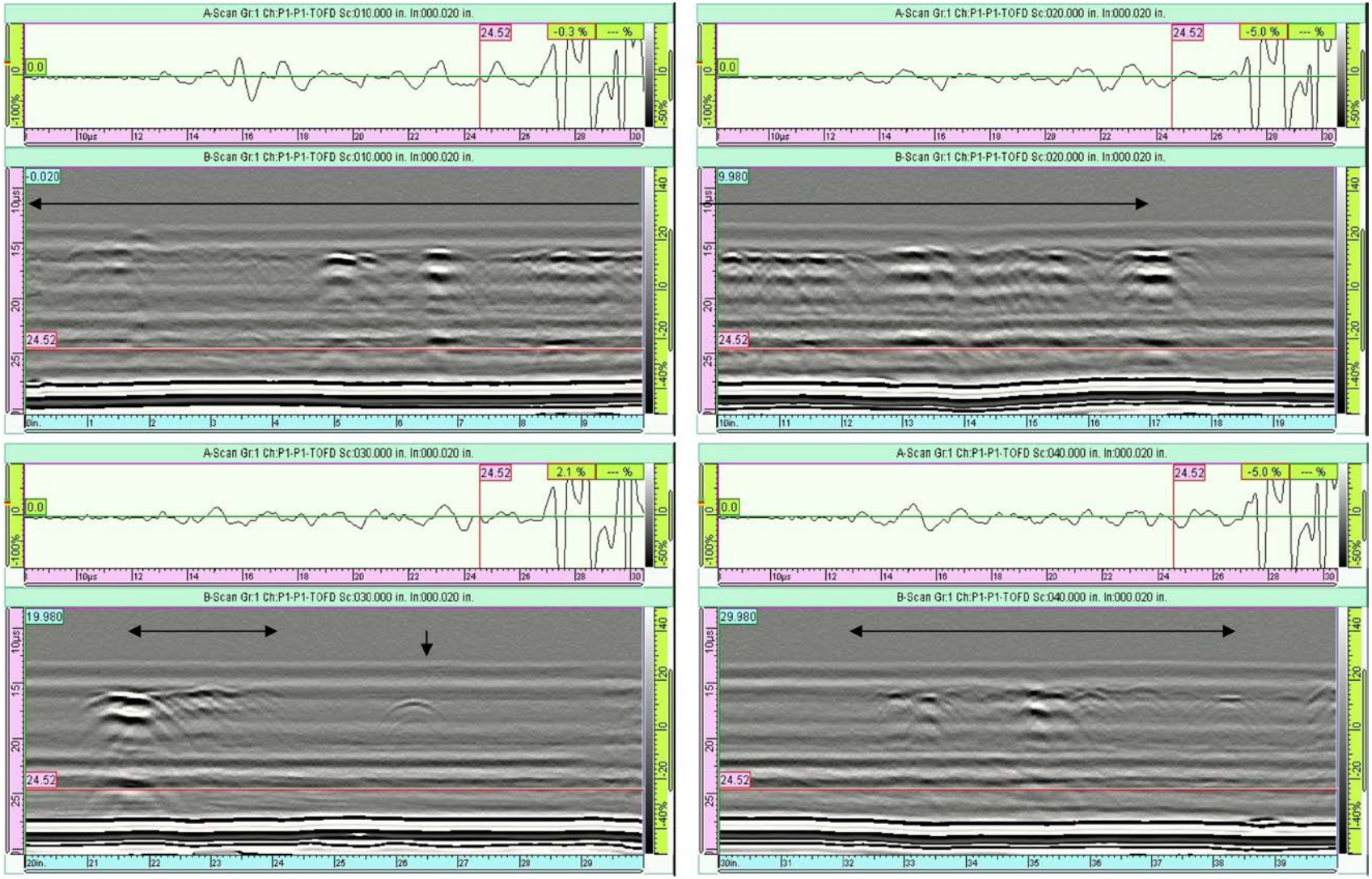

Figure B.8 HDPE Pipe 128, Condition 2

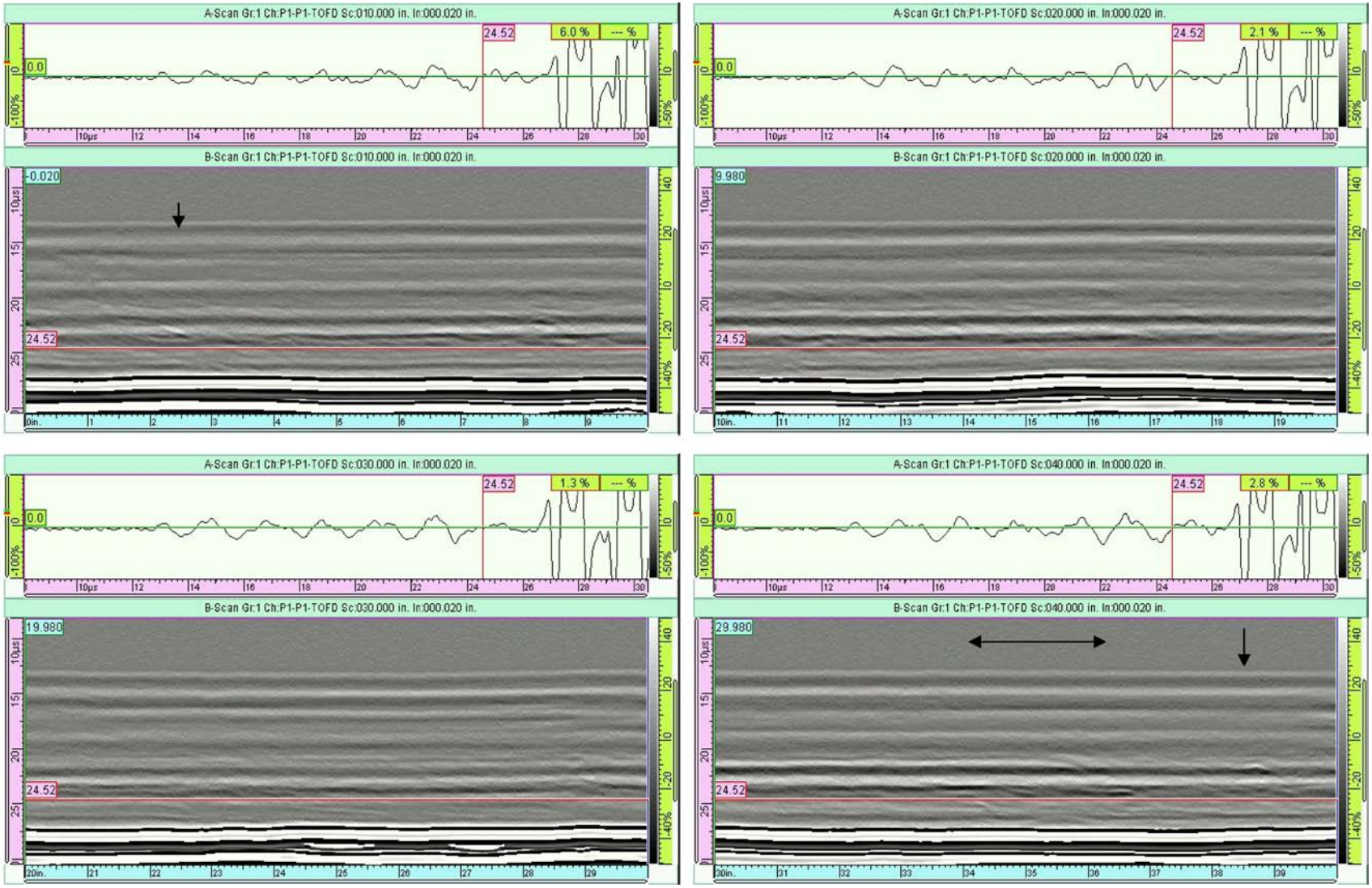

Figure B.9 HDPE Pipe 129, Condition 3

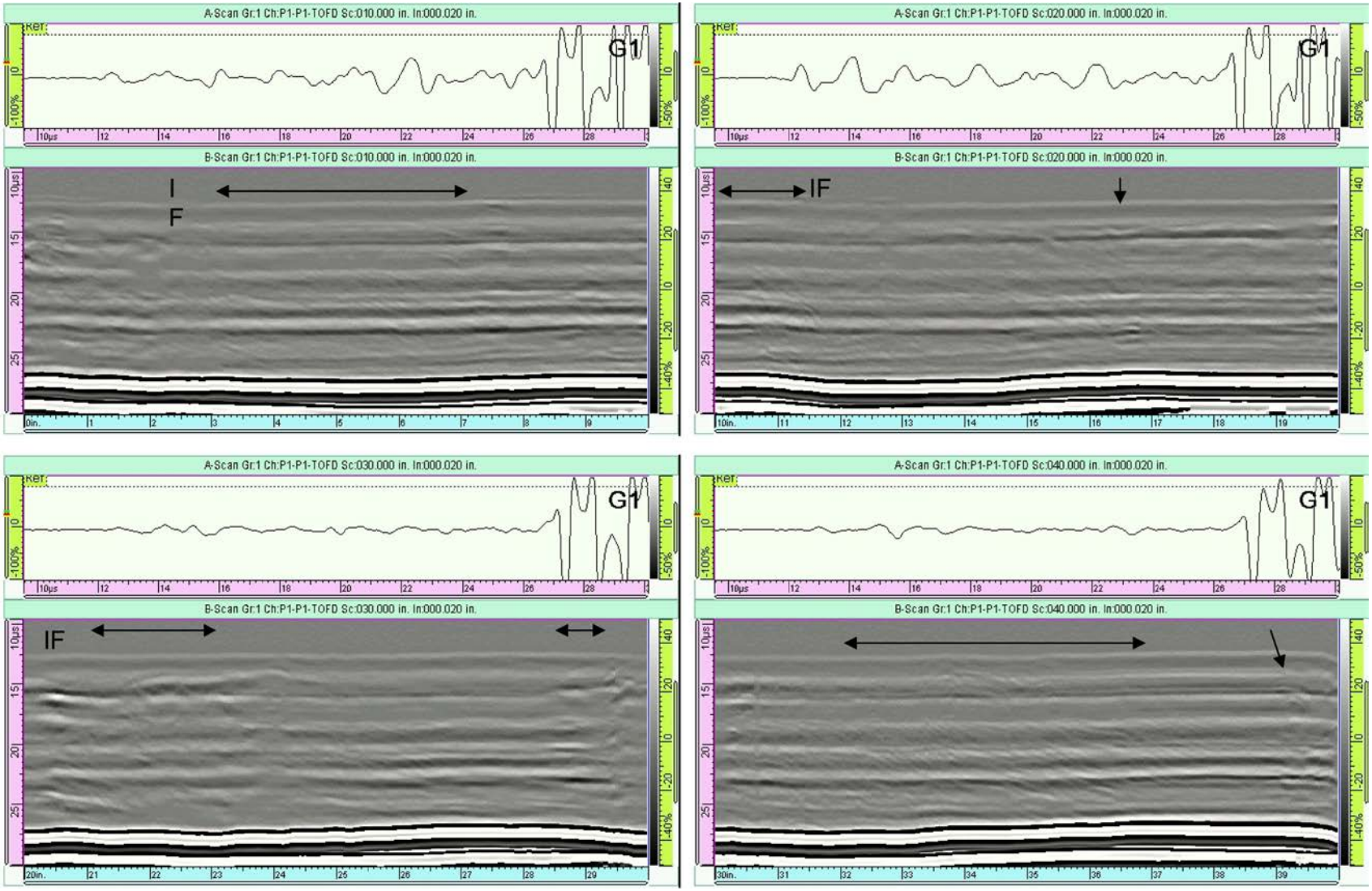

Figure B.10 HDPE Pipe 1210, Condition 3

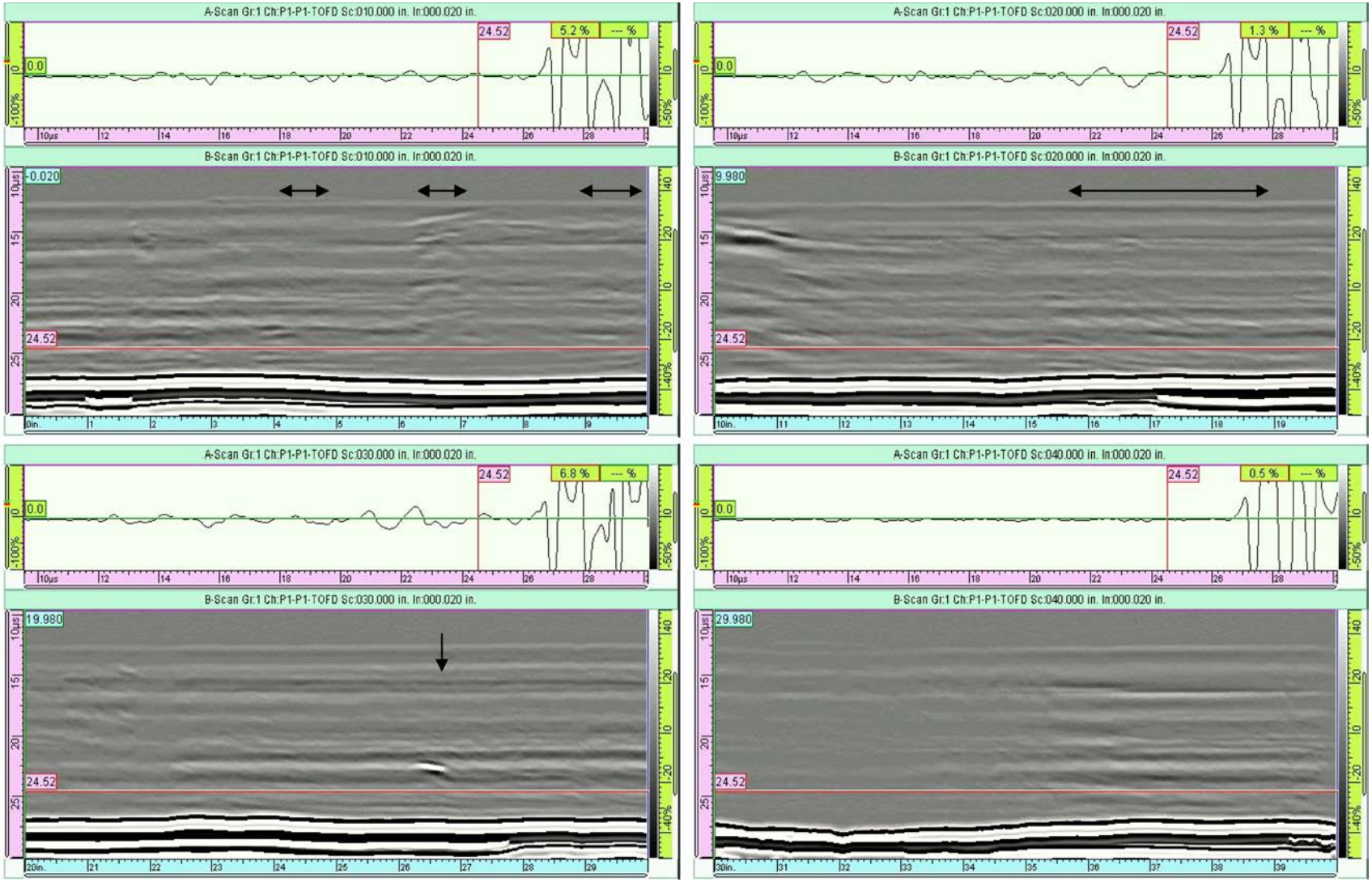

Figure B.11 HDPE Pipe 1211, Condition 3

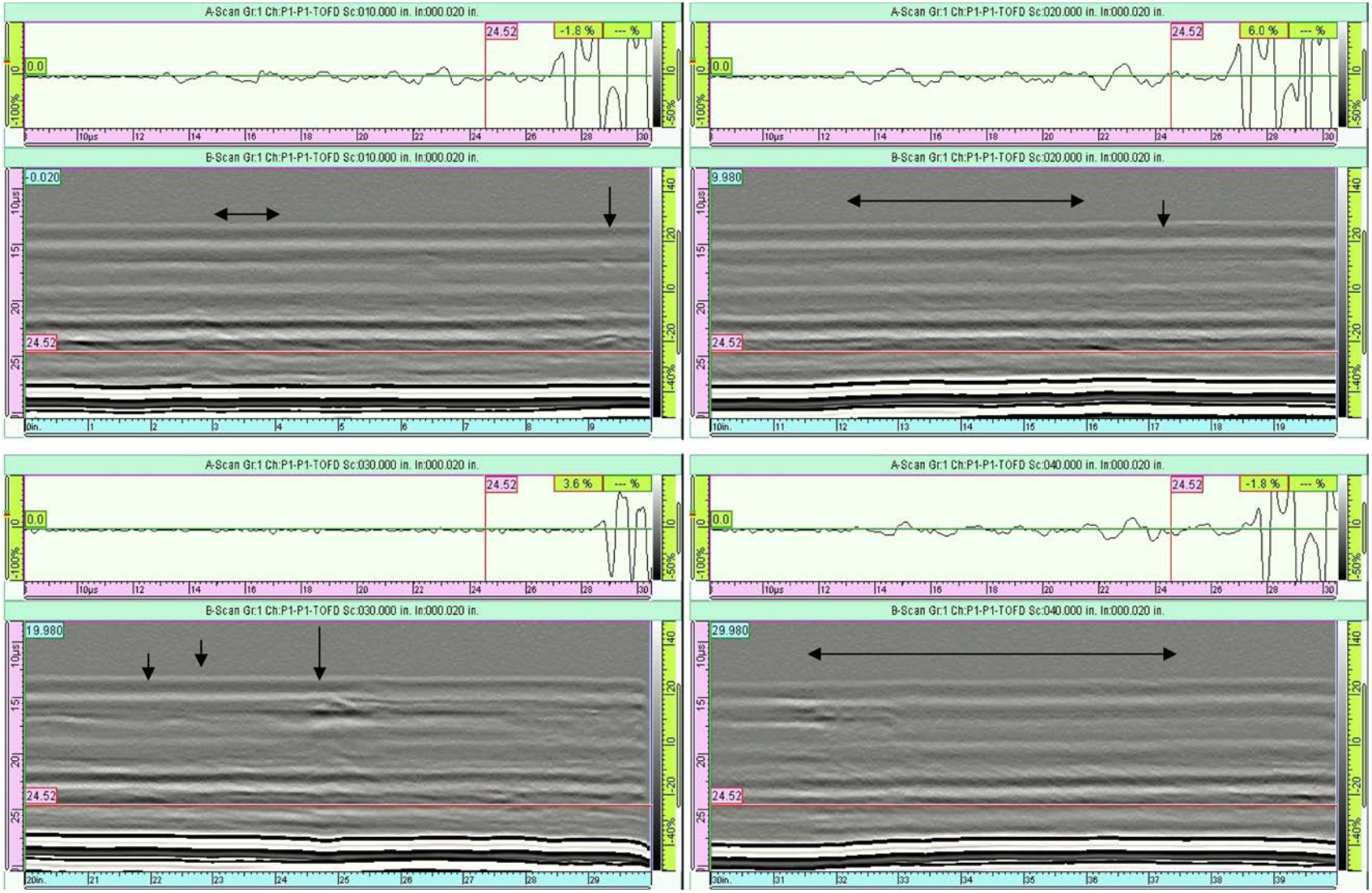

Figure B.12 HDPE Pipe 1212, Condition 3

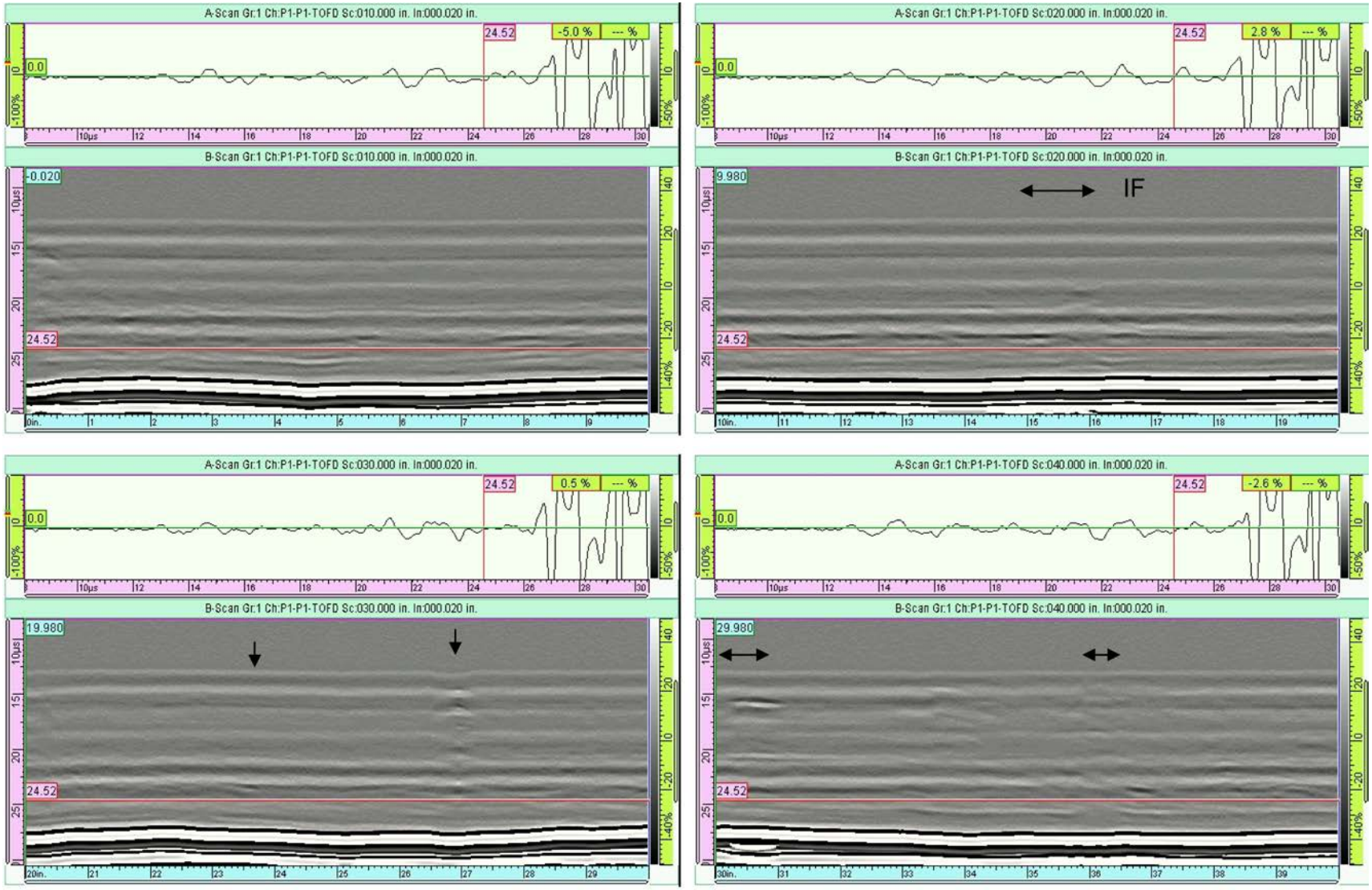

Figure B.13 HDPE Pipe 1213, Condition 4

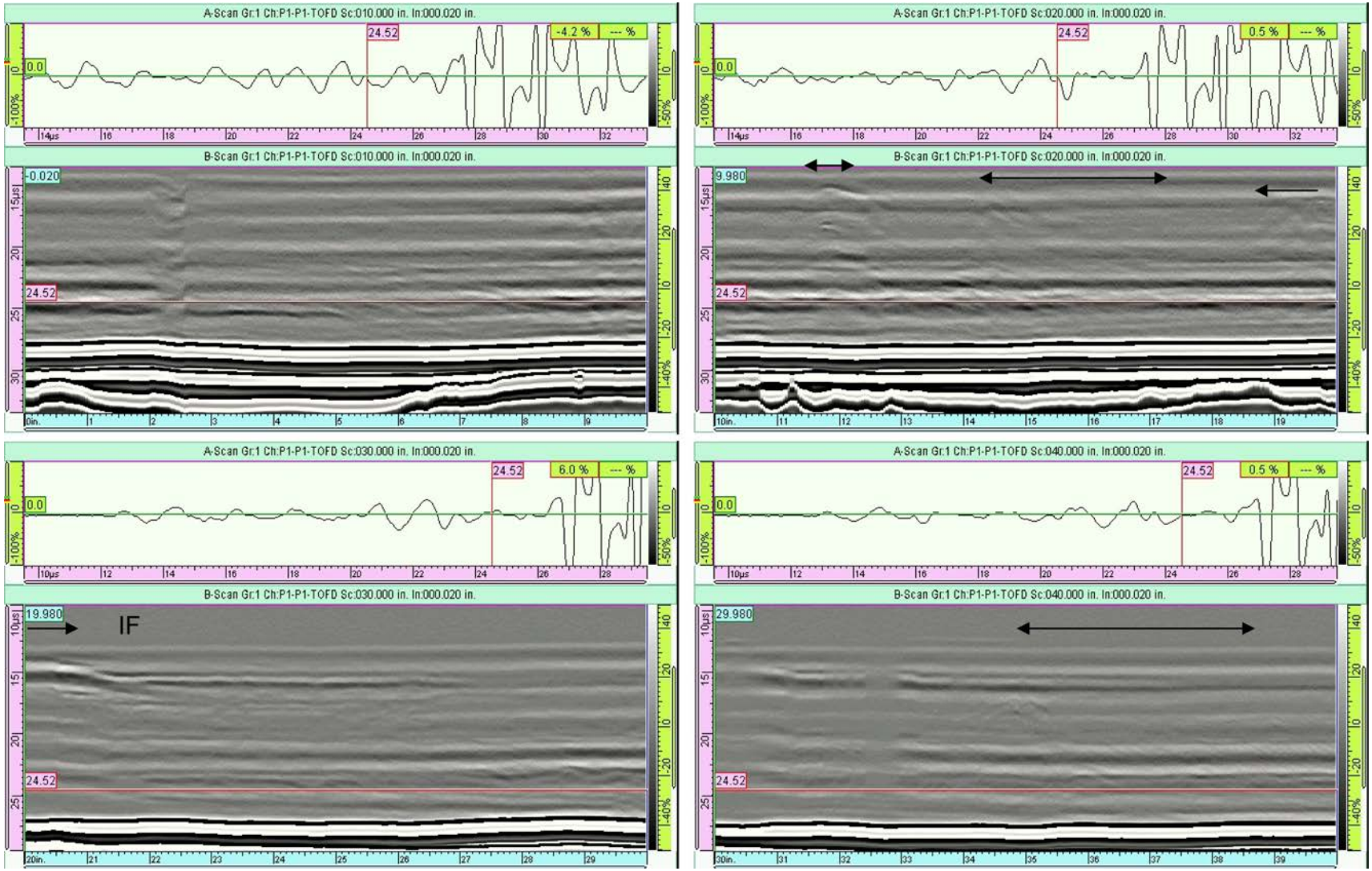

Figure B.14 HDPE Pipe 1214, Condition 4

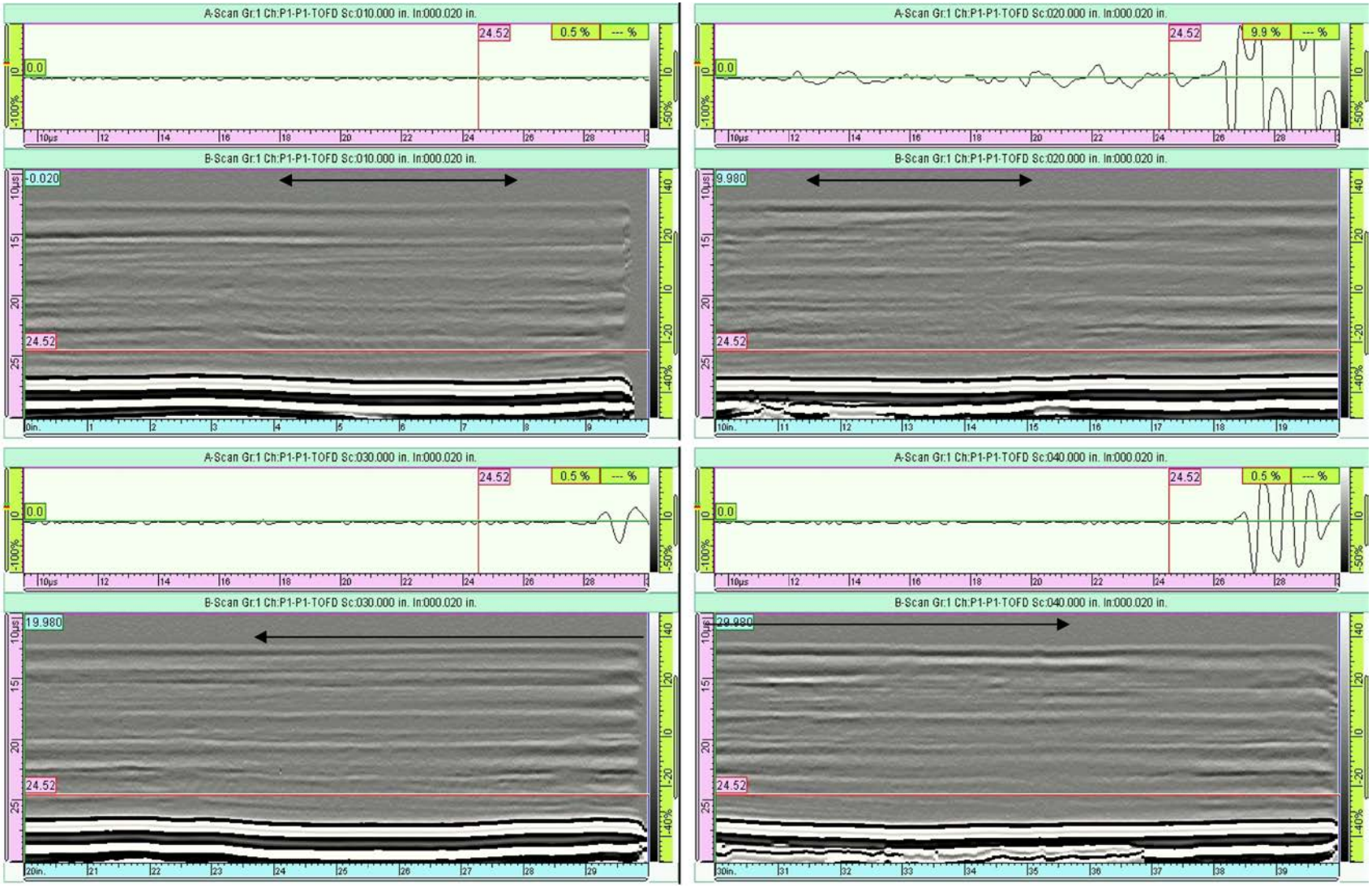

Figure B.15 HDPE Pipe 1215, Condition 4

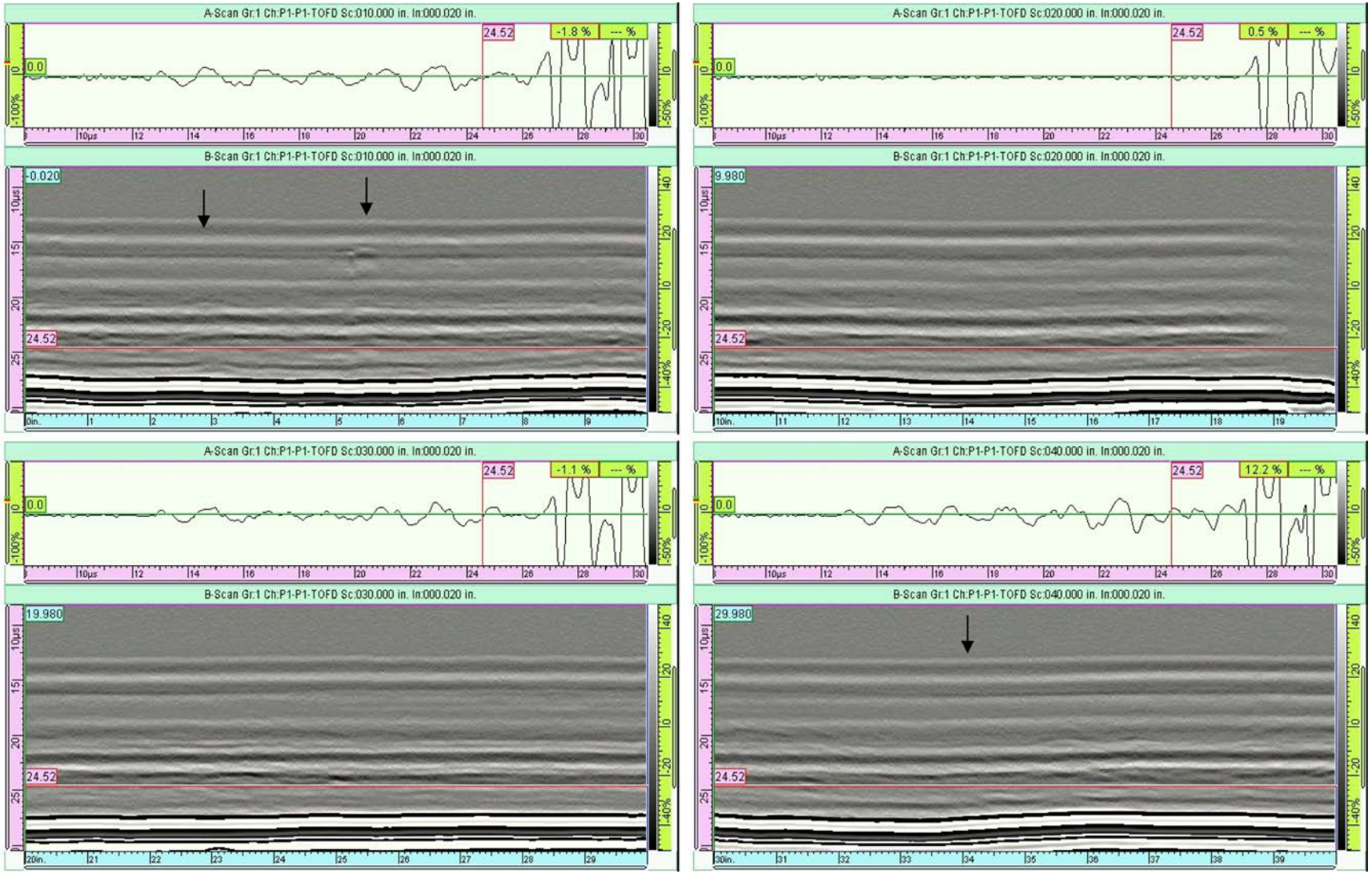

Figure B.16 HDPE Pipe 1216, Condition 4

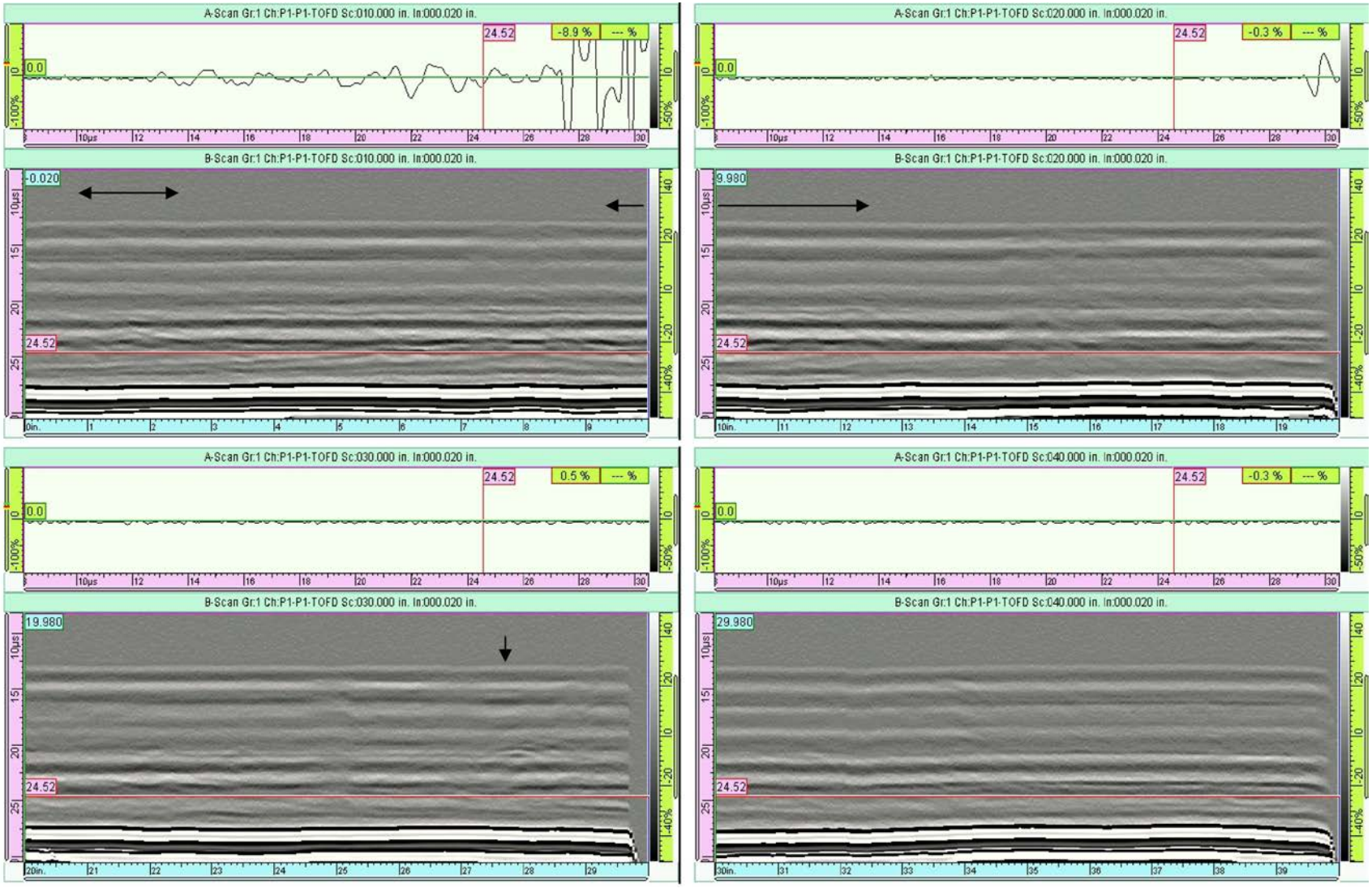

Figure B.17 HDPE Pipe 1217, Condition 5

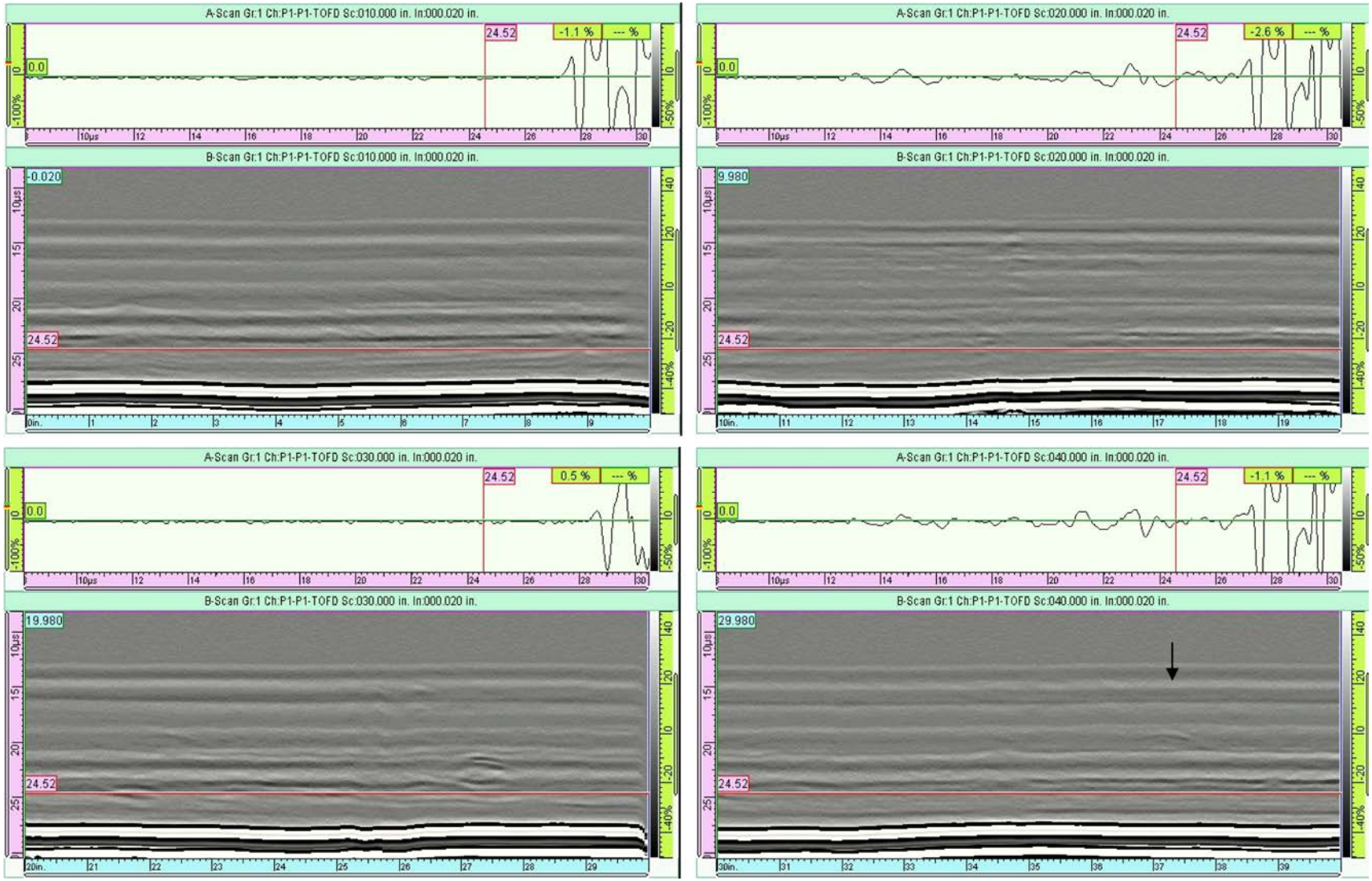

Figure B.18 HDPE Pipe 1218, Condition 5

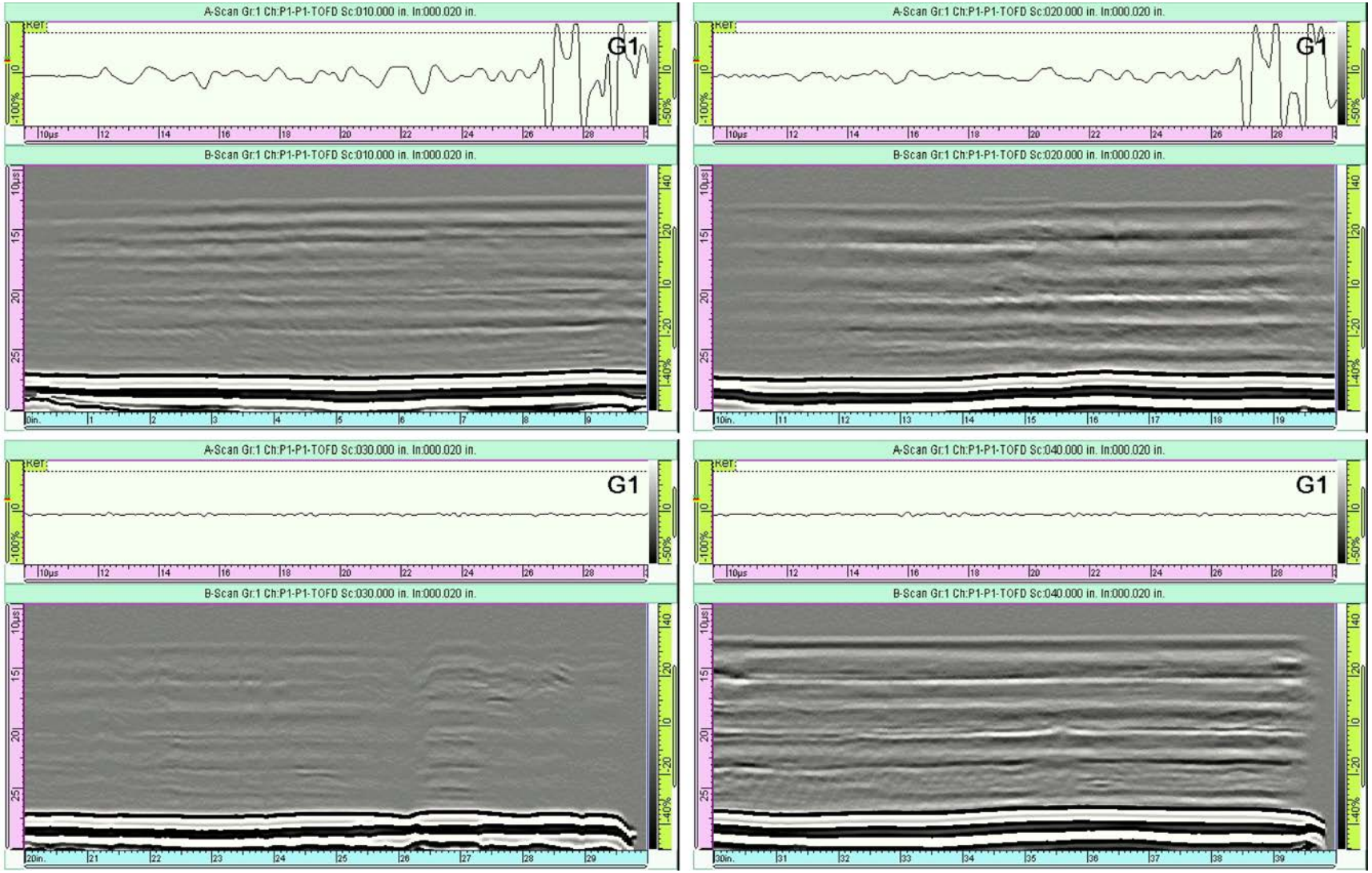

Figure B.19 HDPE Pipe 1219, Condition 5

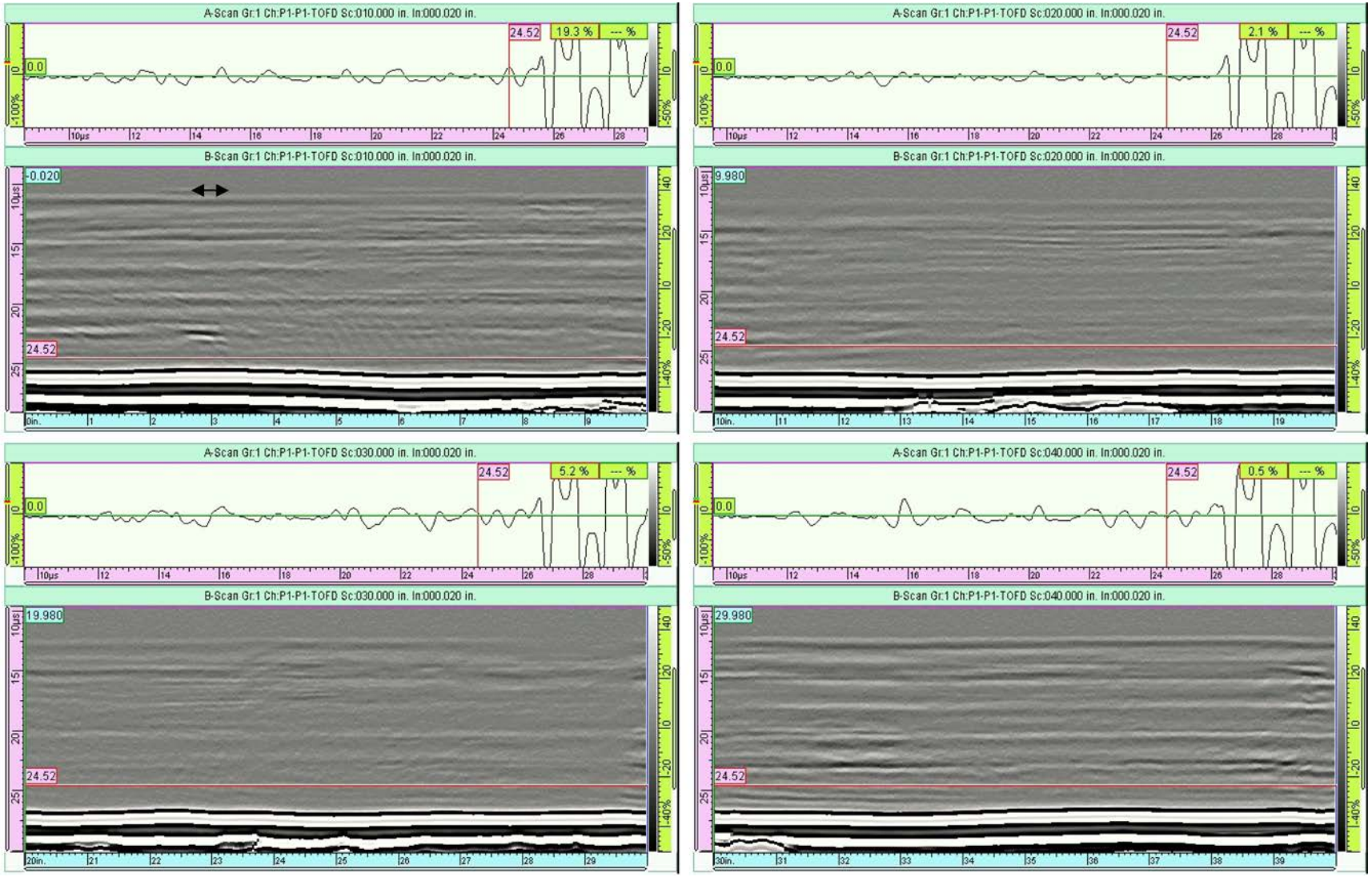

Figure B.20 HDPE Pipe 1220, Condition 5

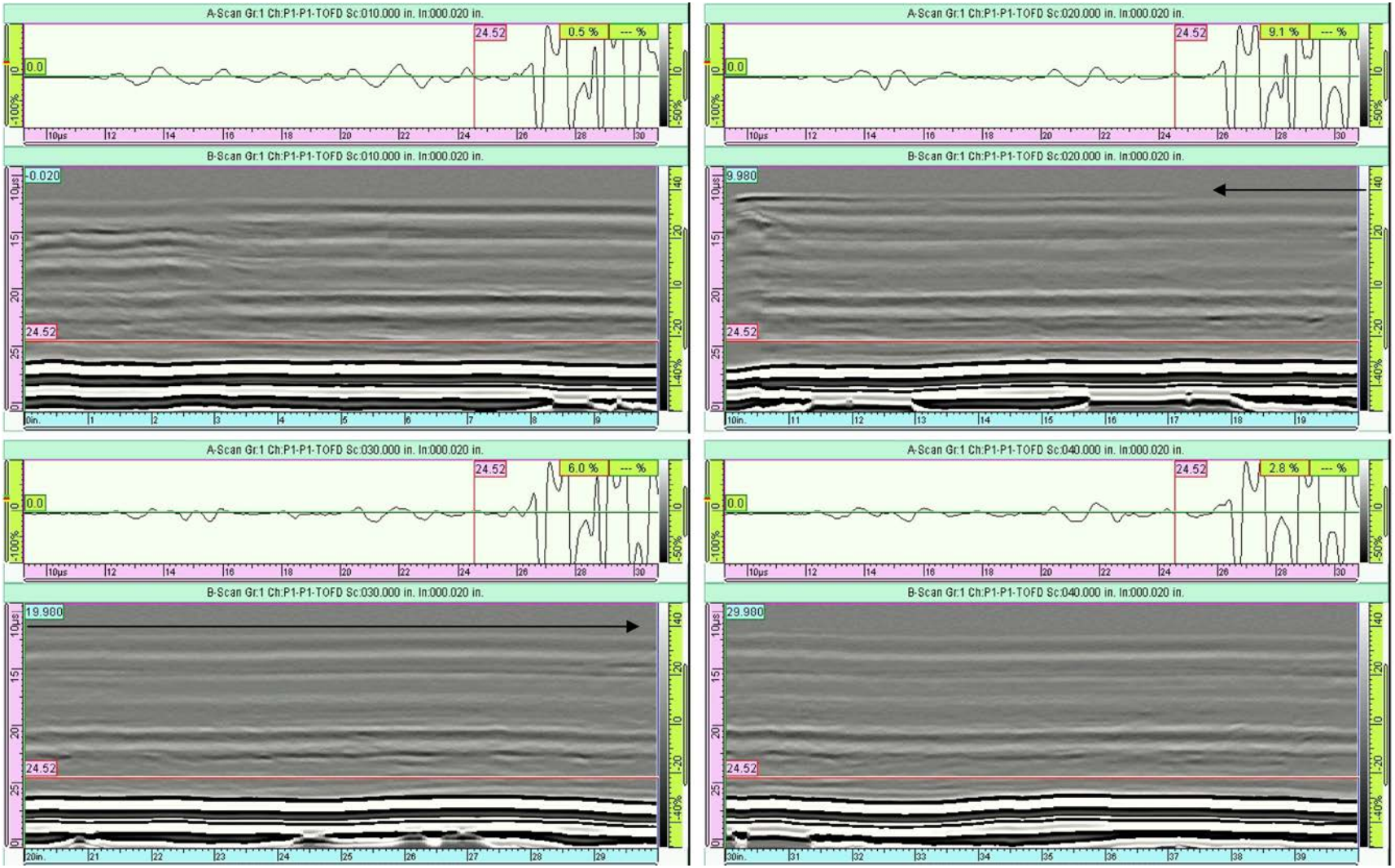

Figure B.21 HDPE Pipe 1221, Condition 6

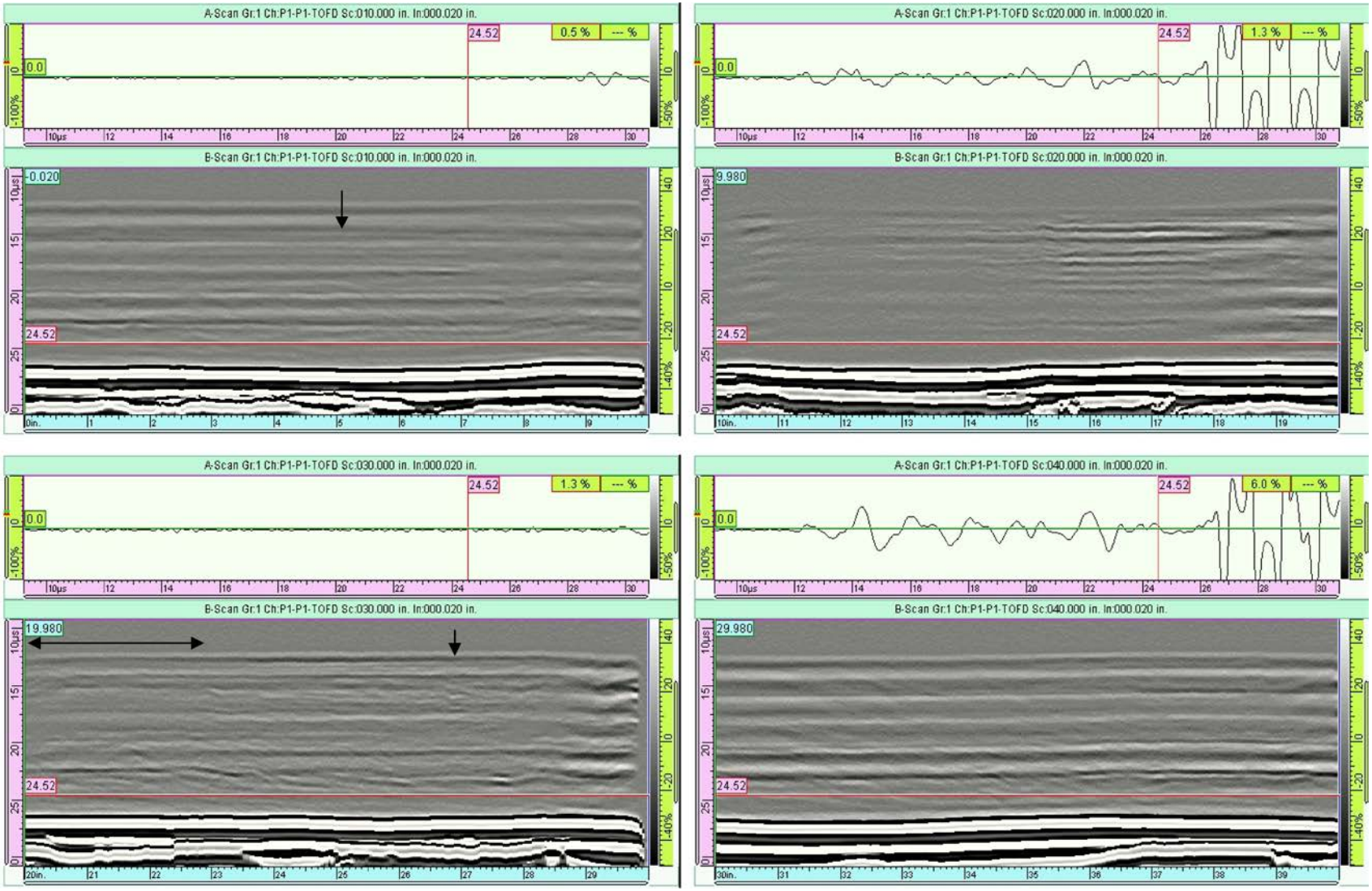

Figure B.22 HDPE Pipe 1222, Condition 6

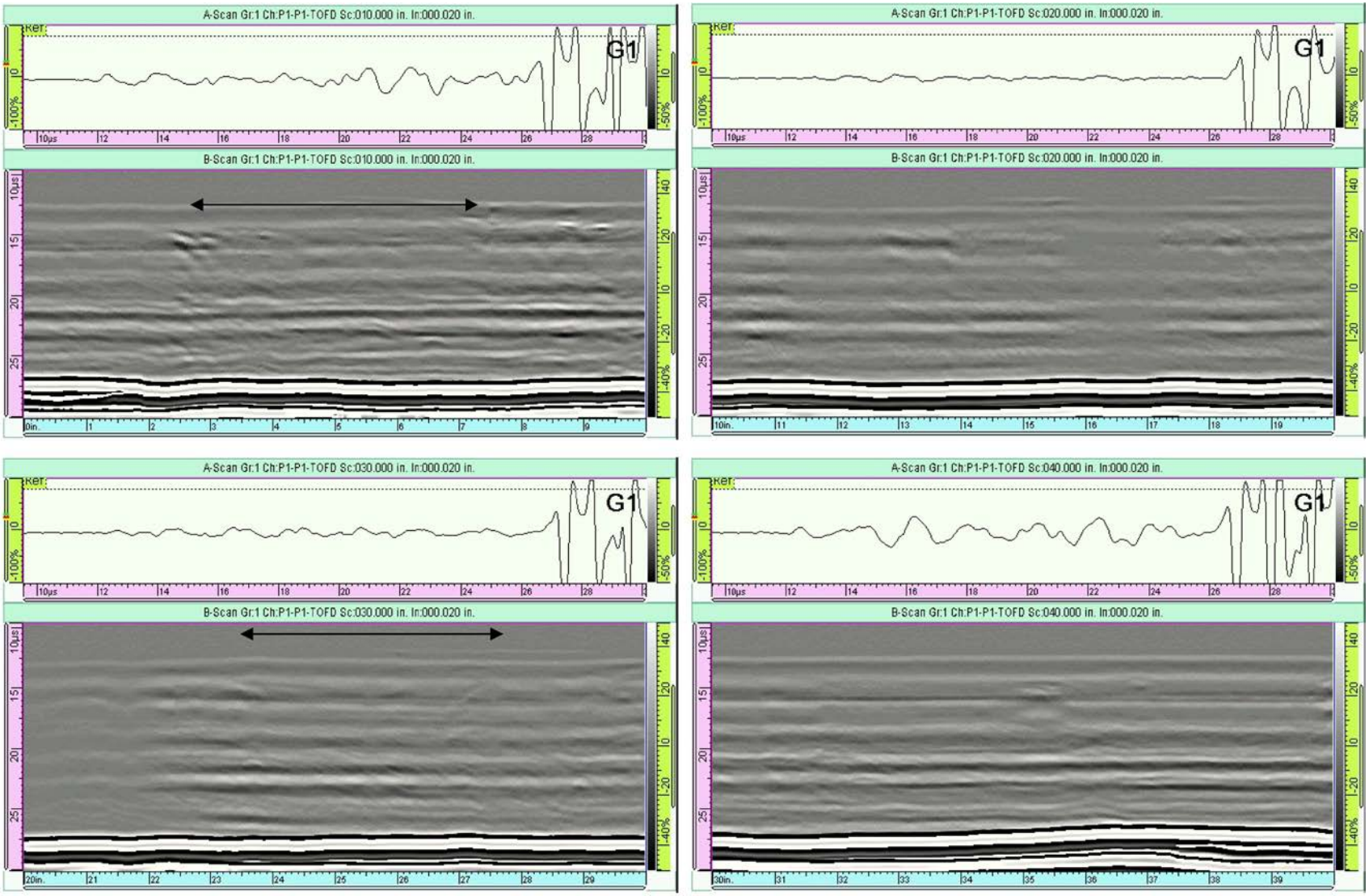

Figure B.23 HDPE Pipe 1223, Condition 6

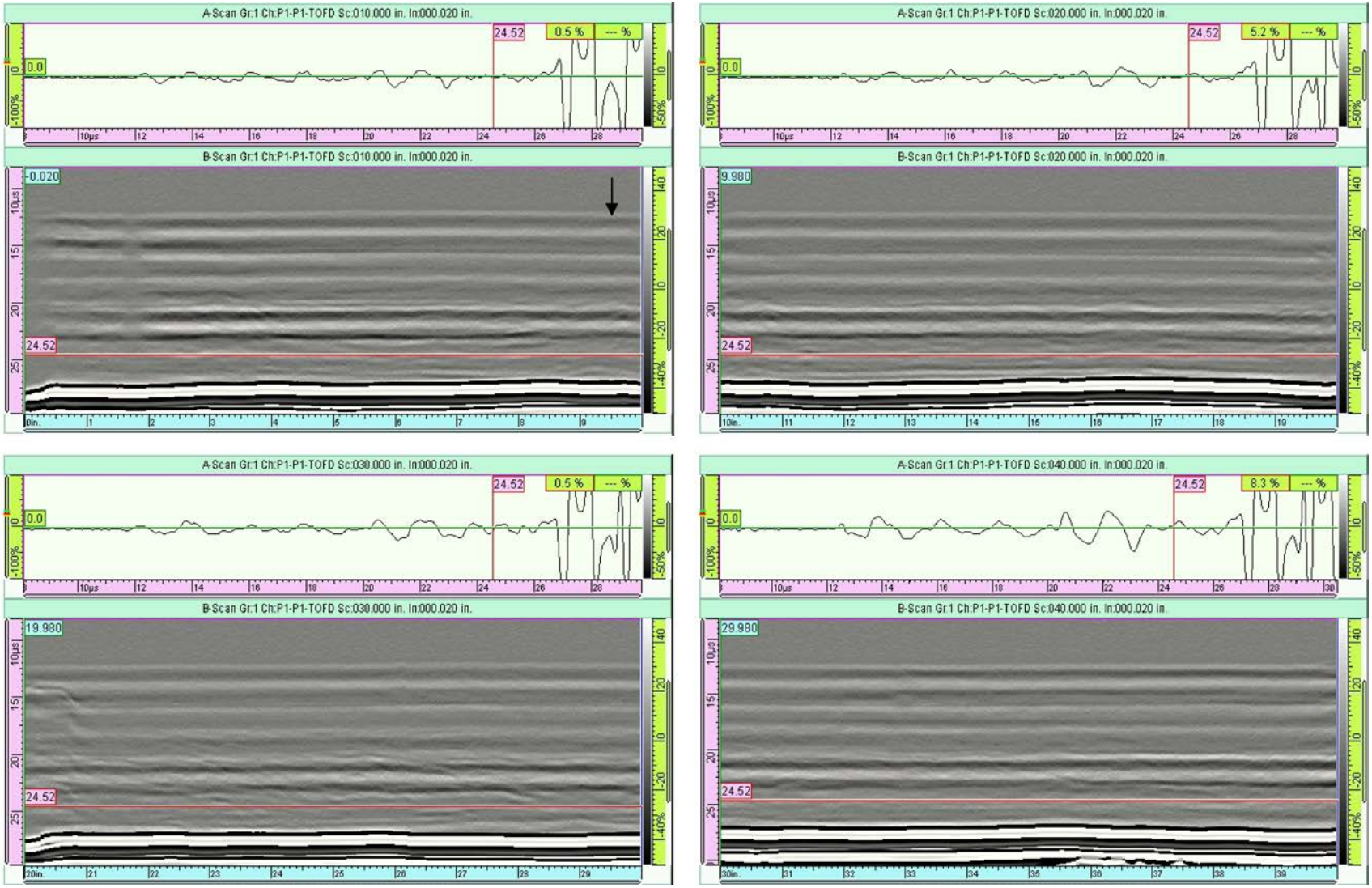

Figure B.24 HDPE Pipe 1224, Condition 6

APPENDIX C

PNNL TOFD INSPECTION RESULTS ON 12 FUSION JOINTS IN 3408 HDPE

APPENDIX C

PNNL TOFD INSPECTION RESULTS ON 12 FUSION JOINTS IN 3408 HDPE

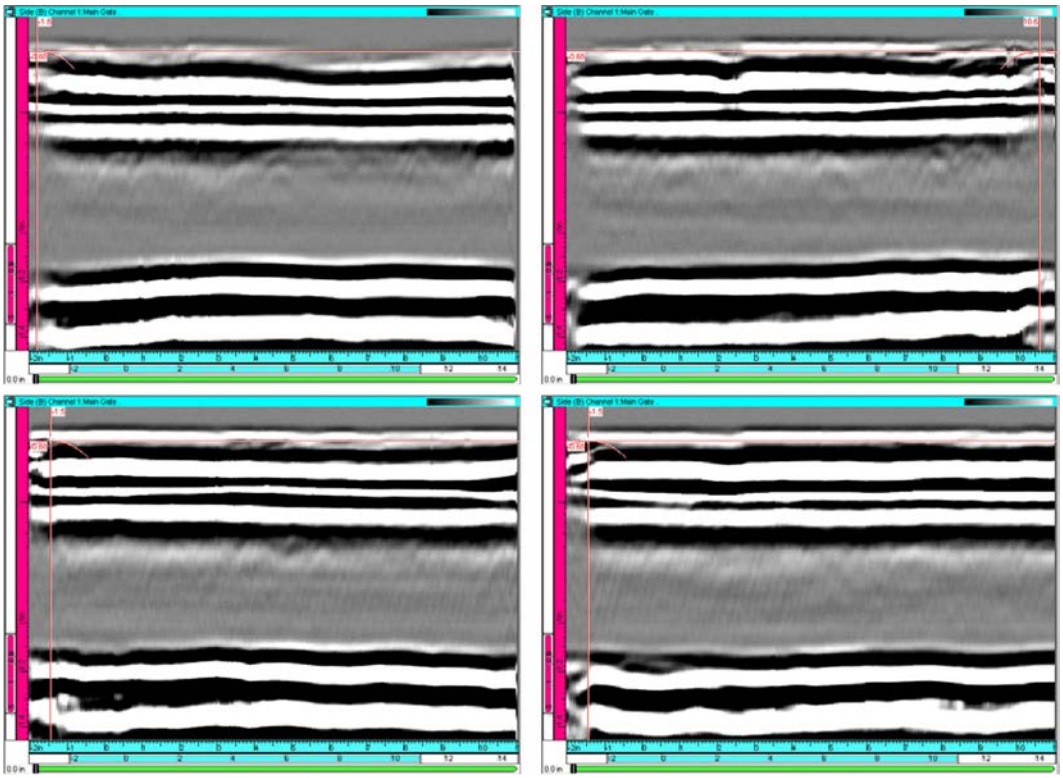

Figure C.1 Pipe Joint 123, 18 dB Gain

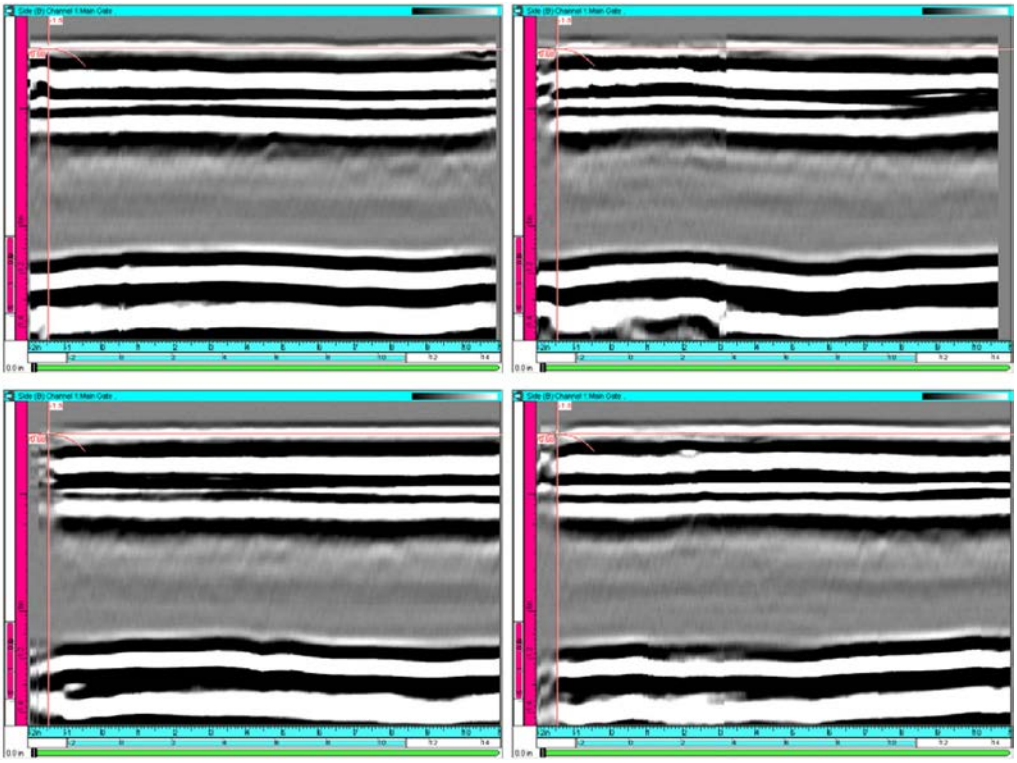

Figure C.2 Pipe Joint 124, 18 dB Gain

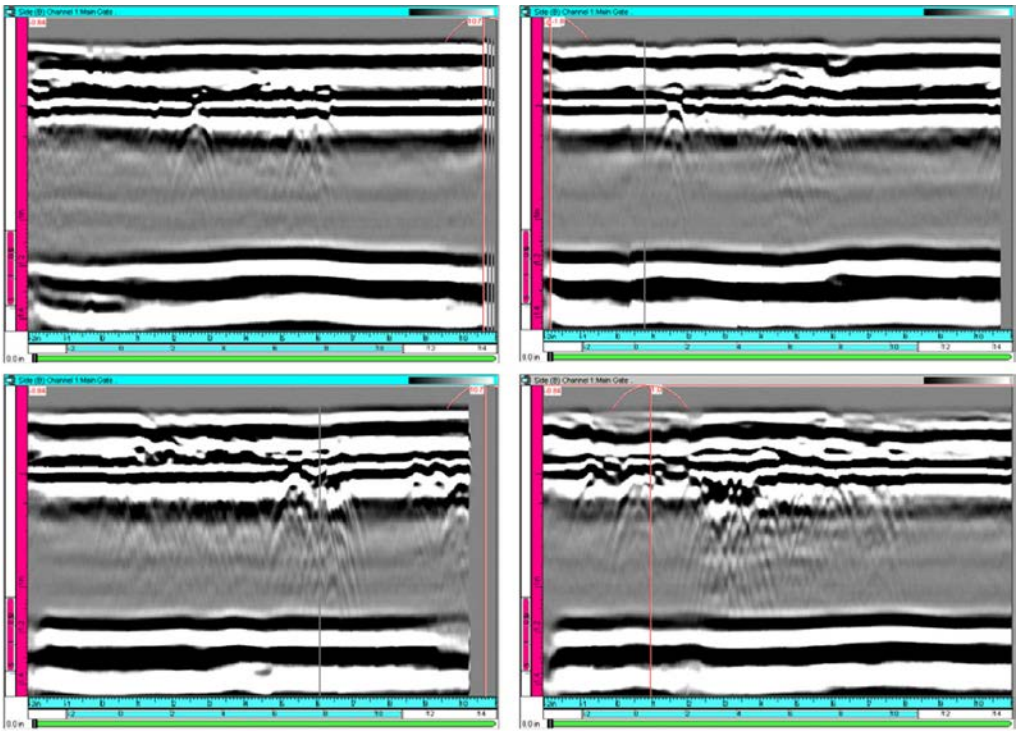

Figure C.3 Pipe Joint 127, 18 dB Gain

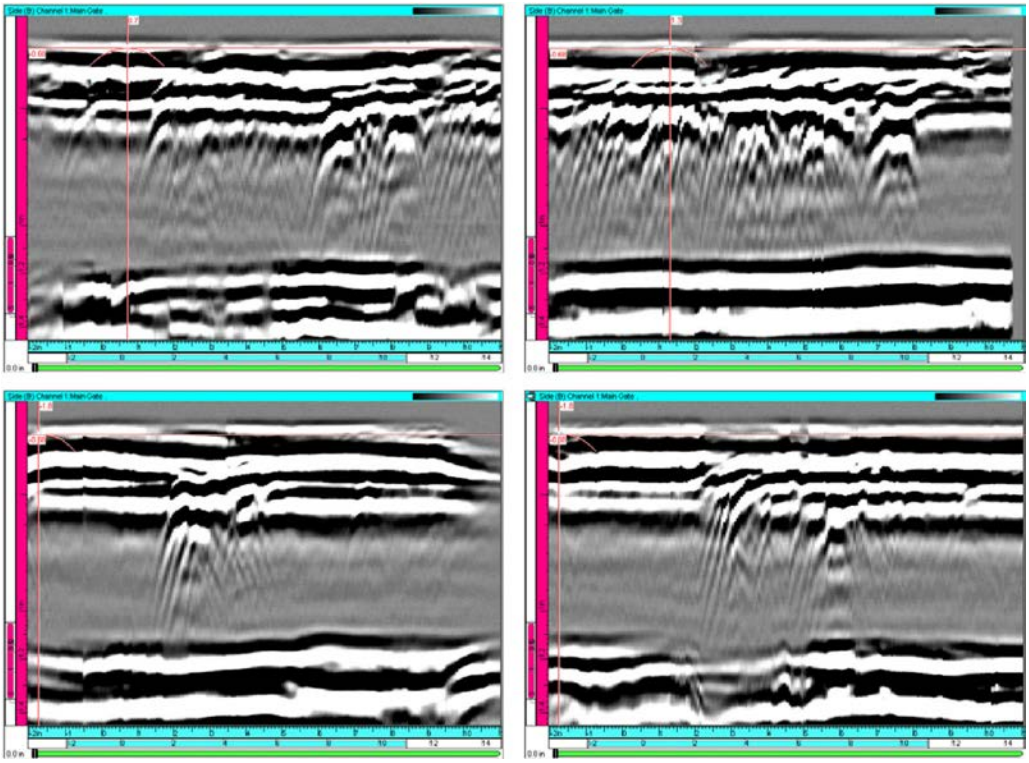

Figure C.4 Pipe Joint 128, 18 dB Gain

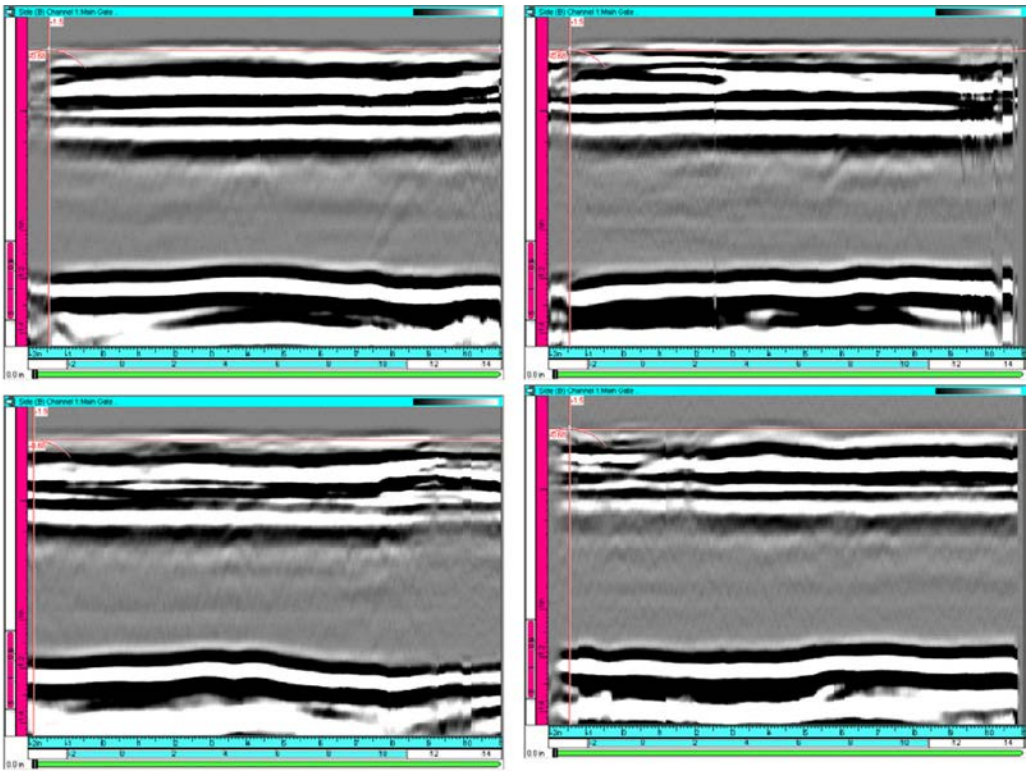

Figure C.5 Pipe Joint 1211, 18 dB Gain

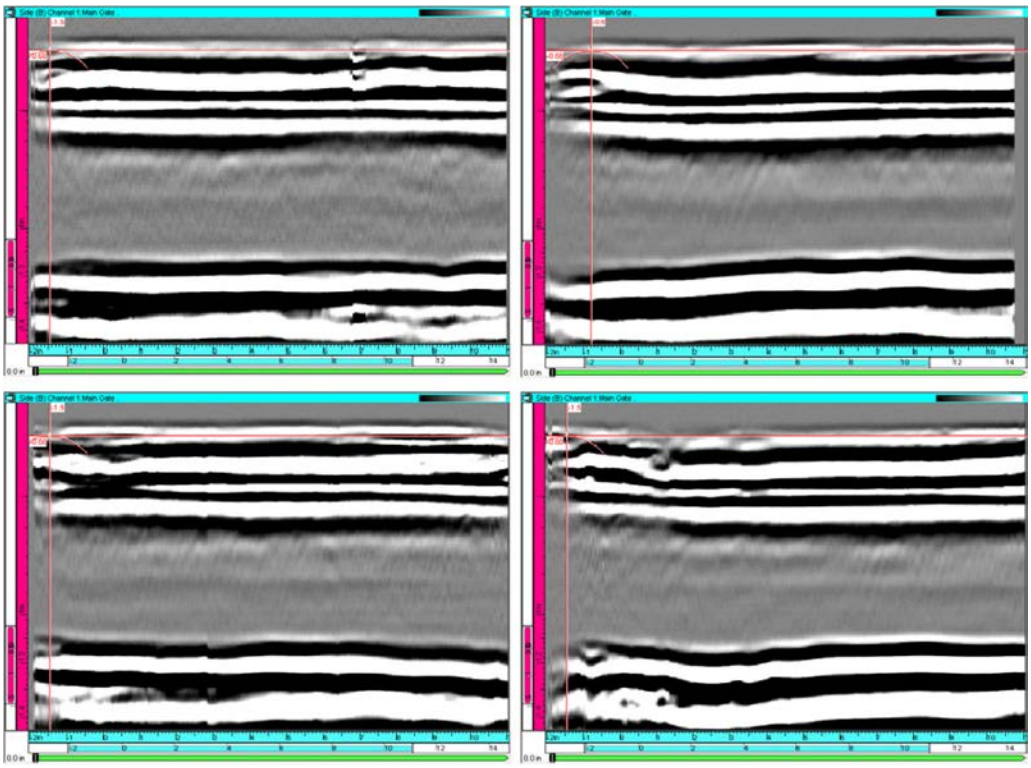

Figure C.6 Pipe Joint 1212, 18 dB Gain

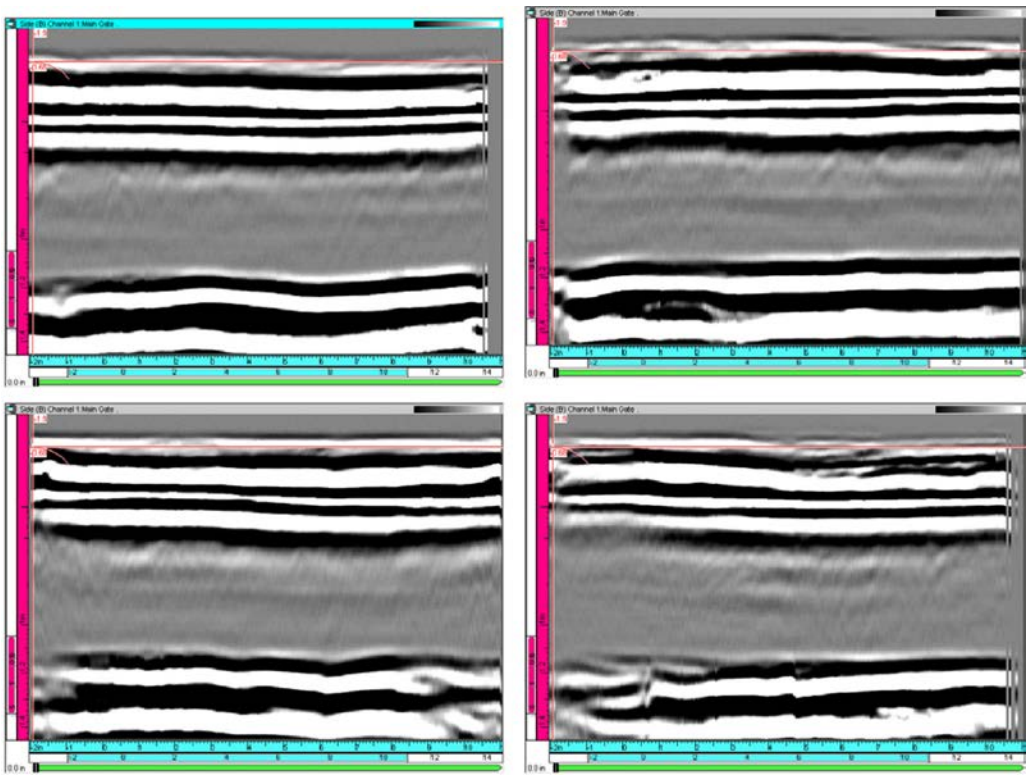

Figure C.7 Pipe Joint 1214, 18 dB Gain

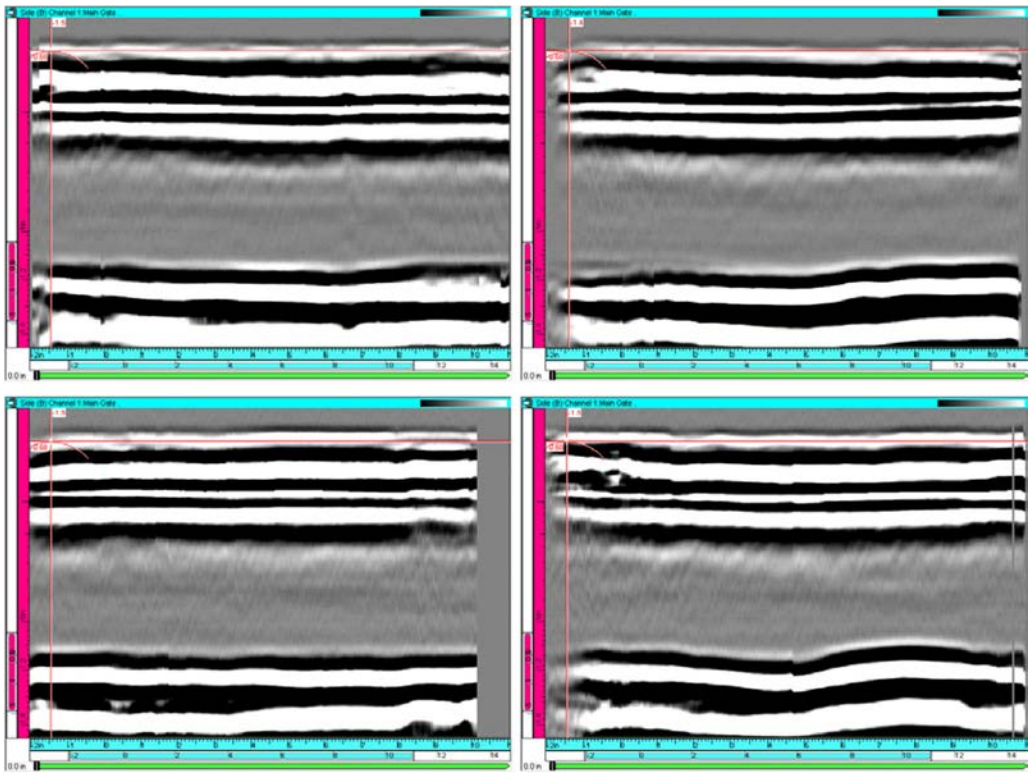

Figure C.8 Pipe Joint 1216, 18 dB Gain

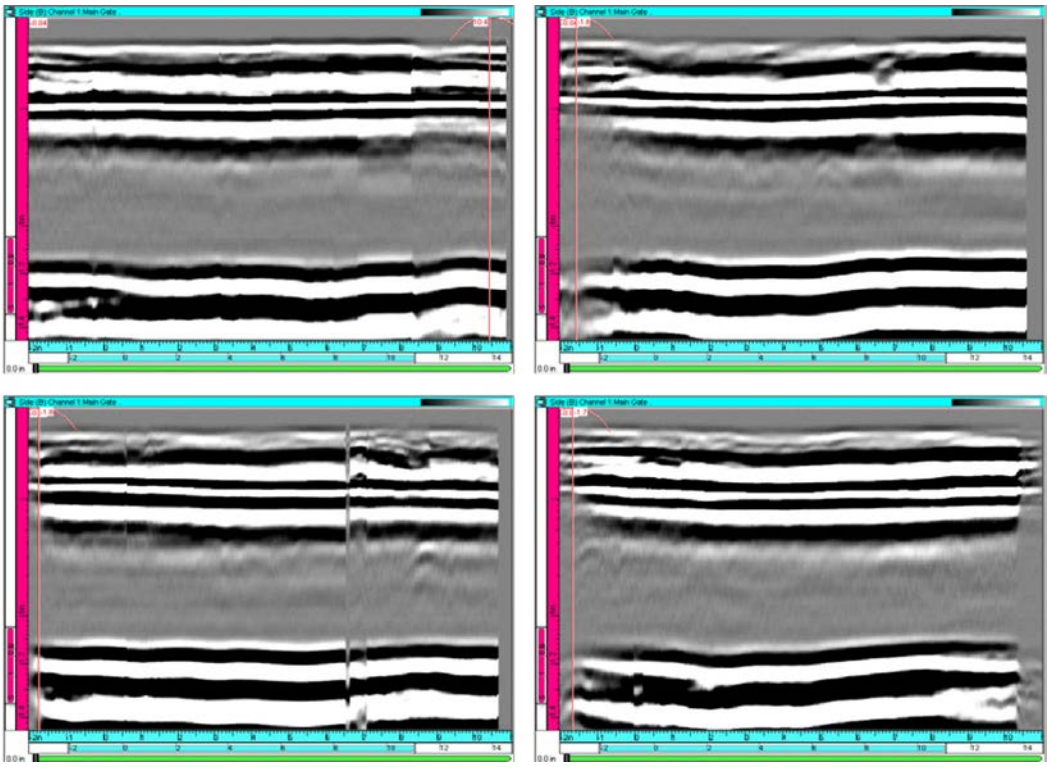

Figure C.9 Pipe Joint 1218, 18 dB Gain

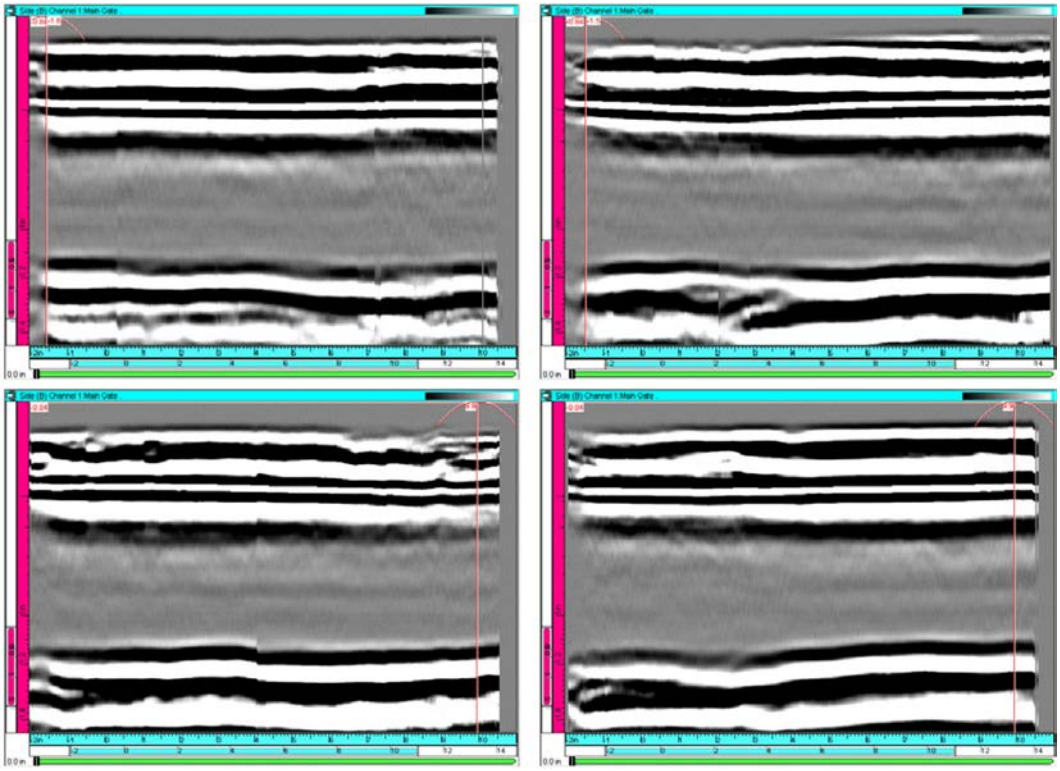

Figure C.10 Pipe Joint 1220, 18 dB Gain

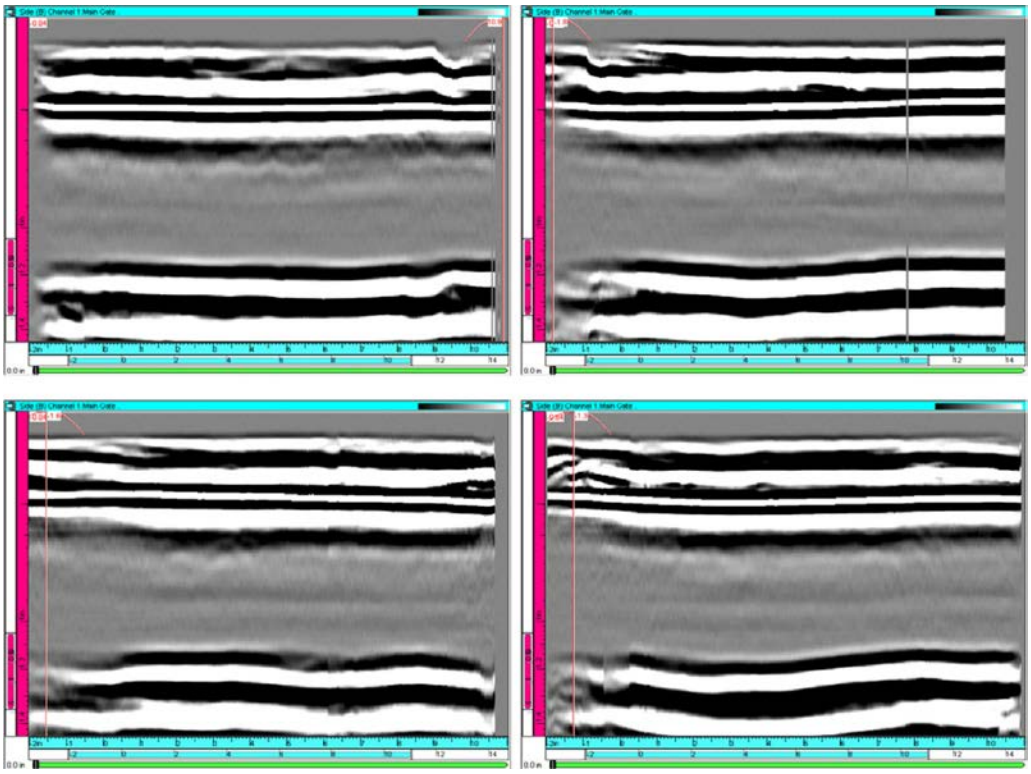

Figure C.11 Pipe Joint 1222, 18 dB Gain

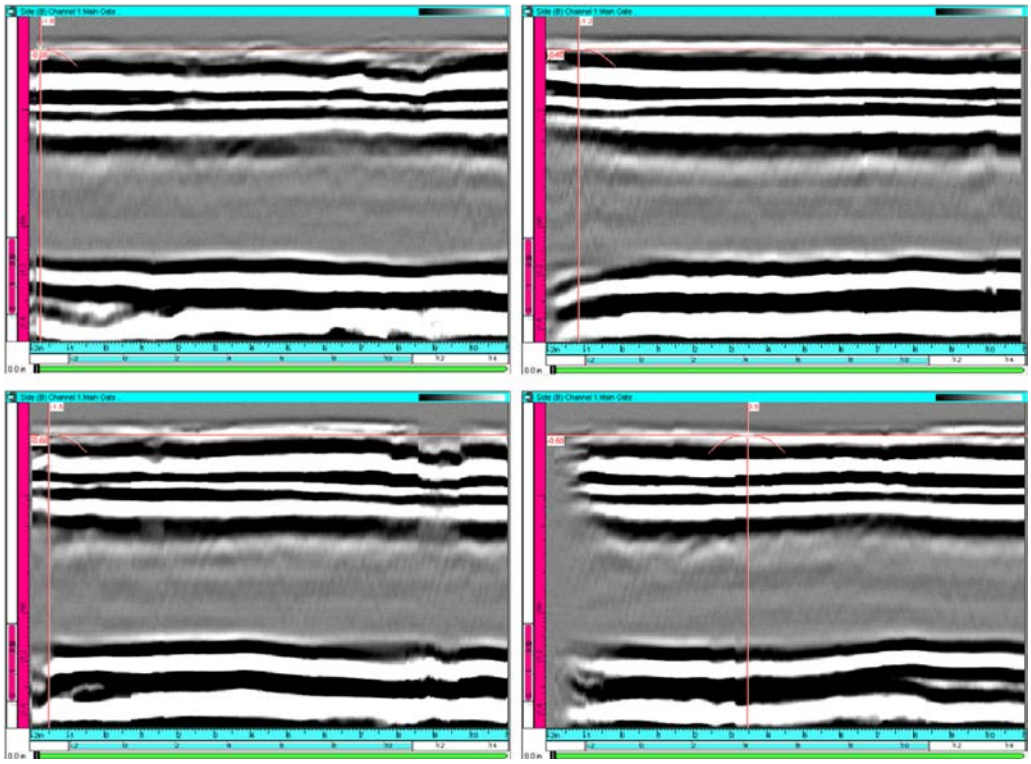

Figure C.12 Pipe Joint 1223, 18 dB Gain

APPENDIX D

PNNL PA INSPECTION RESULTS ON 12 FUSION JOINTS IN 3408 HDPE

APPENDIX D

PNNL PA INSPECTION RESULTS ON 12 FUSION JOINTS IN 3408 HDPE

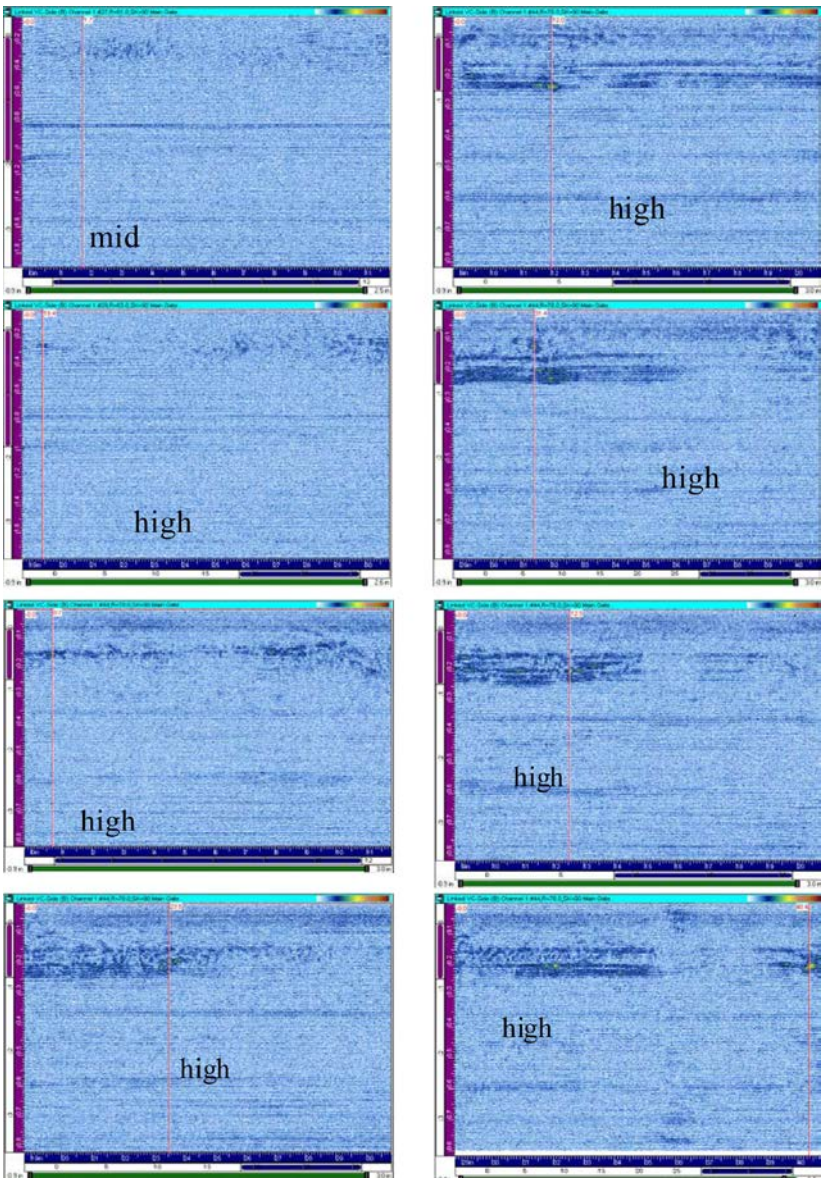

Figure D.1 End View Phased Array Images by Quadrant from Pipe Joint 123 with the Top Four Images from the Stamped Side and the Bottom Four from the Unstamped Side. In a grouping of four, the first quadrant is on the top left, the second quadrant on the top right, the third quadrant on the bottom left and the fourth quadrant on the bottom right. The high, mid, low, etc., notation on the image refers to the inspection angle. Data was acquired from 30 to 78 degrees.

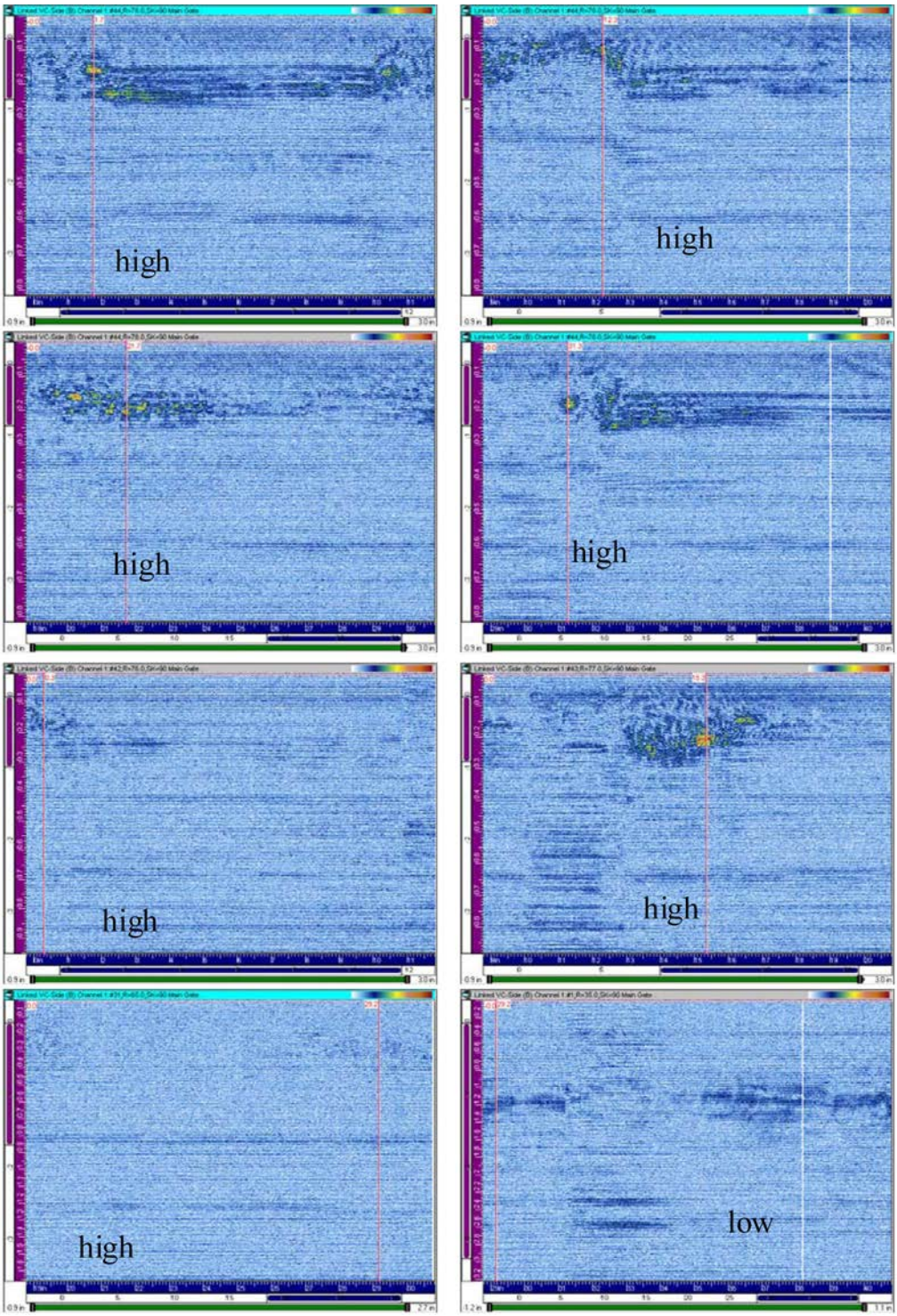

Figure D.2 Phased Array Images by Quadrant from Pipe Joint 124 with the Top Four Images from the Stamped Side and the Bottom Four from the Unstamped Side (30 dB of gain).

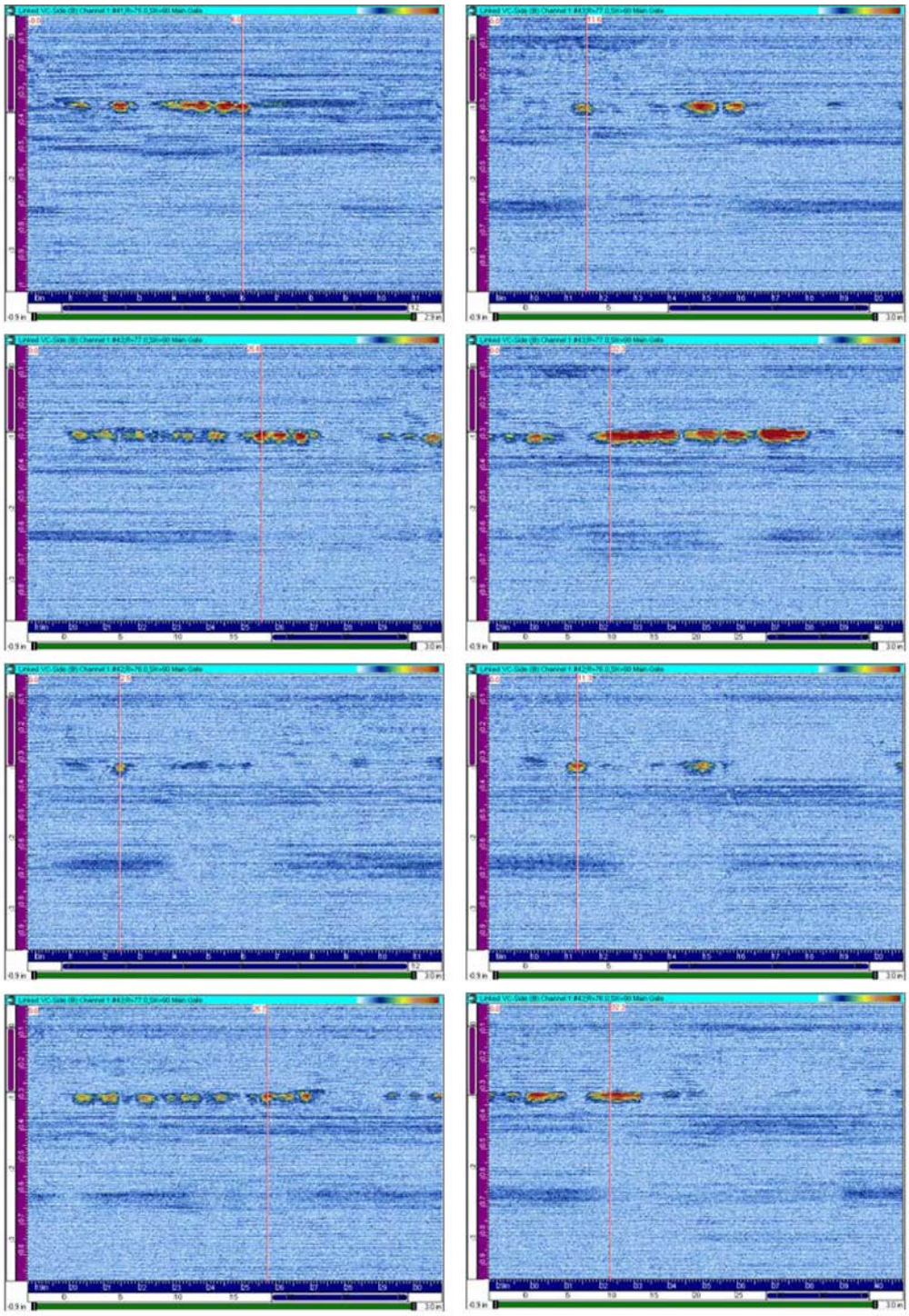

Figure D.3 Phased Array Images by Quadrant from Pipe Joint 127 with the Top Four Images from the Stamped Side and the Bottom Four from the Unstamped Side. All data are from high angles.

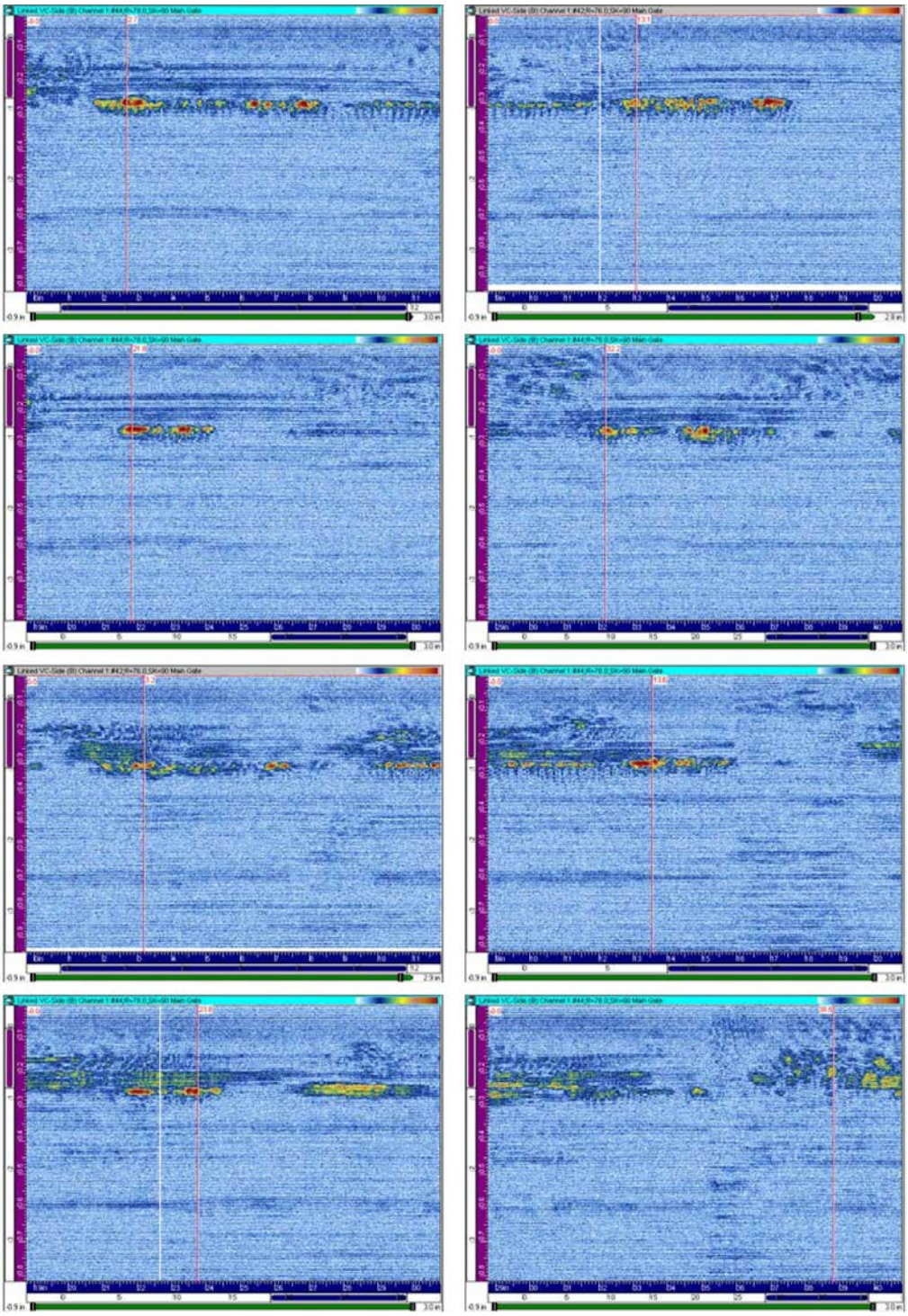

Figure D.4 Phased Array Images by Quadrant from Pipe Joint 128 with the Top Four Images from the Stamped Side and the Bottom Four from the Unstamped Side. All data are from high angles.

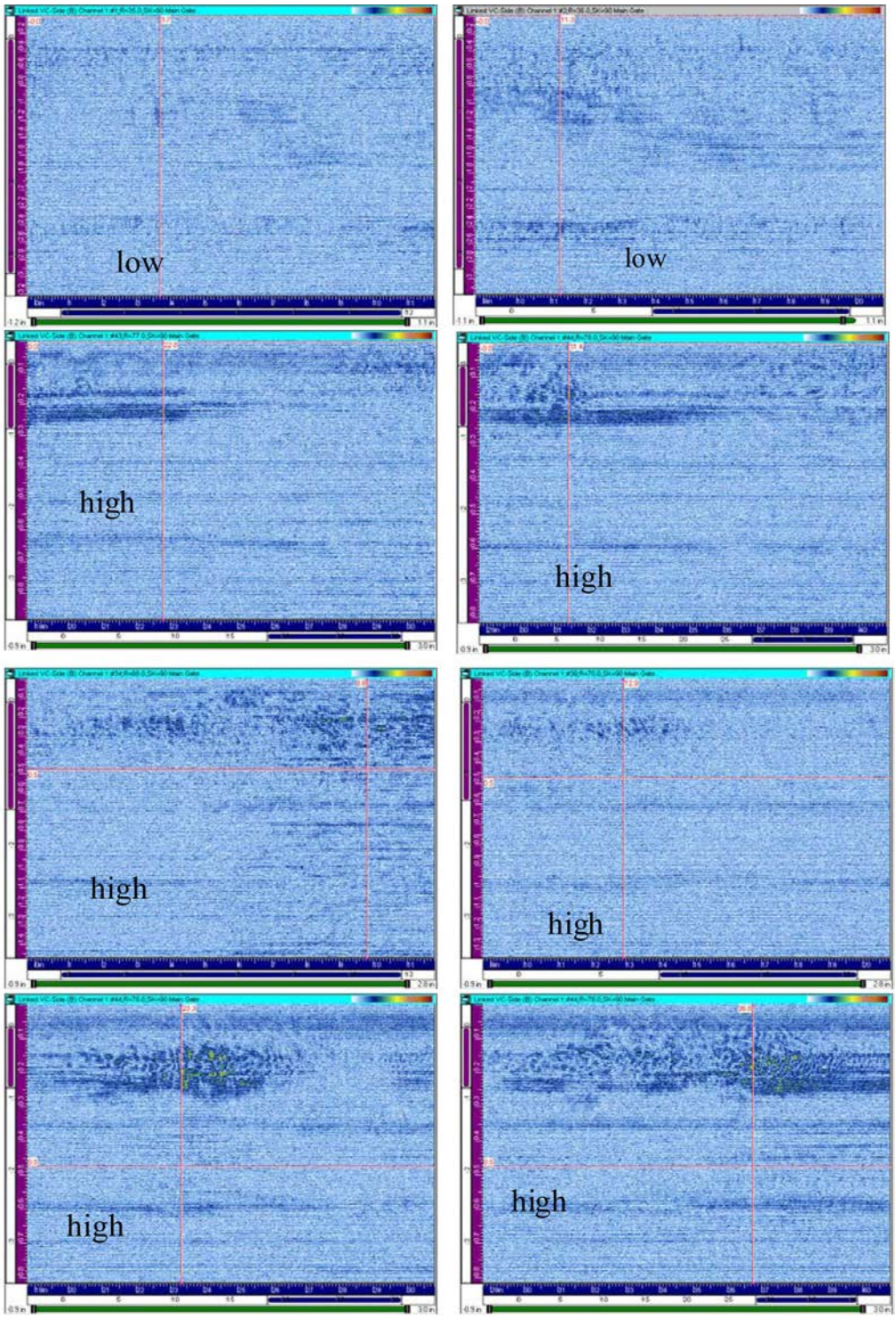

Figure D.5 Phased Array Images by Quadrant from Pipe Joint 1211 with the Top Four Images from the Stamped Side and the Bottom Four from the Unstamped Side

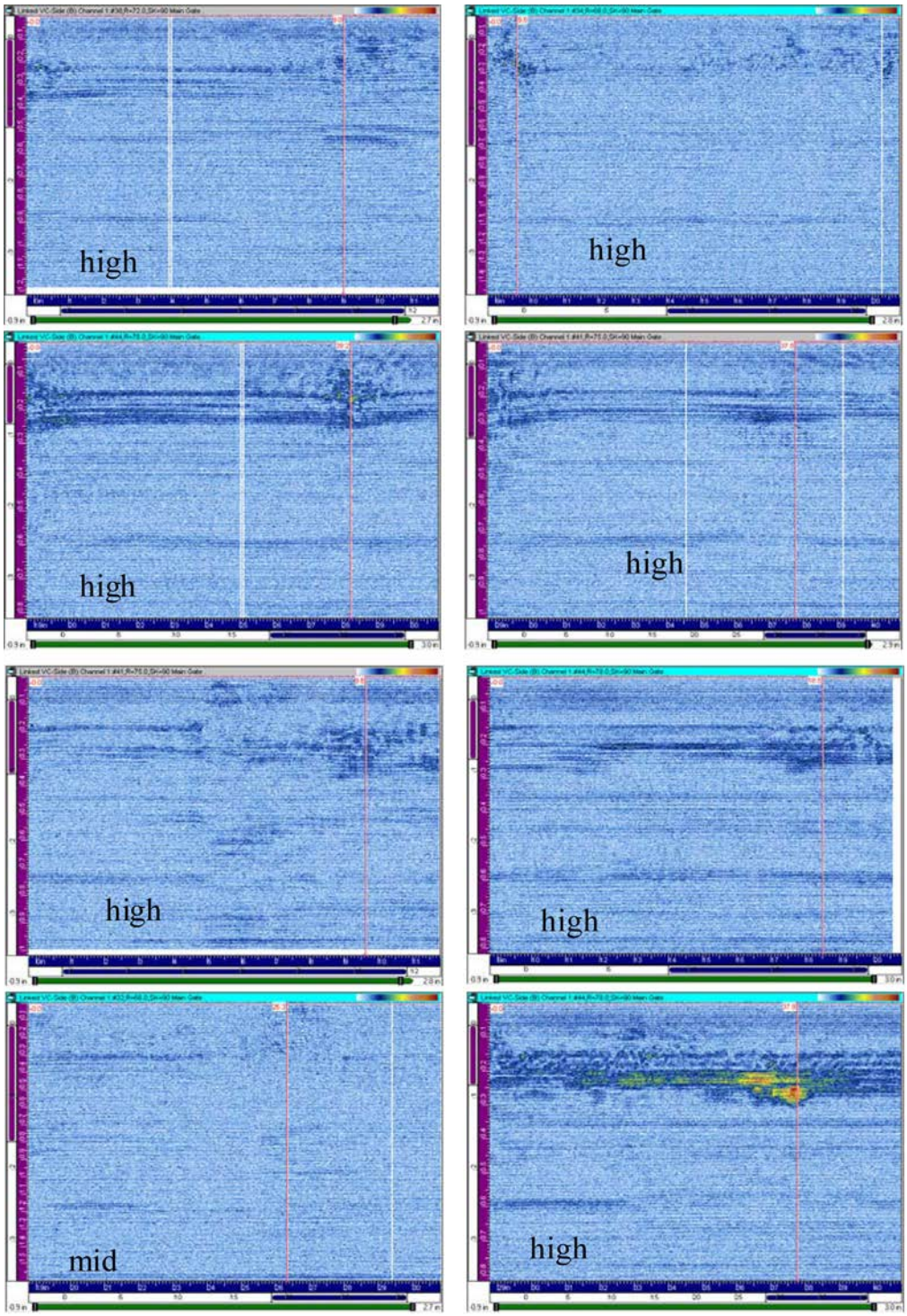

Figure D.6 Phased Array Images by Quadrant from Pipe Joint 1212 with the Top Four Images from the Stamped Side and the Bottom Four from the Unstamped Side

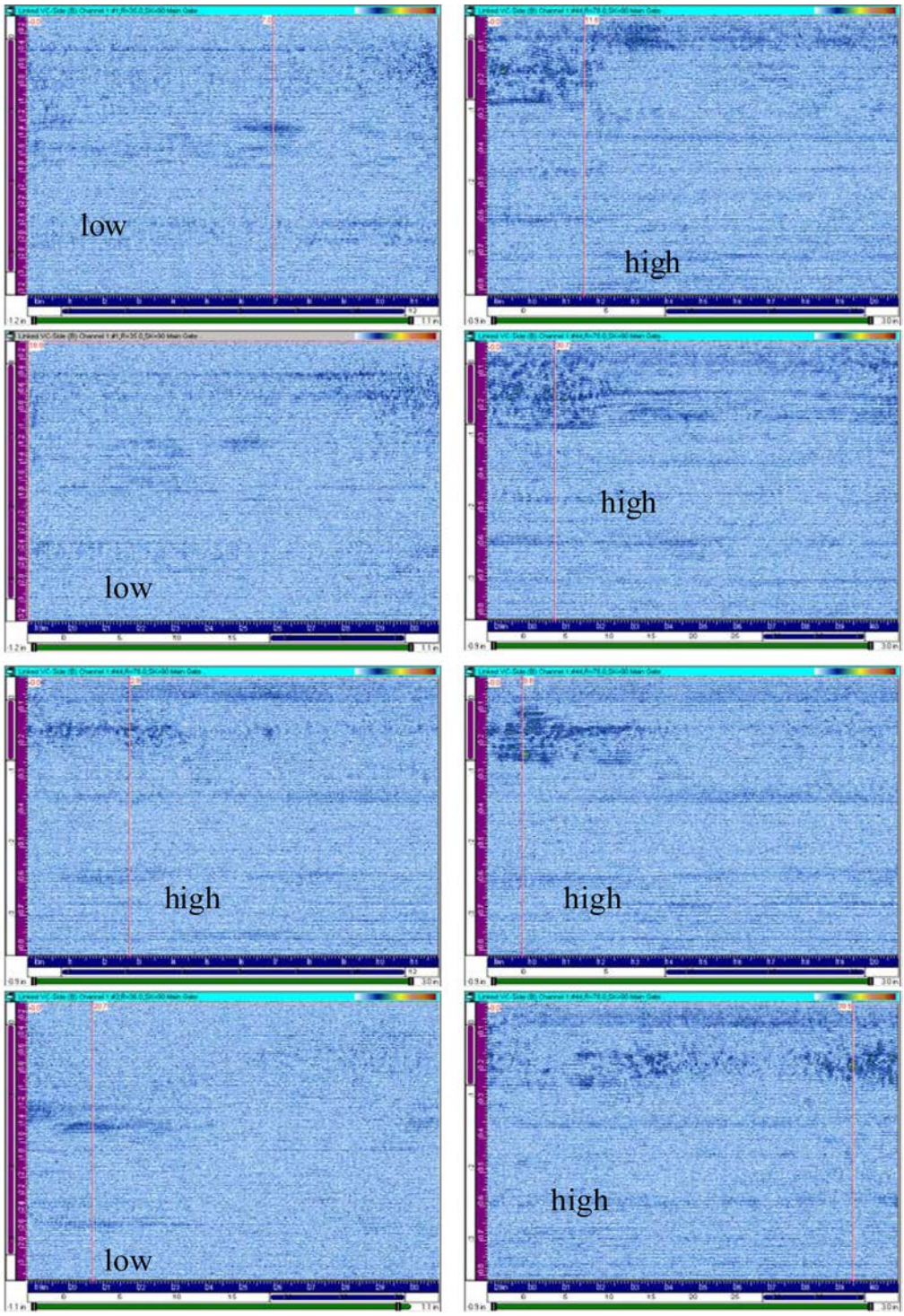

Figure D.7 Phased Array Images by Quadrant from Pipe Joint 1214 with the Top Four Images from the Stamped Side and the Bottom Four from the Unstamped Side

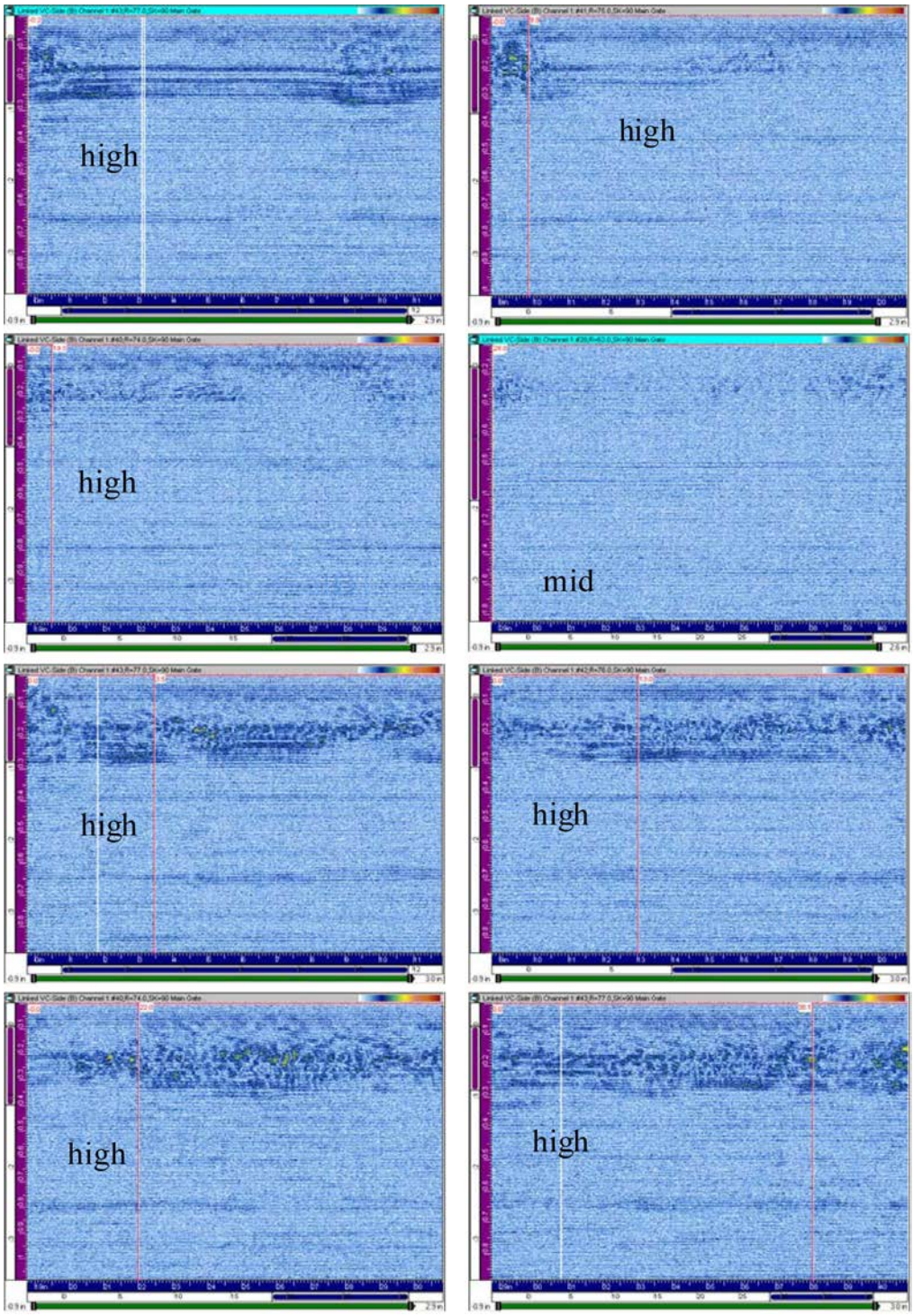

Figure D.8 Phased Array Images by Quadrant from Pipe Joint 1216 with the Top Four Images from the Stamped Side and the Bottom Four from the Unstamped Side

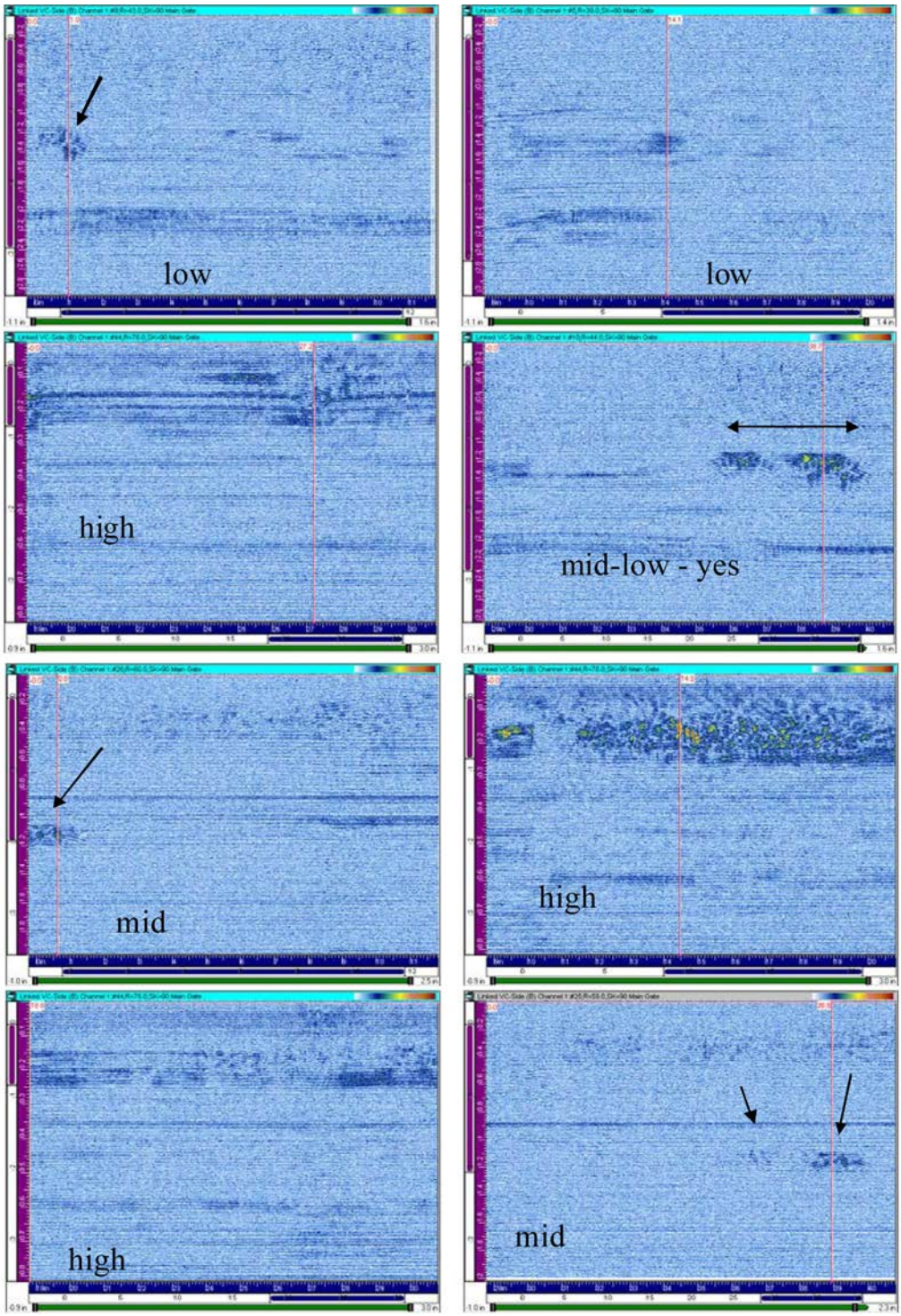

Figure D.9 Phased Array Images by Quadrant from Pipe Joint 1218 with the Top Four Images from the Stamped Side and the Bottom Four from the Unstamped Side

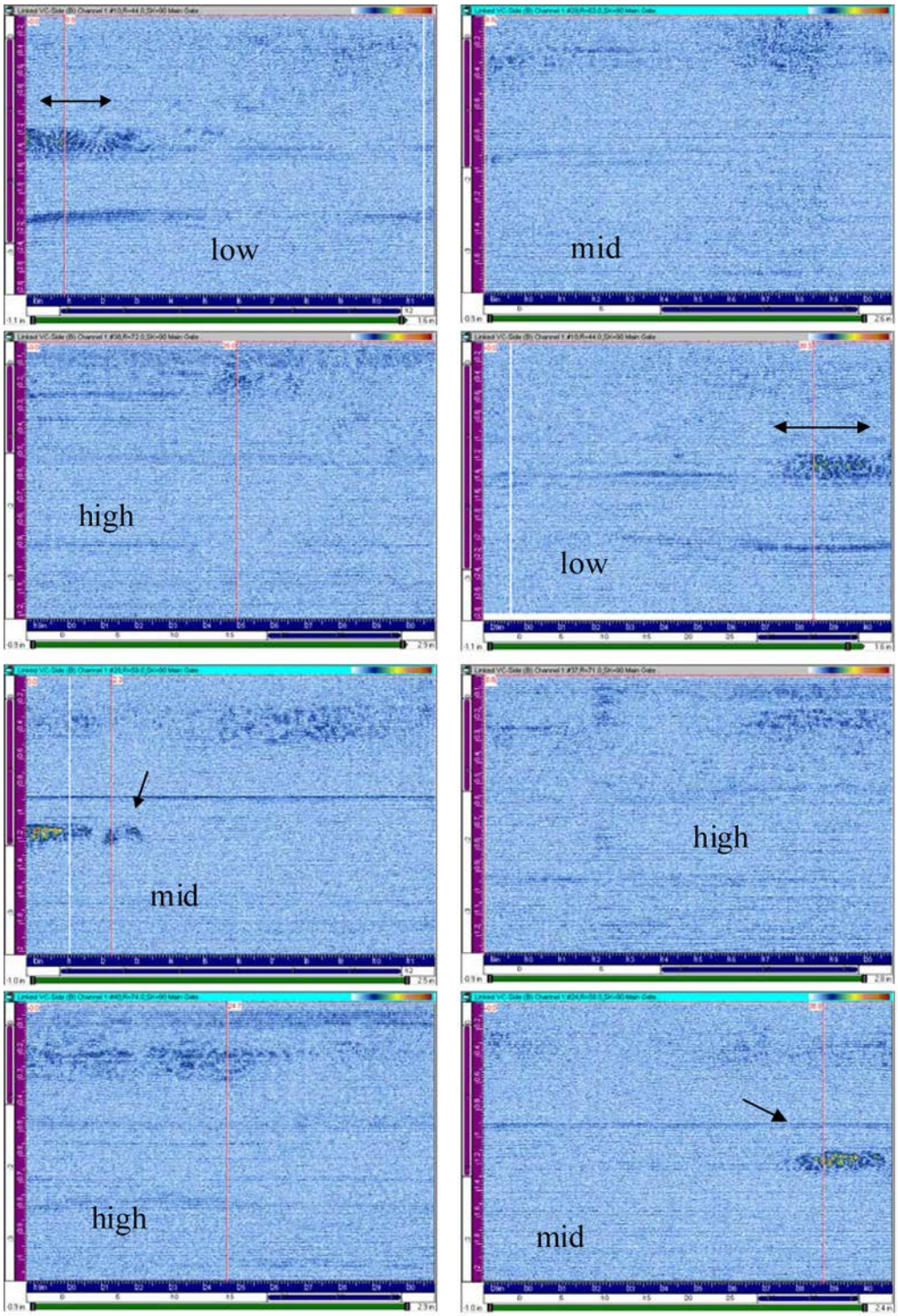

Figure D.10 Phased Array Images by Quadrant from Pipe Joint 1220 with the Top Four Images from the Stamped Side and the Bottom Four from the Unstamped Side

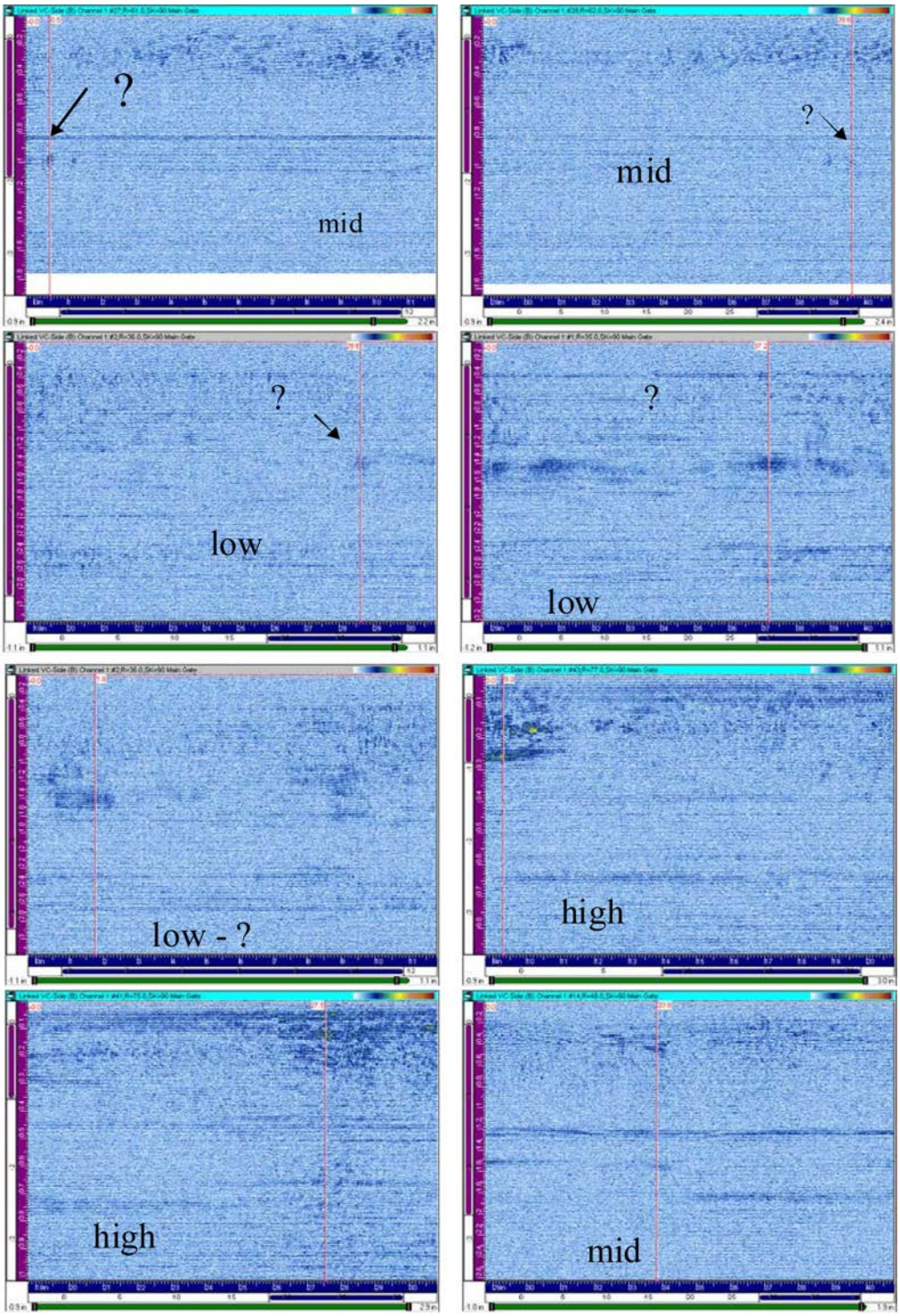

Figure D.11 Phased Array Images by Quadrant from Pipe Joint 1222 with the Top Four Images from the Stamped Side and the Bottom Four from the Unstamped Side

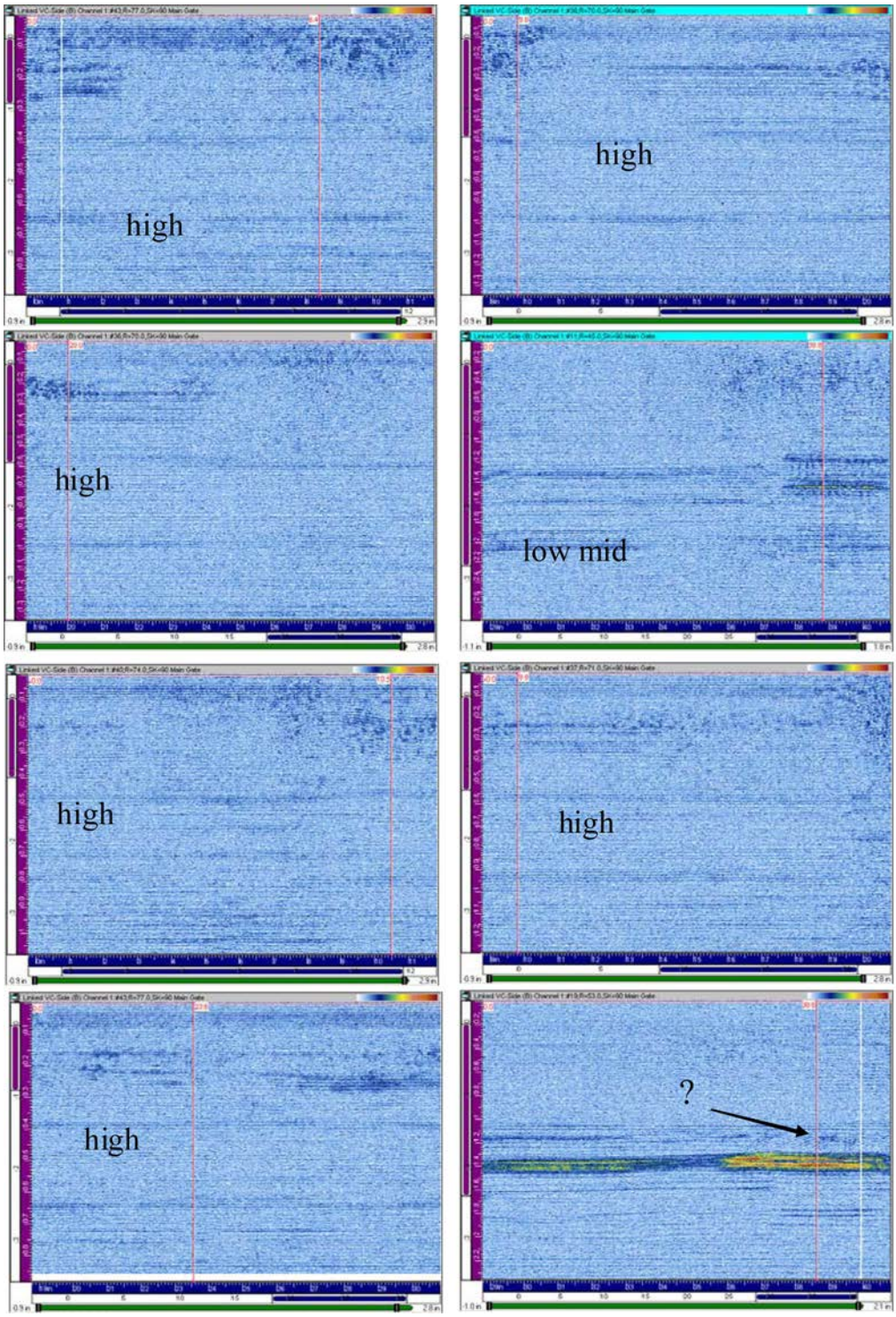

Figure D.12 Phased Array Images by Quadrant from Pipe Joint 1223 with the Top Four Images from the Stamped Side and the Bottom Four from the Unstamped Side

APPENDIX E

SUMMARY PLOTS OF NDE RESULTS IN SPECIMENS NOT SUBJECTED TO DE

APPENDIX E

SUMMARY PLOTS OF NDE RESULTS IN SPECIMENS NOT SUBJECTED TO DE

The following figures summarize the NDE results with the captions commenting on the findings. The visual and bead profile results will not be included in the discussion as the visual results were deemed a surface evaluation and not volumetric, and the bead profile results were an indication of fusion pressure applied during the heat cycle, an abnormal condition. Marginal calls as represented by the dotted lines will not be discussed either since they are not definitive flaw calls. None of these quadrants had any destructive testing performed on them to assess the mechanical integrity of them.

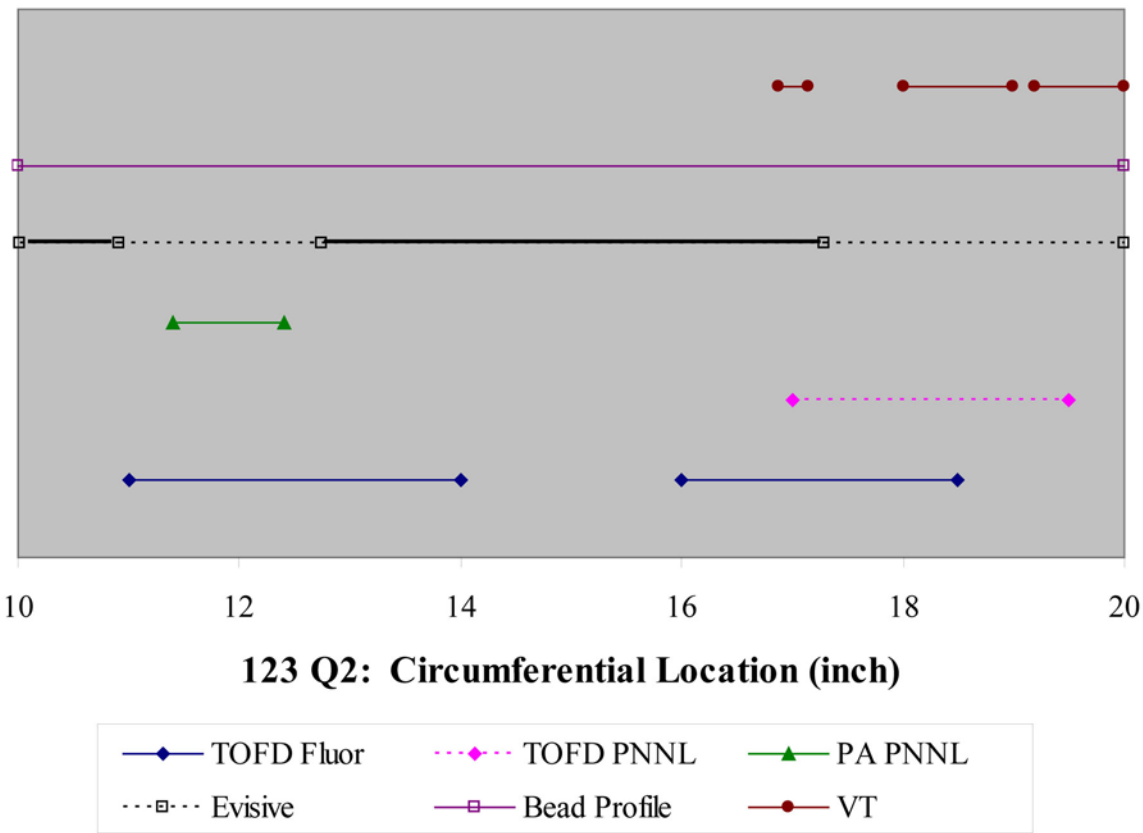

Figure E.1 Evisive, PA PNNL, and TOFD Fluor had areas called defective but the correlation between the three techniques is not very good.

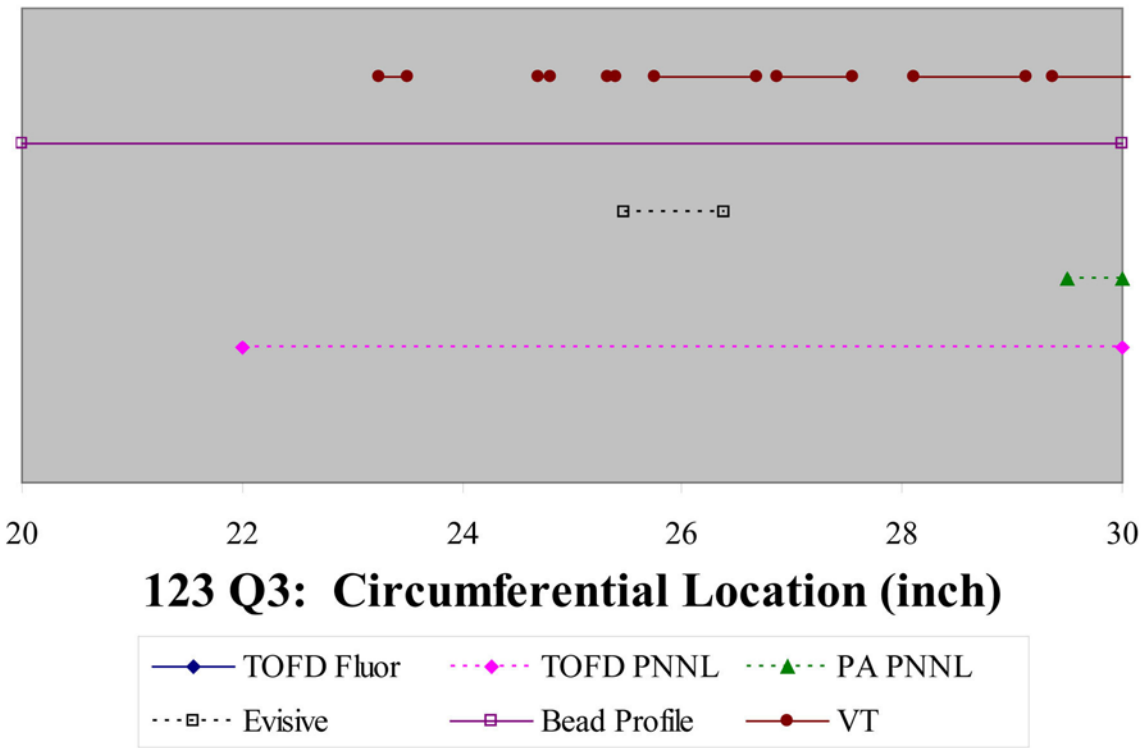

Figure E.2 There were no definitive NDE flaw calls in this quadrant.

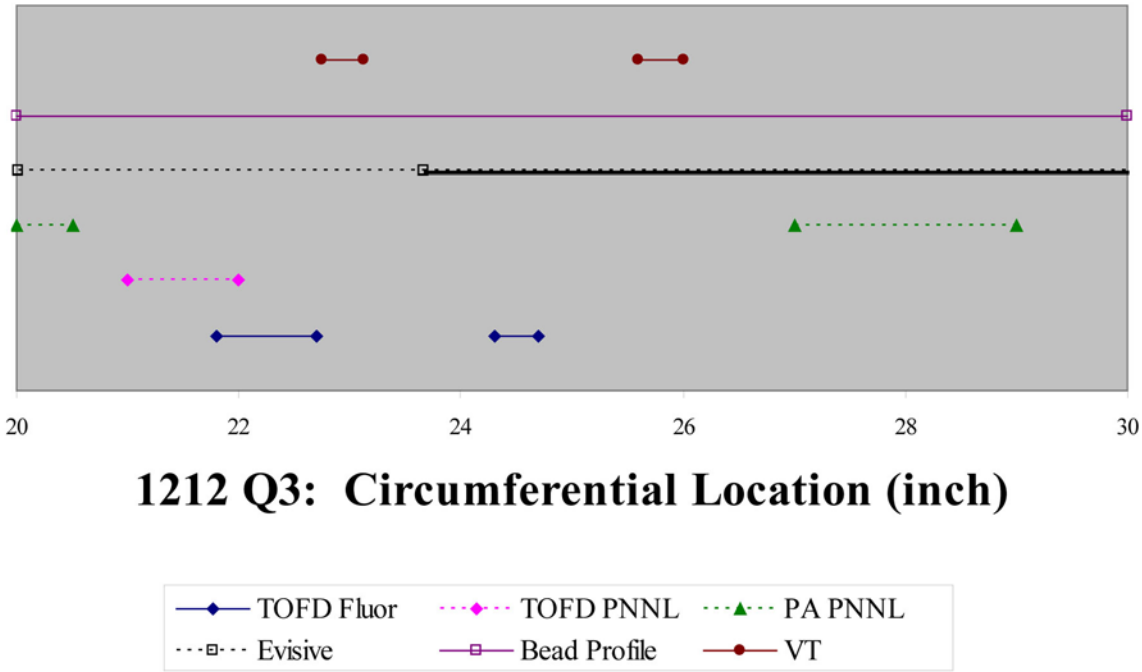

Figure E.3 Evisive called approximately 60% of this quadrant flawed and TOFD Fluor showed two flawed areas, one of which over lapped with the Evisive call.

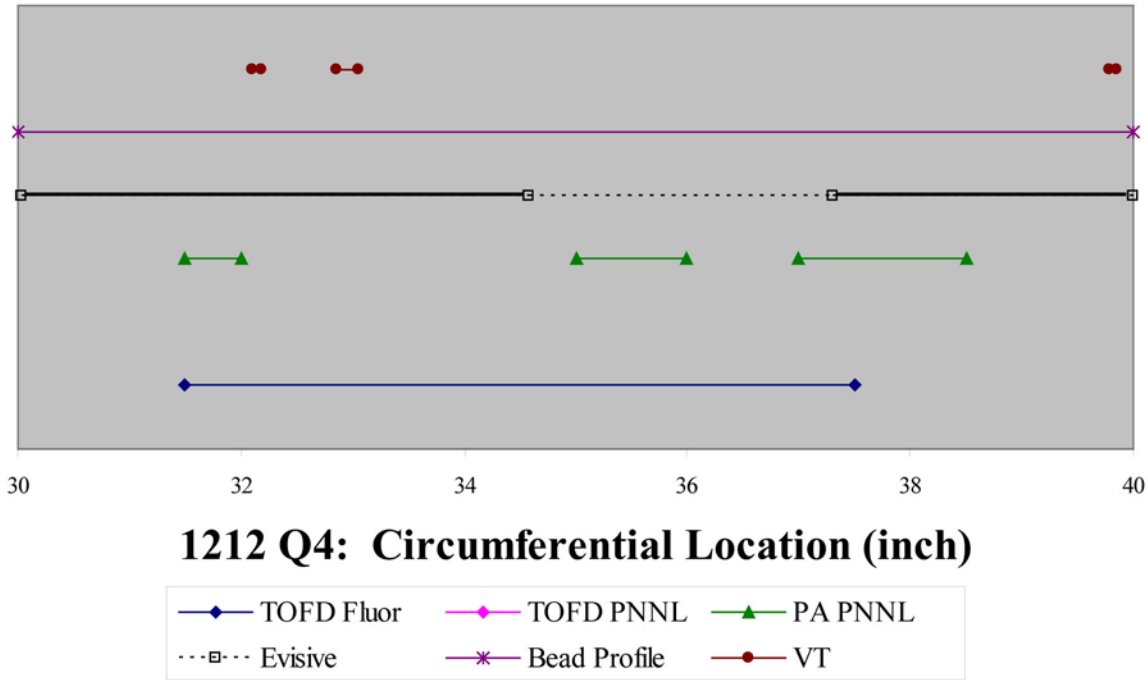

Figure E.4 **Evisive, PA PNNL and TOFD Fluor called defective areas in this quadrant. There was better agreement in the TOFD and PA results than the Evisive results.**

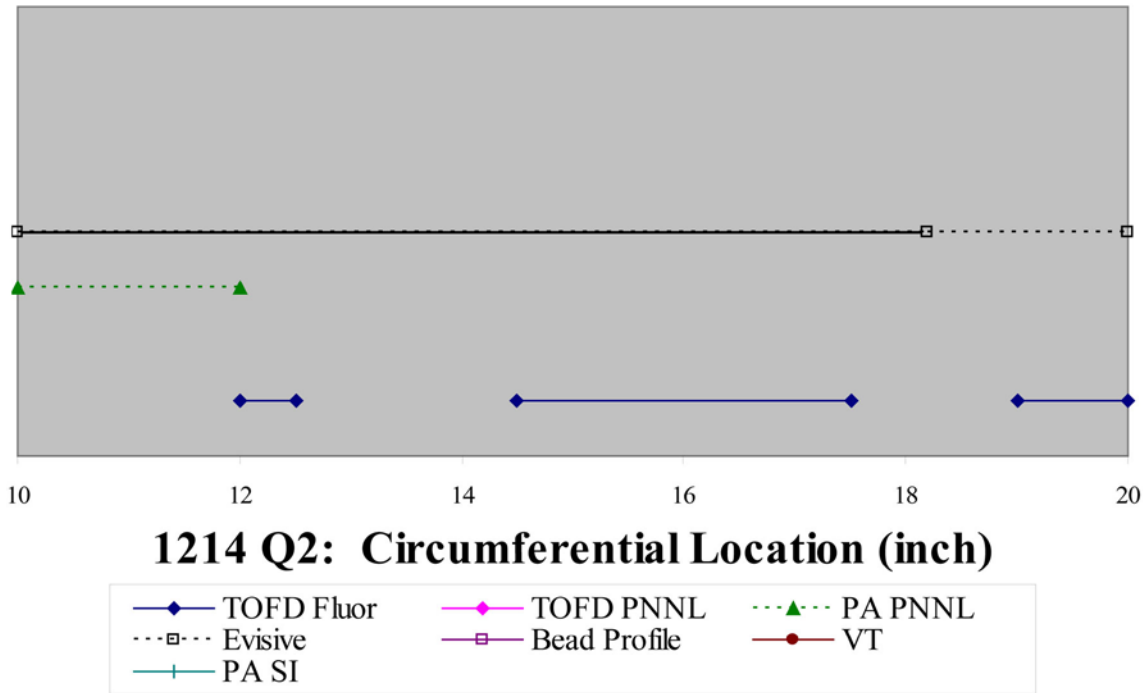

Figure E.5 **Evisive called most of the quadrant defective. TOFD Fluor called three regions defective and two of these regions fell in the Evisive defective area.**

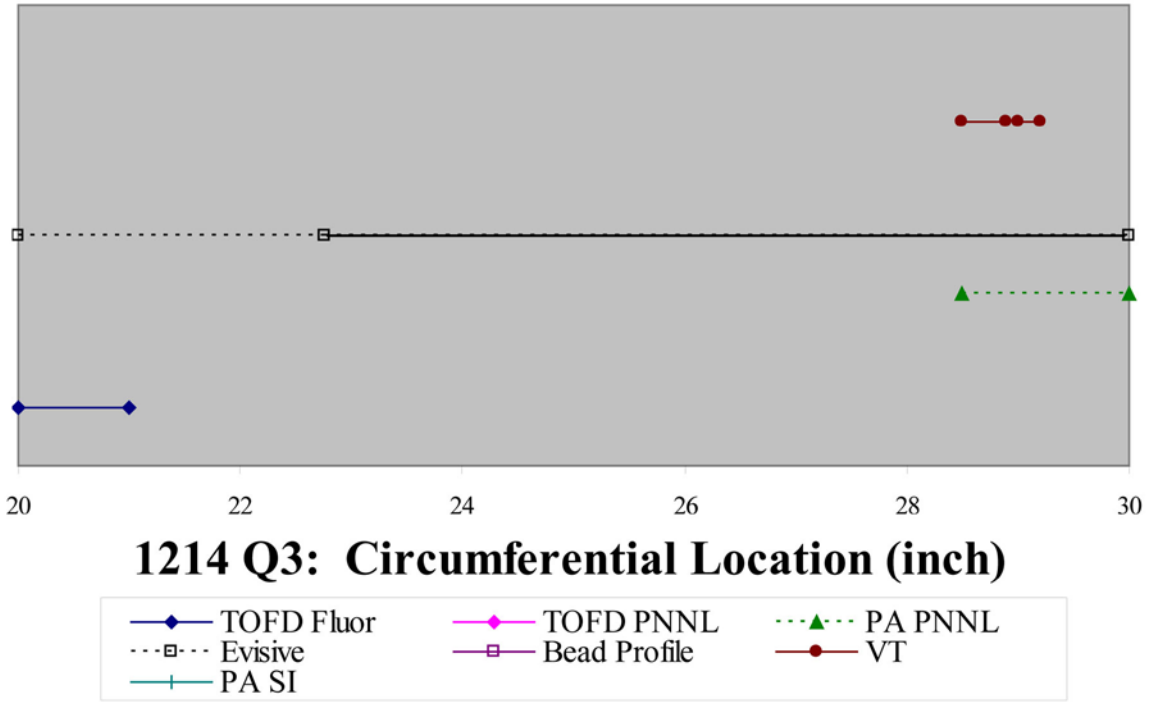

Figure E.6 Evisive called most of the quadrant defective. TOFD Fluor called one small area defective and this did not fall in the Evisive defective area.

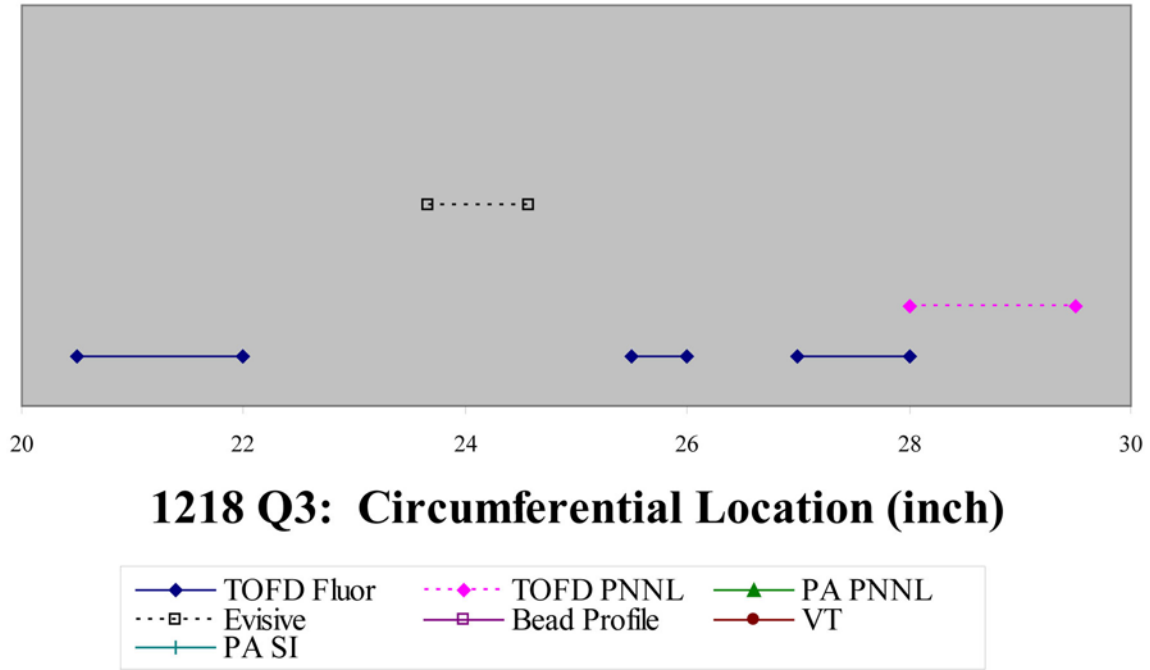

Figure E.7 TOFD Fluor was the only NDE technique to call defective regions.

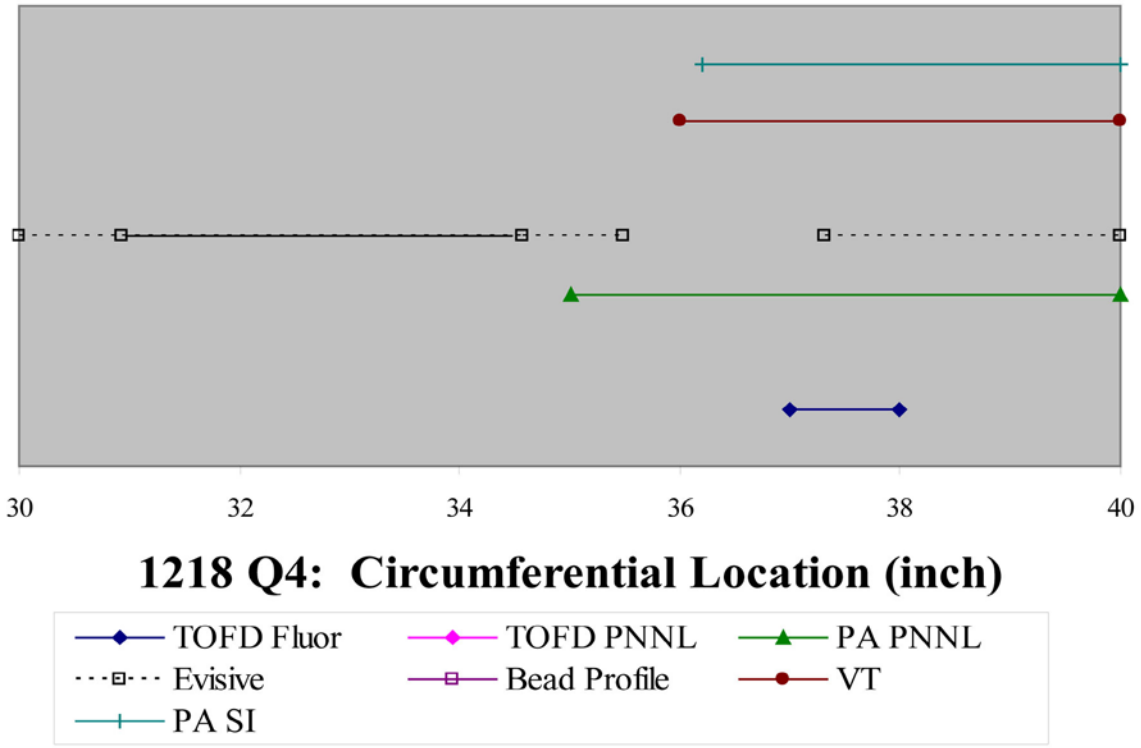

Figure E.8 Evisive and PA PNNL called defective regions but they did not intersect. TOFD Fluor called a small defective region that fell within the PA PNNL called flaw region.

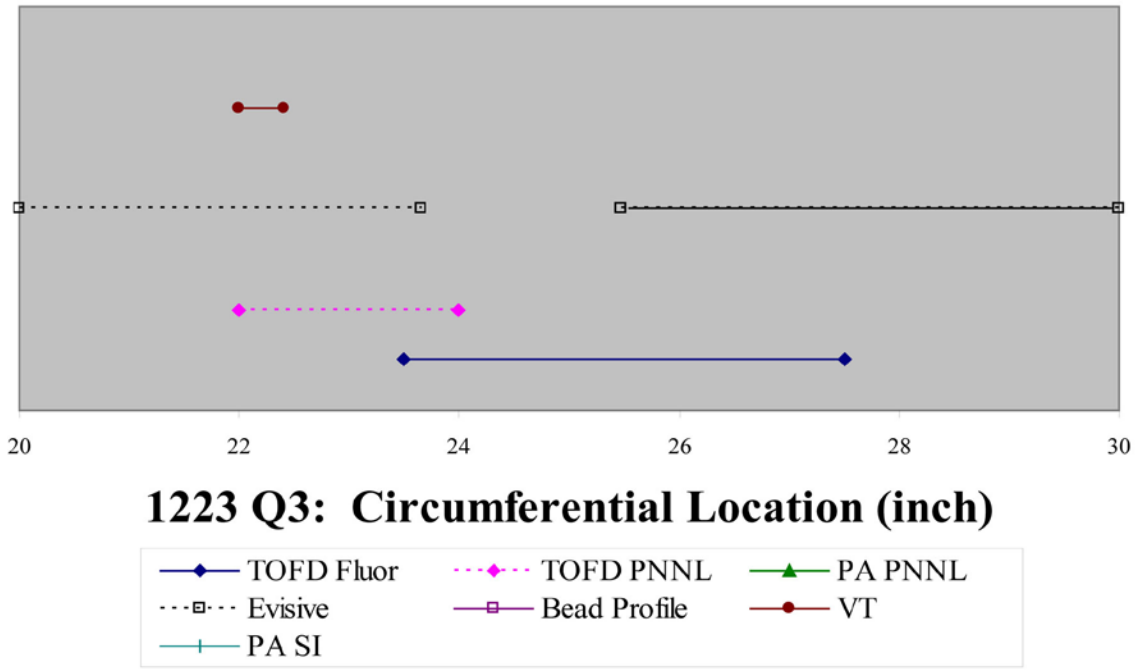

Figure E.9 Evisive and TOFD Fluor called defective regions with an approximate 50% intersection of the called flawed regions.

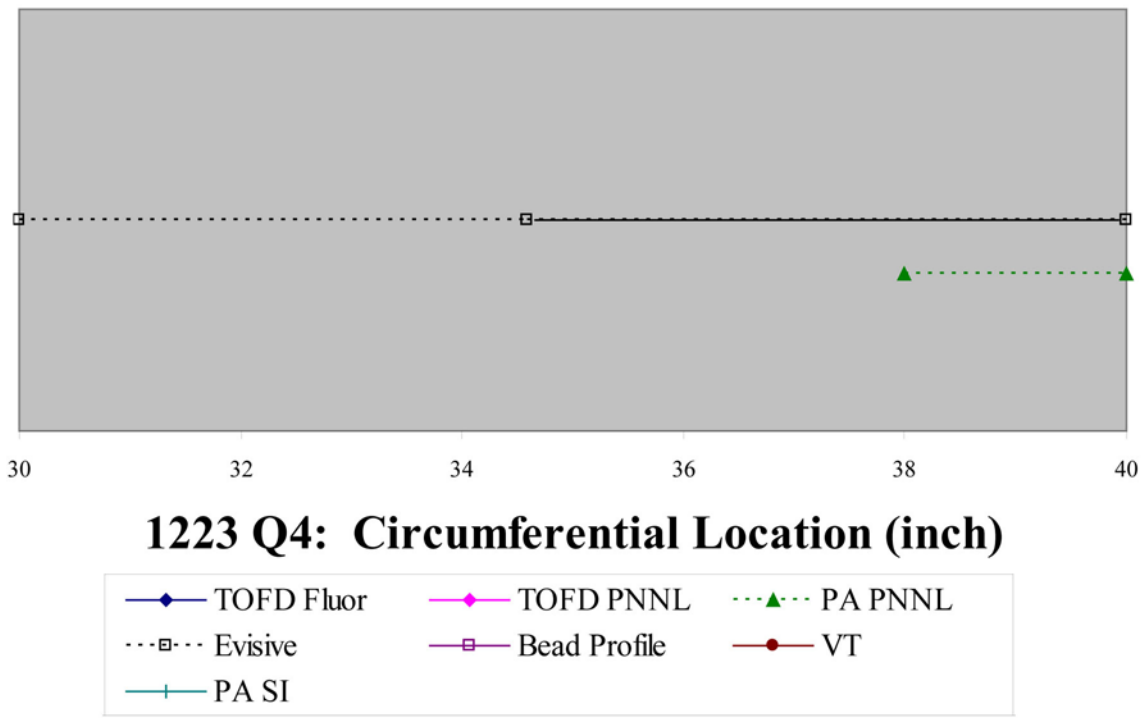

Figure E.10 Evisive called approximately half of the quadrant flawed. There were no other detected flaw regions.

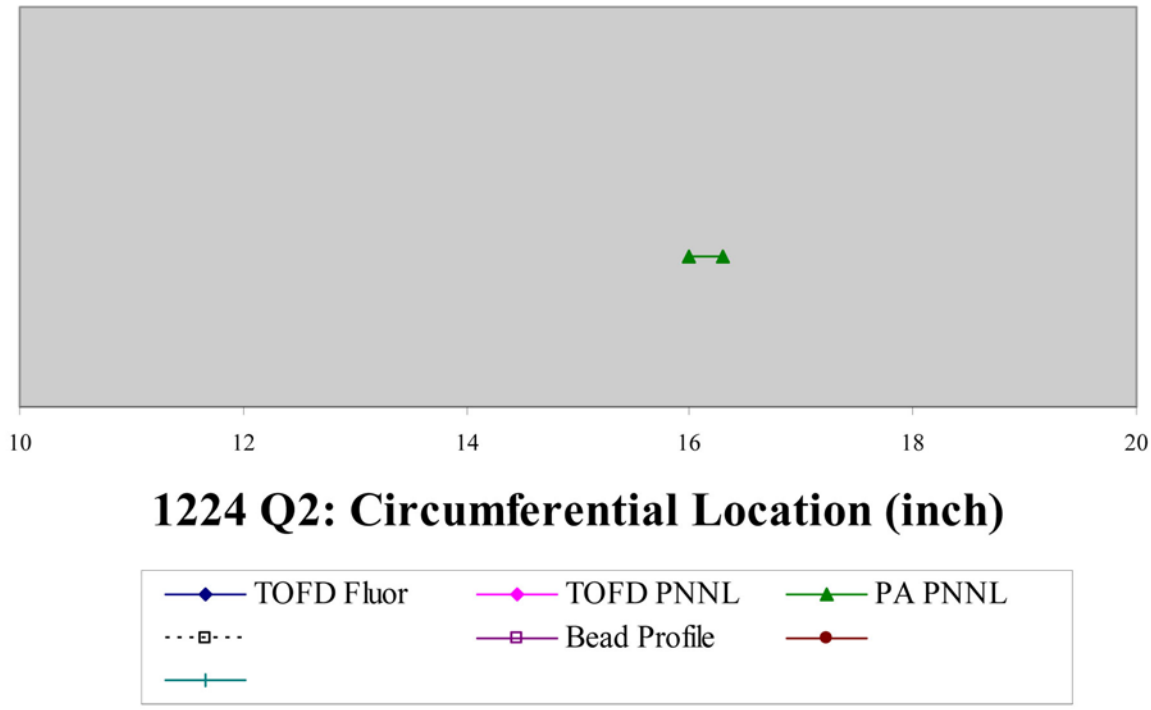

Figure E.11 This quadrant only had one small flaw call by PA PNNL.

NRC FORM 335
(9-2004)
NRCMD 3.7

U.S. NUCLEAR REGULATORY COMMISSION

BIBLIOGRAPHIC DATA SHEET

(See instructions on the reverse)

1. REPORT NUMBER
(Assigned by NRC, Add Vol., Supp., Rev., and Addendum Numbers, if any.)

NUREG/CR-7136

2. TITLE AND SUBTITLE

Assessment of NDE Methods on Inspection of HDPE Butt Fusion Piping Joints for Lack of Fusion

3. DATE REPORT PUBLISHED

MONTH	YEAR
May	2012

4. FIN OR GRANT NUMBER

JCN N6398

5. AUTHOR(S)

S. L. Crawford, S. R. Doctor, A. D. Cinson, M. W. Watts, S. E. Cumblidge, T. E. Hall, and M. T. Anderson

6. TYPE OF REPORT

Technical

7. PERIOD COVERED *(Inclusive Dates)*

9/2006-10/2011

8. PERFORMING ORGANIZATION - NAME AND ADDRESS *(If NRC, provide Division, Office or Region, U.S. Nuclear Regulatory Commission, and mailing address; if contractor, provide name and mailing address.)*

Pacific Northwest National Laboratory
P.O. Box 999
Richland, WA 99352

9. SPONSORING ORGANIZATION - NAME AND ADDRESS *(If NRC, type "Same as above"; if contractor, provide NRC Division, Office or Region, U.S. Nuclear Regulatory Commission, and mailing address.)*

Division of Engineering
Office of Nuclear Regulatory Research
U.S. Nuclear Regulatory Commission
Washington, D.C. 20555-0001

10. SUPPLEMENTARY NOTES

11. ABSTRACT *(200 words or less)*

The U.S. Nuclear Regulatory Commission (NRC) has a multi-year program at the Pacific Northwest National Laboratory (PNNL) to provide engineering studies and assessments of issues. This work was begun in response to requests from commercial nuclear licensees to employ HDPE materials in nuclear power plant systems. HDPE has been widely used in low-pressure, low-temperature applications such as natural gas lines, water, sewer, and petrochemical applications.

The work described in this report is being conducted by the NRC at PNNL to assess whether a volumetric inspection method can be applied to the fusion joint that may reliably detect lack-of-fusion (LOF) conditions. At temperatures at or exceeding the design temperature of HDPE, LOF may result in failure of the piping.

Twenty-four HDPE pipe specimens were butt fused in 3408 material to contain LOF conditions that could be used to assess the effectiveness of NDE methods applied. A range of NDE measurements were performed using ultrasonic and electromagnetic methods. Destructive evaluations were conducted using several different methods, but eventually were focused on a side-bend test procedure. All of the NDE results and destructive test results have been analyzed and documented in this report.

12. KEY WORDS/DESCRIPTORS *(List words or phrases that will assist researchers in locating the report.)*

high density polyethylene, HDPE, butt fusion joints, NDE, phased array UT, time-of-flight diffraction UT, microwave testing, side-bend testing

13. AVAILABILITY STATEMENT

unlimited

14. SECURITY CLASSIFICATION

(This Page)

unclassified

(This Report)

unclassified

15. NUMBER OF PAGES

16. PRICE

PRINTED ON RECYCLED PAPER

Printed
on recycled
paper

Federal Recycling Program

UNITED STATES
NUCLEAR REGULATORY COMMISSION
WASHINGTON, DC 20555-0001

OFFICIAL BUSINESS

NUREG/CR-7136

Assessment of NDE Methods on Inspection of HDPE Butt Fusion Piping Joints for Lack of Fusion

May 2012